Journal of Immunology Research

Vaccines and Therapies for Biodefence Agents

Guest Editors: Julia A. Tree, E. Diane Williamson, Caroline A. Rowland, and Louise M. Pitt

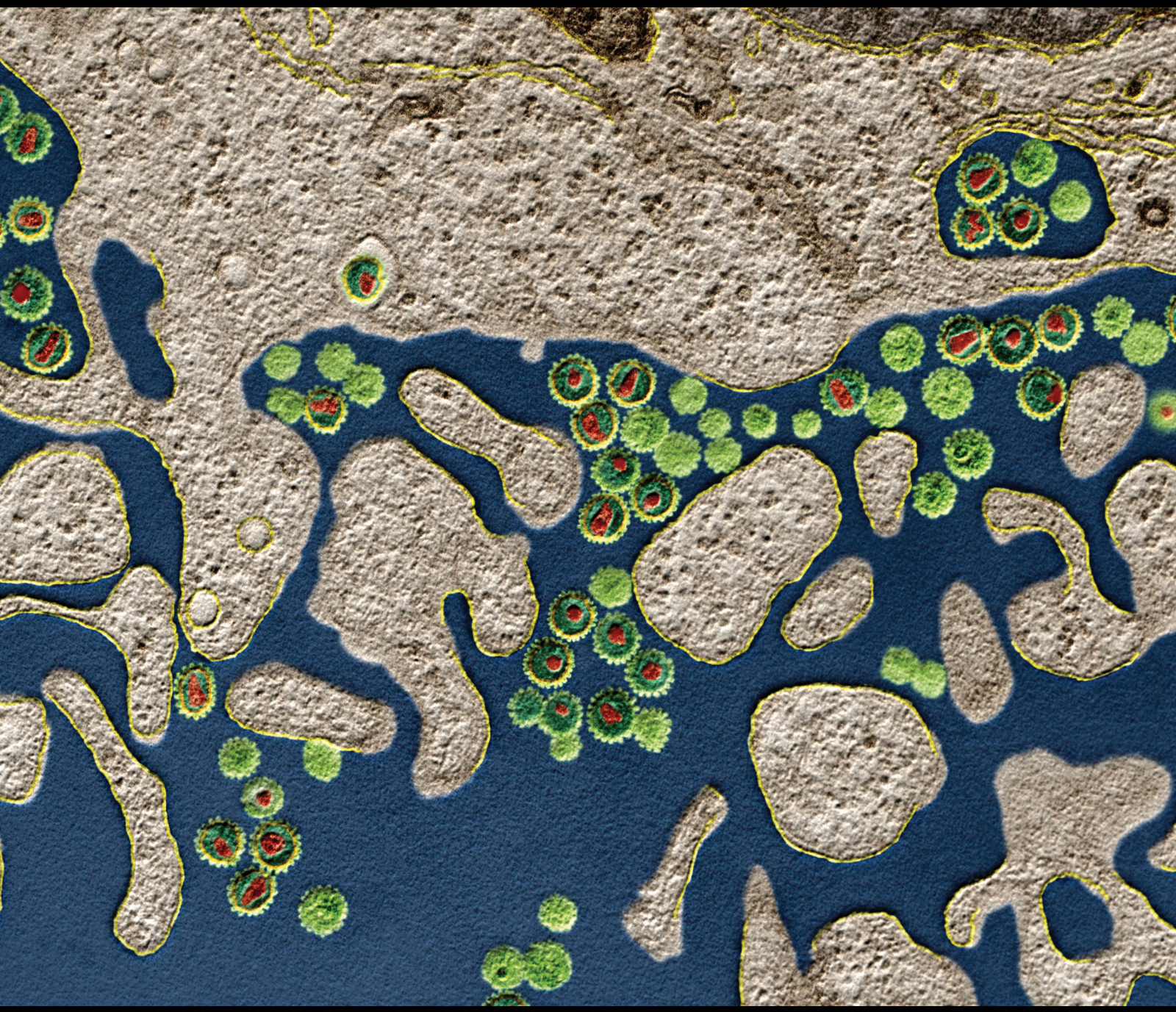

Vaccines and Therapies for Biodefence Agents

Journal of Immunology Research

Vaccines and Therapies for Biodefence Agents

Guest Editors: Julia A. Tree, E. Diane Williamson,
Caroline A. Rowland, and Louise M. Pitt

Editorial Board

Contents

Hindawi Publishing Corporation
Journal of Immunology Research
Volume 2015, Article ID 537319, 2 pages
http://dx.doi.org/10.1155/2015/537319

Editorial

Vaccines and Therapies for Biodefence Agents

Julia A. Tree,[1] E. Diane Williamson,[2] Caroline A. Rowland,[2] and Louise M. Pitt[3]

[1]*Microbiological Services, Public Health England (PHE), Porton Down, Salisbury, Wiltshire SP4 OJG, UK*
[2]*Biomedical Science Department, Defence Science and Technology Laboratory (DSTL), Porton Down, Salisbury, Wiltshire SP4 OJQ, UK*
[3]*Virology Department, United States Army Medical Research Institute of Infectious Diseases (USAMRIID), Fort Detrick, Frederick, MD 21703, USA*

Correspondence should be addressed to Julia A. Tree; julia.tree@phe.gov.uk

Received 9 October 2014; Accepted 9 October 2014

This special issue, dealing with biodefence vaccines and therapies, incorporates two review papers and six original research papers. The review papers introduce concepts and themes underpinning the research papers, including the use of animal models to predict human responses in the transition of candidate vaccines and therapies from research to development and the impact of advances in genomic and imaging technologies on assessing the host immune response to biodefence agents.

Biothreat agents usually cause severe disease so clinical efficacy studies of candidate vaccines or therapies will generally not be ethical or feasible, unless in a field trial situation in a region of endemic disease. Thus there is a need to develop authentic models of the human disease in relevant *in vitro* and *ex vivo* cell culture and *in vivo* animal models and to apply these models to evaluate candidates. This process has been facilitated by the publication of the Animal Rule by the US Food and Drug Agency in 2002, through which a number of antibiotics have recently been approved for inhalational anthrax or plague indications, as have therapies for botulism and anthrax and a next generation vaccine for smallpox. More details about this can be found in the review by E. D. Williamson.

Biodefense agents are dangerous pathogens that pose unique challenges for researchers who often have to work at high biocontainment (levels 3 and 4) making routine experiments difficult to perform. By using various "state of the art" techniques such as optical imaging, biophotonic imaging, next generation sequencing, and microarrays, data derived from each experiment are greatly enhanced and the study of the host response to infection significantly improved. Recent progress using these "omic" and imaging technologies in biodefense research is reviewed by J. A. Tree et al.

Biodefense research benefits from improving and enhancing the utility of specific animal models. In this issue, M. Nelson and M. Loveday describe how they explored the innate immunological response of the common marmoset (*Callithrix jacchus*) to bacterial challenge. The immune response of this nonhuman primate is often understudied because of a lack of reagents. However, M. Nelson and M. Loveday examined the cross-reactivity of commercially available human reagents with marmoset markers and showed that it was possible to characterise the marmoset immune response to infectious disease in terms of phenotype, cell activation status, and key cytokine and chemokine expression. This is particularly useful because there is an increasing body of evidence that suggests that the physiological and immunological responses to biological agents are similar between marmosets and humans.

Progress in the approval of candidate vaccines and therapies is supported by ongoing research which improves the collective understanding of the pathogenesis of disease; two papers in this issue support this area. J. L. Dankmeyer et al. present results about the innate host response to *Yersinia pestis*. They suggest that Toll-like receptor 4 and the adaptor protein Myd88 are important for an optimal antibody response to the subunit F1-V plague vaccine and that Myd88 also appears to be required for protection against a lethal

challenge in vaccinated mice. S. L. Newstead et al. describe the role of nitric oxide in the control of intracellular infection with *F. tularensis*. They infected two murine macrophage cell lines and demonstrated a differential ability to control the intracellular replication of the attenuated live vaccine strain of *F. tularensis* compared with the fully virulent SCHU S4 strain. Some control of SCHU S4 replication was achieved by preactivation of macrophages, indicating the involvement of factors additional to NO production in this effect.

In order for medical countermeasures to be licensed using the Animal Rule there is a need to bridge human immune responses to the animal models to identify surrogate markers of efficacy. This process is highlighted in the research paper modelling pneumonic plague, by V. A. Graham et al., in which an optimised murine model is described. Serum taken from human volunteers vaccinated with a new acellular plague vaccine (containing recombinant proteins rF1 and rV) was assessed for protective efficacy by passive transfer into mice. Mice were subsequently exposed to a lethal aerosol of plague and the delay in mean time-to-death measured. This process was shown to be reproducible and these data indicated that Hsd:NIHS mice may be a better model than BALB/c mice for passive transfer studies with human serum.

The last two papers in this special issue describe research on a generic DNA vaccination approach and a potential immunotherapy treatment for Ebola. S. Qiu and colleagues constructed DNA and recombinant Tiantan vaccinia (rTTV) vaccines encoding OVA-CTB fusion protein. They concluded that, following studies in mice, using an intranasal DNA prime and intramuscular recombinant-vaccinia boost, that fusion-expressed CTB could serve as a potent adjuvant to enhance both systemic and mucosal T-cell responses. S. Dowall et al. describe early studies using *in vitro* models to investigate potential targets for immunomodulatory therapy during infection with the highly infectious Ebola virus. They showed binding of the phosphatidylserine-targeting antibody (bavituximab), which has already progressed through clinical trials (phases I-III) for treatment of tumours, to the surface of host cells infected with Ebola and also to purified Ebola virions. Assessing immune therapies for other indications has the potential to allow repurposing of products for treatment of biodefence agents, potentially saving significantly on research and development time and costs.

In conclusion, this special issue has surveyed a diverse range of approaches to the development of biodefence vaccines and therapies and has explored the likely impact and application to the field of exciting new technological developments.

Julia A. Tree
E. Diane Williamson
Caroline A. Rowland
Louise M. Pitt

Hindawi Publishing Corporation
Journal of Immunology Research
Volume 2015, Article ID 347903, 9 pages
http://dx.doi.org/10.1155/2015/347903

Research Article

Effective Binding of a Phosphatidylserine-Targeting Antibody to Ebola Virus Infected Cells and Purified Virions

S. D. Dowall,[1] V. A. Graham,[1] K. Corbin-Lickfett,[2] C. Empig,[2] K. Schlunegger,[2] C. B. Bruce,[1] L. Easterbrook,[1] and R. Hewson[1]

[1]*Public Health England, Porton Down, Wiltshire, Salisbury SP4 0JG, UK*
[2]*Peregrine Pharmaceuticals, Inc., Tustin, CA 92780, USA*

Correspondence should be addressed to S. D. Dowall; stuart.dowall@phe.gov.uk

Received 25 February 2014; Revised 20 June 2014; Accepted 3 September 2014

Academic Editor: Caroline Rowland

Ebola virus is responsible for causing severe hemorrhagic fevers, with case fatality rates of up to 90%. Currently, no antiviral or vaccine is licensed against Ebola virus. A phosphatidylserine-targeting antibody (PGN401, bavituximab) has previously been shown to have broad-spectrum antiviral activity. Here, we demonstrate that PGN401 specifically binds to Ebola virus and recognizes infected cells. Our study provides the first evidence of phosphatidylserine-targeting antibody reactivity against Ebola virus.

1. Introduction

The family Filoviridae includes two genera, *Ebolavirus* and *Marburgvirus*. The genus *Ebolavirus* includes five species (*Bundibugyo ebolavirus*, *Reston ebolavirus*, *Sudan ebolavirus*, *Taï Forest ebolavirus*, and *Zaire ebolavirus*). *Ebolavirus* strain Ebola (EBOV) is the only member of the *Zaire* species of *Ebolavirus* [1, 2]. EBOV first came to medical attention in 1976 with a disease outbreak in Zaire (now Democratic Republic of Congo (DRC)) [3]. Sporadic outbreaks of Ebola virus disease have occurred naturally since then, sometimes characterised by large epidemics, for example, in the town of Kikwit, DRC, in 1995 (315 cases and 244 deaths) [4]. Since 2001 epidemics have been occurring with increasing frequency which may be related to the increasing encroachment of human beings on tropical rain forests and once-isolated rural villages [5].

Human EBOV infection results in high lethality. Indeed, case-fatality rates of the African EBOV are as high as 90%, with no prophylaxis or treatment available. Consequently the virus is classified as a Risk Group 4 agent, mandating the use of high containment laboratory infrastructure for work with infectious materials. Further classification as a Category A Priority Pathogen by the US NIH/NIAID reflects concern of its potential use as a bioweapon [6]. New therapeutic strategies against EBOV infection are urgently required. Currently these range from antisense technology (chemically modified antisense oligonucleotides that interfere with the translation of viral mRNA) [7, 8] to therapeutic antibodies against specific EBOV proteins [9–11]. While these therapies rely on viral specific interactions, an alternative host-targeted antibody therapy enabling a broader viral specificity has recently gained favour. Bavituximab (PGN401) is a monoclonal human-mouse chimeric antibody. The Fv region was obtained from the mouse IgG3 monoclonal antibody 3G4 specific towards phosphatidylserine (PS) [12] which was subsequently joined to human IgG1κ constant regions [13]. In healthy cells, PS resides predominantly in the inner leaflet of the plasma membrane, where it is inaccessible to circulating antibodies, but translocates to the outer leaflet and externalizes upon cell injury or death [14]. Surface exposure of PS is then accompanied by cell death through apoptosis [15], mediated in part through recognition by T cell immunoglobulin mucin proteins [16]. PS exposure is now accepted as a ubiquitous phenomenon of apoptosis that is independent of cell type and the cell death-inducing trigger [17]. PGN401 was primarily used in mouse models of cancer, which have tumor vasculature with PS expression on endothelial cells [18]. It appears that 3G4 does not bind PS directly but through complexes of the PS-binding plasma protein β2-glycoprotein 1 (β2GP1) [19]. The antibody binds

to PS-expressing membranes by crosslinking two molecules of β2GP1 bound to PS on the membrane [19]. PGN401 has successfully completed several clinical trials, including Phase I in patients with advanced solid tumors [20] and Phase II in patients with advanced breast cancer and non-small cell lung cancer (NSCLC) [13]. It is now entering Phase III trials for NSCLC [21]. Therefore, PGN401 is known to be safe in human studies and the pharmacokinetics of the antibody has been studied.

Surface exposure of PS antigen is also a consequence of viral infection through virus-induced apoptosis events. These also result in a loss of lipid asymmetry due to the translocation of PS from the inner to the outer layer of the infected cells' plasma membrane [22]. Antibodies binding the exposed PS appear to limit viral infection by initiating the removal of enveloped viruses from the bloodstream through the induction of antibody-dependent cellular cytotoxicity (ADCC) which ultimately eliminates virus infected cells [22, 23]. Whilst PS relocation is not the final step in apoptosis, cells expressing it are still likely to be actively producing virus so opsonizing them for ADCC may limit or slow the progression of infection. Major advantages of PGN401 over other antibody treatments against EBOV include specificity for infected cells and independence of virus escape mutations [24]. Antibodies are also attractive anti-infective therapeutics due to their exquisite specificity and their ability to recruit additional immune system components such as complement and natural killer cells, facilitating pathogen inactivation and removal [22]. Most of the antiviral work with PGN401 has been undertaken with hepatitis C virus [25] and has extended to clinical trials [26, 27]. In 2008, Soares et al. reported the efficacy of PGN401 in guinea pigs infected with Pichindé virus [23], a model that closely resembles Lassa fever in humans [28]. Therefore, it was hypothesized that PGN401 may also have therapeutic potential for other hemorrhagic fever viruses. In this report, we evaluate the *in vitro* efficacy of PGN401 to bind to EBOV virions and EBOV-infected cells.

2. Methods

2.1. Virus. EBOV isolate ME718 was used in this work. This was originally isolated during an outbreak in October 1976 [3] in Yambuku, Mongala Province, in what is currently the northern Democratic Republic of the Congo, and simultaneously reported in three publications [29–31]. Virus stocks used for this work were grown in VeroE6 cells (European Collection of Cell Cultures, UK) cultured in Leibovitz's L15 (L15) media containing 5% fetal calf serum (FCS), and aliquots were stored at −80°C. Virus titres were determined by 100-fold dilution with L15 media without any FCS added. 100 μL of each dilution was overlaid onto semiconfluent cell monolayers in four replicate 12.5 cm^2 tissue culture flasks and left to adsorb for 1 hour. A volume of 5 mL media was then added and cells were incubated at 37°C for 6-7 days. Cytopathic effects were observed using microscopy, and the results from each dilution were used to calculate 50% tissue culture infective dose ($TCID_{50}$) using the Reed-Muench method [32].

2.2. Flow Cytometry Assay. VeroE6 cells in 12.5 cm^2 tissue culture flasks were infected with EBOV at a multiplicity of infection (MOI) of approximately 0.5. After five days of infection, the media were removed and the cell monolayer washed with phosphate buffered saline (PBS). For staining with PGN401, the antibody was used at a concentration of 1 μg/mL in flow cytometry buffer consisting of 10 mM HEPES pH 7.4 (Sigma, UK), 140 mM NaCl (Sigma, UK), and 2.5 mM $CaCl_2$ (Sigma, UK) with 50% FCS (Invitrogen, UK). To each flask, 1 mL antibody suspension was added and left on ice for 30 minutes. Unbound antibody was removed by washing with PBS, and cells detached using TrypLE Express solution (Invitrogen, UK) with incubation at 37°C to aid enzymatic activity. Once detached, the cell suspension was transferred to cell culture tubes used for flow cytometry staining. Cells were washed twice with flow cytometry buffer by addition of 2 mL buffer and centrifugation at 400 ×g for 5 minutes. Anti-EBOV antibody (clone FE25, Lifespan Biosciences, USA) was diluted to 100 μg/mL in flow cytometry buffer containing 50% FCS, and 100 μL was added to each cell pellet. Tubes were incubated on ice for 30 minutes to allow binding. Unbound antibody was removed by washing twice with flow cytometry buffer as previously described. Secondary antibody consisted of Alexa-Fluor 647 goat anti-human IgG (Invitrogen, UK) or Alexa-Fluor 488/647 goat anti-mouse IgG (Invitrogen, UK) for detection of the PGN401 and anti-EBOV antibodies, respectively. Secondary antibody was diluted at 1 : 400 with flow cytometry buffer containing 50% FCS, and 100 μL of the appropriate antibody was added to each tube. Tubes were incubated on ice for 30 minutes to allow binding to occur. Unbound antibody was removed by washing twice with flow cytometry buffer as previously described. Cell pellets were fixed in flow cytometry fixation buffer that contained 4% paraformaldehyde (eBioscience, UK). Tubes were fumigated overnight with formalin vapor before removal from the CL4 laboratory. Samples were run on a Beckman Coulter FC500 flow cytometer and analyzed using Cytomics CXP software. Cells were gated using a forward scatter/side scatter density plot. Binding of Alexa Fluor 488 and 647 antibodies was determined by a histogram of fluorescence from the FL1 and FL4 channels, respectively. For dual color staining, a quadrant plot was created to identify single- and dual-labeled cells.

2.3. Immunofluorescence Assay. VeroE6 cells (European Collection of Cell Cultures, UK) were cultured on 8-well LabTek II chamber slides (Thermo Scientific Nunc, UK) and infected with EBOV for 5 days. Antibody preparations of PGN401 and a positive anti-EBOV monoclonal antibody control (clone FE25, Abcam, UK) were diluted with PBS to a concentration of 100 μg/mL before 500 μL was added to the relevant chambers of the slide. PBS alone and isotype antibodies (Erbitux and mouse IgG2a (Abcam, UK)) were used as negative controls. After 1 hour at 37°C the cells were washed 3 times by immersion in PBS and dried. For detection, Alexa Fluor 488-conjugated anti-mouse or anti-human antibody (Invitrogen, UK) was diluted at 1 : 400 and used at 500 μL per well. After 1 hour at 37°C the cells were washed 3 times with PBS and dried. Slides were fixed with a 4%

formaldehyde solution before removal from the Containment Level 4 laboratory. Cells were microscopically observed using an EVOS FL imaging system using a GFP imaging cube (Life Technologies, UK).

2.4. ELISA Assay. For coating with live EBOV virions, fluid from infected cultures were clarified by centrifugation at 400 ×g for 10 minutes. The supernatant fluid was transferred onto sucrose solution (20% sucrose in TH buffer) and particles were purified by ultracentrifugation at 25,500 rpm at 4°C in a SW28 rotor (Beckman Coulter, UK). The sucrose cushion and supernatant fluid was discarded and the pellet air-dried for 10 minutes before resuspending in 3 mL PBS. A 660 nm protein assay (Thermo Scientific Pierce, UK) was used to determine the protein concentration in the purified stocks. Stocks were diluted with PBS to a concentration of 10 μg/mL and 100 μL added to wells of a microplate (Immulon 1B, VWR, UK). For a virus negative control, PBS alone was added. Plates were left overnight at 4°C to allow binding to occur. For coating with PS, hexane solvent (Sigma, UK) was used to dilute PS to a concentration of 5 μg/mL and 100 μL added per well of the microplate. For an antigen negative control, hexane alone was added. Plates were incubated at room temperature in a fume cabinet until the hexane had evaporated and the plates were dry. To assess binding to EBOV glycoprotein, recombinant *Zaire ebolavirus* glycoprotein minus the transmembrane region (rZEBOV GPdTM, IBT Bioservices, US) was diluted to 1 μg/mL with carbonate-bicarbonate buffer (Sigma, UK) and 100 μL added per well of a microplate. To remove unbound antigen, plates were washed with five washes of 200 μL PBS per well. To each well, 200 μL of protein-free blocking buffer (PFBB, Pierce, UK) was added and incubated for 30 minutes at 37°C. Blocking buffer was removed by washing five times with PBS. Dilutions of PGN401 were made in low-binding microplates (Corning, UK) with binding buffer, consisting of 10% dialyzed FCS (Invitrogen, UK) in PBS, before 100 μL was transferred across into the assay plate. Erbitux was used as a non-PS binding isotype control antibody [33]. Mouse anti-ZEBOV GP mAb (clone 4F3, IBT Bioservices, US) was used as a positive control for binding to the recombinant glycoprotein. Plates were incubated for 1-2 hours at 37°C to allow antibody binding to occur. Unbound antigen was removed by washing five times with PBS. Secondary antibody consisted of HRP-conjugated goat anti-human IgG (Jackson ImmunoResearch, USA) diluted at 1 : 2500 in binding buffer, with 100 μL added per well. Plates were left for 1 hour at 37°C before unbound antibody was removed by washing five times with PBS. 3,3′,5,5′-Tetramethylbenzidine (TMB) substrate (Insight Biotechnology, UK) was added to each well at a volume of 100 μL and left for 15 minutes at room temperature to allow the colorimetric reaction to occur. The reaction was stopped by addition of 100 μL of 2 M H_2SO_4 (Fisher Scientific, UK). Absorbances were read by an automated plate spectrometer at a wavelength of 450 nm within 30 minutes of adding the stop solution and analyzed using SoftMax Pro software (Molecular Devices, UK). Data were plotted on a line graph as absorbance at 450 nm *versus* antibody concentration in a log ng/mL scale.

3. Results

3.1. PGN401 Specifically Binds to Cells Infected with EBOV. VeroE6 cells that had been infected with Ebola Zaire virus at a multiplicity of infection (MOI) of approximately 0.5 for five days were used to determine recognition by PGN401 antibody. Staining with an anti-EBOV antibody (clone FE25) showed 9% of cells were specifically labeled (Figure 1(a)). With the PGN401 antibody, 13.5% of cells were specifically stained, compared with 0% for the Erbitux isotype control antibody. This result was repeatable, with a second experiment showing 21.4%, 21.1%, and 0% staining for anti-EBOV, PGN401, and Erbitux, respectively. Dual-colour labeling was used to determine whether the same cells that were stained with the anti-EBOV antibody were also those that PGN401 bound. Results demonstrated that the PGN401 bound to cells to which anti-EBOV antibody was also binding (Figure 1(b)). To support this observation, immunofluorescence testing was conducted using cells infected with EBOV. Results showed specific binding to EBOV-infected cells by the PGN401 and positive control anti-EBOV antibodies with no staining observed with the negative control and isotype antibodies (Figure 2). The immunofluorescence assay was run on two separate occasions and successfully demonstrated that the results were repeatable.

3.2. PGN401 Binds to Purified Ebola Zaire Virions. Concentrated EBOV was used as an antigen to evaluate binding of PGN401 directly to the virus. A quantitative assay on the ultracentrifuged stocks demonstrated an increase in viral titre of approximately 4 logs, from $10^{7.73}$ in the unconcentrated stock to $10^{11.6}$ $TCID_{50}$/mL. A protein quantification assay demonstrated that the concentrated stock contained 620 μg/mL which was then diluted for use in the ELISA studies. Results showed that PGN401 bound specifically to EBOV virus, with no background binding to PBS buffer alone (Figures 3(a) and 3(b)). Under conditions of antigen excess, PGN401 recognition of EBOV in ELISA was equivalent to monoclonal antibody recognition of PS (Figure 3(c)). A further ELISA experiment was conducted using recombinant EBOV glycoprotein to ascertain whether the PGN401 recognized this viral protein. Results showed that PGN401 did not bind to the glycoprotein (Figure 4(a)) whereas the positive control antibody did (Figure 4(b)). All ELISA experiments were repeated at least twice in order to confirm the results achieved.

4. Discussion

The data presented in this study clearly demonstrate that PGN401 has strong binding properties for EBOV virions and EBOV-infected cells. The attachment of the antibody to EBOV virions is indicative of PS being present on the EBOV membrane. Previous studies have shown that PS enhances receptor independent virus entry mechanisms [34]. Additionally, PS found on the surface of the vaccinia virus membrane has been shown to trigger the signaling, blebbing, and macropinocytic event, suggesting that the virus uses an

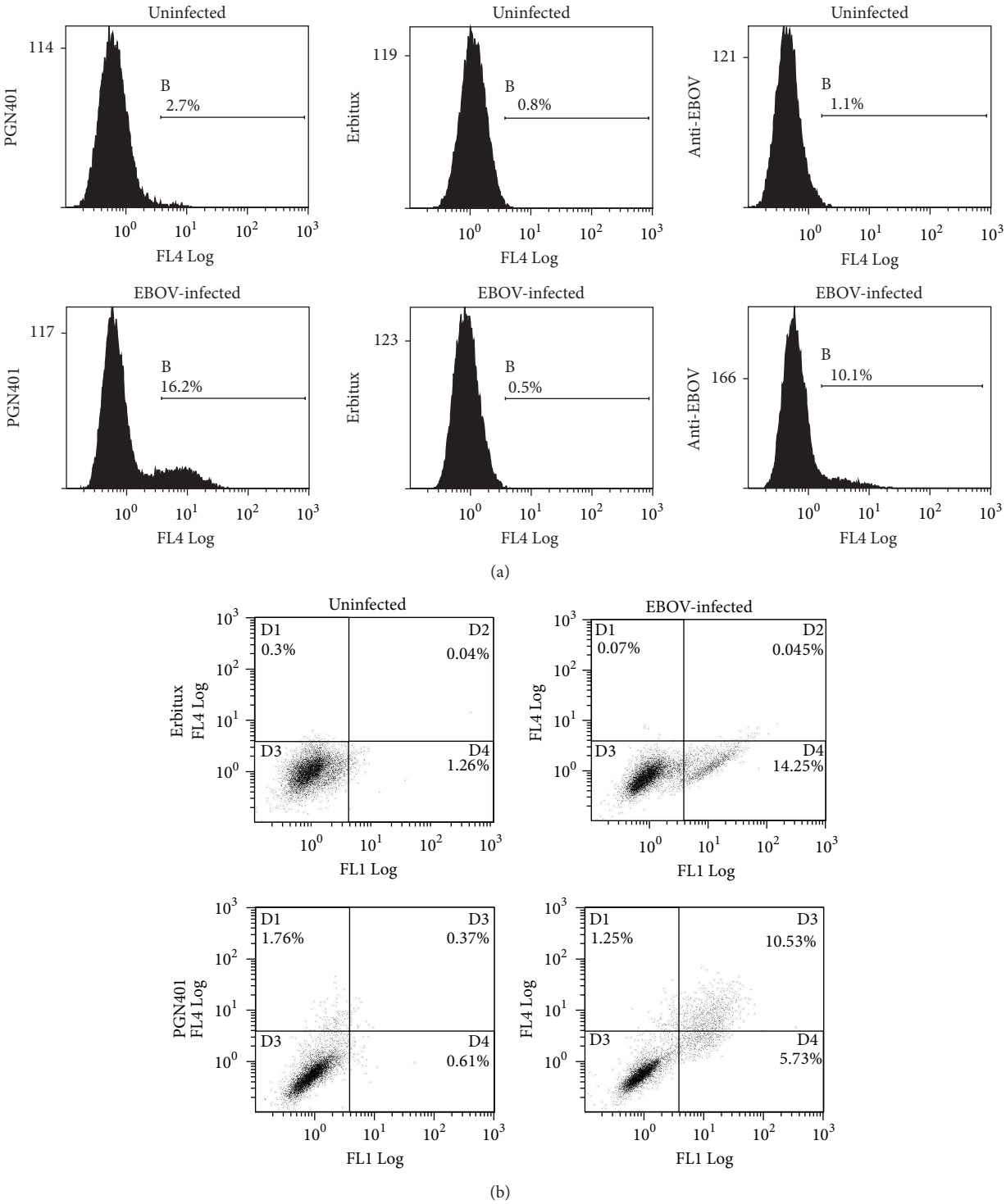

Figure 1: Flow cytometry staining of EBOV-infected cells. (a) Single color staining of cells with anti-EBOV, Erbitux, and PGN401 antibodies. Histograms show frequency of cells versus level of fluorescence intensity. The marker regions quantify the percentage of cells stained above background levels. (b) Dual color labeling with anti-EBOV and PGN401 antibodies. The x-axis relates to the detection of the FL1 channel that detects Alexa-Fluor 488 staining (anti-mouse detector for EBOV antibody) and the y-axis, the FL4 channel that detects Alexa Fluor 647 staining (anti-human detector for PGN401 and Erbitux). Quadplots identify the percentage of cells within each region.

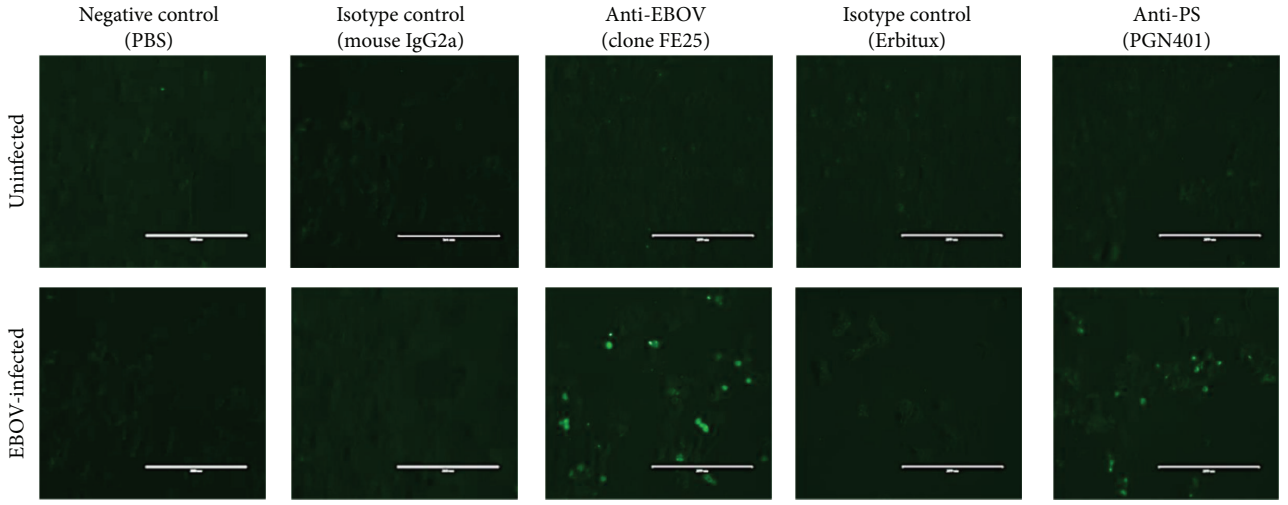

Figure 2: Immunofluorescence staining of uninfected and EBOV-infected cells after staining with antibodies against EBOV (clone FE25), PS (PGN401), and isotype antibodies. Scale bar indicates 200 nm.

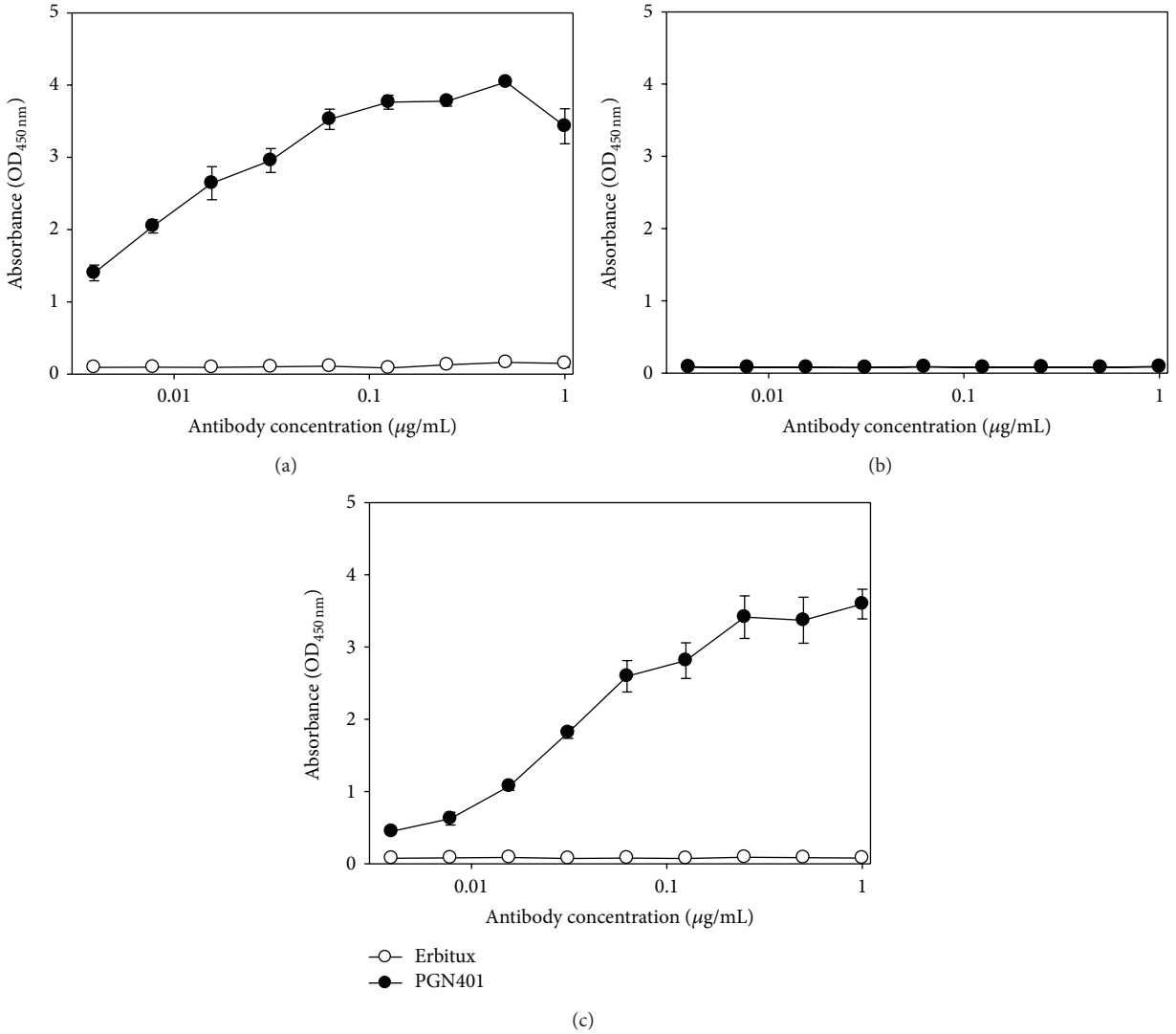

Figure 3: Binding of Erbitux and PGN401 antibodies to plates coated with (a) EBOV, (b) PBS, or (c) PS antigen using a twofold dilution series starting at 1 μg/mL. Binding levels were assessed by measurement of absorbance at a wavelength of 450 nm. Data points show mean values from three replicate wells with error bars denoting standard error.

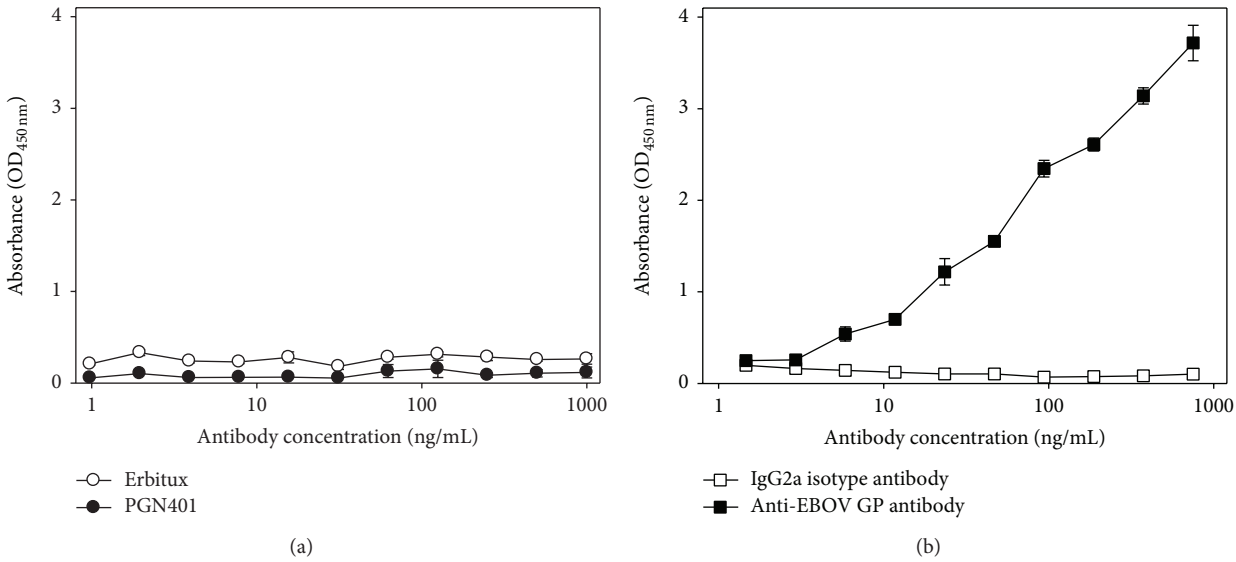

Figure 4: Binding of antibodies to recombinant EBOV glycoprotein. (a) Erbitux and PGN401 antibodies. (b) Polyclonal anti-EBOV glycoprotein antibody and IgG2a isotype control. Data points show mean values from three replicate wells with error bars denoting standard error.

entry mechanism based on mimicry of apoptotic bodies [35]. Apoptotic mimicry provides a route for virus uptake and may also help in the evasion of immune recognition; it has also been observed for hepatitis B virus [36], Lassa fever virus [23], and HIV-1 [37]. Entry via macropinocytosis offers the advantage to the virus of not being exposed to the full range of the immune system, thus delaying immune recognition of the infected cells [35]. In addition, macropinocytic entry gives viruses the mechanisms to broaden their host range and tissue specificity [35]. Many enveloped viruses that bud out from the plasma membrane are assembled in, and bud out of, lipid rafts [38]. This includes EBOV [39]. The lipid rafts are enriched with PS [40] and are structurally modified during apoptosis and are involved with the externalization of PS [41]. Other viruses that are believed to egress from rafts include HIV-1 [42], influenza A virus [43], vesicular stomatitis virus [44], Marburg virus [39], and respiratory syncytial virus [45]. Previous studies have also documented that macropinocytosis is used by EBOV for cell entry [46–48]. Therefore, our results further confirm these findings.

The current studies utilized the VeroE6 cell line as a simple, straightforward, and permissive host *in vitro*. To test for PGN401 binding, we chose the furthest time point from infection before cytopathic effect was observed in order to allow reasonable time for PS to become exposed on the cell surface. Previous studies have shown induction of PS translocation occurs relatively soon after apoptosis [49]. In follow-on studies we aim to detail these findings with the use of primary cells such as macrophages and dendritic cells which are natural targets for EBOV infection [50, 51]; these will also provide the opportunity to specify the postinfection time points when PS becomes exposed on these natural cellular targets. We have assessed the binding of PGN401 independently using two different techniques, flow cytometry, and immunofluorescence. However, the binding of PGN401 to purified virions has only been conducted by ELISA and we are not able to rule out nonspecific binding to impurities in the virus preparation. Nevertheless, this material was purified through a 20% sucrose cushion and there was no evidence of sample degradation which often accompanies the coconcentration of other proteins. Thus we are confident that PGN401 binds PS of EBOV virions.

The mechanism of action of PGN401 is not fully understood. In the elimination of Pichindé virus infection and viremia in the guinea pig model, PGN401 is thought to function via at least two different mechanisms. Firstly, it caused opsonization and clearance of infectious virus from the bloodstream, leaving less virus to infect other tissues and secondly, it induces ADCC of virus infected cells [23]. Other mechanisms by which an antibody may neutralize pathogenic material can include antibody-dependent cellular phagocytosis, complement-dependent cytotoxicity, opsonization, and steric hindrance of ligand activity, almost all of which require the antibody Fc region to interact with cellular receptors [52, 53]. Triggering via the Fc receptor of IgG has also been reported to stimulate chemokine release from natural killer cells, monocytes, and dendritic cells [54–56]. The efficiency of PGN401 may be enhanced by adding extra target molecules to the antibody. For example, adding interleukin (IL)-2 has been shown to enhance immunogenicity of a PS-targeting antibody for use as a breast cancer vaccine [57]. Another option may be to use the antibodies to deliver radionuclides that emanate lethal doses of cytotoxic radiation to target cells [58].

This study has shown that the PS-targeting antibody, PGN401, binds to EBOV-infected cells and to purified EBOV virions. Due to PGN401 having been used for several human clinical trials in cancer, from Phase I to III [13, 20, 21], its repurposing of use for filovirus therapy through licensure or emergency use may present an attractive option.

Due to the anticipated small market size of any antifiloviral treatment, the use of therapies primarily designed for other conditions confers several advantages in reducing the costs of bringing an effective treatment to clinical use due to having already negotiated some of the steps required for regulatory approval. Future work to determine whether this approach elucidates any protective effect using *in vivo* models of EBOV infection is planned.

Conflict of Interests

K. Corbin-Lickfett, C. Empig, and K. Schlunegger are employees of Peregrine Pharmaceuticals, Inc. Peregrine is developing PGN401 and related antibodies as therapeutics for cancer and infectious diseases. The remaining authors declare that there is no conflict of interests regarding the publication of this paper.

Acknowledgments

This work was supported by the Transformational Medical Technologies Program Contract HDTRA1-08-C-003 from the Department of Defense Chemical and Biological Defense Program through the Defense Threat Reduction Agency (DTRA). The views expressed in this publication are those of the authors and not necessarily those of the funding or participant organizations. The authors would like to thank the CL4 staff at the Defence Science and Technology Laboratory (DSTL) for technical assistance in the preparation of concentrated viral stocks for the ELISA assay..

Acknowledgments

This work was supported by the Transformational Medical Technologies Program Contract HDTRA1-08-C-003 from the Department of Defense Chemical and Biological Defense Program through the Defense Threat Reduction Agency (DTRA). The views expressed in this publication are those of the authors and not necessarily those of the funding or participant organizations. The authors would like to thank the CL4 staff at the Defence Science and Technology Laboratory (DSTL) for technical assistance in the preparation of concentrated viral stocks for the ELISA assay.

References

[1] M. J. Adams and E. B. Carstens, "Ratification vote on taxonomic proposals to the international committee on taxonomy of viruses (2012)," *Archives of Virology*, vol. 157, no. 7, pp. 1411–1422, 2012.

[2] J. H. Kuhn, S. Becker, H. Ebihara et al., "Proposal for a revised taxonomy of the family *Filoviridae*: classification, names of taxa and viruses, and virus abbreviations," *Archives of Virology*, vol. 155, no. 12, pp. 2083–2103, 2010.

[3] WHO, "Ebola haemorrhagic fever in Zaire, 1976: report of an international commission," *Bulletin of the World Health Organization*, vol. 56, no. 2, pp. 271–293, 1978.

[4] E. M. Leroy, J.-P. Gonzalez, and S. Baize, "Ebola and Marburg haemorrhagic fever viruses: Major scientific advances, but a relatively minor public health threat for Africa," *Clinical Microbiology and Infection*, vol. 17, no. 7, pp. 964–976, 2011.

[5] N. D. Wolfe, A. T. Prosser, J. K. Carr et al., "Exposure to nonhuman primates in rural Cameroon," *Emerging Infectious Diseases*, vol. 10, no. 12, pp. 2094–2099, 2004.

[6] L. Borio, T. Inglesby, C. J. Peters et al., "Hemorrhagic fever viruses as biological weapons: medical and public health management," *The Journal of the American Medical Association*, vol. 287, no. 18, pp. 2391–2405, 2002.

[7] T. W. Geisbert, A. C. Lee, M. Robbins et al., "Postexposure protection of non-human primates against a lethal Ebola virus challenge with RNA interference: a proof-of-concept study," *The Lancet*, vol. 375, no. 9729, pp. 1896–1905, 2010.

[8] T. K. Warren, K. L. Warfield, J. Wells et al., "Advanced antisense therapies for postexposure protection against lethal filovirus infections," *Nature Medicine*, vol. 16, no. 9, pp. 991–994, 2010.

[9] J. M. Dye, A. S. Herbert, A. I. Kuehne et al., "Postexposure antibody prophylaxis protects nonhuman primates from filovirus disease," *Proceedings of the National Academy of Sciences of the United States of America*, vol. 109, no. 13, pp. 5034–5039, 2012.

[10] G. G. Olinger Jr., J. Pettitt, D. Kim et al., "Delayed treatment of Ebola virus infection with plant-derived monoclonal antibodies provides protection in rhesus macaques," *Proceedings of the National Academy of Sciences of the United States of America*, vol. 109, no. 44, pp. 18030–18035, 2012.

[11] X. Qiu, J. Audet, G. Wong et al., "Successful treatment of ebola virus-infected cynomolgus macaques with monoclonal antibodies," *Science Translational Medicine*, vol. 4, no. 138, Article ID 138ra81, 2012.

[12] S. Ran, J. He, X. Huang, M. Soares, D. Scothorn, and P. E. Thorpe, "Antitumor effects of a monoclonal antibody that binds anionic phospholipids on the surface of tumor blood vessels in mice," *Clinical Cancer Research*, vol. 11, no. 4, pp. 1551–1562, 2005.

[13] P. E. Thorpe, "Targeting anionic phospholipids on tumor blood vessels and tumor cells," *Thrombosis Research*, vol. 125, supplement 2, pp. S134–S137, 2010.

[14] K. Schutters and C. Reutelingsperger, "Phosphatidylserine targeting for diagnosis and treatment of human diseases," *Apoptosis*, vol. 15, no. 9, pp. 1072–1082, 2010.

[15] M. O. Hengartner, "The biochemistry of apoptosis," *Nature*, vol. 407, no. 6805, pp. 770–776, 2000.

[16] N. Kobayashi, P. Karisola, V. Peña-Cruz et al., "TIM-1 and TIM-4 glycoproteins bind phosphatidylserine and mediate uptake of apoptotic cells," *Immunity*, vol. 27, no. 6, pp. 927–940, 2007.

[17] S. J. Martin, D. M. Finucane, G. P. Amarante-Mendes, G. A. O'Brien, and D. R. Green, "Phosphatidylserine externalization during CD95-induced apoptosis of cells and cytoplasts requires ICE/CED-3 protease activity," *The Journal of Biological Chemistry*, vol. 271, no. 46, pp. 28753–28756, 1996.

[18] X. Huang, M. Bennett, and P. E. Thorpe, "A monoclonal antibody that binds anionic phospholipids on tumor blood vessels enhances the antitumor effect of docetaxel on human breast tumors in mice," *Cancer Research*, vol. 65, no. 10, pp. 4408–4416, 2005.

[19] T. A. Luster, J. He, X. Huang et al., "Plasma protein β-2-glycoprotein 1 mediates interaction between the anti-tumor monoclonal antibody 3G4 and anionic phospholipids on endothelial cells," *The Journal of Biological Chemistry*, vol. 281, no. 40, pp. 29863–29871, 2006.

[20] D. E. Gerber, A. T. Stopeck, L. Wong et al., "Phase I safety and pharmacokinetic study of bavituximab, a chimeric phosphatidylserine-targeting monoclonal antibody, in patients with advanced solid tumors," *Clinical Cancer Research*, vol. 17, no. 21, pp. 6888–6896, 2011.

[21] J. M. Reichert, "Antibodies to watch in 2014: mid-year update," *MAbs*, vol. 6, no. 4, pp. 799–802, 2014.

[22] J. C. Pai, J. N. Sutherland, and J. A. Maynard, "Progress towards recombinant anti-infective antibodies," *Recent Patents on Anti-Infective Drug Discovery*, vol. 4, no. 1, pp. 1–17, 2009.

[23] M. M. Soares, S. W. King, and P. E. Thorpe, "Targeting inside-out phosphatidylserine as a therapeutic strategy for viral diseases," *Nature Medicine*, vol. 14, no. 12, pp. 1357–1362, 2008.

[24] H. M. Mir, A. Birerdinc, and Z. M. Younossi, "Monoclonal and polyclonal antibodies against the HCV envelope proteins," *Clinics in Liver Disease*, vol. 13, no. 3, pp. 477–486, 2009.

[25] N. Sakamoto and M. Watanabe, "New therapeutic approaches to hepatitis C virus," *Journal of Gastroenterology*, vol. 44, no. 7, pp. 643–649, 2009.

[26] A. Tomillero and M. A. Moral, "Gateways to clinical trials," *Methods and Findings in Experimental and Clinical Pharmacology*, vol. 30, no. 8, pp. 643–672, 2008.

[27] A. Tomillero and M. A. Moral, "Gateways to clinical trials," *Methods and Findings in Experimental and Clinical Pharmacology*, vol. 30, no. 7, pp. 543–588, 2008.

[28] P. B. Jahrling, R. A. Hesse, J. B. Rhoderick, M. A. Elwell, and J. B. Moe, "Pathogenesis of a pichinde virus strain adapted to produce lethal infections in guinea pigs," *Infection and Immunity*, vol. 32, no. 2, pp. 872–880, 1981.

[29] E. T. Bowen, G. Lloyd, W. J. Harris, G. S. Platt, A. Baskerville, and E. E. Vella, "Viral haemorrhagic fever in southern Sudan and northern Zaire. Preliminary studies on the aetiological agent," *The Lancet*, vol. 1, no. 8011, pp. 571–573, 1977.

[30] K. M. Johnson, P. A. Webb, J. V. Lange, and F. A. Murphy, "Isolation and partial characterisation of a new virus causing acute haemorrhagic fever in Zaire," *The Lancet*, vol. I, no. 8011, pp. 569–571, 1977.

[31] S. Pattyn, W. Jacob, and G. van der Groen, "Isolation of Marburg like virus from a case of haemorrhagic fever in Zaire," *The Lancet*, vol. 1, no. 8011, pp. 573–574, 1977.

[32] L. J. Reed and H. Muench, "A simple method of estimating fifty per cent endpoints," *The American Journal of Epidemiology*, vol. 27, no. 3, pp. 493–497, 1938.

[33] W. Bou-Assaly and S. Mukherji, "Cetuximab (erbitux)," *American Journal of Neuroradiology*, vol. 31, no. 4, pp. 626–627, 2010.

[34] D. A. Coil and A. D. Miller, "Enhancement of enveloped virus entry by phosphatidylserine," *Journal of Virology*, vol. 79, no. 17, pp. 11496–11500, 2005.

[35] J. Mercer and A. Helenius, "Apoptotic mimicry: phosphatidylserine-mediated macropinocytosis of vaccinia virus," *Annals of the New York Academy of Sciences*, vol. 1209, no. 1, pp. 49–55, 2010.

[36] P. Vanlandschoot and G. Leroux-Roels, "Viral apoptotic mimicry: an immune evasion strategy developed by the hepatitis B virus?" *Trends in Immunology*, vol. 24, no. 3, pp. 144–147, 2003.

[37] M. K. Callahan, P. M. Popernack, S. Tsutsui, L. Truong, R. A. Schlegel, and A. J. Henderson, "Phosphatidylserine on HIV envelope is a cofactor for infection of monocytic cells," *Journal of Immunology*, vol. 170, no. 9, pp. 4840–4845, 2003.

[38] J. A. G. Briggs, T. Wilk, and S. D. Fuller, "Do lipid rafts mediate virus assembly and pseudotyping?" *Journal of General Virology*, vol. 84, part 4, pp. 757–768, 2003.

[39] S. Bavari, C. M. Bosio, E. Wiegand et al., "Lipid raft microdomains: a gateway for compartmentalized trafficking of Ebola and Marburg viruses," *Journal of Experimental Medicine*, vol. 195, no. 5, pp. 593–602, 2002.

[40] L. J. Pike, X. Han, K.-N. Chung, and R. W. Gross, "Lipid rafts are enriched in arachidonic acid and plasmenylethanolamine and their composition is independent of caveolin-1 expression: a quantitative electrospray ionization/mass spectrometric analysis," *Biochemistry*, vol. 41, no. 6, pp. 2075–2088, 2002.

[41] H. Ishii, T. Mori, A. Shiratsuchi et al., "Distinct localization of lipid rafts and externalized phosphatidylserine at the surface of apoptotic cells," *Biochemical and Biophysical Research Communications*, vol. 327, no. 1, pp. 94–99, 2005.

[42] A. Ono and E. O. Freed, "Plasma membrane rafts play a critical role in HIV-1 assembly and release," *Proceedings of the National Academy of Sciences of the United States of America*, vol. 98, no. 24, pp. 13925–13930, 2001.

[43] P. Scheiffele, A. Rietveld, T. Wilk, and K. Simons, "Influenza viruses select ordered lipid domains during budding from the plasma membrane," *Journal of Biological Chemistry*, vol. 274, no. 4, pp. 2038–2044, 1999.

[44] W. F. Pickl, F. X. Pimentel-Muiños, and B. Seed, "Lipid rafts and pseudotyping," *Journal of Virology*, vol. 75, no. 15, pp. 7175–7183, 2001.

[45] G. Brown, H. W. M. Rixon, and R. J. Sugrue, "Respiratory syncytial virus assembly occurs in GM1-rich regions of the host-cell membrane and alters the cellular distribution of tyrosine phosphorylated caveolin-1," *Journal of General Virology*, vol. 83, part 8, pp. 1841–1850, 2002.

[46] P. Aleksandrowicz, A. Marzi, N. Biedenkopf et al., "Ebola virus enters host cells by macropinocytosis and clathrin-mediated endocytosis," *Journal of Infectious Diseases*, vol. 204, supplement 3, pp. S957–S967, 2011.

[47] A. Nanbo, M. Imai, S. Watanabe et al., "Ebolavirus is internalized into host cells via macropinocytosis in a viral glycoprotein-dependent manner," *PLoS Pathogens*, vol. 6, no. 9, Article ID e01121, 2010.

[48] M. F. Saeed, A. A. Kolokoltsov, T. Albrecht, and R. A. Davey, "Cellular entry of ebola virus involves uptake by a macropinocytosis-like mechanism and subsequent trafficking through early and late endosomes," *PLoS Pathogens*, vol. 6, no. 9, Article ID e01110, 2010.

[49] M. Mourdjeva, D. Kyurkchiev, A. Mandinova, I. Altankova, I. Kehayov, and S. Kyurkchiev, "Dynamics of membrane translocation of phosphatidylserine during apoptosis detected by a monoclonal antibody," *Apoptosis*, vol. 10, no. 1, pp. 209–217, 2005.

[50] O. Martinez, L. W. Leung, and C. F. Basler, "The role of antigen-presenting cells in filoviral hemorrhagic fever: gaps in current knowledge," *Antiviral Research*, vol. 93, no. 3, pp. 416–428, 2012.

[51] A. Takada, "Filovirus tropism: cellular molecules for viral entry," *Frontiers in Microbiology*, vol. 3, article 34, 2012.

[52] T. Lehner, "Monoclonal antibodies against micro-organisms," *Current Opinion in Immunology*, vol. 1, no. 3, pp. 462–466, 1988.

[53] L. G. Presta, "Molecular engineering and design of therapeutic antibodies," *Current Opinion in Immunology*, vol. 20, no. 4, pp. 460–470, 2008.

[54] N. Fernández, M. Renedo, C. García-Rodríguez, and M. Sánchez Crespo, "Activation of monocytic cells through Fcγ receptors induces the expression of macrophage-inflammatory protein (MIP)-1α, MIP-1β and RANTES," *The Journal of Immunology*, vol. 169, no. 6, pp. 3321–3328, 2002.

[55] D. N. Forthal, G. Landucci, T. B. Phan, and J. Becerra, "Interactions between natural killer cells and antibody Fc result in enhanced antibody neutralization of human immunodeficiency virus type 1," *Journal of Virology*, vol. 79, no. 4, pp. 2042–2049, 2005.

[56] T. R. D. J. Radstake, R. van der Voort, M. Ten Brummelhuis et al., "Increased expression of CCL18, CCL19, and CCL17 by dendritic cells from patients with rheumatoid arthritis, and regulation by Fc gamma receptors," *Annals of the Rheumatic Diseases*, vol. 64, no. 3, pp. 359–367, 2005.

[57] X. Huang, D. Ye, and P. E. Thorpe, "Enhancing the potency of a whole-cell breast cancer vaccine in mice with an antibody-IL-2 immunocytokine that targets exposed phosphatidylserine," *Vaccine*, vol. 29, no. 29-30, pp. 4785–4793, 2011.

[58] D. E. Milenic, E. D. Brady, and M. W. Brechbiel, "Antibody-targeted radiation cancer therapy," *Nature Reviews Drug Discovery*, vol. 3, no. 6, pp. 488–499, 2004.

Hindawi Publishing Corporation
Journal of Immunology Research
Volume 2014, Article ID 237043, 17 pages
http://dx.doi.org/10.1155/2014/237043

Review Article

The Impact of "Omic" and Imaging Technologies on Assessing the Host Immune Response to Biodefence Agents

Julia A. Tree,[1] Helen Flick-Smith,[2] Michael J. Elmore,[1] and Caroline A. Rowland[2]

[1] *Biodefence and PreClinical Evaluation Group, Public Health England (PHE), Porton Down, Salisbury, Wiltshire, SP5 3NU, UK*
[2] *Biomedical Sciences Department, Defence Science and Technology Laboratory (Dstl), Porton Down, Salisbury, Wiltshire, SP4 0JQ, UK*

Correspondence should be addressed to Caroline A. Rowland; carowland@dstl.gov.uk

Received 15 April 2014; Revised 23 July 2014; Accepted 5 August 2014; Published 16 September 2014

Academic Editor: Louise Pitt

Understanding the interactions between host and pathogen is important for the development and assessment of medical countermeasures to infectious agents, including potential biodefence pathogens such as *Bacillus anthracis*, *Ebola virus*, and *Francisella tularensis*. This review focuses on technological advances which allow this interaction to be studied in much greater detail. Namely, the use of "omic" technologies (next generation sequencing, DNA, and protein microarrays) for dissecting the underlying host response to infection at the molecular level; optical imaging techniques (flow cytometry and fluorescence microscopy) for assessing cellular responses to infection; and biophotonic imaging for visualising the infectious disease process. All of these technologies hold great promise for important breakthroughs in the rational development of vaccines and therapeutics for biodefence agents.

1. Introduction

Understanding host-pathogen interactions is important for the development and assessment of medical countermeasures to infectious agents. The advent of new imaging and "omic" technologies has provided the ability to follow these interactions from whole animal to cellular and molecular levels, enabling a greater understanding of the mechanisms involved; this facilitates the development and refinement of new and existing vaccines and therapeutics. For example, advances in bioimaging provide a noninvasive means of identifying the internal systemic spread of infection in animal models and the impact of a prophylaxis or a therapy on the disease process. This can be combined with the analysis of responses at a cellular level using flow cytometry and microscopy techniques. The use of microarrays has also enhanced our understanding of the host response to infection and provides supportive information to help elucidate the innate and adaptive immune mechanisms essential for protection against pathogens, as well as the virulence mechanisms deployed by the pathogen. Although in its infancy, next generation sequencing also holds great potential for defining host-pathogen interactions. This review will assess the impact of these technologies on the ability to assess the host response and how this has been applied to help progress the development of vaccines and immunotherapies against biodefence agents described in the Centers for Disease Control and prevention (CDC) Select Agent list (http://www.selectagents.gov/). Biodefence agents are dangerous pathogens that require high levels of biocontainment and are relatively less-studied (compared with the majority of public health pathogens) and cases are relatively rare. Therefore, studies to test the efficacy of therapeutics in a healthy population from an endemic area are often not feasible and the use of animal models is essential. This review focuses on the use of these new techniques to help us understand host responses in animal models as well as humans. In this context, both "omic" and imaging technologies hold great promise for important breakthroughs in the rational development of vaccines and therapies.

2. "Omic" Technologies

Traditionally, many immunological studies have focused on examining single immune parameters, such as cytokines, using techniques like ELISA and ELISpot. This approach does not highlight interconnecting pathways that control the immune response when the host encounters an infectious agent. With the emergence of transcriptomic technologies, such as microarray and next-generation sequencing, thousands of parameters of the immune system can be measured at the same time at a genome-wide scale. This allows a systematic, unbiased approach to understand how transcript changes correlate with diverse states of the immune system [1]. This section aims to review the use of microarrays and next-generation sequencing in relation to defining the host response against biodefence agents, vaccines, and therapies.

2.1. Microarrays

2.1.1. DNA Microarrays. A DNA microarray consists of a solid surface, usually a glass microscope slide onto which DNA molecules (probes), in picomolar concentrations, are chemically bonded. The purpose of a microarray is to detect the presence and abundance of labelled nucleic acids (targets) in a biological sample, which will hybridise to the DNA on the array. The level of binding between a probe and its target is quantified by measuring the fluorescence emitted by the hybridized targets when scanned. In the majority of microarray experiments the labelled nucleic acids are derived from the mRNA of a sample or tissue, and so the microarray measures gene expression [2].

Most microarrays are prepared so that they cover the whole genome of a species; however, in the absence of a fully sequenced organism, researchers have used smaller focused arrays designed from publically available gene sequences [3, 4]. Alternatively, whole genome microarrays have been used from related animals to predict immune profiles [5] or new arrays have been constructed using cross-species hybridisation bioinformatics to create probes to unsequenced genes [6]. These kinds of approaches are currently being superseded by the use of next-generation sequence analysis which can generate new sequence information rapidly and accurately. On occasion this information has been used to build new microarray platforms; a successful example of this has been applied to the ferret model of influenza [7]. Today, DNA microarrays have been constructed for studying gene expression changes in a number of different species including the mouse, rat, cow, dog, cat, chicken, horse, pig, rabbit, sheep, guinea pig, ferret, chimpanzee, marmoset, rhesus, and cynomolgus macaque.

DNA microarrays have revolutionized our understanding of the host gene expression changes in response to infection with various pathogens. This information has largely been obtained from *in vitro* infection experiments. Primary cells taken from naïve human volunteers [8–15] or continuous cell lines [16–22] have been infected and incubated with a pathogen for different time periods (ranging from 1 to 48 hours) and host gene signatures generated (Table 1). Microarray studies performed in this way provide insights into the cellular response following infection with, for instance, Monkeypox virus. Alkhalil et al. (2010) showed that many genes (89.08%) in MK2 cells underwent downregulation by 1.5-fold changes or more [21] following infection with Monkeypox virus. Bourquain et al. (2013) also found major unresponsiveness of HeLa cells after exposure [16]. Rubins et al. (2011) concluded, from studies on different human cell types, that Monkeypox virus selectively inhibited the expression of genes with critical roles in cell-signalling pathways that activate innate immune responses (such as TNF-α, IL-1 α and β, CCL5, and IL-6) [14]. Thus it would appear that Monkeypox virus downregulates or silences genes so that the host is less responsive to infection.

DNA microarray analysis has been used to improve our understanding of the host response following exposure to the bacterium [18], spores [9], edema toxin [17], and lethal toxin [8] of *Bacillus anthracis*, the causative agent of anthrax. Studies on human peripheral monocytes revealed that anthrax lethal toxin targets multiple normal immune-regulatory pathways that would be expected to protect the host against anthrax infection. They hypothesised that the increase in RGS14 levels and decrease in CCR5, along with IL-1R2, impairs monocyte function and facilitates bacterial survival [8].

Despite the ready availability of DNA microarrays for use with different animal species, relatively few *in vivo* transcription studies have been published using models of infection with biodefence infectious agents compared with public health pathogens such as tuberculosis (TB) or human immunodeficiency virus (HIV). Using the mouse model, gene signatures have been determined in different organs following infection with *Burkholderia pseudomallei* [23, 24], Venezuelan equine encephalitis virus (VEEV) [25, 26], and *Francisella tularensis* [27–30]. Very recently a bovine model has been used for investigating host mRNA expression changes to *Brucella melitensis* by examining the infected Peyer's patch from a calf ligated ileal loop. This study showed that the early infectious process of *Brucella* was primarily accomplished by compromising the mucosal immune barrier and subverting critical immune response mechanisms [31].

Some microarray studies have been performed using nonhuman primates (NHPs) infected with Ebola virus [32] and Variola virus [5]. In studies at Public Health England the mRNA profiles of NHPs infected with Monkeypox virus and *B. anthracis* are currently underway (personal communication, Karen Kempsell). There is scope for many more informative microarray studies to be performed in various animal models of biodefence agents.

2.1.2. Protein Microarrays. Protein microarray is a more recent technology, providing a platform for high-throughput proteomics. Construction is similar to DNA microarrays, except that the immobilised species is a protein or a peptide, and the array aims to represent partially or wholly the entire proteome [52]. Two methods of protein generation are used: (1) the "standard" method where the gene for each protein is amplified, cloned, produced in an *in vitro* expression system (typically in *Escherichia coli*), and printed directly onto glass

Table 1: Microarray studies performed with various Biodefence Agents.

Pathogen	Purpose of study	Arrays used	Material tested	Reference
		Response to infection		
Burkholderia pseudomallei	Profile human antibody responses in healthy and recovered patients.	Protein array containing 154 *B. pseudomallei* proteins.	Human plasma from healthy and recovered melioidosis patients.	[33]
Burkholderia pseudomallei	Gene expression changes following intravenous infection with bacteria in BALB/c mice.	Sentrix MouseRef-8 cDNA array (Illumina).	Liver and spleen from BALB/c mice.	[24]
Burkholderia pseudomallei	Differences in gene expression after 2 hour exposure to *B. pseudomallei* and *B. thailandensis in vitro*.	GeneChip human genome U133 (Affymetrix).	A549 human lung epithelial cells.	[22]
Bacillus anthracis	Gene expression changes in cells exposed to Edema toxin.	GeneChip murine genome (Affymetrix).	RAW 264.7 murine macrophages.	[17]
Bacillus anthracis	Gene expression changes in cells exposed to lethal toxin.	GeneChip human genome U133 plus 2.0 (Affymetrix).	Human monocytes from the blood of naïve volunteers.	[8]
Bacillus anthracis	Murine macrophage gene expression changes following exposure to protective antigen and lethal factor from *B. anthracis*.	PCR product DNA array.	RAW 264.7 murine macrophages.	[18]
Bacillus anthracis spores	Gene expression profiling of human macrophages following infection *in vitro*.	GeneChip human genome U133 Plus 2.0 (Affymetrix).	Human alveolar macrophages following bronchoscopy.	[9]
Brucella melitensis	Gene expression analysis of mucosal epithelial cells following infection *in vitro*.	10K human ESTs microarray (Microarray centre, Ontario, Canada).	Epithelial-like human HeLa cell line.	[19]
Brucella melitensis	Kinetics of human antibody responses to acute and chronic brucellosis.	*Brucella melitensis* protein array.	Sera from brucellosis patients.	[34]
Brucella melitensis	Investigate host gene changes *in vivo* following infection with *Brucella* in a calf ligated ileal loop model.	Custom-made 13K bovine 70 mer oligo array.	Infected Peyer's patch from calf ligated ileal loop.	[31]
Brucella melitensis	Full proteome-wide serological analysis of *B. melitensis* in humans.	Protein microarray containing 3046 proteins from *B. melitensis*.	Sera from brucellosis patients.	[35]
Coxiella burnetii	Profile humoral immune response of naïve and acute Q-fever patients.	Protein microarray containing 84% of *C. burnetii*.	Human sera from Q-fever patients.	[36]
Coxiella burnetii	Comparison of the antibody profiles from acute and chronic Q-fever patients.	Protein microarray containing 93% of *C. burnetii*.	Human sera from Q-fever patients.	[37]
Coxiella burnetii	Define the humoral immune profile using Q-fever patient sera.	Custom-made protein microarray containing 19 proteins from *C. burnetii*.	Human sera from Q-fever patients.	[38]
Ebola and Marburg viruses	Gene signatures following infection *in vitro* with Ebola virus, Marburg virus.	Human cDNA array (Agilent).	Human hepatoblastoma (Huh7) cells.	[20]
Ebola virus	Entry into human macrophages. Infection studies *in vitro*.	GeneChip human genome HG-U95Av2 array (Affymetrix).	Primary human macrophages.	[10]
Francisella tularensis live vaccine strain (LVS)	Human neutrophil gene expression, *in vitro* infection studies.	GeneChip human genome U133 plus 2.0 (Affymetrix).	Polymorphonuclear leukocytes (PMNs) from human blood.	[11]
Francisella tularensis LVS	*In vitro* infection studies using Human PBMCs.	Human gene array (Affymetrix).	Human peripheral blood mononuclear cells (PBMCs).	[12]
Francisella tularensis (SchuS4)	Gene expression following inhalation of *F. tularensis* in BALB/c mice.	Mouse array covering 1500 genes. (Ocimumbio).	Lung tissue taken from infected BALB/c mice.	[27]

Table 1: Continued.

Pathogen	Purpose of study	Arrays used	Material tested	Reference
Francisella tularensis (FSC033/snMF)	Gene expression following aerosol exposure with *F. tularensis* in C57BL/6 mice.	Custom-made mouse cDNA array.	Lung tissue taken from infected C57BL/6 mice.	[30]
Francisella tularensis (SchuS4)	Gene expression of human monocytes infected *in vitro* with *F. tularensis*.	GeneChip human genome U133 plus 2 (Affymetrix).	Naïve human peripheral blood monocytes.	[13]
Francisella tularensis (SchuS4)	Comparison of mouse global transcriptional responses to *F. tularensis, Yersinia pestis, Pseudomonas aeruginosa* and *Legionella pneumophila*.	Mouse whole genome 44K arrays (Agilent).	Lung tissue from infected BALB/c mice.	[29]
Monkeypox and Vaccinia virus	Comparison of gene expression profiles following infection *in vitro* with Monkeypox or Vaccinia virus.	Human cDNA arrays with 406 Variola and Vaccinia virus genes.	Primary human macrophages, primary human fibroblasts and HeLa cells.	[14]
Monkeypox and Vaccinia virus	Comparison of gene expression profiles, *in vitro* infection studies.	Whole human genome oligo microarray (Agilent).	HeLa cells.	[16]
Monkeypox virus	Gene expression changes *in vitro* 3 and 7 hours post-challenge with Monkeypox virus.	Rhesus macaque genome microarrays (Affymetrix).	*Macaca mulatta* kidney cells (MK2).	[21]
Monkeypox virus	Comparison of antibody responses to monkeypox virus infection and human smallpox vaccination.	Protein array covering 92–95% of representative proteins from Monkeypox and Vaccinia virus.	Blood from humans with smallpox vaccination and cyno macaques infected with Monkeypox virus.	[39]
Variola virus	Host gene expression changes in Variola virus infected cynomolgus macaques.	Human cDNA microarrays.	PBMC's sampled from infected monkeys.	[5]
Yersinia pestis	Gene expression changes following infection *in vitro*.	Human nylon blots (1185 cDNA spots) (Clontech).	Primary human monocytes and/or mixed with lymphocytes (PBMCs).	[15]
Venezuelan equine encephalitis virus (VEEV)	Gene expression of VEEV infected mice.	Oligo array mouse 70 mer. (Operon) & GEArray, focused mouse Toll-like receptor signaling microarray.	VEEV infected mouse brain CD-1 mice.	[25, 26]
		Vaccines		
Anthrax vaccine adjuvant CpG ODN	Measure gene expression changes in mice and splenocytes treated with CpG ODN.	Murine oligonucleotide array (custom-made).	Spleens and splenocytes from various breds of mice.	[40–42]
Francisella tularensis LVS	Assess the memory response of PBMCs taken from LVS vaccinated and naïve humans.	GeneChip human genome U133 (Affymetrix).	Re-stimulated PBMCs from LVS vaccinated and naïve humans.	[43]
Killed *Francisella tularensis* (LVS) adjuvanted with ISCOMS admixed with CpG	Define antibody profiles of vaccinated mice.	Whole proteome microarray custom-made.	BALB/c mice vaccinated with LVS.	[44]
Q-fever vaccine	Assess antibody immune profiles of Q-Vax vaccinated humans.	*C. burnetii* protein microarray (custom-made).	Sera from vaccinated humans.	[45]
Smallpox vaccines	Assess antibody profiles generated to MVA, Acam2000 and/or Dryvax smallpox vaccines.	Protein array containing Vaccinia virus proteins [46].	Mouse, rabbit, macaque, black-tailed prairie dog and human sera.	[47–51]
		Therapies		
Anti-coagulant treatments for Ebola virus infection	Comparison of NHP host genome responses responding to candidate therapeutics following infection with Ebola virus.	Human genome cDNA microarray.	PBMC's from rhesus macaques infected with ZEBOV and treated shortly after exposure with rNAPc2 or rhAPC.	[32]

Omission from this table does not constitute absence of data.

slides [46]; (2) an alternative method where the encoding DNA is printed onto the slide and expressed *in situ* at the time required (NAPPA, nucleic acid programmable array) [53].

One of the most powerful applications of protein microarrays is in the study of the humoral immune response to infection. Arrays have been used to assess host antibody profiles (or "immunosignature") in response to infection with *B. melitensis* [34, 35], *B. pseudomallei* [33, 54], Vaccinia/Variola virus [47], Monkeypox virus [39], and *Coxiella burnetii* [36–38] (Table 1). Studies on *C. burnetii*, the etiological agent of Q-fever, have helped to identify new diagnostic antigens [36, 38, 45]. Seven *C. burnetii* proteins (GroEL, YbgF, RplL, Mip, OmpH, Com1, and Dnak) were identified (from protein arrays studies) and then fabricated on a small array and tested with sera from patients with other diseases (Rickettsial spotted fever, *Legionella* pneumonia, or *Streptococcal* pneumonia) as well as Q-fever, in order to develop a diagnostic assay. The selected antigens demonstrated moderate specificity for recognizing Q-fever in patient sera [38]. The use of protein microarrays has also aided the identification of different IgG and IgM profiles for differentiating acute and chronic Q-fever [37] and a proof-of-concept diagnostic assay (immunostrip) to distinguish the two disease states [37]. In addition to identifying antigens for diagnostic tools, antibody profiling, using protein arrays, also provides candidate antigens for subunit vaccine development [37].

2.1.3. Use of Microarrays for the Evaluation of Vaccines and Therapies. Microarray technology has been used to help understand the cell-mediated and humoral immune responses following infection with infectious agents; furthermore it has also improved our understanding of the mechanism of action of therapeutics and biodefence vaccines. For instance a transcriptomic approach, using DNA microarrays, was used to assess the host response to treatment with therapeutic agents (rNAPc2 or rhAPC) designed to block the coagulation pathway during Ebola virus infection in NHPs [32]. Coagulation abnormalities in Ebola hemorrhagic fever have been previously reported [55] suggesting that blocking the development of coagulopathies during Ebola virus infection might limit pathogenesis. Microarray analysis showed that the overall circulating immune response in NHPs was similar both in the presence and absence of coagulation inhibitors; however, the profiles of the surviving NHPs in the treated groups clustered together [32]. Only small numbers (2/8 and 2/11) of animals survived in each treatment group but the study did reveal that several differentially expressed genes correlated with survival, namely, chemokine ligand 8 (CCL8/MCP-2) and coagulation-associated genes TFPI and PDPN [32]. Further work is clearly needed in this area as these genes may provide possible targets for early-stage diagnostics or future therapeutics.

A limited number of studies have been performed using DNA microarrays to understand the underlying protective mechanisms of licensed or novel biodefence vaccines. DNA arrays have been used to examine the immunostimulatory properties of CpG motifs [40–42] which when used as an adjuvant have been shown to significantly prolong the protection induced by anthrax vaccine adsorbed (AVA) [56, 57]. Recently, Paranavitana and colleagues examined the transcriptional profile of human volunteers who had received the live vaccine strain (LVS), an attenuated strain of *F. tularensis* [43]. PBMCs from individuals were restimulated with LVS *in vitro* and memory responses were evaluated. The microarray results revealed that both dendritic cells and macrophages played significant roles in antigen presentation. Significantly differentially expressed genes including IL-15, GM-CSF, IL-9, and IL-10 as well as genes associated with T-cell, B-cell, and natural killer cell activities were identified. Paranavitana et al. concluded that the manipulation of the dendritic cell maturation pathway, with stimuli to promote efficient antigen presentation, may be a way forward for future vaccine development against *Francisella* [43].

The antibody profile evoked by smallpox vaccines has been examined in detail following the development of a Vaccinia proteome microarray by Davies et al. in 2005 [46]. Since then, the immunosignature evoked by three different vaccines (Acam2000, Dryvax, and MVA) in the mouse, rabbit, macaque, prairie dog, and humans have been defined [47–50]. Follow-up studies using protein arrays involved examining the sera from more than 2000 smallpox-vaccinated humans. Six dominant antigens were identified comprising 3 membrane and 3 nonmembrane antigens from the intracellular mature virion [51]. These antigens were then evaluated in an ELISA format with sera from MVA and DryVax vaccinees. Overall, these ELISAs should aid in monitoring the human immune response to MVA in both vaccinia naïve and previously vaccinated individuals, thus assisting with vaccine development in the future.

Protein arrays have also been used to examine the immunosignature of mice vaccinated with killed *F. tularensis* LVS adjuvanted with immune stimulating complexes (ISCOMS) and CpG [44]. Similarly, protein arrays were used to assess the immunosignature of Q-Vax (Q-fever) vaccine [45]. Both studies identified protective proteins which should aid the design of new or improved vaccines.

Advances in "omic" technology have also assisted with the identification of candidate T-cell antigens. An ORFeome flexible cloning approach was developed by Jing and colleagues whilst analysing the CD4 T-cell response to vaccinia virus using PBMCs from Smallpox vaccinated individuals in 2009 [58]. This method has since been used to identify candidate T-cell antigens for herpes simplex virus type 1 (HSV-1) [59]. This could be applied to the identification of T-cell antigens for Biodefence vaccines.

2.2. Next Generation Sequencing. Next generation sequencing (NGS; also known as high-throughput, short-read, or deep sequencing) has revolutionised sequence-based analyses over the last decade. The underlying principle is that it uses micro-/nanotechnologies to run millions of parallel sequencing reactions, generating millions or billions of bases per run (which is up to 6 logs greater than the output using the Sanger method). Read lengths are typically comparatively short, a result of which is that any particular base is sequenced many times (known as coverage or read depth). There are

a number of competing platforms, with Illumina, ABI SOLiD, Roche 454, and Ion Torrent technologies being widely used, each having different characteristics with regard to average read length, total bases sequenced per run, and cost-per-base [60–62]. Other more specialized NGS technologies are PacBio Single Molecule Real Time (SMRT) and Oxford Nanopore [63, 64].

NGS technology can be applied to both DNA (DNA-seq), and RNA (after conversion to cDNA-RNA-seq). RNA-seq analysis aims to identify the transcriptome (the complete set of transcripts of the cell, which includes mRNA, noncoding RNAs, and small RNAs). RNA-seq is increasingly being used as an alternative to microarray as a method of measuring gene expression [65, 66] and uses the sequence read depth of the RNA species as a measure of the absolute level in the sample. The two methods have a high degree of correspondence [67, 68], and similar analytical statistical techniques can be used, although data preprocessing and sample normalization require different bioinformatic techniques [69]. RNA-seq is reported to have significant advantages over microarray, such as less bias/variation, lower background signal, and a larger dynamic range (up to 100-fold greater). Importantly, it does not depend on prior knowledge of a reference transcriptome and therefore can lead to discovery of previously unknown RNA species and of "edited" RNA species such as splice variants [70]. However, certain disadvantages do exist, such as nonuniform read coverage, inability to detect a rare transcript (unless high read depth is obtained), and discrepancy in read depth or library sizes between samples [65].

2.2.1. Use of RNA-Seq to Study Host Response to Pathogens. Upon infection of a host with a pathogen, changes in the expression of both organisms occur. These are usually investigated separately due to the low pathogen:host transcript ratio (up to 200-fold); thus enrichment of the pathogen transcripts is often required [71]. Pathogen expression profiling examples include analysis of the *F. tularensis* transcriptome during infection of mouse macrophages [72] and sRNA expression of *Yersinia pestis* grown *in vitro* and in the mouse lung [73].

RNA-seq has been used to investigate the host response to different virulent strains of *B. melitensis* in mouse peritoneal macrophages [74]. Compared with previous microarray studies, deep sequencing provided a more sensitive and comprehensive unbiased coverage of the host transcriptome, with many alternative and novel transcripts being discovered. In particular, it was shown that a live attenuated vaccine strain (M5-90) had a reduced ability to avoid phagosome-lysosome fusion and activate MAPK pathways when compared with the virulent strain M28. This may account for the difference in the ability of the two strains to survive in the host [74]. A second study examining the microRNA (miRNA) profile of RAW264.7 cells in response to *B. melitensis* infection also used a high throughput sequencing approach [75]. Zheng and colleagues concluded that *Brucella* may establish a chronic infection by regulating the host miRNA profile [75].

The human host response to Dengue virus infection has also been reported using RNA-Seq [76]. A significant amount of previously uncharacterised gene isoforms and alternative transcripts over a range of pathways were shown, and particularly there was a greater number of host differentially regulated transcripts upon infection by an attenuated DENV strain than by the wild-type, suggesting that there may be a previously uncharacterised innate immune response which is largely evaded in wild-type strains [76].

2.2.2. Dual RNA-Seq. Ideally it would be preferable to monitor the gene expression profiles of the pathogen and host simultaneously. This "dual RNA-seq" approach is technically and bioinformatically more challenging [77, 78] but may well become the established method. However, recent examples do exist for the simultaneous profiling of the host and viral [79] or bacterial [29, 80] species. For instance, Walter and colleagues exposed mice to virulent *F. tularensis* and discovered that, while acute infection at four hours was associated with marked suppression of multiple aspects of the innate immune response (relative to other pathogens examined), a subset of immune-related transcripts was uniquely induced by *Francisella*. They also showed that a classical inflammatory response was activated in the lungs of mice, 24 hours after infection and this simultaneously correlated with a dramatic change in bacterial gene expression patterns [29]. These results should help to identify potential virulence factors which target host inflammatory pathways, in the future.

Dual RNA-seq has also been used to evaluate the immune response following smallpox vaccination. PBMCs taken from Dryvax vaccinated individuals were either stimulated with or without live Vaccinia virus for 8 hours [81]. Results showed detection of all annotated Vaccinia genes, with those genes classified as "early" in the viral life cycle expressed at significantly higher levels. On the host side numerous innate genes and pathways were activated upon vaccinia infection. A number of chemokines, cytokines, interferons, and macrophage-associated genes exhibited downregulation upon infection whilst there was an upregulation of histones, IFNβ, IFNγ, and heat shock proteins [81].

2.2.3. Other Uses of NGS Sequencing

T and B Cell Repertoire Diversity. The immunological repertoire is a term defining the collection of surface-expressed B-cell (BCRs) and T-cell receptors (TCRs). Receptor diversity is generated dynamically by sequence rearrangement of specific loci in the germline genome, leading to a vast diversity of differing clones [82]. Classically, studies on the immune repertoire have used techniques that either provide a limited description or sample a limited number of sequences (e.g., CDR3 spectratyping, targeted sequencing [83]). The high-throughput nature of NGS technology allows simultaneous analysis of potentially the entire immune repertoire in a single experiment (using DNA-Seq or RNA-Seq) [84–86]. Recent applications have included studying the changes in the antibody responses to Dengue virus infection [87] and Influenza vaccination [88] and there is clearly scope to apply this technique to monitor the immune repertoire in response to other infectious diseases, vaccines, or therapeutics.

3. Optical Imaging of Host-Pathogen Interactions

Imaging infection using optical sources relies on the detection of specific targets using fluorescence or bioluminescence. Fluorescent light is emitted with a characteristic emission spectrum following excitation at specific wavelengths. Fluorescent molecules may be used to tag specific molecules of interest. Very often the molecule of interest will be an antibody which in turn will be directed to specific targets (e.g., surface receptors on host cells). Alternatively, endogenous proteins can be made to fluoresce, for example, in genetically modified animals or pathogens, or fluorescent dyes can be used to label pathogens or cells. Bioluminescence is produced by the reaction of a luciferase enzyme with its substrate and requires energy and oxygen to occur. Unlike fluorescence imaging, where the signal is still detectable for some hours after the host has died, bioluminescent imaging requires living cells. This section aims to review how our understanding of biodefence pathogens, vaccines, and immunotherapies and their interactions with the host has been greatly aided by imaging techniques such as flow cytometry, fluorescence microscopy and real time *in vivo* biophotonic imaging.

3.1. Flow Cytometry. This technique is routinely used as an important tool for assessing cellular responses to infection and vaccination in both human patients and animal models of infection. It is used for cellular phenotyping and functional assays including fluorescence-based proliferation assays. Bead-based assays are also available to assess levels of soluble factors including cytokines in samples from *in vitro* and *ex vivo* tissues. Intracellular cytokine responses can also be measured by intracellular staining, with fluorochrome labelled antibodies, to determine cellular phenotypes generated following vaccination or therapeutic treatment with specific antigens. Antibodies for specific cell targets are generally available for a number of animal species particularly the mouse and rat, but cell target ranges are limited for less commonly used species such as the marmoset, which in turn can limit the analysis of cellular responses in these models. In order to understand host-responses, fluorescently labelled pathogen-specific antibodies allow the presence of intracellular bacteria to be identified within host cells [89]. Alternatively bacteria expressing fluorescent molecules, for example, green fluorescent protein (GFP) [90], m-cherry red [91] or other fluorescent markers may be used. In combination with specific antibody staining of host cells, fluorescent labelling of pathogens has allowed the location of pathogens within host cells to be identified in both *in vitro* and *in vivo* infection studies using flow cytometry and immunofluorescence microscopy.

3.1.1. Pathogenesis and Assessment of Immunotherapies. Flow cytometry has highlighted a key role for various cell types in murine infection models of *Y. pestis*, the causative agent of plague. The importance of neutrophils in respiratory *Y. pestis* was demonstrated in two early studies [92, 93]. Furthermore, flow cytometry was used to identify the target host cells of *Y. pestis* in a murine pneumonic infection model where alveolar macrophages ($CD11c^+CD11b^+F4/80^+$) were identified as the initial cell type to uptake the bacterium followed by neutrophils [94]. An additional study investigating intratracheal inoculation of *Y. pestis* showed the interaction of this bacterium with $CD11c^+DEC205^+CD11b$- cells in the airways and lung. Depletion of this cell type suggested an important role for it in the initial replication and dissemination of *Y. pestis* from the lung [95]. It is speculated that the difference in cellular tropism of *Y. pestis* described in these respiratory studies maybe due to the difference between aerosol and intratracheal dosing and differing strains of the organism. In an intradermal model of infection, *Y. pestis* was also found to reduce the activation of inflammatory cells, particularly neutrophils, at the site of infection. Using bacterial mutants, the *Y. pestis* virulence plasmid pYV was shown to be involved in this evasion of early inflammatory responses in the skin [96].

Neutrophil inflammatory responses have been characterised following infection in mouse models with both *B. pseudomallei* [97] and *Burkholderia mallei* [98] by flow cytometry where neutrophils were found to be crucial for protection in both respiratory and intraperitoneal forms of these related infections. The role of neutrophils in *Burkholderia* infection in the murine host also aligns with human *ex vivo* studies where phagocytosis and apoptosis of *B. pseudomallei* by human blood neutrophils were impaired in neutrophils from diabetic patients. This impaired neutrophil function may contribute to the increased susceptibility to *Burkholderia* infection observed in diabetic patients [99].

Using flow cytometry to understand host-pathogen interactions has the potential to enable an association between host immune markers with protective effects following treatment with therapeutics and vaccines. A number of studies have assessed the immune response to immunotherapeutic approaches for treatment of infection to further understand potentially protective immune responses in *in vivo* models of infection using immunostimulants including CpG motifs [100]. One study using phosphoantigens as an immunotherapy in a marmoset model of *B. pseudomallei* infection [101] showed that, although there was no effect on survival, strong cell-mediated immune responses were detected which could inform future treatment strategies. In another study, decreased bacterial numbers and increased survival to a novel immunotherapeutic strategy using Acai polysaccharides against pulmonary *F. tularensis* or *B. pseudomallei* infection *in vivo* [102] were associated with IFN-γ production by NK cells in the lung.

Flow cytometry bead-based assays have the potential to aid our understanding of potential protective mechanisms of novel immunotherapeutics by assessing cytokine responses. These assays have been used in studies investigating the effects of IFN-γ therapy in mice during *B. pseudomallei* infection [103] and to understand changes occurring as a result of treatment with an HMGB1-antibody antibiotic combination therapy [104]. This study showed that treated mice had significantly higher IFN-γ levels which correlated with survival. They have also been used to further our understanding of the protective immune responses involved following

a combination of preexposure vaccination and postexposure CpG immunotherapy against *B. pseudomallei* infection *in vivo* [105] where both intranasal and intraperitoneal vaccinations with 2D2 attenuated vaccine strain were found to generate antigen-specific IFN-γ $CD4^+$ T cell responses. A greater pulmonary T cell response was observed following vaccination via the intranasal route which corresponded with increased protection against pulmonary infection.

3.1.2. Vaccine Studies. Immune responses elicited *in vivo* following immunization and *ex vivo* cellular restimulation with specific antigens from vaccinated or infected animals have been used to determine specific, memory-type responses to vaccines. This has broadened our understanding of a number of vaccination strategies for biodefence pathogens including live vaccines for *B. pseudomallei* [106] and *F. tularensis* [107], novel live vaccine strategies against *F. tularensis* infection [108], and heat-killed vaccines to *B. mallei* [109]. Potential immune correlates of protection have also been identified in studies by comparing profiles of lymphocyte populations following vaccination (prior to infection) and their responses during infection with Monkeypox virus [110]. In depth assessment of T-cell signatures in vaccines or individuals with naturally acquired *F. tularensis* infection suggested that these signatures could be used to identify protective correlates of immunity to *F. tularensis* [111]. Additionally, the identification of putative vaccine candidates [112] and the longevity of immune responses to vaccines have also been greatly aided by flow cytometry in follow-on studies of *F. tularensis* live vaccine strain (LVS) vaccination [111, 113]. Immune responses to vaccination have also been used in preclinical animal models (murine and primate) and in Phase I clinical trials to assess host responses to a recombinant plague vaccine. Although a number of memory cell phenotypes were investigated, flow cytometry lacked the sensitivity to detect changes in immune profiles between vaccinated and placebo groups [114]. Understanding immune responses generated by novel vaccines can facilitate the rational development of vaccines which induce the most appropriate immune responses to protect against infection, for example, by engineering the known protective F1-antigen against *Y. pestis* to include B-cell and T-cell epitopes [115].

3.1.3. Other Uses of Flow Cytometric Techniques. In addition to examining lymphocyte responses, the role of antigen-presenting cells in generating protective immunity during vaccination to *B. pseudomallei* (e.g., dendritic cells (DCs) [116]) and *F. tularensis* LVS [107] has also been aided by the use of flow cytometry techniques. The use of a GFP strain (BP82-GFP) of an intradermally delivered live, attenuated *B. pseudomallei* vaccine [117] and specific cell staining demonstrated that the most efficient cell type at uptake and transport of bacteria to the draining lymph node was the neutrophil.

Fluorescent-activated cell sorting and cDNA technologies have recently been used together to generate antigen-specific monoclonal antibodies [118]. The overall aim of this is the provision of antibody treatments for infectious diseases and an example of this has already been applied to emerging coronavirus species including severe acute respiratory syndrome (SARS) [119]. This technology may well be used for developing therapeutics for biodefence agents in the future. Other potential applications of flow cytometry in biosecurity research, outside the area of investigation of host-pathogen interactions, are reviewed in Marrone, 2009 [120].

3.2. Fluorescence Microscopy. A number of recent advances in fluorescent microscopy techniques such as confocal microscopy, intravital 2-photon microscopy, dynamic live cell imaging, and super resolution microscopy have been used to interrogate host-pathogen interactions, based on detection of specific fluorescent signals to provide detailed images of pathogens colocalised with or within host cells. Fluorescence microscopy is also being investigated for its utility in the diagnosis of infections including *B. pseudomallei*. In comparison with flow cytometry, fluorescence microscopy can provide a much more detailed assessment of how pathogens interact with individual host cells. These studies are aided through the use of a range of fluorescent dyes for both the pathogen and cellular structures/organelles including DNA dyes such as DRAQ5 or DAPI which are important for nuclear identification.

3.2.1. In Vitro Infection Models. Fluorescence microscopy has enabled us to understand the intracellular nature and niches of pathogens and their ability to evade immune pathways to enable their survival within host cells. For example, identifying the lysosomal escape mechanism of *F. tularensis* into the cytosol provided an understanding of its ability to survive within host macrophages [121]. Fluorescence microscopy has also been used to investigate the role of complement in uptake of *F. tularensis* into cells [122] and the immune evasion of this pathway by *F. tularensis* [123]. It has also been used to understand the effect of modulators on macrophage function and phagosomal escape of *F. tularensis* LVS [124] and the interaction of *B. mallei* with macrophages *in vitro* to assess which bacterial components are important in the pathogenesis of disease [125]. Understanding the effects of *F. tularensis* LVS strains and their altered interactions with host cells [126] has potential implications for future licensing of these vaccines. Our understanding of the interaction of *F. tularensis* and other bacteria with host cells and its intracellular nature has contributed to development of treatment regimens including delivery of antibiotic therapies suitable for treating intracellular infection. Fluorescence microscopy also has the potential to elucidate host pathway targets which could be therapeutically manipulated to prevent evasion of the host response by bacteria and aid in intracellular clearance. For example, the interaction of *F. tularensis* and *B. pseudomallei* with pathways of autophagic digestion has been assessed using fluorescence microscopy in *in vitro* studies. The interaction of *B. pseudomallei* with autophagosomes using GFP-LC3-expressing RAW 264.7 cells and fluorescently labelled bacteria (both wildtype and mutants) elucidated mechanisms of evasion of the autophagic pathway by *B. pseudomallei* [127]. *F. tularensis* was also found to utilize one autophagic pathway for its survival [111]. Further studies

identified potential new therapeutic compounds to target the autophagic pathway [128, 129]. It was demonstrated that inducing alternative autophagic pathways using the novel inducer AR-12 reduced bacterial growth in *F. tularensis* infection [112]. Confocal scanning microscopy has enhanced our understanding of the interaction of *C. burnetii* with host-cells and intracellular vacuoles [130]. The dynamics between vacuoles, lysosomes, and the processes which regulate actin dynamics in formation of vacuoles, including GTPases and associated proteins, have been investigated in detail using *C. burnetii* mutants [107]. This has led to identification of host targets with the potential for therapeutic targeting. Confocal microscopy has also been utilised to develop a high content imaging assay to understand the formation of multinucleated giant cells (MNGCs) during *B. pseudomallei* infection which is a unique mechanism used by *Burkholderia* spp. and is thought to allow spread of the infection without detection by the immune system [131]. This quantitative method allowed the effect of bacterial mutants, thought to subvert the formation of MNGCs, to be assessed. Importantly, this method was also used to investigate the effect of small molecule inhibitors on MNGC formation and thus has the potential to be used as a screening tool for novel therapeutics. Confocal microscopy has also been used to investigate the interaction of viral pathogens including filoviruses such as Ebola virus with host cells [132, 133] and by mapping the interaction between the viral proteins polymerase L and its cofactor VP-35. In this model *in vitro* system, immunofluorescence analysis demonstrated that this interaction was disrupted by mutants containing the VP-35 binding site which led to reduced Ebola virus replication, thus identifying a potential target for development as a novel antiviral therapy [134].

3.2.2. In Vivo Infection Models. *F. tularensis* was detected by phase-contrast and fluorescence microscopy using *in situ* hybridization [135] and an m-cherry red strain of *B. melitensis* identified bacteria associated with host cells in tissue sections from *in vivo* infection models [91]. This study showed the *in situ* colocalisation of *B. melitensis* with a number of different cellular phenotypes within granulomas in the spleen and liver. Understanding these immune-pathological lesions using complex immunohistochemistry and fluorescent bacterial strains has the potential to allow identification of new treatments for bacteria which so effectively evade and manipulate host responses to enable their survival. The binding of monoclonal antibody therapies to the *Y. pestis* bacterium using immunofluorescence demonstrated the specificity of potential therapies for bubonic plague. This prior testing of monoclonal antibody therapies was important to determine the specificity of any protection observed in *in vivo* studies [136]. Intravital microscopy, which adds an additional parameter of time to microscopy studies, was used to identify the rapidity of the neutrophil response *in situ* during intradermal infection with ds-red expressing *Y. pestis* strain in a GFP-expressing neutrophil transgenic mouse model [137]. The dynamic interactions between ds-red *Y. pestis* and GFP-neutrophils following intradermal infection and the association between *Y. pestis* and neutrophils were confirmed by confocal microscopy which specifically demonstrated that, within 4 hours, *Y. pestis* had been phagocytosed by neutrophils and was intracellular and not just associated with cells. This led the authors to investigate the role of neutrophils in dissemination of plague to the lymph nodes using antibody depletion which suggested that *Y. pestis* subverted the host response very early in infection to prevent dissemination to the lymph nodes.

3.3. Biphotonic Imaging: Real-Time In Vivo Imaging. Visualising the infectious disease process as it occurs inside a living animal is of major benefit to the development of medical countermeasures. This can be achieved using biphotonic imaging (BPI), a sensitive and noninvasive method of detecting light emitted either as a bioluminescent (BL) or fluorescent (FL) signal, using photon detectors such as those based on a charge coupled device (CCD) camera. BPI has enabled new insights into pathogen dissemination, host responses to infection, interactions between host and pathogen, and the effects of antimicrobials and vaccines. This technique can also be used to refine animal experiments with each animal acting as its own control, therefore, increasing the power of these studies. The creation of BL or FL strains of pathogenic organisms has enabled this field to progress and description of the processes involved in BPI and creation of these strains are comprehensively reviewed in Andreu et al. [138].

Using BPI different patterns of pathogen dissemination can be readily observed allowing discrimination of the growth and spread of different forms of the pathogen or target organs depending on route of infection. For example, BL expressing variants of *B. anthracis* Sterne strain that only produced a BL signal during either spore germination or vegetative growth of the bacterium have permitted identification of sites of germination and spread during the early stages of anthrax infection [139]. BPI studies helped determine the site of anthrax spore germination after inhalational infection [140] where light emitting bacteria in the upper respiratory tract and lung were observed within 30 min of inhalational infection [140, 141].

BPI studies showed that dissemination of *Y. pestis* was found to vary depending on route of infection [142, 143]. Subcutaneous (s.c.) administration in the abdominal *linea alba* region resulted in pathogen spread from the inguinal lymph node (LN) to axillary LN, then to liver and spleen whereas s.c. infection in the more traditional cervical "scruff" region, base of the tail, in the footpad [144] or ear pinna [143] resulted in a different pattern of signal intensity originating at the site of injection. Intranasal (i.n.) challenge with BL *Y. pestis* leads to a detectable BL signal [143, 145] in the upper abdominal region which was confirmed to originate from the lung by *ex vivo* imaging of tissues. BPI has also been used to investigate the dissemination of BL strains of *F. tularensis* type A (SCHU S4) and type B (LVS) [146]. Visualising areas of BL LVS infection and bacterial spread [147] provided important information on the effects of instillation volume and anaesthesia in delivery of i.n. bacterial challenge with the potential to impact on the wider development of *in vivo* pulmonary infection models.

The pattern of dissemination of BL *B. pseudomallei* following inhalational challenge has been investigated [148, 149]. The spread of both wild type and capsule mutant strains of *B. pseudomallei* has been compared in the BALB/c mouse model with an immunocompentent, hairless SKH-1 mouse strain, that is, particularly useful for FL imaging studies due to low autofluorescent background usually generated by fur. Infection studies with a BL strain of *B. mallei* have also been reported [150, 151] with a BL signal detectable in the lung after i.n. challenge from 48 h after infection (p.i.), before progressing to the liver and spleen.

These pathogen dissemination models have subsequently been used to assess the effect of antibiotics and immunotherapies. A substantial reduction of bacterial signal was found in *B. mallei*-infected mice treated with the antibiotic levofloxacin compared to untreated mice [150]; however, when the antibiotic was discontinued at 96 h p.i., reemergence of the BL bacterial signal was observed. This mouse model of *B. mallei* infection has been further used to investigate the effects of CpG treatment alone, previously shown to provide protection against *B. mallei* infection when given preexposure to mice [152]. Mott et al. (2013) [151] used dual signal imaging to elucidate the role of CpGs on neutrophil activation using a neutrophil-specific fluorescent probe. This cyanine 7-conjugate, PEG modified hexapeptide reagent specifically binds to the formylpeptide receptor of neutrophils [136]. This has allowed real-time colocalisation of BL bacterial spread with FL neutrophil responses in the lung during the course of infection.

The effects of immunisation with protective antigen (PA) vaccine demonstrated that, in immunised mice, dissemination of BL *B. anthracis* beyond the nasopharynx region was prevented. The effect of PA vaccine immunisation on anthrax spore germination and bacterial spread has also been assessed [141]. This work clearly demonstrated that although spore germination and bacterial growth occur at the same rate in both immunised and unimmunised mice, bacterial growth was quickly neutralised in the immunised mice whereas BL bacteria spread rapidly in unimmunised controls. BL expressing *B. anthracis* strains modified to express only one of the anthrax toxins stimulated different patterns of early immune response after cutaneous infection of the ear pinna [153]. In this study, draining LN were removed following BPI and immune cell populations were analysed by flow cytometry. The Lethal toxin-expressing strain stimulated increases in the total cell populations of neutrophils, $CD4^+$ and $CD8^+$ T-cells whereas the immunosuppressive edema toxin-expressing strain stimulated only an increase in $CD8^+$ T-cells.

3.4. Emerging Technologies

3.4.1. Imaging Flow Cytometry. Recent developments in flow cytometry include the development of imaging flow cytometers including the ImagestreamX. Imaging flow cytometry adds another dimension to flow cytometric applications with images of each cell being produced in addition to fluorescence readouts and has the ability to further advance our understanding of host-pathogen interactions. It is particularly suitable for assessing the colocalisation of pathogens within host cells and for examining cellular processes for uptake and processing of pathogens, for example, phagocytosis, autophagy, and apoptosis. The number of publications which incorporate use of ImagestreamX for investigating host-pathogen interactions is growing each year with a limited number of publications on a wide range of public health related pathogens including *Yersinia enterocolitica* [154], *Plasmodium falciparum* [155, 156], and *Neisseria meningitidis* [157]. As yet, no studies for biodefence pathogens have been published. However, pathogens which have been used to model biodefence pathogens, such as *Yersinia pseudotuberculosis* as a model for *Yersinia pestis*, have been documented [158] demonstrating the potential of this technology. At Defense Science and Technology Laboratory, we are currently using the ImagestreamX to examine the interactions of *B. pseudomallei*, *F. tularensis*, and other pathogens with cellular targets in samples from both *in vivo* and *in vitro* studies (Figure 1). This technique has the potential of providing a high-throughput imaging technique for the analysis of host-pathogen interactions and assessment of immunotherapeutics for biodefence pathogens.

3.4.2. Other Imaging Technologies. Ultrasound magnetic resonance imaging (MRI) and radiography are all technologies which have been used clinically in the diagnosis of infectious diseases including anthrax and tuberculosis. Some of these technologies have been used in biodefence research, for example, positron emission tomography (PET)/computer tomography (CT) imaging was used to examine inflammation patterns in Monkeypox virus infection of primates [159]. The use of these imaging technologies in high containment, alongside optical imaging technologies, has the potential to provide a multi-faceted approach to imaging to further enhance our understanding of the pathogenesis of infection with Biodefence agents in the future. The use of other imaging technologies and their potential application to biodefence disease in the clinic is reviewed in [160].

4. Conclusions

Biodefence agents are dangerous pathogens that pose unique challenges for researchers. Human cases of these diseases are relatively rare and therefore animal models play a key role in helping to understand pathogenesis. Imaging and "omic" technologies have greatly aided our ability to study the host response during the course of an infection and have thus provided important insights. Also since it is neither ethical nor feasible to conduct conventional phase III efficacy trials, using biodefence agents in human volunteers, these key technologies can play an important role in the evaluation of vaccines and therapies. They provide evidence to support the concepts defined by the Food and Drug Agency (FDA) Animal Rule [161] for licensing new medical countermeasures.

Currently the majority of studies using the "omic" and imaging techniques, described in this review, have examined the host response independently from pathogen virulence. In the future, however, due to rapid advances in NGS platform

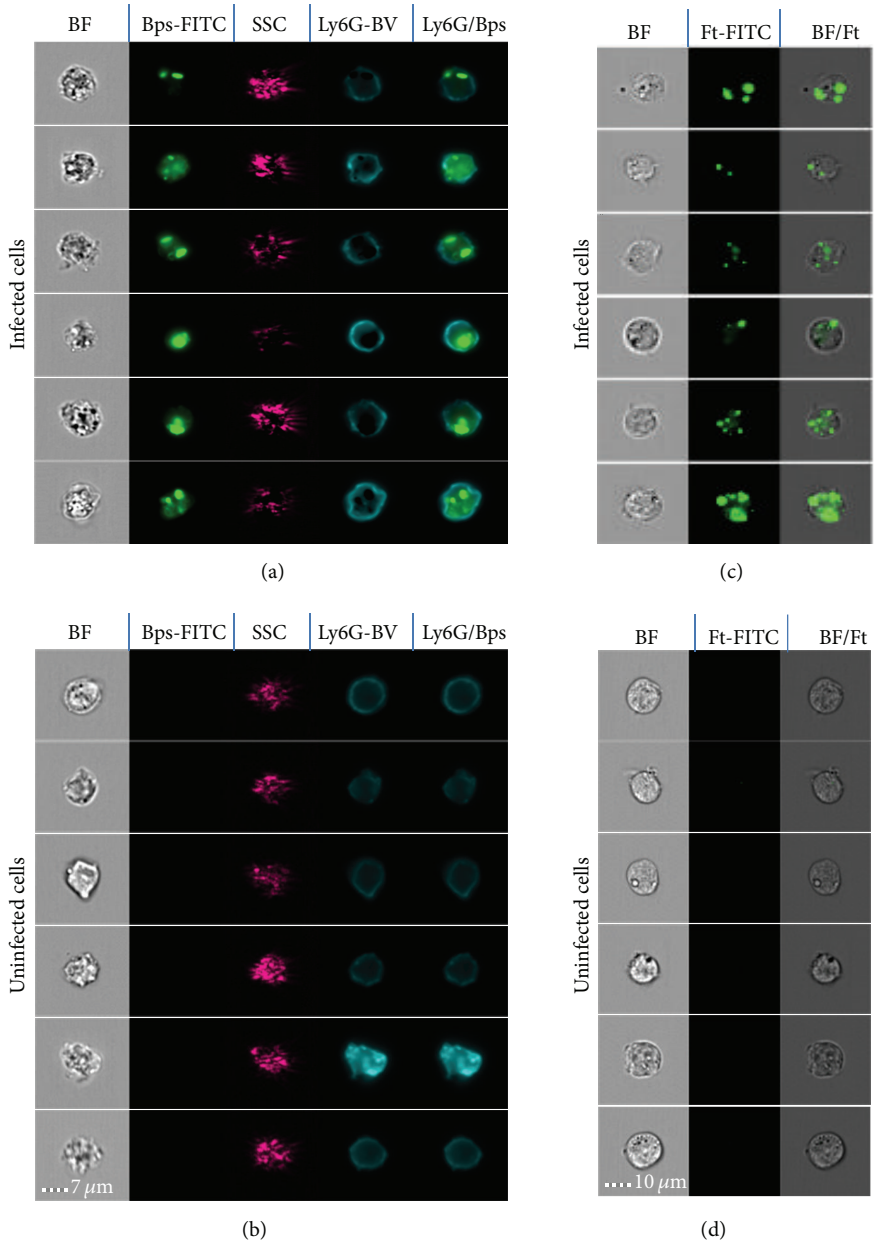

Figure 1: ImageStreamX Mk1 imaging depicting intracellular infection of *ex vivo* and *in vitro* cells. (a) Infected and (b) uninfected *ex vivo* lung cells stained with fluorescently labelled antibodies specific for *Burkholderia pseudomallei* (Bps) and the neutrophil marker Ly6G. A composite (overlayed) fluorescence image shows intracellular Bps inside neutrophils (Ly6G/Bps). Mouse macrophage cell line (P388D.1) infected (c) *in vitro* with *F. tularensis* SCHU S4 (Ft) or uninfected controls (d). Each Image series shows 6 representative cells from one sample. SSC = Side Scatter; BF = Brightfield; FITC = Fluorescein Isothiocyanate; BV = Brilliant Violet.

technologies and imaging technologies, it is anticipated that examining pathogen virulence whilst simultaneously interrogating host responses will be achieved. Overall, this should reduce and refine animal experiments and thus allow the identification of both host and pathogen markers during infection at the same time. This will further enhance our knowledge of host-pathogen interactions and aid in the development of vaccines and therapeutics for these dangerous pathogens.

Conflict of Interests

The authors declare that there is no conflict of interests regarding the publication of this paper.

Acknowledgment

The authors would like to acknowledge Dominic Jenner (Dstl) for his contribution to this review.

References

[1] B. A. Kidd, L. A. Peters, E. E. Schadt, and J. T. Dudley, "Unifying immunology with informatics and multiscale biology," *Nature Immunology*, vol. 15, no. 2, pp. 118–127, 2014.

[2] D. Stekel, *Microarray Bioinformatics*, Cambridge University Press, Cambridge, UK, 2003.

[3] J. A. Tree, M. J. Elmore, S. Javed, A. Williams, and P. D. Marsh, "Development of a guinea pig immune response-related microarray and its use to define the host response following *Mycobacterium bovis* BCG vaccination," *Infection and Immunity*, vol. 74, no. 2, pp. 1436–1441, 2006.

[4] N. A. Datson, M. C. Morsink, S. Atanasova et al., "Development of the first marmoset-specific DNA microarray (EUMAMA): a new genetic tool for large-scale expression profiling in a non-human primate," *BMC Genomics*, vol. 8, article 190, 2007.

[5] K. H. Rubins, L. E. Hensley, P. B. Jahrling et al., "The host response to smallpox: analysis of the gene expression program in peripheral blood cells in a nonhuman primate model," *Proceedings of the National Academy of Sciences of the United States of America*, vol. 101, no. 42, pp. 15190–15195, 2004.

[6] R. Jain, B. Dey, and A. K. Tyagi, "Development of the first oligonucleotide microarray for global gene expression profiling in guinea pigs: defining the transcription signature of infectious diseases," *BMC Genomics*, vol. 13, no. 1, article 520, 2012.

[7] C. E. Bruder, S. Yao, F. Larson et al., "Transcriptome sequencing and development of an expression microarray platform for the domestic ferret," *BMC Genomics*, vol. 11, article 251, no. 1, 2010.

[8] K. M. Chauncey, M. C. Lopez, G. Sidhu et al., "Bacillus anthracis'lethal toxin induces broad transcriptional responses in human peripheral monocytes," *BMC Immunology*, vol. 13, article 33, 2012.

[9] M. Dozmorov, W. Wu, K. Chakrabarty et al., "Gene expression profiling of human alveolar macrophages infected by B. anthracis spores demonstrates TNF-α and NF-κb are key components of the innate immune response to the pathogen," *BMC Infectious Diseases*, vol. 9, article 152, 2009.

[10] V. Wahl-Jensen, S. Kurz, F. Feldmann et al., "Ebola virion attachment and entry into human macrophages profoundly effects early cellular gene expression," *PLoS Neglected Tropical Diseases*, vol. 5, no. 10, Article ID e1359, 2011.

[11] J. T. Schwartz, S. Bandyopadhyay, S. D. Kobayashi et al., "Francisella tularensis alters human neutrophil gene expression: insights into the molecular basis of delayed neutrophil apoptosis," *Journal of Innate Immunity*, vol. 5, no. 2, pp. 124–136, 2013.

[12] C. Paranavitana, P. R. Pittman, M. Velauthapillai, E. Zelazowska, and L. DaSilva, "Transcriptional profiling of Francisella tularensis infected peripheral blood mononuclear cells: a predictive tool for tularemia," *FEMS Immunology and Medical Microbiology*, vol. 54, no. 1, pp. 92–103, 2008.

[13] J. P. Butchar, T. J. Cremer, C. D. Clay et al., "Microarray analysis of human monocytes infected with Francisella tularensis identifies new targets of host response subversion," *PLoS ONE*, vol. 3, no. 8, Article ID e2924, 2008.

[14] K. H. Rubins, L. E. Hensley, D. A. Relman, and P. O. Brown, "Stunned silence: gene expression programs in human cells infected with monkeypox or vaccinia virus," *PLoS ONE*, vol. 6, no. 1, Article ID e15615, 2011.

[15] R. Das, A. Dhokalia, X.-Z. Huang et al., "Study of proinflammatory responses induced by *Yersinia pestis* in human monocytes using cDNA arrays," *Genes and Immunity*, vol. 8, no. 4, pp. 308–319, 2007.

[16] D. Bourquain, P. W. Dabrowski, and A. Nitsche, "Comparison of host cell gene expression in cowpox, monkeypox or vaccinia virus-infected cells reveals virus-specific regulation of immune response genes," *Virology Journal*, vol. 10, article 61, 2013.

[17] J. E. Comer, C. L. Galindo, F. Zhang et al., "Murine macrophage transcriptional and functional responses to *Bacillus anthracis* edema toxin," *Microbial Pathogenesis*, vol. 41, no. 2-3, pp. 96–110, 2006.

[18] N. H. Bergman, K. D. Passalacqua, R. Gaspard, L. M. Shetron-Rama, J. Quackenbush, and P. C. Hanna, "Murine macrophage transcriptional responses to Bacillus anthracis infection and intoxication," *Infection and Immunity*, vol. 73, no. 2, pp. 1069–1080, 2005.

[19] C. A. Rossetti, K. L. Drake, and L. G. Adams, "Transcriptome analysis of HeLa cells response to *Brucella melitensis* infection: a molecular approach to understand the role of the mucosal epithelium in the onset of the *Brucella pathogenesis*," *Microbes and Infection*, vol. 14, no. 9, pp. 756–767, 2012.

[20] J. C. Kash, E. Mühlberger, V. Carter et al., "Global suppression of the host antiviral response by Ebola- and Marburgviruses: increased antagonism of the type I interferon response is associated with enhanced virulence," *Journal of Virology*, vol. 80, no. 6, pp. 3009–3020, 2006.

[21] A. Alkhalil, R. Hammamieh, J. Hardick, M. A. Ichou, M. Jett, and S. Ibrahim, "Gene expression profiling of monkeypox virus-infected cells reveals novel interfaces for host-virus interactions," *Virology Journal*, vol. 7, article 173, 2010.

[22] P. Wongprompitak, S. Sirisinha, and S. C. Chaiyaroj, "Differential gene expression profiles of lung epithelial cells exposed to Burkholderia pseudomallei and Burkholderia thailandensis during the initial phase of infection," *Asian Pacific Journal of Allergy and Immunology*, vol. 27, no. 1, pp. 59–70, 2009.

[23] C.-Y. Chin, D. M. Monack, and S. Nathan, "Delayed activation of host innate immune pathways in streptozotocin-induced diabetic hosts leads to more severe disease during infection with *Burkholderia pseudomallei*," *Immunology*, vol. 135, no. 4, pp. 312–332, 2012.

[24] C.-Y. Chin, D. M. Monack, and S. Nathan, "Genome wide transcriptome profiling of a murine acute melioidosis model reveals new insights into how Burkholderia pseudomallei overcomes host innate immunity," *BMC Genomics*, vol. 11, no. 1, article 672, 2010.

[25] A. Sharma and R. K. Maheshwari, "Oligonucleotide array analysis of Toll-like receptors and associated signalling genes in Venezuelan equine encephalitis virus-infected mouse brain," *Journal of General Virology*, vol. 90, no. 8, pp. 1836–1847, 2009.

[26] A. Sharma, B. Bhattacharya, R. K. Puri, and R. K. Maheshwari, "Venezuelan equine encephalitis virus infection causes modulation of inflammatory and immune response genes in mouse brain," *BMC Genomics*, vol. 9, article 289, 2008.

[27] J. David, A. J. Gates, G. D. Griffiths, and R. A. Lukaszewski, "Gene expression following low dose inhalational *Francisella tularensis* (SchuS4) exposure in Balb/c mice and the potential role of the epithelium and cell adhesion," *Microbes and Infection*, vol. 14, no. 4, pp. 369–379, 2012.

[28] H. Andersson, B. Hartmanová, P. Rydén, L. Noppa, L. Näslund, and A. Sjöstedt, "A microarray analysis of the murine macrophage response to infection with Francisella tularensis LVS," *Journal of Medical Microbiology*, vol. 55, no. 8, pp. 1023–1033, 2006.

[29] K.-A. Walters, R. Olsufka, R. E. Kuestner et al., "Francisella tularensis subsp. tularensis induces a unique pulmonary inflammatory response: role of bacterial gene expression in temporal regulation of host defense responses," *PLoS ONE*, vol. 8, no. 5, Article ID e62412, 2013.

[30] H. Andersson, B. Hartmanová, R. KuoLee et al., "Transcriptional profiling of host responses in mouse lungs following aerosol infection with type A Francisella tularensis," *Journal of Medical Microbiology*, vol. 55, no. 3, pp. 263–271, 2006.

[31] C. A. Rossetti, K. L. Drake, P. Siddavatam et al., "Systems biology analysis of brucella infected peyer's patch reveals rapid invasion with modest transient perturbations of the host transcriptome," *PLoS ONE*, vol. 8, no. 12, Article ID e81719, 2013.

[32] J. Y. Yen, S. Garamszegi, J. B. Geisbert et al., "Therapeutics of Ebola hemorrhagic fever: whole-genome transcriptional analysis of successful disease mitigation," *Journal of Infectious Diseases*, vol. 204, supplement 3, pp. S1043–S1052, 2011.

[33] D. Suwannasaen, J. Mahawantung, W. Chaowagul et al., "Human immune responses to Burkholderia pseudomallei characterized by protein microarray analysis," *Journal of Infectious Diseases*, vol. 203, no. 7, pp. 1002–1011, 2011.

[34] A. P. Cannella, J. C. Lin, L. Liang et al., "Serial kinetics of the antibody response against the complete Brucella melitensis ORFeome in focal vertebral brucellosis," *Journal of Clinical Microbiology*, vol. 50, no. 3, pp. 922–926, 2012.

[35] L. Liang, X. Tan, S. Juarez et al., "Systems biology approach predicts antibody signature associated with Brucella melitensis infection in humans," *Journal of Proteome Research*, vol. 10, no. 10, pp. 4813–4824, 2011.

[36] A. Vigil, R. Ortega, R. Nakajima-Sasaki et al., "Genome-wide profiling of humoral immune response to Coxiella burnetii infection by protein microarray," *Proteomics*, vol. 10, no. 12, pp. 2259–2269, 2010.

[37] A. Vigil, C. Chen, A. Jain et al., "Profiling the humoral immune response of acute and chronic Q fever by protein microarray," *Molecular & Cellular Proteomics*, vol. 10, no. 10, 2011.

[38] X. Xiong, X. Wang, B. Wen, S. Graves, and J. Stenos, "Potential serodiagnostic markers for Q fever identified in *Coxiella burnetii* by immunoproteomic and protein microarray approaches," *BMC Microbiology*, vol. 12, article 35, 2012.

[39] S. Keasey, C. Pugh, A. Tikhonov et al., "Proteomic basis of the antibody response to monkeypox virus infection examined in cynomolgus macaques and a comparison to human smallpox vaccination," *PLoS ONE*, vol. 5, no. 12, Article ID e15547, 2010.

[40] D. M. Klinman, S. Klaschik, K. Tomaru, H. Shirota, D. Tross, and H. Ikeuchi, "Immunostimulatory CpG oligonucleotides: effect on gene expression and utility as vaccine adjuvants," *Vaccine*, vol. 28, no. 8, pp. 1919–1923, 2010.

[41] S. Klaschik, I. Gursel, and D. M. Klinman, "CpG-mediated changes in gene expression in murine spleen cells identified by microarray analysis," *Molecular Immunology*, vol. 44, no. 6, pp. 1095–1104, 2007.

[42] S. Klaschik, D. Tross, and D. M. Klinman, "Inductive and suppressive networks regulate TLR9-dependent gene expression in vivo," *Journal of Leukocyte Biology*, vol. 85, no. 5, pp. 788–795, 2009.

[43] C. Paranavitana, L. DaSilva, A. Vladimirova, P. R. Pittman, M. Velauthapillai, and M. Nikolich, "Transcriptional profiling of recall responses to Francisella live vaccine strain," *Pathogens and Disease*, vol. 70, no. 2, pp. 141–152, 2014.

[44] J. E. Eyles, B. Unal, M. G. Hartley et al., "Immunodominant Francisella tularensis antigens identified using proteome microarray," *Proteomics*, vol. 7, no. 13, pp. 2172–2183, 2007.

[45] P. A. Beare, C. Chen, T. Bouman et al., "Candidate antigens for Q fever serodiagnosis revealed by immunoscreening of a Coxiella burnetii protein microarray," *Clinical and Vaccine Immunology*, vol. 15, no. 12, pp. 1771–1779, 2008.

[46] D. H. Davies, X. Liang, J. E. Hernandez et al., "Profiling the humoral immune response to infection by using proteome microarrays: high-throughput vaccine and diagnostic antigen discovery," *Proceedings of the National Academy of Sciences of the United States of America*, vol. 102, no. 3, pp. 547–552, 2005.

[47] D. H. Davies, D. M. Molina, J. Wrammert et al., "Proteome-wide analysis of the serological response to vaccinia and smallpox," *Proteomics*, vol. 7, no. 10, pp. 1678–1686, 2007.

[48] D. H. Davies, L. S. Wyatt, F. K. Newman et al., "Antibody profiling by proteome microarray reveals the immunogenicity of the attenuated smallpox vaccine modified vaccinia virus Ankara is comparable to that of Dryvax," *Journal of Virology*, vol. 82, no. 2, pp. 652–663, 2008.

[49] D. H. Davies, M. M. McCausland, C. Valdez et al., "Vaccinia virus H3L envelope protein is a major target of neutralizing antibodies in humans and elicits protection against lethal challenge in mice," *Journal of Virology*, vol. 79, no. 18, pp. 11724–11733, 2005.

[50] M. B. Townsend, M. S. Keckler, N. Patel et al., "Humoral immunity to smallpox vaccines and monkeypox virus challenge: proteomic assessment and clinical correlations," *Journal of Virology*, vol. 87, no. 2, pp. 900–911, 2013.

[51] G. Hermanson, S. Chun, J. Felgner et al., "Measurement of antibody responses to Modified Vaccinia virus Ankara (MVA) and Dryvax using proteome microarrays and development of recombinant protein ELISAs," *Vaccine*, vol. 30, no. 3, pp. 614–625, 2012.

[52] F. X. Sutandy, J. Qian, C. S. Chen, and H. Zhu, "Overview of protein microarrays," in *Current Protocols in Protein Science*, chapter 27, unit 27.1, 2013.

[53] N. Ramachandran, J. V. Raphael, E. Hainsworth et al., "Next-generation high-density self-assembling functional protein arrays," *Nature Methods*, vol. 5, no. 6, pp. 535–538, 2008.

[54] P. L. Felgner, M. A. Kayala, A. Vigil et al., "A Burkholderia pseudomallei protein microarray reveals serodiagnostic and cross-reactive antigens," *Proceedings of the National Academy of Sciences of the United States of America*, vol. 106, no. 32, pp. 13499–13504, 2009.

[55] T. W. Geisbert, H. A. Young, P. B. Jahrling, K. J. Davis, E. Kagan, and L. E. Hensley, "Mechanisms underlying coagulation abnormalities in ebola hemorrhagic fever: overexpression of tissue factor in primate monocytes/macrophages is a key event," *Journal of Infectious Diseases*, vol. 188, no. 11, pp. 1618–1629, 2003.

[56] H. Xie, I. Gursel, B. E. Ivins et al., "CpG oligodeoxynucleotides adsorbed onto polylactide-co-glycolide microparticles improve the immunogenicity and protective activity of the licensed anthrax vaccine," *Infection and Immunity*, vol. 73, no. 2, pp. 828–833, 2005.

[57] D. M. Klinman, H. Xie, and B. E. Ivins, "CpG oligonucleotides improve the protective immune response induced by the licensed anthrax vaccine," *Annals of the New York Academy of Sciences*, vol. 1082, pp. 137–150, 2006.

[58] L. Jing, S. M. McCaughey, D. H. Davies et al., "ORFeome approach to the clonal, HLA allele-specific CD4 T-cell response

to a complex pathogen in humans," *Journal of Immunological Methods*, vol. 347, no. 1-2, pp. 36–45, 2009.

[59] L. Jing, J. Haas, T. M. Chong et al., "Cross-presentation and genome-wide screening reveal candidate T cells antigens for a herpes simplex virus type 1 vaccine," *Journal of Clinical Investigation*, vol. 122, no. 8, p. 3024, 2012.

[60] M. A. Quail, M. Smith, P. Coupland et al., "A tale of three next generation sequencing platforms: comparison of Ion Torrent, Pacific Biosciences and Illumina MiSeq sequencers," *BMC Genomics*, vol. 13, no. 1, article 341, 2012.

[61] M. L. Metzker, "Sequencing technologies—the next generation," *Nature Reviews Genetics*, vol. 11, no. 1, pp. 31–46, 2010.

[62] N. J. Loman, R. V. Misra, T. J. Dallman et al., "Performance comparison of benchtop high-throughput sequencing platforms," *Nature Biotechnology*, vol. 30, no. 5, pp. 434–439, 2012.

[63] R. J. Roberts, M. O. Carneiro, and M. C. Schatz, "The advantages of SMRT sequencing," *Genome Biology*, vol. 14, no. 6, p. 405, 2013.

[64] G. F. Schneider and C. Dekker, "DNA sequencing with nanopores," *Nature Biotechnology*, vol. 30, no. 4, pp. 326–328, 2012.

[65] Z. Wang, M. Gerstein, and M. Snyder, "RNA-Seq: a revolutionary tool for transcriptomics," *Nature Reviews Genetics*, vol. 10, no. 1, pp. 57–63, 2009.

[66] A. Oshlack, M. D. Robinson, and M. D. Young, "From RNA-seq reads to differential expression results," *Genome Biology*, vol. 11, no. 12, article 220, 2010.

[67] J. R. Bradford, Y. Hey, T. Yates, Y. Li, S. D. Pepper, and C. J. Miller, "A comparison of massively parallel nucleotide sequencing with oligonucleotide microarrays for global transcription profiling," *BMC Genomics*, vol. 11, article 282, no. 1, 2010.

[68] S. Kogenaru, Y. Qing, Y. Guo, and N. Wang, "RNA-seq and microarray complement each other in transcriptome profiling," *BMC Genomics*, vol. 13, no. 1, article 629, 2012.

[69] C. Soneson and M. Delorenzi, "A comparison of methods for differential expression analysis of RNA-seq data," *BMC Bioinformatics*, vol. 14, article 91, 2013.

[70] S. Zhao, W. P. Fung-Leung, A. Bittner, K. Ngo, and X. Liu, "Comparison of RNA-Seq and microarray in transcriptome profiling of activated T cells," *PLoS ONE*, vol. 9, no. 1, Article ID e78644, 2014.

[71] Z. W. Bent, M. B. Tran-Gyamfi, S. A. Langevin et al., "Enriching pathogen transcripts from infected samples: a capture-based approach to enhanced host-pathogen RNA sequencing," *Analytical Biochemistry*, vol. 438, no. 1, pp. 90–96, 2013.

[72] Z. W. Bent, D. M. Brazel, M. B. Tran-Gyamfi, R. Y. Hamblin, V. A. VanderNoot, and S. S. Branda, "Use of a capture-based pathogen transcript enrichment strategy for RNA-Seq analysis of the Francisella Tularensis LVS transcriptome during infection of murine macrophages," *PLoS ONE*, vol. 8, no. 10, Article ID e77834, 2013.

[73] Y. Yan, S. Su, X. Meng et al., "Determination of sRNA expressions by RNA-seq in Yersinia pestis grown in vitro and during infection," *PLoS ONE*, vol. 8, no. 9, Article ID e74495, 2013.

[74] F. Wang, S. Hu, W. Liu, Z. Qiao, Y. Gao, and Z. Bu, "Deep-sequencing analysis of the mouse transcriptome response to infection with brucella melitensis strains of differing virulence," *PLoS ONE*, vol. 6, no. 12, Article ID e28485, 2011.

[75] K. Zheng, D.-S. Chen, Y.-Q. Wu et al., "MicroRNA expression profile in RAW264.7 cells in response to *Brucella melitensis* infection," *International Journal of Biological Sciences*, vol. 8, no. 7, pp. 1013–1022, 2012.

[76] O. M. Sessions, Y. Tan, K. C. Goh et al., "Host cell transcriptome profile during wild-type and attenuated dengue virus infection," *PLoS Neglected Tropical Diseases*, vol. 7, no. 3, Article ID e2107, 2013.

[77] A. J. Westermann, S. A. Gorski, and J. Vogel, "Dual RNA-seq of pathogen and host," *Nature Reviews Microbiology*, vol. 10, no. 9, pp. 618–630, 2012.

[78] G. Xu, E. K. Flemington, C. M. Taylor et al., "RNA CoMPASS: a dual approach for pathogen and host transcriptome analysis of RNA-seq datasets," *PLoS ONE*, vol. 9, no. 2, Article ID e89445, 2014.

[79] Z. Yang, D. P. Bruno, C. A. Martens, S. F. Porcella, and B. Moss, "Simultaneous high-resolution analysis of vaccinia virus and host cell transcriptomes by deep RNA sequencing," *Proceedings of the National Academy of Sciences of the United States of America*, vol. 107, no. 25, pp. 11513–11518, 2010.

[80] M. S. Humphrys, T. Creasy, Y. Sun et al., "Simultaneous transcriptional profiling of bacteria and their host cells," *PLoS ONE*, vol. 8, Article ID e80597, 2013.

[81] R. B. Kennedy, A. L. Oberg, I. G. Ovsyannikova, I. H. Haralambieva, D. Grill, and G. A. Poland, "Transcriptomic profiles of high and low antibody responders to smallpox vaccine," *Genes and Immunity*, vol. 14, no. 5, pp. 277–285, 2013.

[82] H. Robins, "Immunosequencing: applications of immune repertoire deep sequencing," *Current Opinion in Immunology*, vol. 25, no. 5, pp. 646–652, 2013.

[83] A. Six, M. E. Mariotti-Ferrandiz, W. Chaara et al., "The past, present, and future of immune repertoire biology—the rise of next-generation repertoire analysis," *Frontiers in Immunology*, vol. 4, p. 413, 2013.

[84] G. Georgiou, G. C. Ippolito, J. Beausang et al., "The promise and challenge of high-throughput sequencing of the antibody repertoire," *Nature Biotechnology*, vol. 32, no. 2, pp. 158–168, 2014.

[85] P. D. Baum, V. Venturi, and D. A. Price, "Wrestling with the repertoire: The promise and perils of next generation sequencing for antigen receptors," *European Journal of Immunology*, vol. 42, no. 11, pp. 2834–2839, 2012.

[86] J. Benichou, R. Ben-Hamo, Y. Louzoun, and S. Efroni, "Rep-Seq:uncovering the immunological repertoire through next-generation sequencing," *Immunology*, vol. 135, no. 3, pp. 183–191, 2012.

[87] P. Parameswaran, Y. Liu, K. M. Roskin et al., "Convergent antibody signatures in human dengue," *Cell Host & Microbe*, vol. 13, no. 6, pp. 691–700, 2013.

[88] J. D. Galson, A. J. Pollardemail, J. Trück, and D. F. Kelly, "Studying the antibody repertoire after vaccination: practical applications," *Trends in Immunology*, vol. 35, no. 7, pp. 319–331, 2014.

[89] J. A. Edwards, D. Rockx-Brouwer, V. Nair, and J. Celli, "Restricted cytosolic growth of Francisella tularensis subsp. tularensis by IFN-γ activation of macrophages," *Microbiology*, vol. 156, no. 2, pp. 327–339, 2010.

[90] A. M. Balagopal, A. S. MacFarlane, N. Mohapatra, S. Soni, J. S. Gunn, and L. S. Schlesinger, "Characterization of the receptor-ligand pathways important for entry and survival of Francisella tularensis in human macrophages," *Infection and Immunity*, vol. 74, no. 9, pp. 5114–5125, 2006.

[91] R. Copin, M. A. Vitry, D. Hanot Mambres et al., "In situ microscopy analysis reveals local innate immune response

developed around Brucella infected cells in resistant and susceptible mice," *PLoS Pathogens*, vol. 8, no. 3, Article ID e1002575, 2012.

[92] R. A. Lukaszewski, D. J. Kenny, R. Taylor, D. G. C. Rees, M. G. Hartley, and P. C. F. Oyston, "Pathogenesis of *Yersinia pestis* infection in BALB/c mice: effects on host macrophages and neutrophils," *Infection and Immunity*, vol. 73, no. 11, pp. 7142–7150, 2005.

[93] T. R. Laws, M. S. Davey, R. W. Titball, and R. Lukaszewski, "Neutrophils are important in early control of lung infection by Yersinia pestis," *Microbes and Infection*, vol. 12, no. 4, pp. 331–335, 2010.

[94] R. D. Pechous, V. Sivaraman, P. A. Price, N. M. Stasulli, and W. E. Goldman, "Early host cell targets of *Yersinia pestis* during primary pneumonic plague," *PLoS Pathogens*, vol. 9, no. 10, Article ID e1003679, 2013.

[95] C. M. G. Bosio, A. W. Goodyear, and S. W. Dow, "Early interaction of *Yersinia pestis* with APCs in the lung," *The Journal of Immunology*, vol. 175, no. 10, pp. 6750–6756, 2005.

[96] C. F. Bosio, C. O. Jarrett, D. Gardner, and B. J. Hinnebusch, "Kinetics of innate immune response to Yersinia pestis after intradermal infection in a mouse model," *Infection and Immunity*, vol. 80, no. 11, pp. 4034–4045, 2012.

[97] T. R. Laws, S. J. Smither, R. A. Lukaszewski, and H. S. Atkins, "Neutrophils are the predominant cell-type to associate with Burkholderia pseudomallei in a BALB/c mouse model of respiratory melioidosis," *Microbial Pathogenesis*, vol. 51, no. 6, pp. 471–475, 2011.

[98] C. A. Rowland, M. S. Lever, K. F. Griffin, G. J. Bancroft, and R. A. Lukaszewski, "Protective cellular responses to Burkholderia mallei infection," *Microbes and Infection*, vol. 12, no. 11, pp. 846–853, 2010.

[99] S. Chanchamroen, C. Kewcharoenwong, W. Susaengrat, M. Ato, and G. Lertmemongkolchai, "Human polymorphonuclear neutrophil responses to *Burkholderia pseudomallei* in healthy and diabetic subjects," *Infection and Immunity*, vol. 77, no. 1, pp. 456–463, 2009.

[100] B. M. Judy, K. Taylor, A. Deeraksa et al., "Prophylactic application of CpG oligonucleotides augments the early host response and confers protection in acute melioidosis," *PLoS ONE*, vol. 7, no. 3, Article ID e34176, 2012.

[101] T. R. Laws, "In vivo Manipulation of $\gamma 9^+$ T cells in the common marmoset (*Callithrix Jacchus*) with phosphoantigen and effect on the progression of respiratory melioidosis," *PLoS ONE*, vol. 8, no. 9, Article ID e74789, 2013.

[102] J. A. Skyberg, M. F. Rollins, J. S. Holderness et al., "Nasal acai polysaccharides potentiate innate immunity to protect against pulmonary Francisella tularensis and Burkholderia pseudomallei infections," *PLoS Pathogens*, vol. 8, no. 3, Article ID e1002587, 2012.

[103] K. L. Propst, R. M. Troyer, L. M. Kellihan, H. P. Schweizer, and S. W. Dow, "Immunotherapy markedly increases the effectiveness of antimicrobial therapy for treatment of Burkholderia pseudomallei infection," *Antimicrobial Agents and Chemotherapy*, vol. 54, no. 5, pp. 1785–1792, 2010.

[104] R. V. D'Elia, T. R. Laws, A. Carter, R. Lukaszewski, and G. C. Clark, "Targeting the "rising DAMP" during a Francisella tularensis infection," *Antimicrobial Agents and Chemotherapy*, vol. 57, no. 9, pp. 4222–4228, 2013.

[105] A. Easton, K. Chu, N. Patel et al., "Combining vaccination and postexposure CpG therapy provides optimal protection against lethal sepsis in a biodefense model of human melioidosis," *Journal of Infectious Diseases*, vol. 204, no. 4, pp. 636–644, 2011.

[106] A. Haque, K. Chu, A. Easton et al., "A live experimental vaccine against Burkholderia pseudomallei elicits CD4+ T cell-mediated immunity, priming T cells specific for 2 type III secretion system proteins," *Journal of Infectious Diseases*, vol. 194, no. 9, pp. 1241–1248, 2006.

[107] D. M. Schmitt, D. M. O'Dee, J. Horzempa et al., "A Francisella tularensis live vaccine strain that improves stimulation of antigen-presenting cells does not enhance vaccine efficacy," *PLoS ONE*, vol. 7, no. 2, Article ID e31172, 2012.

[108] Q. Jia, R. Bowen, J. Sahakian, B. J. Dillon, and M. A. Horwitz, "A heterologous prime-boost vaccination strategy comprising the *Francisella tularensis* live vaccine strain *capB* mutant and recombinant attenuated *Listeria monocytogenes* expressing *F. tularensis* IglC induces potent protective immunity in mice against virulent *F. tularensis* aerosol challenge," *Infection and Immunity*, vol. 81, no. 5, pp. 1550–1561, 2013.

[109] G. C. Whitlock, R. A. Lukaszewski, B. M. Judy, S. Paessler, A. G. Torres, and D. M. Estes, "Host immunity in the protective response to vaccination with heat-killed Burkholderia mallei," *BMC Immunology*, vol. 9, article 55, 2008.

[110] G. J. Hatch, V. A. Graham, K. R. Bewley et al., "Assessment of the protective effect of imvamune and Acam2000 vaccines against aerosolized monkeypox virus in cynomolgus macaques," *Journal of Virology*, vol. 87, no. 14, pp. 7805–7815, 2013.

[111] K. Eneslätt, M. Normark, R. Björk et al., "Signatures of T cells as correlates of immunity to *Francisella tularensis*," *PLoS ONE*, vol. 7, no. 3, Article ID e32367, 2012.

[112] A. Sjöstedt, M. Eriksson, G. Sandström, and A. Tärnvik, "Various membrane proteins of Francisella tularensis induce interferon-γ production in both CD4+ and CD8+ T cells of primed humans," *Immunology*, vol. 76, no. 4, pp. 584–592, 1992.

[113] A. Tarnvik, M. L. Lofgren, S. Lofgren, G. Sandström, and H. Wolf-Watz, "Long-lasting cell-mediated immunity induced by a live Francisella tularensis vaccine," *Journal of Clinical Microbiology*, vol. 22, no. 4, pp. 527–530, 1985.

[114] E. D. Williamson, H. C. Flick-Smith, C. LeButt et al., "Human immune response to a plague vaccine comprising recombinant F1 and V antigens," *Infection and Immunity*, vol. 73, no. 6, pp. 3598–3608, 2005.

[115] R. Ali, R. A. Naqvi, S. Kumar, A. A. Bhat, and D. N. Rao, "Multiple Antigen Peptide Containing B and T Cell Epitopes of F1 Antigen of Yersinia pestis Showed Enhanced Th1 Immune Response in Murine Model," *Scandinavian Journal of Immunology*, vol. 77, no. 5, pp. 361–371, 2013.

[116] P. P. Tippayawat, M. Pinsiri, D. Rinchai et al., "*Burkholderia pseudomallei* proteins presented by monocyte-derived dendritic cells stimulate human memory T cells *in vitro*," *Infection and Immunity*, vol. 79, no. 1, pp. 305–313, 2011.

[117] E. B. Silva, A. Goodyear, M. D. Sutherland et al., "Correlates of immune protection following cutaneous immunization with an attenuated *Burkholderia pseudomallei* vaccine," *Infection and Immunity*, vol. 81, no. 12, pp. 4626–4634, 2013.

[118] N. Kurosawa, M. Yoshioka, R. Fujimoto, F. Yamagishi, and M. Isobe, "Rapid production of antigen-specific monoclonal antibodies from a variety of animals," *BMC Biology*, vol. 10, p. 80, 2012.

[119] M. M. Coughlin and B. S. Prabhakar, "Neutralizing human monoclonal antibodies to severe acute respiratory syndrome coronavirus: target, mechanism of action, and therapeutic

potential," *Reviews in Medical Virology*, vol. 22, no. 1, pp. 2–17, 2012.

[120] B. L. Marrone, "Flow cytometry: a multipurpose technology for a wide spectrum of global biosecurity applications ," *Journal of the Association for Laboratory Automation*, vol. 14, no. 3, pp. 148–156, 2009.

[121] M. Santic, R. Asare, I. Skrobonja, S. Jones, and Y. A. Kwaik, "Acquisition of the vacuolar ATPase proton pump and phagosome acidification are essential for escape of *Francisella tularensis* into the macrophage cytosol," *Infection and Immunity*, vol. 76, no. 6, pp. 2671–2677, 2008.

[122] J. T. Schwartz, J. H. Barker, M. E. Long, J. Kaufman, J. McCracken, and L.-A. H. Allen, "Natural IgM mediates complement-dependent uptake of *Francisella tularensis* by human neutrophils via complement receptors 1 and 3 in nonimmune serum," *The Journal of Immunology*, vol. 189, no. 6, pp. 3064–3077, 2012.

[123] S. Dai, M. V. S. Rajaram, H. M. Curry, R. Leander, and L. S. Schlesinger, "Fine Tuning Inflammation at the Front Door: Macrophage Complement Receptor 3-mediates Phagocytosis and Immune Suppression for Francisella tularensis," *PLoS Pathogens*, vol. 9, no. 1, Article ID e1003114, 2013.

[124] D. L. Clemens, B.-Y. Lee, and M. A. Horwitz, "Francisella tularensis phagosomal escape does not require acidification of the phagosome," *Infection and Immunity*, vol. 77, no. 5, pp. 1757–1773, 2009.

[125] M. N. Burtnick, D. DeShazer, V. Nair, F. C. Gherardini, and P. J. Brett, "*Burkholderia mallei* cluster 1 type VI secretion mutants exhibit growth and actin polymerization defects in RAW 264.7 murine macrophages," *Infection and Immunity*, vol. 78, no. 1, pp. 88–99, 2010.

[126] D. L. Clemens, B.-Y. Lee, and M. A. Horwitz, "O-antigen-deficient francisella tularensis live vaccine strain mutants are ingested via an aberrant form of looping phagocytosis and show altered kinetics of intracellular trafficking in human macrophages," *Infection and Immunity*, vol. 80, no. 3, pp. 952–967, 2012.

[127] M. Cullinane, L. Gong, X. Li et al., "Stimulation of autophagy suppresses the intracellular survival of Burkholderia pseudomallei in mammalian cell lines," *Autophagy*, vol. 4, no. 6, pp. 744–753, 2008.

[128] S. Steele, J. Brunton, B. Ziehr, S. Taft-Benz, N. Moorman, and T. Kawula, "Francisella tularensis Harvests Nutrients Derived via ATG5-Independent Autophagy to Support Intracellular Growth," *PLoS Pathogens*, vol. 9, no. 8, Article ID e1003562, 2013.

[129] H.-C. Chiu, S. Soni, S. K. Kulp et al., "Eradication of intracellular Francisella tularensis in THP-1 human macrophages with a novel autophagy inducing agent," *Journal of Biomedical Science*, vol. 16, article 110, no. 1, 2009.

[130] M. Aguilera, R. Salinas, E. Rosales, S. Carminati, M. I. Colombo, and W. Berón, "Actin dynamics and Rho GTPases regulate the size and formation of parasitophorous vacuoles containing *Coxiella burnetii*," *Infection and Immunity*, vol. 77, no. 10, pp. 4609–4620, 2009.

[131] G. Pegoraro, B. P. Eaton, R. L. Ulrich et al., "A high-content imaging assay for the quantification of the Burkholderia pseudomallei induced multinucleated giant cell (MNGC) phenotype in murine macrophages," *BMC Microbiology*, vol. 14, p. 98, 2014.

[132] C. J. Empig and M. A. Goldsmith, "Association of the caveola vesicular system with cellular entry by filoviruses," *Journal of Virology*, vol. 76, no. 10, pp. 5266–5270, 2002.

[133] E. Adu-Gyamfi, M. A. Digman, E. Gratton, and R. V. Stahelin, "Investigation of Ebola VP40 assembly and oligomerization in live cells using number and brightness analysis," *Biophysical Journal*, vol. 102, no. 11, pp. 2517–2525, 2012.

[134] M. Trunschke, D. Conrad, S. Enterlein, J. Olejnik, K. Brauburger, and E. Mühlberger, "The L-VP35 and L-L interaction domains reside in the amino terminus of the Ebola virus L protein and are potential targets for antivirals," *Virology*, vol. 441, no. 2, pp. 135–145, 2013.

[135] W. D. Splettstoesser, E. Seibold, E. Zeman, K. Trebesius, and A. Podbielski, "Rapid differentiation of *Francisella* species and subspecies by fluorescent in situ hybridization targeting the 23S rRNA," *BMC Microbiology*, vol. 10, article 72, 2010.

[136] X. Xiao, Z. Zhu, J. L. Dankmeyer et al., "Human anti-plague monoclonal antibodies protect mice from Yersinia pestis in a bubonic plague model," *PLoS ONE*, vol. 5, no. 10, Article ID e13047, 2010.

[137] J. G. H. Shannon, A. M. Dorward, D. W. Nair, V. Carmody, A. B. Hinnebusch, and B. J. Yersinia pestis, "Yersinia pestis subverts the dermal neutrophil response in a mouse model of bubonic plague," *mBio*, vol. 4, no. 5, p. e00170, 2013.

[138] N. Andreu, A. Zelmer, and S. Wiles, "Noninvasive biophotonic imaging for studies of infectious disease," *FEMS Microbiology Reviews*, vol. 35, no. 2, pp. 360–394, 2011.

[139] P. Sanz, L. D. Teel, F. Alem, H. M. Carvalho, S. C. Darnell, and A. D. O'Brien, "Detection of Bacillus anthracis spore germination in vivo by bioluminescence imaging," *Infection and Immunity*, vol. 76, no. 3, pp. 1036–1047, 2008.

[140] I. J. Glomski, F. Dumetz, G. Jouvion, M. R. Huerre, M. Mock, and P. L. Goossens, "Inhaled non-capsulated *Bacillus anthracis* in A/J mice: nasopharynx and alveolar space as dual portals of entry, delayed dissemination, and specific organ targeting," *Microbes and Infection*, vol. 10, no. 12-13, pp. 1398–1404, 2008.

[141] I. J. Glomski, J.-P. Corre, M. Mock, and P. L. Goossens, "Noncapsulated toxinogenic Bacillus anthracis presents a specific growth and dissemination pattern in naive and protective antigen-immune mice," *Infection and Immunity*, vol. 75, no. 10, pp. 4754–4761, 2007.

[142] T. Nham, S. Filali, C. Danne, A. Derbise, and E. Carniel, "Imaging of bubonic plague dynamics by in vivo tracking of bioluminescent yersinia pestis," *PLoS ONE*, vol. 7, no. 4, Article ID e34714, 2012.

[143] R. J. Gonzalez, E. H. Weening, R. Frothingham, G. D. Sempowski, and V. L. Miller, "Bioluminescence imaging to track bacterial dissemination of Yersinia pestis using different routes of infection in mice," *BMC Microbiology*, vol. 12, article 147, 2012.

[144] Y. Sun, M. G. Connor, J. M. Pennington, and M. B. Lawrenz, "Development of bioluminescent bioreporters for in vitro and in vivo tracking of *Yersinia pestis*," *PLoS ONE*, vol. 7, no. 10, Article ID e47123, 2012.

[145] J. Sha, J. A. Rosenzweig, M. L. Kirtley et al., "A non-invasive *in vivo* imaging system to study dissemination of bioluminescent *Yersinia pestis* CO92 in a mouse model of pneumonic plague," *Microbial Pathogenesis*, vol. 55, no. 1, pp. 39–50, 2013.

[146] X. R. Bina, M. A. Miller, and J. E. Bina, "Construction of a bioluminescence reporter plasmid for Francisella tularensis," *Plasmid*, vol. 64, no. 3, pp. 156–161, 2010.

[147] M. A. Miller, J. M. Stabenow, J. Parvathareddy et al., "Visualization of murine intranasal dosing efficiency using luminescent Francisella tularensis: effect of instillation volume and form of anesthesia," *PLoS ONE*, vol. 7, no. 2, Article ID e31359, 2012.

[148] J. M. Warawa, D. Long, R. Rosenke, D. Gardner, and F. C. Gherardini, "Bioluminescent diagnostic imaging to characterize altered respiratory tract colonization by the Burkholderia pseudomallei capsule mutant," *Frontiers in Microbiology*, vol. 2, article 133, 2011.

[149] S. J. Owen, M. Batzloff, F. Chehrehasa et al., "Nasal-associated lymphoid tissue and olfactory epithelium as portals of entry for burkholderia pseudomallei in murine melioidosis," *Journal of Infectious Diseases*, vol. 199, no. 12, pp. 1761–1770, 2009.

[150] S. Massey, K. Johnston, T. M. Mott et al., "In vivo bioluminescence imaging of burkholderia mallei respiratory infection and treatment in the mouse model," *Frontiers in Microbiology*, vol. 2, article 174, 2011.

[151] T. M. Mott, R. Katie Johnston, S. Vijayakumar et al., "Monitoring therapeutic treatments against infections using imaging techniques," *Pathogens*, vol. 2, no. 2, pp. 383–401, 2013.

[152] D. M. Waag, M. J. McCluskie, N. Zhang, and A. M. Krieg, "A CpG oligonucleotide can protect mice from a low aerosol challenge dose of *Burkholderia mallei*," *Infection and Immunity*, vol. 74, no. 3, pp. 1944–1948, 2006.

[153] F. Dumetz, G. Jouvion, H. Khun et al., "Noninvasive imaging technologies reveal edema toxin as a key virulence factor in anthrax," *The American Journal of Pathology*, vol. 178, no. 6, pp. 2523–2535, 2011.

[154] S. E. Autenrieth, P. Warnke, G. H. Wabnitz et al., "Depletion of dendritic cells enhances innate anti-bacterial host defense through modulation of phagocyte homeostasis," *PLoS Pathogens*, vol. 8, no. 2, Article ID e1002552, 2012.

[155] I. Safeukui, P. A. Buffet, S. Perrot et al., "Surface area loss and increased sphericity account for the splenic entrapment of subpopulations of Plasmodium falciparum ring-infected erythrocytes," *PLoS ONE*, vol. 8, no. 3, Article ID e60150, 2013.

[156] P.-Y. Mantel, A. N. Hoang, I. Goldowitz et al., "Malaria-infected erythrocyte-derived microvesicles mediate cellular communication within the parasite population and with the host immune system," *Cell Host & Microbe*, vol. 13, no. 5, pp. 521–534, 2013.

[157] S. N. Bartley, Y.-L. Tzeng, K. Heel et al., "Attachment and invasion of neisseria meningitidis to host cells is related to surface hydrophobicity, bacterial cell size and capsule," *PLoS ONE*, vol. 8, no. 2, Article ID e55798, 2013.

[158] E. A. Durand, F. J. Maldonado-Arocho, C. Castillo, R. L. Walsh, and J. Mecsas, "The presence of professional phagocytes dictates the number of host cells targeted for Yop translocation during infection," *Cellular Microbiology*, vol. 12, no. 8, pp. 1064–1082, 2010.

[159] J. Dyall, R. F. Johnson, D.-Y. Chen et al., "Evaluation of monkeypox disease progression by molecular imaging," *Journal of Infectious Diseases*, vol. 204, no. 12, pp. 1902–1911, 2011.

[160] K. Li, D. Thomasson, L. Ketai et al., "Potential applications of conventional and molecular imaging to biodefense research," *Clinical Infectious Diseases*, vol. 40, no. 10, pp. 1471–1480, 2005.

[161] H. H. S. Food and Drug Administration, "New drug and biological drug products; evidence needed to demonstrate effectiveness of new drugs when human efficacy studies are not ethical or feasible. Final rule," *Federal Register*, vol. 67, no. 105, pp. 37988–37998, 2002.

Hindawi Publishing Corporation
Journal of Immunology Research
Volume 2014, Article ID 913632, 8 pages
http://dx.doi.org/10.1155/2014/913632

Research Article

Exploring the Innate Immunological Response of an Alternative Nonhuman Primate Model of Infectious Disease; the Common Marmoset

M. Nelson and M. Loveday

Biomedical Science Department, DSTL, Porton Down, Salisbury SP4 0JQ, UK

Correspondence should be addressed to M. Nelson; mnelson@dstl.gov.uk

Received 19 February 2014; Revised 6 May 2014; Accepted 20 May 2014; Published 22 July 2014

Academic Editor: Louise Pitt

The common marmoset (*Callithrix jacchus*) is increasingly being utilised as a nonhuman primate model for human disease, ranging from autoimmune to infectious disease. In order to fully exploit these models, meaningful comparison to the human host response is necessary. Commercially available reagents, primarily targeted to human cells, were utilised to assess the phenotype and activation status of key immune cell types and cytokines in naive and infected animals. Single cell suspensions of blood, spleen, and lung were examined. Generally, the phenotype of cells was comparable between humans and marmosets, with approximately 63% of all lymphocytes in the blood of marmosets being T cells, 25% B-cells, and 12% NK cells. The percentage of neutrophils in marmoset blood were more similar to human values than mouse values. Comparison of the activation status of cells following experimental systemic or inhalational infection exhibited different trends in different tissues, most obvious in cell types active in the innate immune response. This work significantly enhances the ability to understand the immune response in these animals and fortifies their use as models of infectious disease.

1. Introduction

The common marmoset (*Callithrix jacchus*), a New World monkey (NWM) species is a small, arboreal nonhuman primate (NHP), native to the Atlantic Coastal Forest in Northeast Brazil and parts of South East Brazil. In recent years the common marmoset has become more widely used in applied biomedical research, and an increasing body of evidence suggests the physiological and immunological responses to biological insults are similar between marmosets and humans [1]. In the field of infectious disease, the marmoset is primarily being investigated as an alternative NHP model to complement the more traditionally used Old World monkeys (OWM) (e.g., rhesus and cynomolgus macaques). Evolutionarily, both NWM and OWM sit within the simiiformes infraorder of the suborder *Haplorhini* of primates [2]. Marmosets sit within the family Callitrichidae of the Platyrrhini parvorder, while OWM sit within the Cercopithecidae family of the Catarrhini Parvorder. Marmosets therefore are separated from Old World monkeys by one ancestral step and are a lower order primate.

Marmosets have been used to model the infection syndrome caused by a number of public health pathogens including Lassa virus [3], Hepatitis C virus [4], Dengue virus [5], Herpesvirus [6], Junin virus [7] Rift Valley Fever [8], and SARS [9]. Marmosets have also been used to model a number of biodefense pathogens including Eastern Equine Encephalitis virus [10], *Bacillus anthracis* [11], *Francisella tularensis* [12, 13], *Burkholderia pseudomallei* [14], Marburg haemorrhagic fever virus [15, 16], Ebola haemorrhagic fever virus [16], and Variola virus [17]. The utility of marmosets to assess medical countermeasures has also been demonstrated; a vaccine has been tested for Lassa fever [18] and the efficacy of ciprofloxacin and levofloxacin has been tested as postexposure therapies for anthrax and tularemia, respectively [19, 20].

In order to exploit these models fully and to allow meaningful comparison with the human condition, the response of the immune system to infection/therapy needs to be

characterised and understood. Generally, NHPs have a close molecular, immunological, reproductive, and neurological similarity with humans making them ideal surrogates for humans and the study of infectious diseases. There is a high level of gene homology between humans and NHPs which underlies physiological and biochemical similarities. Similarities at the genetic level extend to the phenotypical level making NHPs well suited to modelling pathophysiological responses in man [21]. Immunologically, there is a high degree of homology between humans and marmosets [22]. The similarity of various immunological factors produced by humans and marmosets has been investigated at both the genetic and protein levels. There is at least 95% homology between human costimulatory molecules (e.g., CD80, CD86 etc.) and those of marmosets [23]. Also the immunoglobulin and T-cell receptor repertoire of humans and marmosets show at least 80% homology [24, 25].

Currently, the availability of commercial reagents specifically designed for the marmoset is limited although a number of antibodies designed for use with human samples have been shown to cross-react with leucocytes from marmoset blood [26–28]. However, these reagents have not been exploited to investigate the immune response to infectious disease. To date, investigation of the immune response in marmosets has primarily been achieved using pathogen-specific antibodies to determine the serological response using ELISA such as in the smallpox, Dengue, Rift Valley Fever, and Herpes models [5, 6, 8, 17] or by immunohistochemistry to identify, for example, CD8+, CD3+, CD20+ cells, and IL-6 in the smallpox model [17]; neutrophils and macrophages in the Herpes model [6]; or CD3+ and CD20+ cells in the Lassa model [3].

The work presented here focuses on understanding the immune profile of the naive marmoset as well as identifying and quantifying the immune response to infectious disease. The aim of this work is to determine key changes and identify correlates of infection or protection.

2. Materials and Methods

2.1. Marmosets. Healthy sexually mature common marmosets (*C. jacchus*) were obtained from the Dstl Porton Down breeding colony and housed in vasectomized male and female pairs. The Dstl colony was established during the 1970s and is a closed colony with a stable genotype. Animals included in these studies were mixed sex pairs, between 18 months and 5 years old and weighing between 320 g to 500 g. All animals were allowed free access to food and water as well as environmental enrichment. All animal studies were carried out in accordance with the UK Animals (Scientific Procedures) Act of 1986 and the Codes of Practice for the Housing and Care of Animals used in Scientific Procedures 1989. Animals were challenged with an intracellular pathogen by either the subcutaneous or inhalational route and were humanely killed at various time points after challenge. Prior to the infection study, animals were bled to determine baseline immunological parameters. Studies were performed to establish infection models in order to evaluate the efficacy of suitable therapies for transition ultimately to the clinic.

2.2. Flow Cytometry on Leucocyte Populations. Blood and tissue samples were homogenised to provide single cell suspensions [12]. Red blood cells were lysed, and the mixed leucocyte population was washed and stained with various combinations of the following fluorescent antibody stains: CD3 (SP34-2), CD8 (LT8), CD11c (SHCL3), CD14 (M5E2), CD16 (3G8), CD20 (Bly1), CD45RA (5H9), CD54 (HCD54), CD56 (B159), CD69 (FN50), CD163 (GHI/61), and MCHII (L243) (BD Bioscience, Insight Bioscience, AbD serotec). Samples were fixed in 4% paraformaldehyde for 48 hrs at 4°C and analysed by flow cytometry (FACScanto II BD) within 72 hours of staining.

Levels of circulating cytokines and chemokines were also quantified in the blood of marmosets from the Dstl colony using human multiplex kits available commercially (BD cytokine flex beads and the Luminex system). These systems show significant cross-reactivity with the marmoset suggesting a high degree of conservation between the two species for IL-6, MIP-1α, MIP-1β, and MCP-1 [29]. However, for other cytokines that are pivotal in the innate response, TNFα and IFNγ reagents were obtained from U-CyTech Biosciences and Mabtech AB, respectively, due to a lack of cross-reactivity observed within the kit obtained from BD [13].

3. Results and Discussion

In order to fully characterise the immune response to infectious agent in the marmoset, single cell suspensions of lung and spleen tissue were also examined in conjunction with the traditionally used blood cells. These tissue homogenates are of particular interest in relation to target sites of infection: the lung as the site of initial infection following an inhalational challenge and the spleen as a representative organ following a parental challenge. Cell types targeted during this analysis include cells important in the innate response (e.g., neutrophils, macrophages, and NK cells) and the adaptive response (T and B cells) with a view to determine the response to infection and vaccination and to derive immune correlates of infection/protection. Dapi was included as a nuclear marker to ensure that the initial gating included only intact cells. Basic cell types in blood were easily identified by measuring size (forward) and granularity (side) scatter (Figure 1(a)). Identification of cell types in tissue samples was more difficult as the scatter profiles are less clearly compartmentalized. The common leukocyte antigen (CD45) normally used to locate all leukocytes in human samples also worked well in marmoset blood but failed to provide relevant information in the tissue samples. Confirmation of neutrophil identification was done by nuclear morphology and macrophages were identified by their adherent nature in initial experiments (data not shown). Neutrophils were stained as CD11c dim CD14− and macrophages as CD11c + CD14+ regardless of tissue origin (Figure 1(b)). Figure 1(c)

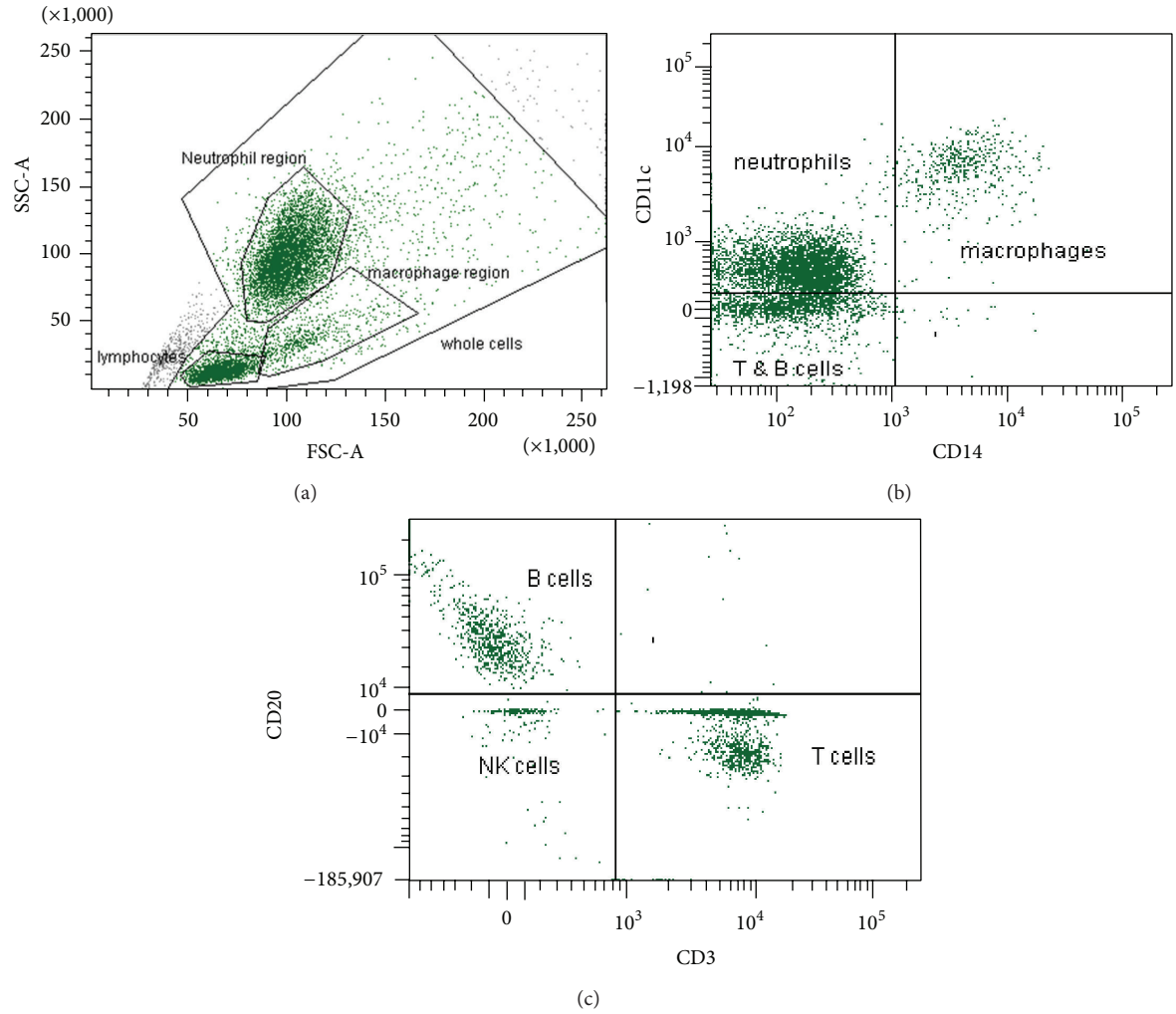

Figure 1: Flow cytometry plots. (a) Typical scatter profile from naïve marmoset blood showing the difference in size (FSC) and granularity (SSC) of the basic cell types. (b) Expression of CD11c and CD14 on monocytes/macrophages and neutrophils and (c) CD20 and CD3 expression on lymphocytes.

shows the basic division of lymphocytes between T, B, and NK cells from a healthy blood sample.

Using this approach, the percentage of NK cells, B-cells, total T-cells, CD8+ T-cells, neutrophils, and monocytes was determined in the blood of naive marmosets (Figure 2(a), Table 1); approximately 63% of all lymphocytes were T cells, 25% B cells, and 12% NK cells. The variability of the data is depicted in Figure 2(a) with the greatest variability observed in the proportion of neutrophils. There were no obvious differences attributable to age or sex of the animals. This analysis was also applied to lung and spleen homogenates from naive marmosets (Figures 2(b) and 2(c)). Greater variability was observed in the data relating to the identification of cell types in tissue samples, attributed to the inherent difficulties in identifying cell types in tissue homogenates by size and granularity and also the smaller cohort of animals. As expected, low numbers of neutrophils are found in naive spleen or lung tissue (8% both). Healthy mouse spleens typically have approximately 1-2% granulocytes [30]. Understandably, there are few reports on the typical cell percentages expected in healthy human individuals for these tissues. However, it is reported that B cells are more prevalent in the spleens of humans at a ratio of 5 to 4 B to T cells than in the lungs which have a ratio of 1 to 8 B to T cells [34]. In marmoset data reported here, a ratio of 2 to 3 B to T cells in the spleen and 1 to 6 B to T-cells in the lungs was observed compared to a ratio of 3 to 2 B to T cells in mouse spleens [30].

Upon comparison, the marmoset data is generally consistent with previously reported data which is only available for marmoset blood samples [27] and information available for human blood [32, 33] (Table 1). However, one report found the proportion of CD8+ T-cells was almost three times greater in marmosets than humans, 61% to 21% respectively [35] compared to the 30% observed in this study and the work previously reported by Brok et al. [27]. Brok's study involved a small number of animals (eight) and also used a different CD8+ clone to identify cells. Contrastingly, in mice,

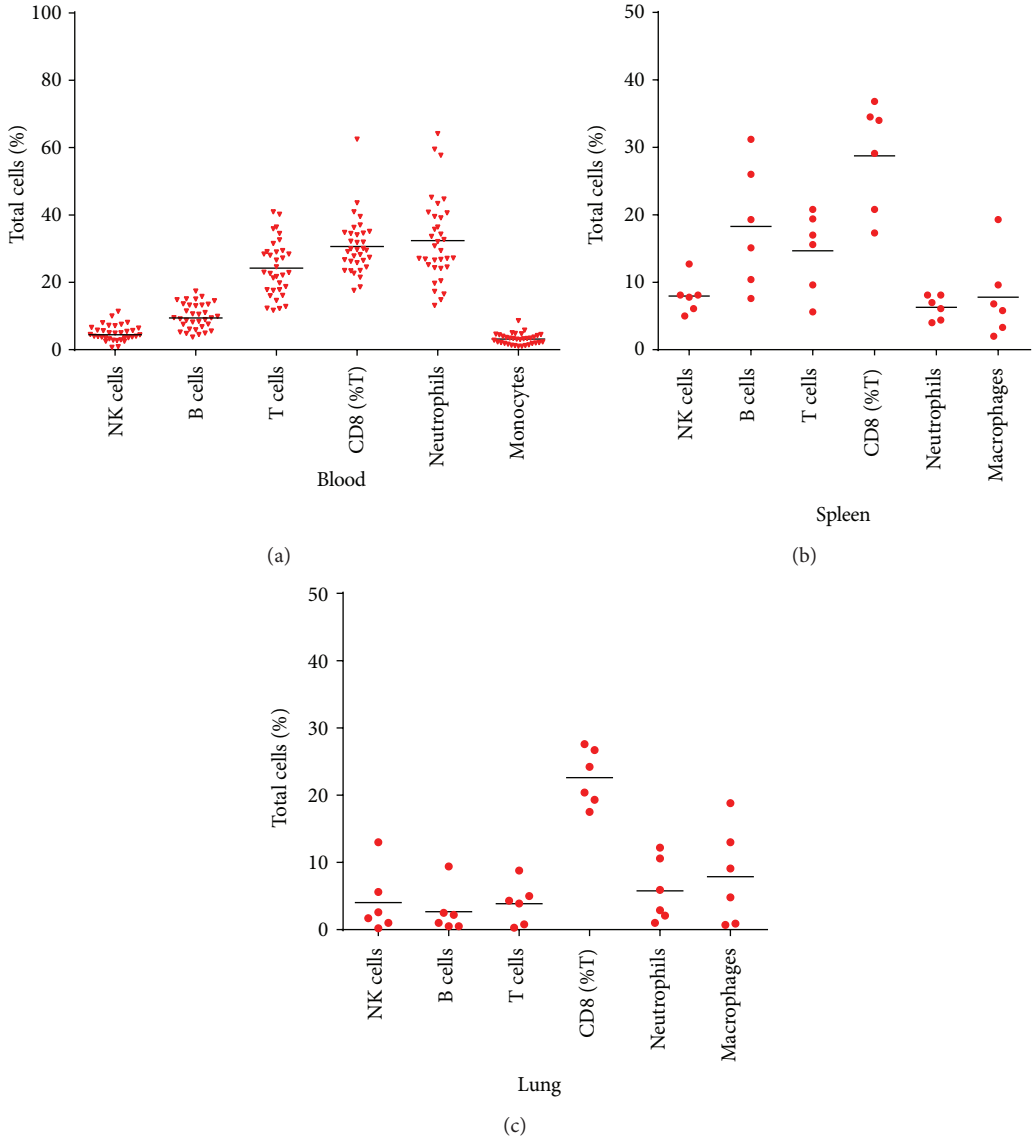

Figure 2: The percentage of the total leucocyte count for various cell types identified in naive marmosets (a) cells in naïve blood, (b) in naive spleens, and (c) in naive lungs. CD8 T cells are expressed as a percentage of CD3+ cells. Bar represents the median value.

differences are observed in the proportion of both B cells and neutrophils [31], although these differences are highly strain specific. C57BL/6J mice are reported to have 67% B cells and BALB/C mice 46%; both of which are consistently higher than the percentage found in marmosets and humans of approximately 25% (Table 1) [27, 31]. The proportion of neutrophils found in the blood of C57BL/6J mice at 13% is lower than the 35% found in marmosets and the 40–75% expected for healthy human blood. This is encouraging as neutrophils play a pivotal role in the innate response to infection [36]. A cross-species comparison suggests that monocytes comprise 3% of leukocytes (Table 1).

Levels of circulating cytokines and chemokines (IL-6, IL-1β, MIP-1β, MCP-1, Rantes, TNFα, and IFNγ) were also quantified in the blood, lung, and spleen of naïve marmosets from the Dstl colony. None of these cytokines were detected in blood samples from uninfected animals; however low levels of MIP-1β, MCP-1, and Rantes were found in spleen and lung tissue.

Preliminary investigation of the immune response has supported the development of marmoset model of infection at Dstl. The levels of different cell types were measured at specific times after challenge with inhalational *F. tularensis, B. pseudomallei,* and Marburg virus [13–15]. Following challenge with *F. tularensis,* increasing levels of NK cells, neutrophils, T cells, and macrophages were observed, peaking at 48 hours after challenge before rapidly declining. This study also demonstrated the importance of investigating the immunological response in key target organs, as an increase in CD8+ T cells and $\gamma\delta$ T cells was observed in the spleen and lungs but not in the blood. Increasing levels of various cytokines, MCP-1, MIP-1α, MIP-1β, IL-6, and IL-1β, were observed in

Table 1: Comparison of the percentages of different cell types observed in the blood from healthy marmosets, mice, and humans.

Cell type	Identification markers	Marmoset (present data)	Reported percentage observed in blood (%)			
			Marmoset [27]	Mouse[4] [30, 31]	Human Asian [32]	Human Caucasian [33]
Number of samples		130+	20		230	200+
[1]B cells	CD20+ CD3−	25 (10–45)	10–25	60 (21–85)	18	7–23
[1]NK	CD20− CD3− CD56+	12.5 (2–30)	25–50	nd	15	6–29
[1]T cells	CD20− CD3+	62.5 (25–90)	50–75	49 (24–99)	67	61–85
[2]CD8+ T cells	CD20− CD3+ CD8+	30 (20–65)	25–50	30 (24–37)	27	15–40
[3]Neutrophils	CD11c dim CD14−	35 (20–65)	nd	13 (8–16)	nd	nd
[3]Monocytes	CD11c dim CD14−	3 (1–10)	nd	1-2	nd	nd

[1]Reported as percentage of lymphocytes.
[2]Reported as percentage of T cells.
[3]Reported as percentage of leukocytes.
[4]Recalculated as average mouse values from reported strains.
nd: not determined.

the lungs, spleen, and blood as the disease progressed (TNFα and IFNγ were not measured in this study).

Following inhalational challenge of marmosets with *B. pseudomallei*, an increase in the number of neutrophils was observed in the blood at 36 hours after challenge, followed by a rapid decline that was associated with an influx of neutrophils into the lung at 46 hours after challenge. A subsequent decline in the number of neutrophils in the lung was associated with the increased number in the spleen of animals that exhibited severe disease and were humanely killed. There was a gradual increase in the number of macrophages in the spleen as the disease progressed with numbers of macrophages peaking in the blood and lungs at 36 hours after challenge. A rapid decline in the number of macrophages in the lungs and blood was observed by 46 hours after challenge.

The levels of various cell types and cytokines were also measured in the blood of animals following inhalational challenge with Marburg virus [15]. In these animals a general increase in the numbers of T cells, NK cells, macrophages IFN-γ, IL-1β, and MCP-1 was observed with time (TNFα was not measured).

In order to gain more information from these acute bacterial infection models, we have sought out other markers from the literature. Primarily this was from marmoset models of autoimmune disorders such as rheumatoid arthritis and multiple sclerosis where the cross-reactivity of human antibodies was investigated, as well as the functionality of cells [37–40]. More recent work at Dstl has reported further cross-reactivity between marmoset cells and human cytokines to induce activity in marmoset T cells [36, 41]. These studies, combined with increasing information available on the cross-reactivity of human antibodies to various NHPs (e.g., NIH NHP reagent resource, http://www.nhpreagents.org/NHP/default.aspx), has expanded the ability to assess activation markers for disease. Detection of the following cell surface markers with human antibodies was trialed: CD54 (ICAM-1) associated with cellular adhesion, inflammation, and leukocyte extravasation; CD69 the early activation marker; CD16 as a macrophage activation marker; CD163 the alternative macrophage activation marker; and MHC class II (HLA-DR). CD56 was originally included to identify NK cells; however, it was noted that its expression on T cells was upregulated during disease and that cells defined as CD3+ CD16− CD56+ have been shown to be functionally cytotoxic in marmosets [37, 42].

These markers have been used to expand on our previously published work to determine changes in the activation status of basic cell types in response to an acute bacterial infection. Animals were challenged with bacteria at a comparable dose either by inhalation ($n = 22$) or by a systemic route ($n = 12$) and humanely killed once they had reached a humane endpoint (between day 4 and day 5 after challenge). Figure 3 illustrates the cellular activity in representative tissues following inhalational (Figures 3(b) and 3(e)) or systemic challenge (Figures 3(c) and 3(f)) and in naïve samples (Figures 3(a) and 3(d)). Naïve T and NK cells appear to have similar resting activation states regardless of origin, whereas neutrophils and macrophages have differential expression of activation, for example, CD16. In response to disease, the proportions of the cell types appear to remain relativity constant; however, the activation markers provide more detailed information and show involvement of all the cell types explored. Extensive activation was to be expected considering that the samples were taken at the humane endpoint. There is also extensive variation between

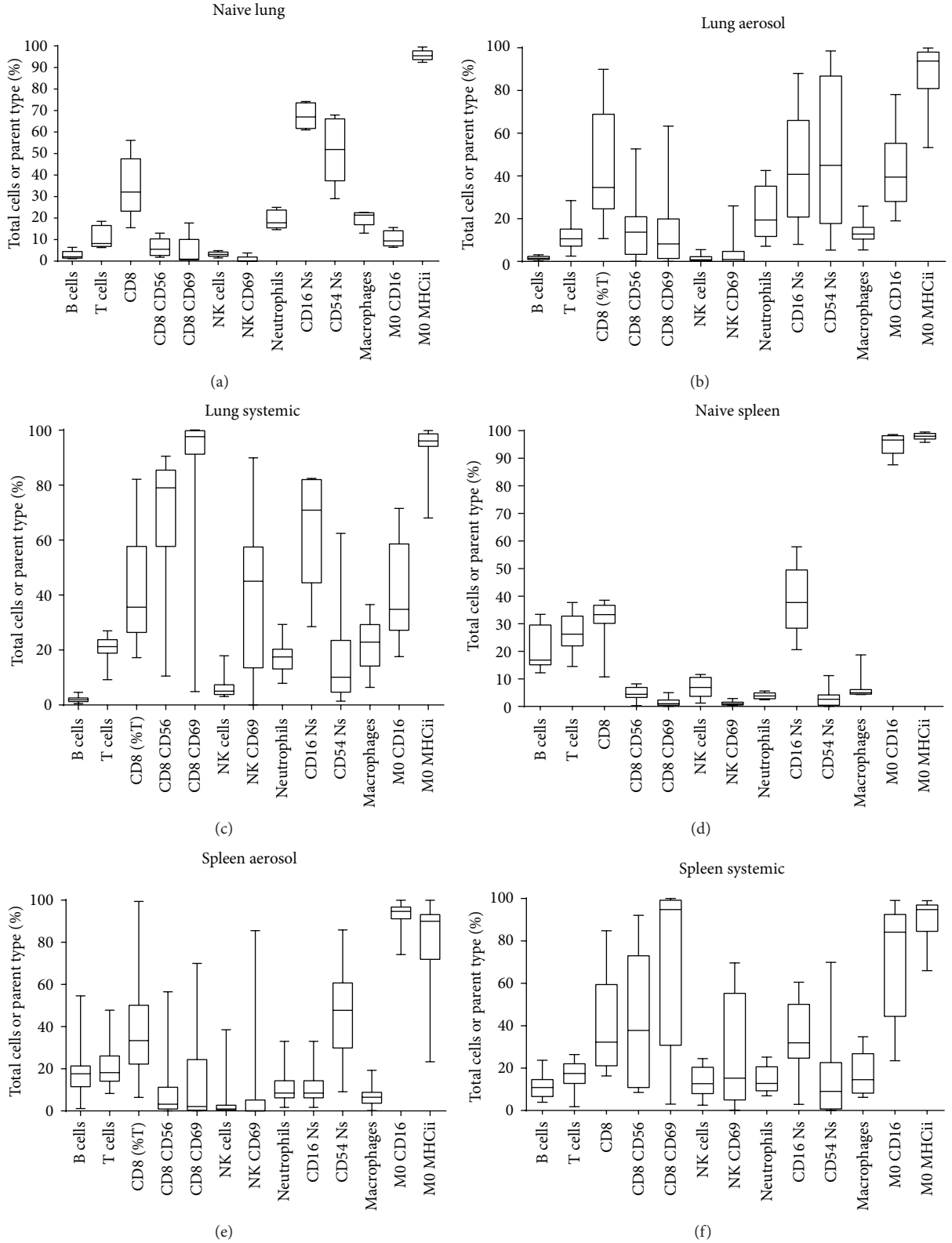

Figure 3: Cell types and activation markers from naïve and after an acute bacterial infection in spleen and lung tissues. Samples were taken at the humane endpoint approx. 4 days after challenge. B, T, NK cells, neutrophils, and macrophages expressed as percentage total whole cells, activation markers as percentages of parent cell type. (a) Naïve lung, (b) lung after aerosol challenge, (c) lung after systemic challenge, (d) naïve spleen, (e) spleen after aerosol challenge, and (f) spleen after systemic challenge.

the samples from the infected animals, again indicative of the late time point in infection.

The spleen was chosen as a representative organ of systemic disease, and the cell activity shows that it is more actively involved in the systemic form of the disease with extensive activation in T cells, NK cells, and neutrophils. In the pneumonic form of disease, only the neutrophils and macrophages show changes in median values.

The response to infection within the lungs has similarities across disease routes in terms of neutrophil reduced expression of CD16 and CD54 and macrophage increased expression of CD16 and reduction in MHCII. Unexpectedly, the T and NK cells appear to be more actively involved in systemic disease, indicating that the disease develops a pneumonic element regardless of initial route of infection.

Levels of circulating cytokines and chemokines (IL-6, IL-1β, MIP-1β, MCP-1, Rantes, TNFα, and IFNγ) were also quantified in the lung and spleen samples. All of the cytokines (with the exception of Rantes) were expressed at high levels (ng/mg) in all samples, which was expected as the animals had succumbed to terminal disease.

4. Conclusion

The work presented here adds significant relevant information to the marmoset models of infection and to the understanding of the immune response in these animals. This work extends marmoset immunology from autoimmune disorders into the field of infectious diseases; this coupled with an increase in the information available on cross-reactivity of human reagents to a variety of NHPs increases the utility/application of marmosets as models of human disease. In conclusion, the immune response in marmosets to infectious disease can be characterised in terms of the phenotype and activation status of all the major immune cells and key cytokine and chemokine expression. This can aid in the identification of correlates of infection or protection in medical countermeasures assessment studies. This information can also potentially be used for pivotal studies to support licensure of products under the FDA Animal Rule.

This, in conjunction with the small size of marmosets, their immune response to infection that is comparable to humans, and the ability to house more statistically relevant numbers within high containment, makes the marmoset an appropriate animal model for biodefense-related pathogens.

Conflict of Interests

The authors declare that there is no conflict of interests regarding the publication of this paper.

References

[1] K. Mansfield, "Marmoset models commonly used in biomedical research," *Comparative Medicine*, vol. 53, no. 4, pp. 383–392, 2003.

[2] C. Groves, D. E. Wilson, and D. M. Reeder, Eds., *Mammal Species of the World*, Johns Hopkins University Press, Baltimore, Md, USA, 3rd edition, 2005.

[3] R. Carrion Jr., K. Brasky, K. Mansfield et al., "Lassa virus infection in experimentally infected marmosets: liver pathology and immunophenotypic alterations in target tissues," *Journal of Virology*, vol. 81, no. 12, pp. 6482–6490, 2007.

[4] T. Weatherford, D. Chavez, K. M. Brasky, S. M. Lemon, A. Martin, and R. E. Lanford, "Lack of adaptation of chimeric GB virus B/hepatitis C virus in the marmoset model: possible effects of bottleneck," *Journal of Virology*, vol. 83, no. 16, pp. 8062–8075, 2009.

[5] T. Omatsu, M. L. Moi, T. Hirayama et al., "Common marmoset (*Callithrix jacchus*) as a primate model of dengue virus infection: development of high levels of viraemia and demonstration of protective immunity," *Journal of General Virology*, vol. 92, no. 10, pp. 2272–2280, 2011.

[6] E. Leibovitch, J. E. Wohler, S. M. Cummings Macri et al., "Novel marmoset (*Callithrix jacchus*) model of human herpesvirus 6A and 6B infections: immunologic, virologic and radiologic characterization," *PLoS Pathogens*, vol. 9, no. 1, Article ID e1003138, 2013.

[7] M. C. Weissenbacher, M. A. Calello, O. J. Colillas, S. N. Rondinone, and M. J. Frigerio, "Argentine hemorrhagic fever: a primate model," *Intervirology*, vol. 11, no. 6, pp. 363–365, 1979.

[8] D. R. Smith, B. H. Bird, B. Lewis et al., "Development of a novel nonhuman primate model for Rift Valley fever," *Journal of Virology*, vol. 86, no. 4, pp. 2109–2120, 2012.

[9] T. C. Greenough, A. Carville, J. Coderre et al., "Pneumonitis and multi-organ system disease in common marmosets (*Callithrix jacchus*) infected with the severe acute respiratory syndrome-associated coronavirus," *American Journal of Pathology*, vol. 167, no. 2, pp. 455–463, 2005.

[10] A. P. Adams, J. F. Aronson, S. D. Tardif et al., "Common marmosets (*Callithrix jacchus*) as a nonhuman primate model to assess the virulence of eastern equine encephalitis virus strains," *Journal of Virology*, vol. 82, no. 18, pp. 9035–9042, 2008.

[11] M. S. Lever, A. J. Stagg, M. Nelson et al., "Experimental respiratory anthrax infection in the common marmoset (*Callithrix jacchus*)," *International Journal of Experimental Pathology*, vol. 89, no. 3, pp. 171–179, 2008.

[12] M. Nelson, M. S. Lever, V. L. Savage et al., "Establishment of lethal inhalational infection with *Francisella tularensis* (tularaemia) in the common marmoset (*Callithrix jacchus*)," *International Journal of Experimental Pathology*, vol. 90, no. 2, pp. 109–118, 2009.

[13] M. Nelson, M. S. Lever, R. E. Dean et al., "Characterization of lethal inhalational infection with *Francisella tularensis* in the common marmoset (*Callithrix jacchus*)," *Journal of Medical Microbiology*, vol. 59, no. 9, pp. 1107–1113, 2010.

[14] M. Nelson, R. E. Dean, F. J. Salguero et al., "Development of an acute model of inhalational melioidosis in the common marmoset (*Callithrix jacchus*)," *International Journal of Experimental Pathology*, vol. 92, no. 6, pp. 428–435, 2011.

[15] S. J. Smither, M. Nelson, L. Eastaugh et al., "Experimental respiratory marburg virus haemorrhagic fever infection in the common marmoset (*Callithrix jacchus*)," *International Journal of Experimental Pathology*, vol. 94, no. 2, pp. 156–168, 2013.

[16] R. Carrion Jr., Y. Ro, K. Hoosien et al., "A small nonhuman primate model for filovirus-induced disease," *Virology*, vol. 420, no. 2, pp. 117–124, 2011.

[17] M. Kramski, K. Mätz-Rensing, C. Stahl-Hennig et al., "A novel highly reproducible and lethal nonhuman primate model for

orthopox virus infection," *PLoS ONE*, vol. 5, no. 4, Article ID e10412, 2010.

[18] I. S. Lukashevich, R. Carrion Jr., M. S. Salvato et al., "Safety, immunogenicity, and efficacy of the ML29 reassortant vaccine for Lassa fever in small non-human primates," *Vaccine*, vol. 26, no. 41, pp. 5246–5254, 2008.

[19] M. Nelson, A. J. Stagg, D. J. Stevens et al., "Post-exposure therapy of inhalational anthrax in the common marmoset," *International Journal of Antimicrobial Agents*, vol. 38, no. 1, pp. 60–64, 2011.

[20] M. Nelson, M. S. Lever, R. E. Dean, P. C. Pearce, D. J. Stevens, and A. J. H. Simpson, "Bioavailability and efficacy of levofloxacin against *Francisella tularensis* in the common marmoset (*Callithrix jacchus*)," *Antimicrobial Agents and Chemotherapy*, vol. 54, no. 9, pp. 3922–3926, 2010.

[21] W. H. Stone, R. C. S. Treichel, and J. L. van de Berg, "Genetic significance of some common primate models in biomedical research," in *Animal Models: Assessing the Scope of Their Use in Biomedical Research*, J. Kawamata and E. C. Melby Jr., Eds., pp. 73–93, Alan R. Liss, New York, NY, USA, 1987.

[22] B. A. 't Hart, J. D. Laman, J. Bauer, E. Blezer, Y. van Kooyk, and R. Q. Hintzen, "Modelling of multiple sclerosis: lessons learned in a non-human primate," *The Lancet Neurology*, vol. 3, no. 10, pp. 588–597, 2004.

[23] F. Villinger, P. Bostik, A. Mayne et al., "Cloning, sequencing, and homology analysis of nonhuman primate Fas/Fas-ligand and co-stimulatory molecules," *Immunogenetics*, vol. 53, no. 4, pp. 315–328, 2001.

[24] H.-C. von Budingen, S. L. Hauser, C. B. Nabavi, and C. P. Genain, "Characterization of the expressed immunoglobulin IGHV repertoire in the New World marmoset *Callithrix jacchus*," *Immunogenetics*, vol. 53, no. 7, pp. 557–563, 2001.

[25] A. Uccelli, J. R. Oksenberg, M. C. Jeong et al., "Characterization of the TCRB chain repertoire in the New World monkey *Callithrix jacchus*," *The Journal of Immunology*, vol. 158, no. 3, pp. 1201–1207, 1997.

[26] R. Neubert, M. Foerster, A. C. Nogueira, and H. Helge, "Cross-reactivity of antihuman monoclonal antibodies with cell surface receptors in the common marmoset," *Life Sciences*, vol. 58, no. 4, pp. 317–324, 1995.

[27] H. Brok, R. Hornby, G. Griffiths, L. Scott, and B. A. 't Hart, "An extensive monoclonal antibody panel for the phenotyping of leukocyte subsets in the common marmoset and the cotton-top tamarin," *Cytometry*, vol. 45, no. 4, pp. 293–303, 2001.

[28] Y. S. Kap, M. van Meurs, N. van Driel et al., "A monoclonal antibody selection for immunohistochemical examination of lymphoid tissues from non-human primates," *Journal of Histochemistry and Cytochemistry*, vol. 57, no. 12, pp. 1159–1167, 2009.

[29] S. Kireta, H. Zola, R. B. Gilchrist, and P. T. H. Coates, "Cross-reactivity of anti-human chemokine receptor and anti-TNF family antibodies with common marmoset (*Callithrix jacchus*) leukocytes," *Cellular Immunology*, vol. 236, no. 1-2, pp. 115–122, 2005.

[30] The Jackson lab leukocyte, "lymphocyte base line levels," http://jaxmice.jax.org/support/phenotyping/B6data000664.pdf.

[31] J. Chen and D. E. Harrison, "Quantitative trait loci regulating relative lymphocyte proportions in mouse peripheral blood," *Blood*, vol. 99, no. 2, pp. 561–566, 2002.

[32] W. J. Chng, G. B. Tan, and P. Kuperan, "Establishment of adult peripheral blood lymphocyte subset reference range for Asian populations by single platform flow cytometry: influence of age, sex, and race and comparison with other published studies," *Clinical and Diagnostic Laboratory Immunology*, vol. 11, no. 1, pp. 168–173, 2004.

[33] T. Reichert, M. DeBruyere, V. Deneys et al., "Lymphocyte subset reference ranges in adult caucasians," *Clinical Immunology and Immunopathology*, vol. 60, no. 2, pp. 190–208, 1991.

[34] J. Westermann and R. Pabst, "Distribution of lymphocyte subsets and natural killer cells in the human body," *Clinical Investigator*, vol. 70, no. 7, pp. 539–544, 1992.

[35] Y. Fujii, K. Kitaura, T. Matsutani et al., "Immune-related gene expression profile in laboratory common marmosets assessed by an accurate quantitative real-time PCR using selected reference genes," *PLoS ONE*, vol. 8, no. 2, Article ID e56296, 2013.

[36] C. A. Rowland, T. R. Laws, and P. C. F. Oyston, "An assessment of common marmoset (*Callithrix jacchus)* $\gamma 9^+$ T cells and their response to phosphoantigen *in vitro*," *Cellular Immunology*, vol. 280, no. 2, pp. 132–137, 2012.

[37] S. A. Jagessar, B. Gran, N. Heijmans et al., "Discrepant effects of human interferon-gamma on clinical and immunological disease parameters in a novel marmoset model for multiple sclerosis," *Journal of Neuroimmune Pharmacology*, vol. 7, no. 1, pp. 253–265, 2012.

[38] S. Ohta, Y. Ueda, M. Yaguchi et al., "Isolation and characterization of dendritic cells from common marmosets for preclinical cell therapy studies," *Immunology*, vol. 123, no. 4, pp. 566–574, 2008.

[39] S. Seehase, H. D. Lauenstein, C. Schlumbohm et al., "LPS-induced lung inflammation in marmoset monkeys—an acute model for anti-inflammatory drug testing," *PLoS ONE*, vol. 7, no. 8, Article ID e43709, 2012.

[40] M. P. M. Vierboom, E. Breedveld, I. Kondova, and B. A. 't Hart, "Collagen-induced arthritis in common marmosets: a new nonhuman primate model for chronic arthritis," *Arthritis Research & Therapy*, vol. 12, no. 5, article R200, 2010.

[41] T. R. Laws, M. Nelson, C. Bonnafous et al., "*In Vivo* manipulation of $\gamma 9^+$ T cells in the common marmoset (*Callithrix jacchus*) with phosphoantigen and effect on the progression of respiratory melioidosis," *PLoS ONE*, vol. 8, no. 9, Article ID e74789, 2013.

[42] Y. S. Kap, P. Smith, S. A. Jagessar et al., "A fast progression of recombinant human myelin/oligodendrocyte glycoprotein (MOG)-induced experimental autoimmune encephalomyelitis in marmosets is associated with the activation of MOG_{34-56}-specific cytotoxic T cells," *The Journal of Immunology*, vol. 180, pp. 1326–1337, 2008.

Hindawi Publishing Corporation
Journal of Immunology Research
Volume 2014, Article ID 694717, 8 pages
http://dx.doi.org/10.1155/2014/694717

Research Article

Control of Intracellular *Francisella tularensis* by Different Cell Types and the Role of Nitric Oxide

Sarah L. Newstead, Amanda J. Gates, M. Gillian Hartley, Caroline A. Rowland, E. Diane Williamson, and Roman A. Lukaszewski

Dstl, Porton Down, Salisbury SP4 0JQ, UK

Correspondence should be addressed to Sarah L. Newstead; slnewstead@dstl.gov.uk

Received 10 February 2014; Revised 14 May 2014; Accepted 10 June 2014; Published 21 July 2014

Academic Editor: Julia Tree

Reactive nitrogen is critical for the clearance of *Francisella tularensis* infections. Here we assess the role of nitric oxide in control of intracellular infections in two murine macrophage cell lines of different provenance: the alveolar macrophage cell line, MH-S, and the widely used peritoneal macrophage cell line, J774A.1. Cells were infected with the highly virulent Schu S4 strain or with the avirulent live vaccine strain (LVS) with and without stimuli. Compared to MH-S cells, J774A.1 cells were unresponsive to stimulation and were able to control the intracellular replication of LVS bacteria, but not of Schu S4. In MH-S cells, Schu S4 demonstrated control over cellular NO production. Despite this, MH-S cells stimulated with LPS or LPS and IFN-γ were able to control intracellular Schu S4 numbers. However, only stimulation with LPS induced significant cellular NO production. Combined stimulation with LPS and IFN-γ produced a significant reduction in intracellular bacteria that occurred whether high levels of NO were produced or not, indicating that NO secretion is not the only defensive cellular mechanism operating in virulent *Francisella* infections. Understanding how *F. tularensis* interacts with host macrophages will help in the rational design of new and effective therapies.

1. Introduction

Francisella tularensis is a Gram-negative, facultative intracellular bacterium, which is the causative organism of the disease tularemia [1]. There are two main biovars of *F. tularensis* which cause disease in humans: *F. tularensis* subsp. *tularensis*, which is highly virulent and potentially fatal (designated type A), and the less virulent *F. tularensis* subsp. *holartica* (designated type B), a mutation of which has resulted in further attenuation and its development as a live attenuated vaccine, the live vaccine strain (LVS). In parts of the world (Scandinavia, North America, and parts of Asia) *F. tularensis* is harboured by the local wildlife, for example, rabbits or deer, that can transmit the bacterium to humans [2].

Protection against an inhaled infection with *F. tularensis* is highly desired, as it is estimated that as little as 25 colony-forming units (cfu) can cause fatal disease [3]. Currently, there is no licensed vaccine for tularemia and antibiotics have limited efficacy due to the infection being intracellular in nature and somewhat difficult to diagnose [4]. Protection against inhalational exposure with *F. tularensis* Schu S4 would be facilitated by further understanding of the mechanisms of resistance operating in the respiratory tract and the lungs. As alveolar macrophages reside in the lungs, they provide a first line of defence against an aerosol infection and, to date, infection of these cells with *F. tularensis* has not been extensively studied.

MH-S cells are a murine alveolar macrophage cell line, created by obtaining cells from a bronchoalveolar lavage, which were then transformed with simian virus 40 (SV40) to produce a rapidly proliferating cell line [5]. J774A.1 cells are a well-defined and widely used murine peritoneal macrophage cell line. Both these macrophage cell types can support the growth of intracellular pathogens such as *F. tularensis, Mycobacterium tuberculosis* [6], and *Legionella pneumophila* [7] and both can secrete cytokines and nitric oxide [8].

Here, we have compared the cellular responses of these two macrophage cell lines, J774A.1 and MH-S, to infection with *F. tularensis*.

Selected isolated components of bacteria such as peptidoglycan, lipopolysaccharide, synthetic CpG, and proinflammatory cytokines have all been used to study activation and the protective responses of macrophages *in vitro* [9]. One of the known macrophage resistance mechanisms against *F. tularensis* is the induction of nitric oxide synthase (iNOS) and NO secretion [10–12]. NO is a short-lived inorganic free radical gas derived from L-arginine by NOS activity [13], which has an antimicrobial effect important in the innate immune system.

The observed ability of more virulent *F. tularensis* strains to survive within macrophages and other cells may depend on their capacity to suppress such antibacterial activities of the host cells [14]. It has been previously reported that type A strains of *F. tularensis* possess the enzyme citrulline ureidase (ctu) [15], which recently has been described as a virulence factor, enabling the bacteria to limit the amount of arginine available to the host cell and thereby restrict the production of reactive nitrogen [16]. A Δctu mutant of *F. tularensis* Schu S4 was significantly attenuated in mice and, when used to infect macrophages *in vitro,* was more susceptible to killing due to the observed enhanced levels of nitrite production (measured as the stable oxidative product of NO and an indicator of NO production), compared with Schu S4-infected macrophages [16]. These findings led us to question whether NO production is effective in countering the virulence of the Schu S4 strain and whether it is the only effective mechanism available to host cells.

We have tested the ability of combinations of stimulants to induce significant NO synthesis in the J774A.1 and MH-S cell lines. We have also used the chemical inhibitor of NO synthesis, N^G-monomethyl-L-arginine, to investigate the specific influence of NO induction on the resistance of mammalian cells to infection with tularemia strains of differing virulence *in vivo*. We have also assessed the effect of the induced NO on the intracellular growth of *F. tularensis* in each cell line to determine whether any observed difference in functionality can be correlated with cellular source.

2. Materials and Methods

2.1. Bacteria. *F. tularensis* LVS was derived directly from an original NDBR 101, lot 4 vaccine ampoule produced during the 1960s. Prior to reconstitution, vaccine ampoules were stored at −20°C. *F. tularensis* Schu S4 was originally isolated from a human case of tularemia in 1941 and has been passaged through animals.

2.2. Cell Lines. MH-S alveolar macrophages and J774A.1 peritoneal macrophages (ECACC, PHE, Porton Down, UK) were cultured in RPMI1640 (plus 10% FCS and 2% L-glutamine) or DMEM (10% FCS and 2% L-glutamine), respectively (all from Invitrogen Ltd, Paisley, UK). Both cell lines were cultivated in 5% CO_2 at 37°C in a humidified environment. Cells were seeded into 24-well plates (Corning) at a density of 5×10^5 cells/mL and allowed to adhere overnight. Immediately before infection the cells were visually inspected to ensure a confluent monolayer (1×10^6/well).

2.3. Stimulation. Confluent monolayers of cells were stimulated with 2.5 μg/mL lipopolysaccharide from *Escherichia coli* (Sigma, Gillingham, UK) or 1 μg/mL recombinant mouse interferon gamma (IFN-γ) (R&D systems Europe Ltd, Abingdon, UK) or 10 μg/mL CpG 10109 (Coley Pharmaceuticals, USA) or peptidoglycan (Sigma, Gillingham, UK) at 20 μg/mL or TNF-α (AbD Serotec, Kidlington, UK) at 20 μg/mL. These concentrations were selected following optimisation for maximum production of nitric oxide over a period of 24 hr.

2.4. Cytokine Release. Cytokine release was measured in the supernatant of uninfected cells following 24 hours of stimulation. The suite of cytokines measured using flow cytometry and mouse inflammation cytometric bead array (CBA) kits (BD Biosciences, UK) was TNF-α, IFN-γ, IL-6, IL-12, and CCL2. The CBA kits were used in accordance with the manufacturer's instructions and analysed using FACScanto II (BD).

2.5. Measuring Nitric Oxide Production and Inhibition. NO concentration was measured as the stable oxidized metabolite and nitrite (NO_2^-) using a Griess reaction kit (Promega UK Ltd, Southampton, UK). The limit of detection (LOD) was 2.5 μM (125 pmol). Manufacturer's instructions were followed. Briefly, 50 μL of sample and 50 μL of sulfanilamide solution (1% sulfanilamide in 5% phosphoric acid) were incubated at room temperature and protected from light for 5–10 minutes. Subsequently, 50 μL of 0.1% N-1-naphthylethylenediamine dihydrochloride in water was added, reincubated, and protected from light for a further 5–10 minutes. The absorbance was read at 540 nm and compared to a known standard.

The nitric oxide inhibitor N^G-monomethyl-L-arginine (L-NMMA) (Sigma, Gillingham, UK) was used at a concentration of 4 mM and added after stimulation and remained for the duration of the assay.

2.6. Infection and Stimulation of Cells with Bacteria. All infection experiments were performed under containment level 3 (CL3) conditions (necessary for infection studies with type A strains of *F. tularensis*) with a range of stimulants.

Both strains of *F. tularensis* were cultured on blood cysteine glucose agar supplemented with 50% glucose, 10% histine, 10% cysteine, and defibrinated horse blood at 50°C. The multiplicity of infections (MOI) required to achieve comparable levels of infections between the strains and cells was determined in initial experiments. MOIs used in NO experiments were LVS 100 : 1, Schu S4 10 : 1 for MH-S cells, and LVS 10 : 1, Schu S4 1 : 1 for J774A.1 cells. Bacteria and cells were incubated for 30 minutes. Following this all of the supernatant was removed, the cells were not washed, and 10 μg/mL gentamicin (Sigma, Gillingham, UK) was added for 30 minutes to kill any extracellular bacteria. Workup of the

method demonstrated that this concentration of gentamicin is sufficient to kill all extracellular *Francisella* of either strain. This was deemed time 0 and stimulants were added. Gas packs (Biomerieux, Basingstoke, UK) were used to supply CO_2 during the infection and stimulation of the cell lines.

Supernatant from the wells was taken for measurement of nitrite and cytokine production and bacteria were enumerated.

2.7. Intracellular Counts. Intracellular bacterial counts were achieved by lysing the macrophages with distilled water and vigorous pipetting for approximately five minutes. Relevant dilutions (made in PBS) were then pipetted out onto BCGA agar and incubated at 37°C for three days before colonies were counted.

2.8. Bacterial Sensitivity to NO. Spermine NONOate was used as an NO donor. This compound is stable under alkaline conditions but disassociates releasing free NO at pH 7.4 or below. Increasing concentrations of Spermine NONOate were used to determine if the *Francisella* strains had similar sensitivity to NO under extracellular conditions (PBS room temperature). Spermine NONOate (Cambridge Bioscience, UK) was used according to the manufacturer's instructions.

2.9. Statistical Analysis. In order to quantify the NO response of either cell line to stimulation or inhibition, at least 3 independent replicates were used to derive mean values ± standard errors of the mean (SEM). For the bacterial growth assays, the increase in intracellular bacterial counts achieved after 24 hours in unstimulated (media only) cells was taken as 100% and the change in bacterial counts from stimulated cells was expressed as a percentage of this. Under this system, a percentage increase of less than 1% denotes an actual decrease in bacterial numbers from the $t = 0$ initial infection. Thus the data from independent experiments were combined. Student's t-test was used to analyse the data and determine significant differences at the levels of $P < 0.05$ (*), $P < 0.01$ (**), and $P < 0.001$ (***).

3. Results

3.1. Response of Cell Lines to Infection with F. tularensis. Before stimulation and infection studies were conducted, the ability of both Schu S4 and LVS to be phagocytosed by and colonise J774A.1 and MH-S cells was compared.

In either cell line, at both time points, Schu S4 colonised cells significantly faster than LVS ($P < 0.005$, Table 1). After 30 mins of infection with a multiplicity of infection (MOI) of 10 : 1 (bacteria to cells) J774A.1 cells contained significantly more bacteria (Schu S4 or LVS) than MH-S cells ($P < 0.002$); however this difference was not significant at the 120-minute time point.

Once infection was established, survival of bacteria within unstimulated macrophages (regardless of cell line) was not significantly different between the two strains, each achieving on average 2 logs of growth over 24 hours of incubation (data not shown).

Table 1: Comparison of *F. tularensis* colonisation of cell lines at 30 minutes of exposure at an MOI of 10 : 1 and 120 minutes at MOI of 1 : 1, measured in cfu/mL. Under either condition in either cell line Schu S4 infected in significantly higher numbers ($P < 0.005$ by Student's t-test). Values are the means from at least three independent experiments.

	30 min 10 : 1		120 min 1 : 1	
	LVS	Schu S4	LVS	Schu S4
J774A.1	$\mathbf{1.53 \times 10^2}$	$\mathbf{3.28 \times 10^3}$	$\mathbf{9.30 \times 10^2}$	$\mathbf{5.93 \times 10^4}$
(±SD)	4.16×10^1	1.90×10^2	1.44×10^2	1.79×10^4
MH-S	$\mathbf{4.05 \times 10^1}$	$\mathbf{1.03 \times 10^2}$	$\mathbf{2.57 \times 10^2}$	$\mathbf{8.00 \times 10^3}$
(±SD)	1.84×10^2	3.86×10^1	1.63×10^2	1.21×10^3

The MOIs were adjusted in subsequent experiments to compensate for differences in uptake, ensuring comparable infection rates between bacterial strains and cell lines. The starting infection established was in the region of 100 bacteria per 10^6 cells per mL. The following MOIs were used on MH-S cells: LVS 100 : 1, Schu S4 10 : 1 and on J774A.1 cells: LVS 10 : 1, Schu S4 1 : 1.

3.2. Cytokine Production. Cytokine production was compared between J774A.1 and MH-S cells. The cytokine profiles of the cells were similar in that low levels of cytokines were detected in unstimulated cells with the exception of CCL2 (MCP-1). Also both cell lines stimulated with LPS (used here as an immunostimulant at supraphysiological levels) induced IL-6 and TNF-α production (Figures 1(a) and 1(b)). IFN-γ stimulation produced further release of IFN-γ and peptidoglycan stimulation produced high levels of IL-6 and TNF-α (data not shown). J774A.1 cells produce significantly more TNF-α than MH-S cells under all conditions tested except for response to LPS ($P < 0.005$). Combined stimulation with LPS and IFN-γ was not tested.

3.3. Nitrite Production. Production of nitrite from unstimulated cells of either cell line was consistently below 10 μM (media Figure 2). Infection with either LVS or Schu S4 did not cause an increase in either cell line in the production of nitrite.

When stimulated without infection, J774A.1 cells produced NO in response to LPS and IFN-γ plus LPS (both $P < 0.05$) but not to IFN-γ only or CpG (Figure 2(a)). The MH-S cells did not respond to LPS by the production of NO but produced NO in response to IFN-γ plus LPS and to CpG ($P < 0.05$ Figure 2(b)).

Infection of J774A.1 with either LVS or Schu S4 did not alter the production of NO above the effect of the stimulant (Figure 2(a)). In contrast infection of the MH-S cell line with LVS leads to increased production of NO which was significant for the IFN-γ plus LPS and for the CpG treated cells ($P < 0.01$) (Figure 2(b)). Infection with Schu S4 (Figure 2(b)) had a dramatic effect on the MH-S production of nitrite, reducing it in all stimulated groups and significantly so in cells stimulated with both IFN-γ plus LPS and CpG ($P < 0.05$).

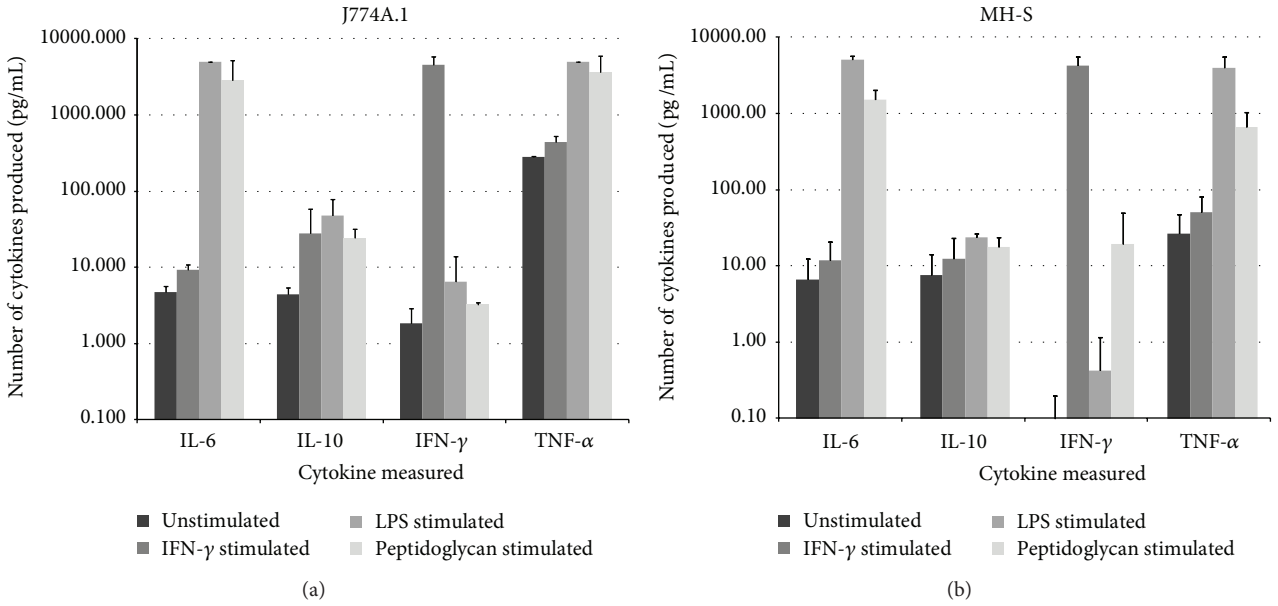

Figure 1: ((a) and (b)) Cytokine production from stimulated J774A.1 and MH-S cells. Cytokine concentrations were measured 24 hours after stimulation with LPS (5 μg/mL) or IFN-γ (1 μg/mL). Values are the means and SEM from at least three independent experiments. There were significant differences in TNF-α production between the cell lines for unstimulated, LPS stimulated and peptidoglycan stimulated cells.

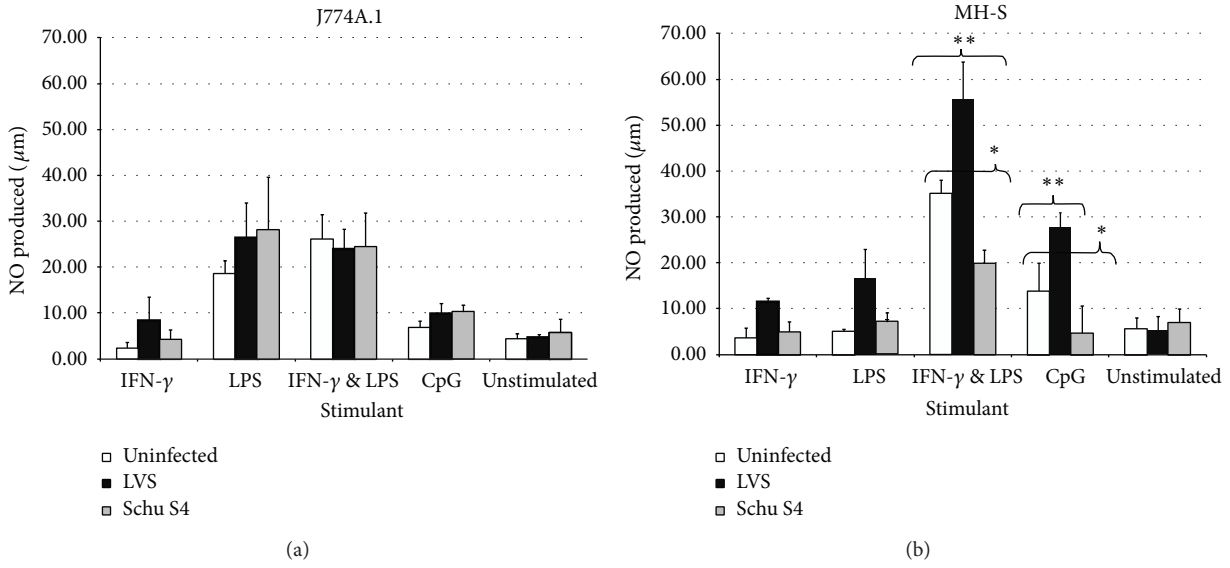

Figure 2: ((a) and (b)) Nitrite production from stimulated cells: J774A.1 (a) and MH-S (b). Stimulant concentrations added were IFN-γ (1 μg/mL), LPS (5 μg/mL), and IFN-γ + LPS (1 μg/mL + 5 μg/mL). Nitrite measurements were taken 24 hours after stimulation and/or infection. Values are the means and SEM from at least three independent experiments. Significant differences in production of nitrite from stimulation or stimulation and infection are marked with asterisks. Significance levels of $^{*}P < 0.05$, $^{**}P < 0.01$, and $^{***}P < 0.001$ by Student's t-test.

3.4. Bacterial Sensitivity to Extracellular NO. The LVS and Schu S4 strains were tested for their relative sensitivity to extracellular NO. When tested at concentrations ranging from 0 mM to 2 mM NO in PBS, both strains were sensitive to extracellular NO, with a maximal reduction in viable counts (for both strains) of 1 log over 1 hour of exposure to 2 mM (Table 2).

3.5. Intracellular Bacterial Counts of Stimulated Macrophages. Intracellular bacteria were enumerated from cells that were stimulated with CpG, LPS, IFN-γ separately, or LPS and IFN-γ combined and infected with either LVS or Schu S4 (Figures 3(a) and 3(b)). The results presented in Figure 3 are combined from at least 3 replica experiments by converting the growth achieved by the bacterial strain in unstimulated cells to 100%,

Table 2: Effect of increased concentration of nitric oxide on bacterial counts (cfu/mL) after 1 hr incubation in PBS.

Nitric oxide concentration (μM)	Schu S4	LVS
0	3.23×10^4	5.00×10^4
0.125	1.90×10^4	4.98×10^4
0.25	1.55×10^4	2.00×10^4
0.5	8.75×10^3	9.00×10^3
1	6.25×10^3	9.97×10^3
2	2.75×10^3	6.00×10^3

with the starting count ($t = 0$) being equal to 1%. Thus the growth achieved by the bacteria in stimulated cells is expressed as a percentage of maximal growth possible: 1% equates to no change from the starting infection and values of less than 1% represent a reduction from the initial level of infection at $t = 0$. The initial infection was generally in the region of 100 bacteria to 1×10^6 cells.

Intracellular growth of LVS was significantly reduced in either cell line under all of the stimulating conditions compared to growth in unstimulated cells ($P < 0.001$). This was more pronounced in MH-S cells stimulated with either LPS or CpG where there was a reduction in intracellular bacteria compared to the infecting ($t = 0$) count (Figure 3(b)). Both MH-S and J774A.1 cells were able to clear all LVS when stimulated with LPS and IFN-γ in combination. The inhibition of bacterial growth appeared to correlate with the measurable levels of nitrite (Figures 2(a) and 2(b)).

Intracellular growth of Schu S4 was less inhibited than LVS growth by the effects of the stimulants in either cell line and was unaffected by stimulation with either IFN-γ alone or CpG. In stimulated MH-S cells, Schu S4 growth was reduced by stimulation by LPS or LPS combined with IFN-γ, compared to growth in unstimulated cells (Figure 3(b); $P < 0.001$). This occurred despite little or no measurable nitrite production. Stimulation of MH-S cells with IFN-γ plus LPS resulted in a significant reduction in Schu S4 from the starting infection with only 1 out of 3 experiments having detectable bacteria. By contrast Schu S4 growth in J774A.1 cells (Figure 3(a)) was largely unaffected by stimulation, despite levels of nitrite that had appeared to control LVS growth previously. The only exception to this was from stimulation with LPS and IFN-γ in combination, which significantly reduced intracellular Schu S4 ($P < 0.05$).

3.6. Effect of NO Inhibition. Stimulation with IFN-γ, LPS alone or in combination, or CpG alone in the presence of the nitric oxide synthase inhibitor (L-NMMA) of either cell line prevented nitrite production (concentrations consistently below 10 μM, data not shown).

Compared with the levels of intracellular LVS seen in stimulated cells, stimulation combined with inhibition of nitric oxide synthase (NOS) resulted in an increase of intracellular LVS for most groups (Figure 3). In particular, the intracellular counts of LVS in stimulated CpG (both cell types) and stimulated LPS (MH-S only) were no longer significantly depressed compared to media only controls.

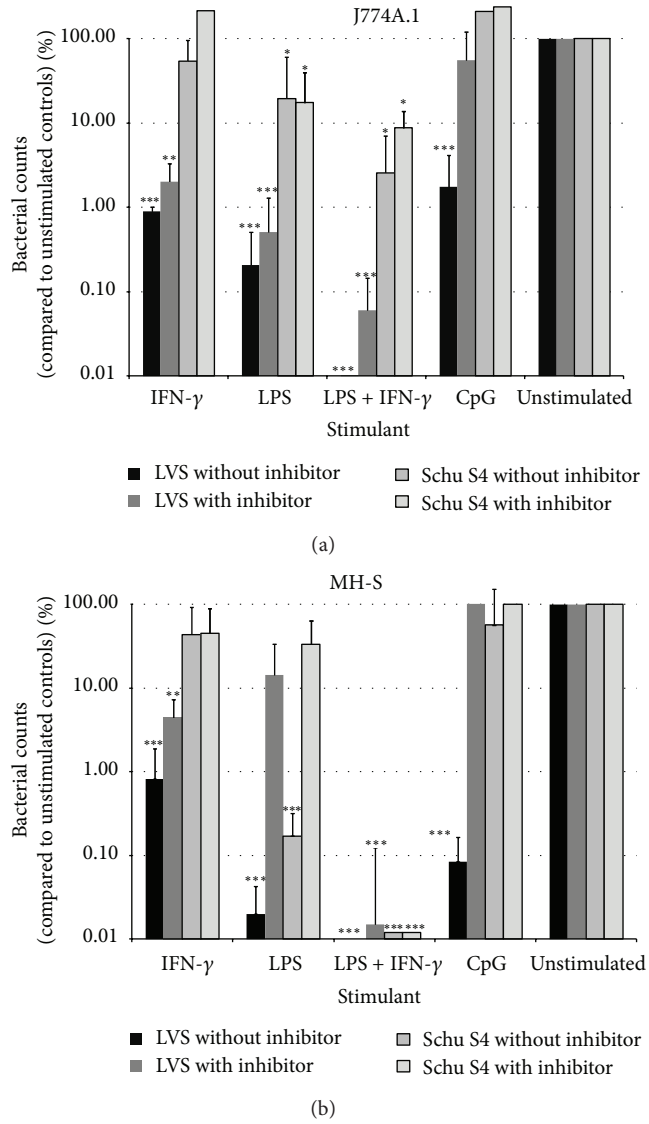

Figure 3: ((a) and (b)) Intracellular counts 24 hours after stimulation and infection of J774A.1 cells (a) and MH-S cells (b). Stimulant concentrations added were IFN-γ (1 μg/mL), LPS (5 μg/mL), IFN-γ + LPS (1 μg/mL + 5 μg/mL), and CpG (10 μg/mL). Nitric oxide production was inhibited by 4 mM N^G-monomethyl-L-arginine added before stimulation. Values are the means and SEM from at least three independent experiments, with the starting infection given a value of 1% and the maximal growth achieved (in unstimulated cells) as 100%. Significant differences in intracellular counts between stimulated and unstimulated cells are shown (significance $^*P < 0.05$, $^{**}P < 0.01$, and $^{***}P < 0.001$ by Student's t-test).

However inhibition of NOS together with LPS and IFN-γ stimulation of MH-S-cells did not result in an increase in counts of intracellular LVS.

Schu S4 counts in L-NMMA-blocked and stimulated cells were almost unchanged by inhibiting nitrite production in either J774A.1 or MH-S cells. The only significant increase in growth occurred in the MH-S cells stimulated with LPS ($P < 0.005$) (Figure 3(b)). This was unexpected as

nitrite production by MH-S cells stimulated with LPS in the presence of Schu S4 was not increased (Figure 2(b)). Despite inhibition of NOS in MH-S cells stimulated with LPS and IFN-γ, there was no increase in intracellular counts; there was a nonsignificant increase in the equivalent J774A.1 cells. This suggests that MH-S cells can control bacterial growth of either Schu S4 or LVS by additional pathway(s), possibly not present in J774A.1 cells.

4. Discussion

Initial infection studies illustrated that our strain of Schu S4 was significantly more infectious than our strain of LVS (although once infected the growth rate was comparable) and this was consistent not only for the macrophage cell lines reported here but also for epithelial cell lines such as A549 (personal observation). To our knowledge this has not been previously reported by others comparing these bacterial strains and is likely to be the result of our LVS being directly obtained from a vaccine vial and not passaged through animals as the ACTC strain is documented as being so.

4.1. Cell Differences Allow Greater Understanding of Intracellular Control. Here we have assessed the role of NO in the control of intracellular infections in two murine macrophage cell lines of different provenance: the alveolar MH-S cells and the peritoneal J774A.1 cells.

The two cell lines used in this study were deliberately selected based on their provenance. Due to their differing provenance, these cell lines might be expected to have different characteristics, through adaptation to their function *in vivo*, although continuous cell lines do not always retain the full characteristics of the primary cell [17]. In this study, we aimed to determine whether this difference in aetiology would affect the relative susceptibility of J774A.1 and MH-S cells to infection and the extent of subsequent intracellular growth of bacteria and to determine the role of NO production in limiting intracellular growth.

We have found a major difference between the cell lines in their resistance to infection with *Francisella* bacteria and our data indicate that MH-S cells are 10 times more resistant to infection than J774A.1 macrophages. In our studies, Schu S4 was consistently and significantly more rapidly phagocytosed in either cell line than the avirulent LVS, an observation not reported by others [18, 19]. However in agreement with these studies, once an infection was established, there was no difference in bacterial growth rate, between strains or cell types.

Stimulation of the cell lines to induce cytokine release revealed a similar cytokine profile; the only significant difference was increased TNF-α production in J774A.1 cells. In the absence of infection, nitrite levels in MH-S and J774A.1 cells varied with stimulant, in no particular pattern. The fact that J774A.1 cells failed to produce measurable increases in NO to infection under any of the test conditions is interesting. Previous studies have shown that concentrations of available arginine are crucial for production of NO [20]. Although there is more available arginine in RPMI used to maintain the MH-S cells than in DMEM used for the J774A.1 cells (Invitrogen) both media were supplemented with 10% foetal calf serum which increased the free arginine so there was no difference between culture conditions for the two cell lines. Others have used the same strategy; for example, clearance of *Burkholderia mallei* has been reported from cultured RAW macrophages in DMEM with 10% serum and attributed to the activation of NOS [21].

4.2. Nitric Oxide Is Important in Controlling LVS Infections But Not Schu S4. Infection of either cell type *in vitro* with either strain of *Francisella* did not induce nitrite production. This was expected since it is well documented that *Francisella* spp. possess a relatively inert form of LPS that fails to stimulate macrophages [22].

However stimulation of cells with a selection of native or synthetic bacterial products (LPS and CpG) alone or in combination with the proinflammatory IFN-γ, together with infection with LVS, resulted in enhanced nitrite production, which was significant for MH-S cells. The induction of nitrite levels in response to stimulation correlated with significant suppression of intracellular counts of LVS. Blocking NOS with L-NMMA resulted in increased intracellular counts in cells stimulated with LPS or CpG and this finding correlates well with previous reports [10, 14]. The fact that stimulated macrophages can produce TNF-α and consequently sufficient NO to prevent LVS replication has been reported before [1]; however, inhibition of J774A.1 cells occurs at high MOIs when the majority of macrophages are heavily infected [23].

In contrast to infection with LVS, infection of cells with Schu S4 in combination with stimulation caused no increase in nitrite production; stimulation of cells with IFN-γ or LPS was less protective against Schu S4 infection than against LVS infection. Interestingly, although CpG appeared to be a relatively poor stimulator of nitrite production, the inhibition of NOS was permissive for the intracellular growth of LVS as well as Schu S4, suggesting that CpG was not activating any other mechanisms of cellular resistance. This in part may explain why CpGs provide protection against lethal challenge of mice with LVS but are not able to protect against Schu S4 [24–26].

Few studies have explored Schu S4 growth in macrophages. Lindgren et al. [27] reported that cells stimulated with IFN-γ were more resistant to Schu S4 and also found that Schu S4 was more resistant than LVS to exposure to extracellular NO, something we were not able to demonstrate. Ireland et al. [28] found that pretreatment of cells with IFN-γ ensured sufficient NO activity to have a controlling effect on intracellular Schu S4 counts. We did not pretreat cells with stimulants, in order to avoid any effects on phagocytosis. However Ireland et al. [28] do note that posttreatment of cells with IFN-γ did not result in control of intracellular infections.

There is a significant problem with reactive nitrogen studies in the fact that measuring the stable end-product gives little information on the speed of generation of the reactive burst [29]. This is illustrated by our findings of control of Schu S4 numbers in MH-S cells stimulated with LPS and increased intracellular growth when NO production

was blocked, despite any detectable increase in the overall production of nitrite.

4.3. Schu S4 Restricts NO Production. Schu S4 appears to have a mechanism, lacking in LVS, which prevents cellular nitrite production and this may be a significant factor in its virulence [16]. When macrophages generate NO, arginine is converted to citrulline, which can then be recycled by the cell to enable a sustained production of NO. Citrulline ureidase breaks down the citrulline, preventing further NO generation. Thus only in high concentrations of arginine can enough NO be generated to restrict Schu S4 growth. Interestingly although primarily isolated macrophages have been shown to limit intracellular growth of Schu S4 following stimulation with IFN-γ, these cells are not capable of producing NO [30]. Schu S4 appeared more able to restrict NO production in MH-S than in J774A.1 cells suggesting that J774A.1 cells hold more arginine intracellularly than MH-S cells.

This mechanism occurs over and above the activity of the superoxide dismutase that neutralises both reactive oxygen and nitrogen spp. [31] and is just one of many mechanisms employed by *F. tularensis* to manipulate and evade the host response [32].

4.4. Fully Stimulated Cells Do Not Rely upon NO. The LPS and IFN-γ mixed stimulus was able to fully inhibit bacterial growth for both Schu S4 and LVS in MH-S macrophages, despite the inhibition of cellular NOS. The combination of LPS and IFN-γ would be expected to have pleiotropic effects on macrophages in culture, apart from the induced nitrite secretion observed here for both cell lines. LPS and IFN-γ stimulation has also been reported to induce apoptosis [33]. This effect was not tested in our assay, but induction of apoptosis would significantly reduce intracellular bacterial counts.

In conclusion, NO production is a significant defence mechanism against bacterial infection in macrophages. Our results indicate that NO production in macrophage cell lines of different physiological provenance is sufficient to curtail the intracellular replication of LVS but not adequate on its own to control Schu S4. However, alveolar-derived MH-S macrophages were ten times more resistant to infection than J774A.1 cells, which are of peritoneal provenance. These data highlight both the importance of NO production to protect mammalian cells against intracellular infection and also the importance of choosing the cell line most appropriate to the route of infection to analyse host-pathogen interactions *in vitro*. In combination *in vitro*, LPS and IFN-γ are potent stimulators of mammalian cells and NO induction is a significant component in the cellular response. Here, we have demonstrated that such stimulation has resulted in a significant enhancement of the resistance to infection *in vitro*, even to the highly virulent Schu S4 strain.

Recent *in vitro* and *in vivo* studies have addressed the effects of LVS or Schu S4 infection on cytokine responses in a range of lung cells and more specifically alveolar macrophages at both the protein [34] and gene [35] levels, in the context of identifying responses which may correlate with protection. The current study has extended these data by demonstrating the importance of NO production by macrophages in resistance to infection. It further confirms the findings of Mahawar [16] by demonstrating that the differential infectivity of LVS and Schu S4 is partly due to differences in their capacity to restrict NO production by host cells. The fact that the virulent Schu S4 strain should express so many factors aimed at limiting reactive nitrogen serves to demonstrate what an effective protective cellular mechanism this is [32]. This work takes further steps towards understanding differences in mammalian cell responses to the virulent *Francisella* type A strain and LVS, an avirulent type B strain.

Conflict of Interests

The authors declare that there is no conflict of interests regarding the publication of this paper.

References

[1] A. H. Fortier, T. Polsinelli, S. J. Green, and C. A. Nacy, "Activation of macrophages for destruction of Francisella tularensis: identification of cytokines, effector cells, and effector molecules," *Infection and Immunity*, vol. 60, no. 3, pp. 817–825, 1992.

[2] N. Männikkö, "Etymologia, Francisella tularensis," *Emerging Infectious Diseases*, vol. 17, no. 5, p. 799, 2011.

[3] P. C. F. Oyston, A. Sjöstedt, and R. W. Titball, "Tularaemia: bioterrorism defence renews interest in *Francisella tularensis*," *Nature Reviews Microbiology*, vol. 2, no. 12, pp. 967–978, 2004.

[4] M. J. Hepburn and A. J. H. Simpson, "Tularemia: current diagnosis and treatment options," *Expert Review of Anti-Infective Therapy*, vol. 6, no. 2, pp. 231–240, 2008.

[5] I. N. Mbawuike and H. B. Herscowitz, "MH-S, a murine alveolar macrophage cell line: Morphological, cytochemical, and functional characteristics," *Journal of Leukocyte Biology*, vol. 46, no. 2, pp. 119–127, 1989.

[6] M. D. Melo and R. W. Stokes, "Interactioon of *Mycobacterium tuberculosis* with MH-S, an immortilized murine alveolar macrophage cell line: a comparison with primary murine macrophages," *Tubercle and Lung Disease*, vol. 80, no. 1, pp. 35–46, 2000.

[7] L. Yan and J. D. Cirillo, "Infection of murine macrophage cell lines by *Legionella pneumophila*," *FEMS Microbiology Letters*, vol. 230, no. 1, pp. 147–152, 2004.

[8] D. Damte, S.-. Lee, M.-. Hwang et al., "Inflammatory responses to Mycoplasma hyopneumoniae in murine alveolar macrophage cell lines," *New Zealand Veterinary Journal*, vol. 59, no. 4, pp. 185–190, 2011.

[9] A. Classen, J. Lloberas, and A. Celada, "Macrophage activation: classical vs. alternative," *Methods in Molecular Biology*, vol. 531, pp. 29–43, 2009.

[10] L. S. D. Anthony, P. J. Morrissey, and F. E. Nano, "Growth inhibition of *Francisella tularensis* live vaccine strain by IFN-γ- activated macrophages is mediated by reactive nitrogen intermediates derived from L-arginine metabolism," *Journal of Immunology*, vol. 148, no. 6, pp. 1829–1834, 1992.

[11] L. C. Green, D. A. Wagner, J. Glogowski, P. L. Skipper, J. S. Wishnok, and S. R. Tannenbaum, "Analysis of nitrate, nitrite,

and [15N]nitrate in biological fluids," *Analytical Biochemistry*, vol. 126, no. 1, pp. 131–138, 1982.

[12] T. Polsinelli, M. S. Meltzer, and A. H. Fortier, "Nitric oxide-independent killing of Francisella tularensis by IFN-γ- stimulated murine alveolar macrophages," *Journal of Immunology*, vol. 153, no. 3, pp. 1238–1245, 1994.

[13] R. M. J. Palmer, D. S. Ashton, and S. Moncada, "Vascular endothelial cells synthesize nitric oxide from L-arginine," *Nature*, vol. 333, no. 6174, pp. 664–666, 1988.

[14] H. Lindgren, S. Stenmark, W. Chen, A. Tärnvik, and A. Sjöstedt, "Distinct roles of reactive nitrogen and oxygen species to control infection with the facultative intracellular bacterium Francisella tularensis," *Infection and Immunity*, vol. 72, no. 12, pp. 7172–7182, 2004.

[15] J. Farlow, D. M. Wagner, M. Dukerich et al., "Francisella tularensis in the United States," *Emerging Infectious Diseases*, vol. 11, no. 12, pp. 1835–1841, 2005.

[16] M. Mahawar, G. S. Kirimanjeswara, D. W. Metzger, and C. S. Bakshi, "Contribution of citrulline ureidase to *Francisella tularensis* strain Schu S4 pathogenesis," *Journal of Bacteriology*, vol. 191, no. 15, pp. 4798–4806, 2009.

[17] R. Snyderman, M. C. Pike, D. G. Fischer, and H. S. Koren, "Biologic and biochemical activities of continuous macrophage cell lines P388D1 and J774.1," *Journal of Immunology*, vol. 119, no. 6, pp. 2060–2066, 1977.

[18] D. L. Clemens, B.-Y. Lee, and M. A. Horwitz, "Virulent and avirulent strains of *Francisella tularensis* prevent acidification and maturation of their phagosomes and escape into the cytoplasm in human macrophages," *Infection & Immunity*, vol. 72, no. 6, pp. 3204–3217, 2004.

[19] A. A. Melillo, C. S. Bakshi, and J. A. Melendez, "Francisella tularensis antioxidants harness reactive oxygen species to restrict macrophage signaling and cytokine production," *The Journal of Biological Chemistry*, vol. 285, no. 36, pp. 27553–27560, 2010.

[20] A. P. Gobert, D. J. McGee, M. Akhtar et al., "Helicobacter pylori arginase inhibits nitric oxide production by eukaryotic cells: a strategy for bacterial survival," *Proceedings of the National Academy of Sciences of the United States of America*, vol. 98, no. 24, pp. 13844–13849, 2001.

[21] P. J. Brett, M. N. Burtnick, H. Su, V. Nair, and F. C. Gherardini, "iNOS activity is critical for the clearance of Burkholderia mallei from infected RAW 264.7 murine macrophages," *Cellular Microbiology*, vol. 10, no. 2, pp. 487–498, 2008.

[22] G. Hartley, R. Taylor, J. Prior et al., "Grey variants of the live vaccine strain of Francisella tularensis lack lipopolysaccharide O-antigen, show reduced ability to survive in macrophages and do not induce protective immunity in mice," *Vaccine*, vol. 24, no. 7, pp. 989–996, 2006.

[23] M. Telepnev, I. Golovliov, T. Grundström, A. Tärnvik, and A. Sjöstedt, "*Francisella tularensis* inhibits Toll-like receptor-mediated activation of intracellular signalling and secretion of TNF-α and IL-1 from murine macrophages," *Cellular Microbiology*, vol. 5, no. 1, pp. 41–51, 2003.

[24] K. L. Elkins, T. R. Rhinehart-Jones, S. Stibitz, J. S. Conover, and D. M. Klinman, "Bacterial DNA containing CpG motifs stimulates lymphocyte-dependent protection of mice against lethal infection with intracellular bacteria," *Journal of Immunology*, vol. 162, no. 4, pp. 2291–2298, 1999.

[25] D. A. Rozak, H. C. Gelhaus, M. Smith et al., "CpG oligodeoxyribonucleotides protect mice from *Burkholderia pseudomallei* but not *Francisella tularensis* Schu S4 aerosols," *Journal of Immune Based Therapies and Vaccines*, vol. 8, article 2, 2010.

[26] D. G. C. Rees, M. G. Hartley, M. Green et al., "The ability of CpG oligonucleotides to protect mice against *Francisella tularensis* live vaccine strain but not fully virulent F. tularensis subspecies holarctica is reflected in cell-based assays," *Microbial Pathogenesis*, vol. 63, pp. 16–18, 2013.

[27] H. Lindgren, H. Shen, C. Zingmark, I. Golovliov, W. Conlan, and A. Sjöstedt, "Resistance of *Francisella tularensis* strains against reactive nitrogen and oxygen species with special reference to the role of KatG," *Infection and Immunity*, vol. 75, no. 3, pp. 1303–1309, 2007.

[28] R. Ireland, N. Olivares-Zavaleta, J. M. Warawa et al., "Effective, broad spectrum control of virulent bacterial infections using cationic DNA liposome complexes combined with bacterial antigens," *PLoS Pathogens*, vol. 6, no. 5, Article ID e1000921, pp. 1–16, 2010.

[29] M. M. Tarpey, D. A. Wink, and M. B. Grisham, "Methods for detection of reactive metabolites of oxygen and nitrogen: in vitro and in vivo considerations," *The American Journal of Physiology: Regulatory Integrative and Comparative Physiology*, vol. 286, no. 3, pp. R431–R444, 2004.

[30] J. A. Edwards, D. Rockx-Brouwer, V. Nair, and J. Celli, "Restricted cytosolic growth of Francisella tularensis subsp. tularensis by IFN-γ activation of macrophages," *Microbiology*, vol. 156, no. 2, pp. 327–339, 2010.

[31] A. A. Melillo, M. Mahawar, T. J. Sellati et al., "Identification of Francisella tularensis live vaccine strain CuZn superoxide dismutase as critical for resistance to extracellularly generated reactive oxygen species," *Journal of Bacteriology*, vol. 191, no. 20, pp. 6447–6456, 2009.

[32] C. M. Bosio, "The subversion of the immune system by *Francisella tularensis*," *Frontiers in Microbiology*, vol. 2, no. 9, Article ID Article 9, pp. 1–5, 2011.

[33] T. Gotoh and M. Mori, "Arginase II downregulates nitric oxide (NO) production and prevents NO-mediated apoptosis in murine macrophage-derived RAW 264.7 cells," *Journal of Cell Biology*, vol. 144, no. 3, pp. 427–434, 1999.

[34] R. D'Elia, D. C. Jenner, T. R. Laws et al., "Inhibition of *Francisella tularensis* LVS infection of macrophages results in a reduced inflammatory response: evaluation of a therapeutic strategy for intracellular bacteria," *FEMS Immunology & Medical Microbiology*, vol. 62, no. 3, pp. 348–361, 2011.

[35] J. David, A. J. Gates, G. D. Griffiths, and R. A. Lukaszewski, "Gene expression following low dose inhalational *Francisella tularensis* (SchuS4) exposure in Balb/c mice and the potential role of the epithelium and cell adhesion," *Microbes and Infection*, vol. 14, no. 4, pp. 369–379, 2012.

Hindawi Publishing Corporation
Journal of Immunology Research
Volume 2014, Article ID 807564, 11 pages
http://dx.doi.org/10.1155/2014/807564

Research Article

Efficacy of Primate Humoral Passive Transfer in a Murine Model of Pneumonic Plague Is Mouse Strain-Dependent

V. A. Graham, G. J. Hatch, K. R. Bewley, K. Steeds, A. Lansley, S. R. Bate, and S. G. P. Funnell

Microbiological Services, Public Health England, Porton Down, Salisbury, Wiltshire SP4 0JG, UK

Correspondence should be addressed to S. G. P. Funnell; simon.funnell@phe.gov.uk

Received 28 February 2014; Revised 21 May 2014; Accepted 18 June 2014; Published 6 July 2014

Academic Editor: E. Diane Williamson

New vaccines against biodefense-related and emerging pathogens are being prepared for licensure using the US Federal Drug Administration's "Animal Rule." This allows licensure of drugs and vaccines using protection data generated in animal models. A new acellular plague vaccine composed of two separate recombinant proteins (rF1 and rV) has been developed and assessed for immunogenicity in humans. Using serum obtained from human volunteers immunised with various doses of this vaccine and from immunised cynomolgus macaques, we assessed the pharmacokinetic properties of human and cynomolgus macaque IgG in BALB/c and the NIH Swiss derived Hsd:NIHS mice, respectively. Using human and cynomolgus macaque serum with known ELISA antibody titres against both vaccine components, we have shown that passive immunisation of human and nonhuman primate serum provides a reproducible delay in median time to death in mice exposed to a lethal aerosol of plague. In addition, we have shown that Hsd:NIHS mice are a better model for humoral passive transfer studies than BALB/c mice.

1. Introduction

Plague is caused by the gram-negative bacterium *Yersinia pestis*; it is primarily a disease of rodents, which can cause zoonotic disease directly via the aerosol route or indirectly via arthropod vectors. Throughout history, human pandemics have been caused, the greatest being during the Middle Ages where at least 25% of the population was killed [1]. There is a general perception that plague is nonexistent; however, there are several regions in the world where plague is still endemic and there is a consistent annual morbidity and mortality rate with the potential to cause large outbreaks [2]. Worldwide, from 2000 to 2009, at least 21,725 people were infected with plague and 1,612 people died, including 7 deaths in the United States [3].

Humans are extremely susceptible to plague and the aetiology of the disease is dependent upon the route and source of the infection, resulting in one of the three principal clinical forms: bubonic, septicaemic, and pneumonic plague [2]. Pneumonic plague follows inhalation of aerosolised droplets containing *Y. pestis*. It has the highest fatality rate of the three forms of plague, with a 1–3 day incubation period. It has a 100% fatality rate unless antibiotics are given the same day as symptoms develop [3]. Once inhaled the plague bacteria multiply in the alveolar spaces, and the patient is usually infectious 1-2 days after infection; during this time the patient produces highly contagious aerosolised *Y. pestis* in fine droplets, which can be inhaled deep into the respiratory tract of close contacts [2].

Antibiotics have been used for the treatment of plague and, to date, there have been two reports of antibiotic resistant plague strains [4, 5]. Laboratory experiments have shown that it is possible for *Y. pestis* to acquire plasmids which contain antibiotic resistant genes [3, 5]. Due to the rapid onset and the high case fatality rate of pneumonic plague, the potential bioterrorist threat, and the potential emergence of antibiotic resistant strains, the production of a vaccine to enable protection from this form of plague is required.

Vaccines against plague have previously been limited to live-attenuated or formalin-killed whole cell *Y. pestis*. They have not shown protection against primary pneumonic plague and have shown adverse reactions to the vaccine

itself [6, 7]. Therefore, there is a requirement for vaccines which will provide long-lasting protection against all forms of plague infection with minimal side-effects.

It has been shown that both humoral and cellular immunity are required for complete plague immunity [8–12]; however, antibodies against two natural virulence proteins F1 and V are associated with protection during a natural infection and have been shown to be protective in mouse models of pneumonic plague when given as recombinant proteins [11, 13–15]. The F1 capsular protein is unique to *Y. pestis* and is an antiphagocytic protein capsule, the gene for which is located on the pFra plasmid. The V protein is an outer membrane protein encoded by the pYV plasmid and is part of the Type III secretion system [3, 8, 11]. These (rF1 and rV) are the major constituents of new subunit plague vaccines [12, 16–24].

Due to the lack of an endemic population within which new plague vaccines could be assessed the FDA will allow licensure based on the animal rule (21CFR 601.91 Subpart H). There are several critical components in evaluating vaccine efficacy under this rule. Licensure will require the use of an assay(s) that measures a functional component of the immune response and is reasonably likely to predict clinical benefit. Scientists and regulatory authorities have for many years been looking for a functional assay which will enable measurement of a correlate of protection against pneumonic plague. Passive immune protection studies in animals, using antibodies isolated from vaccinated individuals, may provide this assay [14, 15, 25, 26].

The experiments described here detail the development of a pneumonic plague mouse model and the subsequent use of this model to test the *Y. pestis* subunit vaccine containing recombinant F1 and recombinant V (rF1 and rV) by the passive transfer of unfractionated serum and plasma from immunised cynomolgus macaques and humans.

This is the first paper to assess the ability of the rF1 and rV vaccine to generate protection from an aerosol challenge of the CO92 strain of *Y. pestis* by passive transfer of unfractionated serum. Previous papers have assessed the combined rF1V fusion protein [13]. Known titres of anti-rF1 and anti-rV antibodies were then transferred into groups of immunologically naïve mice to assess the ability of humoral immunity to protect against pneumonic plague.

2. Materials and Methods

2.1. Bacterial Strain. *Y. pestis* strain CO92 (biovar Orientalis, NR641, BEI Repositories) was supplied by the Biodefence and Emerging Infections (BEI) Research Repository (USA) in accordance with International Export and Import Regulatory Requirements. The organism was stored and handled in accordance with US Biological Select Agent or Toxin requirements.

2.2. Bacterial Growth and Subculture. The generation of the master stock was performed by streaking *Y. pestis* onto tryptic soy agar (TSA) (VWR, UK) and incubated at 26°C for 48 hours. This was used to inoculate tryptone soya broth (TSB) (Media Services, PHE) which was incubated overnight at 26°C. This broth was then used to inoculate a further suspension of TSB, which was incubated at 26°C overnight. A 50% glycerol (Sigma, UK) solution was added to the broth to a final concentration of 40% (v/v) glycerol. The master stocks were frozen at −80°C. Working stocks were generated from a vial of master stock. This was performed by streaking the master stock of *Y. pestis* onto TSA and incubating at 26°C for 72 hours. A strike through of the lawn was used to inoculate a large volume of TSB and was incubated overnight at 26°C. A 50% glycerol solution was added to the broth to a final concentration of 40% (v/v) glycerol. The working stocks were frozen at −80°C. Master stock certificate of analysis was produced; characterisation of these stocks included microscopic staining (Wayson's), colony morphology and purity checks on TSA, Congo red uptake on Congo red agar, multiple loci (5 target) PCR, 16S rRNA sequencing, and VNTR for genetic integrity checks. Subcutaneous lethality checks were performed on BALB/c mice and stocks were 100% lethal (data not shown). All experimental and confirmatory studies were performed using the working stock vials; therefore they had a maximum passage number of 3.

2.3. Preparation of Inoculum. All inocula were prepared in the same way. A vial from the working stock was thawed at ambient temperature and then streaked onto TSA and incubated at 26°C for 54 hours for subculture and purity check. The contents of individual streak plates were washed into 25 mL total of TSB. To obtain maximal yields, the broth was incubated with orbital agitation at 26°C for 18 hours. Following incubation, 25 mL fresh TSB was added and the optical density was measured at 600 nm wavelength. The broths were then reincubated with orbital agitation for 3 hours at 26°C. The broths were harvested when the $OD_{600\,nm}$ values were over 3, with an aliquot taken for real time PCR analysis.

2.4. Determination of Bacterial Challenge Dose. Retrospective quantification of colony forming unit concentration of inocula was conducted using a spread plate method. Briefly, serial ten-fold dilutions were created to bring the bacterial suspensions into a countable range. In duplicate, 100 μL of each diluted bacterial suspension was spread across the surface of a TSA plate. After 48 hours incubation, the plates were manually counted for colony forming unit content and the average counts used to determine colony forming unit concentration (CFU/mL). Immediately prior to aerosol exposure of mice all inocula were checked for the presence of plasmids and essential genetic characteristics by PCR, as described below. *In vivo* studies were not initiated without confirmation of genetic integrity by PCR for each batch of inocula culture.

2.5. Confirmation of Strain Virulence. A four target real time PCR was utilised to ensure genetic integrity and stability for each batch of inocula used for *in vivo* studies. This confirmed the presence of all three plasmids and the *pgm* virulence locus

Table 1: Genetic primer targets of the PCR test used to ensure integrity of the inoculum. All primer probe design was based on GenBank accession number NC_003143 (*Yersinia pestis* CO92, complete genome). MGB is *minor groove binder/nonfluorescent quencher* covalently bound to the 3′ end of the probe. All probes have a 5′ fluorescein (FAM) label.

Gene	Sequence (5′ → 3′)
HmsF (chromosomal *pgm* locus)	
Forward	CGGAGAAGCCAACGTTCGT
Reverse	TCTTTCACTTTGCGGCAATG
Probe (MGB)	CCGCCTGCACAACG
F1 (pMT1)	
Forward	TTGGCGGCTATAAAACAGGAA
Reverse	CACCCGCGGCATCTGTA
Probe (MGB)	CACTAGCACATCTGTTAAC
Pst (pPCP1)	
Forward	CGGCAATCGTTCCCTCAA
Reverse	GGTCAGGAAAAAGACGGTGTGA
Probe (MGB)	AACCATGACACGGTAGACT
VAg (pCD1)	
Forward	CGGCGGTTAAAGAGAAATGC
Reverse	CATCGCCGAATACACAATGG
Probe (MGB)	TACTGCCATGAACGCC

[27] of the bacterial chromosome. The PCR was based on the targets detailed in Table 1. PCR reaction constituents consist of 2× fast universal master mix (Applied Biosystems) 10 μL; forward primer (900 nM); reverse primer (900 nM); probe (250 nM); DNA template 2 μL; and nuclease-free water to a final volume of 20 μL. PCR thermal cycling consisted of 40 cycles (ABI 7500 fast protocol) comprising 95°C, 3 seconds, and 60°C, 30 seconds.

2.6. Mice. In accordance with UK Home Office regulations, BALB/c and Hsd:NIHS mice were obtained from UK accredited suppliers (Harlan, UK, or Charles River, UK). In all studies described, mice were required to comply with both age and weight selective criteria: age minimum 8–10 weeks and a minimum body weight of 17 grams. Mice were randomly assigned and housed in groups of between five and ten. Food and water available to all mic *ad libitum*, and were exposed to 12 hour. Pilot studies were performed with groups of 5 or 6 mice. Details for all the challenge experiments can be found in Table 2. All animal procedures were conducted under the authority of and in accordance with a UK Home Office license.

2.7. Health Monitoring. For three days before infection and throughout the remainder of the studies, mice were weighed in the morning and afternoon to monitor diurnal bodyweight fluctuation. In addition, the health status of each mouse was checked on at least two occasions every day. When mice began to show signs of infection, the monitoring frequency was increased to at least four occasions every day. When mice were seen to have restricted movement and reflexes they were humanely euthanised using a UK Home Office schedule 1 procedure.

2.8. Human Serum. All human serum samples were from individuals vaccinated with either 40, 80, or 120 μg of recombinant plague vaccine using the same dosing regimen and serum isolated 35, 196, or 365 days postvaccination. All human serum samples were provided by NIAID (through Avecia and PharmAthene) under contract number N01-AI30062.

2.9. Pharmacokinetic Analysis of Human Antibodies. Pooled human serum with known ELISA titres against rF1 and rV proteins was injected into four groups of five BALB/c mice via the intraperitoneal route (250 μL/mouse). Groups of mice were serially sacrificed at 1.5, 3, 6, and 12 hours after injection. One group of 5 mice was injected with 250 μL/mouse negative control serum for a control. The levels of circulating human IgG antibody levels specific for rF1 and rV were determined by ELISA (performed by Huntingdon Life Sciences, UK).

2.10. Passive Humoral Therapy of Human Serum. Three to six hours before aerosol infection, groups of five mice were administered with 250 μL of human serum via the intraperitoneal route. Mice were administered with either test, positive control or negative control human serum. The mice were then transferred into high-containment isolators before being loaded into restraint tubes for aerosol administration.

2.11. Aerosol Challenge of Mice. Groups of mice were challenged for 10 minutes with a dynamic aerosol of *Y. pestis* (<2 μm, mass median aerodynamic diameter) using a contained modified Henderson apparatus [28]. The challenge aerosol was generated using a three-jet Collison nebulizer (BGI, Waltham, USA) containing 20 mL *Y. pestis* in TSB. The resulting aerosol was mixed with conditioned air (65% relative humidity, 22°C) in the spray tube and delivered to the nose of each animal via an exposure tube in which the unanaesthetised mice are held in restraint tubes. Samples of the aerosol were collected into 20 mL TSB using an SKC Biosampler (SKC, Dorset, UK) operating at 12.5 L/min. In the later studies using the Hsd:NIHS mice, aerosol samples were collected using an All Glass Impinger (AGI30, Ace Glass, USA) [29] operating at 6 L/min and an Aerodynamic Particle Sizer (TSI Instruments Ltd., Bucks, UK), controlled using the AeroMP management platform (Biaera Technologies LLC., MD, USA). Counts were used to calculate the inhaled dose using a derived respiratory minute volume estimated from the average weight of the animals [30].

2.12. ELISA. Recombinant F protein (rF1) and V protein (rV) (provided by Pharmathene via NIAID) were coated

Table 2: A tabular summary of the murine data for each of the challenge experiments described.

Study	Number of mice per group	Minimum body weight (g)	Sex of mice	Source of mice	Strain of mice
Study 1	6	17.7	Female	Harlan	BALB/c
Study 2	10	17.5	Female	Charles Rivers	BALB/c
Study 3	10	17.1	Female	Charles Rivers	BALB/c
Study 4	5	18.0	Female Male	Harlan	BALB/c Hsd:NIHS
Study 5	10	18.0	Female	Harlan	BALB/c Hsd:NIHS
Study 6	10	18.0	Female	Harlan	Hsd:NIHS

in carbonate coating buffer separately into wells of 96-well microplate (Nunc Maxisorp C96, Fisher Scientific, UK) and incubated overnight at 4°C. The plates were washed in PBS containing 0.05% w/v Tween-20 (Sigma, UK) before and after each absorptive reagent addition. Plates were blocked for 2 hours with PBS containing 3% w/v bovine serum albumin (BSA) (Sigma, UK). Where necessary, samples were prediluted using PBS containing 1% w/v BSA and 0.05% Tween-20. Murine samples containing human antibody were incubated for 1 hour, and vaccinated-goat serum was used as a positive control (rF1 14182 Pro-Sci, USA; rV 14181 Pro-Sci, USA). Bound antibody was detected with horseradish peroxidase conjugated to protein-G (Pierce, USA). Bound conjugate was detected by addition of ABTS peroxidase substrate system (Kirkegaard and Perry Laboratories, USA), and the reaction stopped with ABTS peroxidase stop solution (Kirkegaard and Perry Laboratories, USA). Plates were read at a wavelength of 405 nm using an automated ELISA reader (VersaMax, Molecular Devices, CA, USA) and data was analysed using Softmax Pro version 4.7.1. (Molecular Devices, CA, USA). The goat positive control sera (anti-rF1 or anti-rV) were assigned arbitrary values of 10000 units per mL. The human and cynomolgus macaque sera titres were extrapolated from the goat positive control sera.

2.13. Cynomolgus Macaques (Macaca fascicularis). Two female cynomolgus macaques of Mauritian origin were obtained from a UK breeding colony for use in this study. Both animals weighed more than 2.5 kg and were over 2 years of age at immunization. Animals were housed according to the Home Office (UK) Code of Practice for the Housing and Care of Animals Used in Scientific Procedures (1989) and the National Committee for Refinement, Reduction and Replacement (NC3Rs) Guidelines on Primate Accommodation, Care and Use, August 2006. When a procedure required the removal of a primate from a cage it was sedated by intramuscular (*i.m.*) injection with ketamine hydrochloride (10 mg/kg) (Ketaset, Fort Dodge Animal Health Ltd., Southampton, UK). All procedures were conducted under a project license approved by the Ethical Review Process of Public Health England, Salisbury, UK, and the UK Home Office. None of the animals had previously been used for experimental procedures.

2.14. Generation of Cynomolgus Macaque Immune Serum. Two cynomolgus macaques were immunized then twice boosted with a recombinant plague vaccine consisting of rF1 and rV antigens with an alhydrogel adjuvant (plague (recombinant) vaccine suspension, 873082-H01, Batch 7051, Avecia Biologics Ltd., UK). A 20 ug/mL solution was prepared by adding 0.25 mL of the vaccine (which contained 240 ug/mL of each antigen adjuvanted with 0.26% (w/w) alhydrogel) to 2.75 mL 0.26% (w/w) alhydrogel in a sterile vessel and mixed thoroughly. The vaccination schedule comprised of three intramuscular injections of 10 μg of total antigen with a 21 day interval between injections.

2.15. Pharmacokinetic Analysis of Cynomolgus Macaque Antibodies. Pooled cynomolgus macaque serum with known ELISA titres against rF1 and rV proteins was injected into groups of five Hsd:NIHS mice via the intraperitoneal route (250 μL/animal). Groups of five mice were serially sacrificed, preinjection or at 1.5, 3, 6, and 12 hours postinjection. The levels of circulating cynomolgus macaque IgG antibody were determined by ELISA as previously described.

2.16. Passive Humoral Therapy of Cynomolgus Macaque Serum. Three to six hours before aerosol infection, groups of five mice were administered with 250 μL/mouse of test cynomolgus macaque serum, positive control vaccinated human serum, or as a negative control nonvaccinated human serum via the intraperitoneal route. The mice were then transferred into high containment isolators before being loaded into restraint tubes for aerosol administration.

2.17. Statistical Analysis. Survival analysis was performed using Kaplan-Meier survival curves and comparisons were performed using Wilcoxon rank sum for P values [31].

3. Results

3.1. Aerosol BALB/c Murine Infection Model. An aerosol model of plague was developed using BALB/c mice to enable assessment of the efficacy of passive transfer of antibodies against pneumonic plague. An exposure to 2.4 LD_{50}

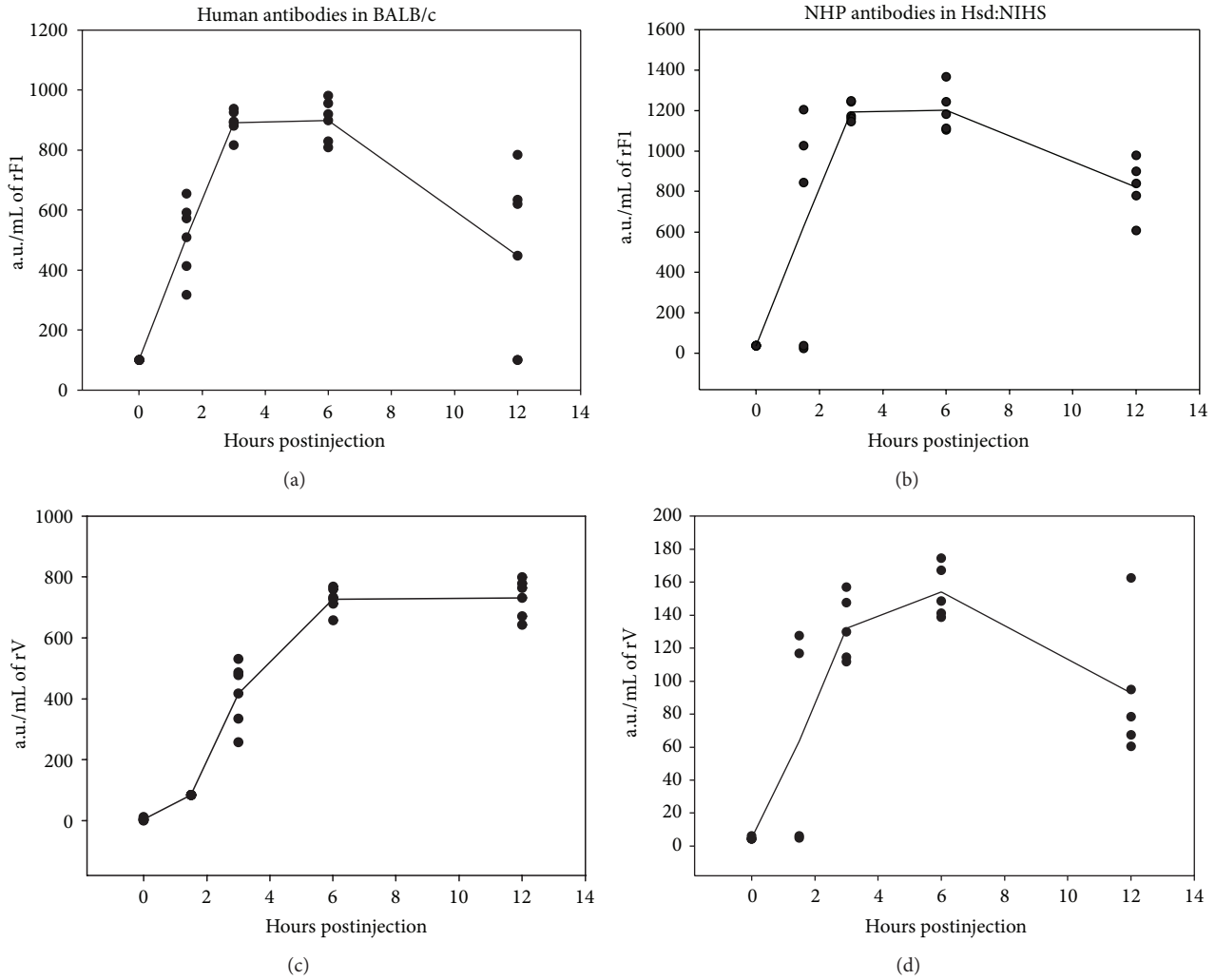

Figure 1: Pharmacokinetics of human or cynomolgus macaque antibody in BALB/c and Hsd:NIHS mice, respectively. 0.25 mL human ((a) and (c)) or cynomolgus macaque ((b) and (d)) plague vaccine serum was injected via the intraperitoneal route into BALB/c ($n = 20$) or Hsd:NIHS ($n = 20$) mice, respectively. The mice were serially sacrificed and the presence of anti-rF1 ((a) and (b)) or anti-rV ((c) and (d)) antibody was assessed by ELISA. Additional groups of mice ($n = 5$) were sacrificed preinjection to provide baseline data. The data suggests that the time delay between passive antibody administration and optimal serum concentration in the murine serum was between 3 and 6 hours. a.u., arbitrary units.

aerosolised *Y. pestis* CO92 or above was found to produce a mean time to death of 4.2 days (±0.5 SE).

The presented dose used in a range of humoral passive transfer experiments was extremely consistent and only varied between 10.6 and 13.9 LD_{50}s.

3.2. Passive Protection of Human Antibody within BALB/c Mice. To maximise the efficacy of passively transferred antibodies, we examined the pharmacokinetics of human antibody in the circulating blood stream of BALB/c mice (Figure 1). The results indicated that optimal human antibody concentrations were reached between three and six hours after intraperitoneal administration into mice.

A pool of high titre serum obtained from human volunteers that had been vaccinated with experimental recombinant plague vaccine was initially used to assess the concept that passive human antibody therapy would provide some form of protection against pneumonic plague in BALB/c mice. The combined Kaplan-Meier survival curves of three studies are presented in Figure 2. All BALB/c mice were infected three hours after intraperitoneal administration of 250 μL of either nonimmune human serum or a pool of serum from vaccinated volunteers. The serum had a significant protective effect ($P < 0.001$, Wilcoxon test), as defined by a delay of the median time to death (MTD) of 1 to 2 days (Table 3).

3.3. Assessment of Vaccine Dose and Longevity of Protection. The dose of the vaccine required to provide protection was investigated by examining the protective effect of human sera taken from vaccines 35 days after they received one

Table 3: A tabular summary of presented dose of aerosolised *Y. pestis*, passive immune therapy treatment, and MTD in BALB/c and Hsd:NIHS mice. The median time to death (MTD) was calculated using a Kaplan-Meier survival plot. N/D: not determined; over 50% of the mice survived to the end of these experiments; therefore an MTD could not be calculated.

Presented dose		Mouse strain	Study	Passive immune treatment	MTD
(CFU)	LD_{50}				
240	0.05	BALB/c	4	No treatment	N/D
3,000	0.6	BALB/c	4	No treatment	N/D
12,000	2.4	BALB/c	4	No treatment	3.7
62,026	12.4	BALB/c	1	Human reference serum	4.92
57,746	11.5	BALB/c	2	Human reference serum	4.18
69,390	13.9	BALB/c	3	Human reference serum	4.71
62,026	12.4	BALB/c	1	Human control negative serum	3.42
57,746	11.5	BALB/c	2	Human control negative serum	2.94
69,390	13.9	BALB/c	3	Human control negative serum	3.17
57,746	11.5	BALB/c	2	D35 40 μg	3.94
57,746	11.5	BALB/c	2	D35 80 μg	4.18
57,746	11.5	BALB/c	2	D35 120 μg	4.18
69,390	13.9	BALB/c	3	D196 40 μg	5.17
69,390	13.9	BALB/c	3	D196 80 μg	5.17
69,390	13.9	BALB/c	3	D196 120 μg	4.71
69,390	13.9	BALB/c	3	D365 40 μg	4.33
69,390	13.9	BALB/c	3	D365 80 μg	4.71
69,390	13.9	BALB/c	3	D365 120 μg	4.71
240	0.05	Hsd:NIHS	4	No treatment	N/D
3,000	0.6	Hsd:NIHS	4	No treatment	3.46
12,000	2.4	Hsd:NIHS	4	No treatment	3.96
53,000	10.6	BALB/c	5	Human vaccine serum	5.48
53,000	10.6	BALB/c	5	Human control negative serum	3.48
53,000	10.6	Hsd:NIHS	5	Human vaccine serum	7.73
53,000	10.6	Hsd:NIHS	5	Human control negative serum	3.48
62,000	12	Hsd:NIHS	6	Human vaccine serum	7.75
62,000	12	Hsd:NIHS	6	Human control negative serum	3.25
62,000	12	Hsd:NIHS	6	Cynomolgus macaque vaccinated serum	N/D

of three different doses (40 μg, 80 μg, and 120 μg). The sera showed a significant protective effect ($P < 0.001$, Wilcoxon test) in survival analysis (Figure 3) as defined by a delay of the MTD from 2.94 days to between 3.92 and 4.18 days (Table 3). However, there was no significant difference ($P > 0.02$, Wilcoxon test) between the three doses of vaccine.

The length of the protective effect of immunisation was also tested by comparing the passive protective effect of human vaccine sera taken at 35, 196, and 365 days postimmunisation in the BALB/c pneumonic plague model (Figures 3 and 4). There was no significant difference ($P > 0.02$, Wilcoxon test) in the passive protection of the mice from the human sera from three different doses and 35, 196, and 365 days postvaccination.

In order to assess the relationship between ELISA titre and MTD, all the data from the different dose experiments were combined. As illustrated in Figure 5, a good correlation was obtained between MTD and the ELISA titre of the sera against both rF1 ($R^2 = 0.91$) and rV ($R^2 = 0.92$).

The pneumonic plague model was initially developed in BALB/c mice. However, even when using the highest titre human sera available, passive transfer only resulted in a delay in the MTD in BALB/c mice in our hands. We were aware that other published literature had previously described 100% survival in other murine strains [13]. As a result, Hsd:NIHS mice were investigated to determine whether the protection conferred by the human antibodies would be more effective in the different mouse strain.

3.4. Aerosol Hsd:NIHS Murine Infection Model. An aerosol model of murine plague using Hsd:NIHS mice was developed to enable assessment of the efficacy of passive transfer of

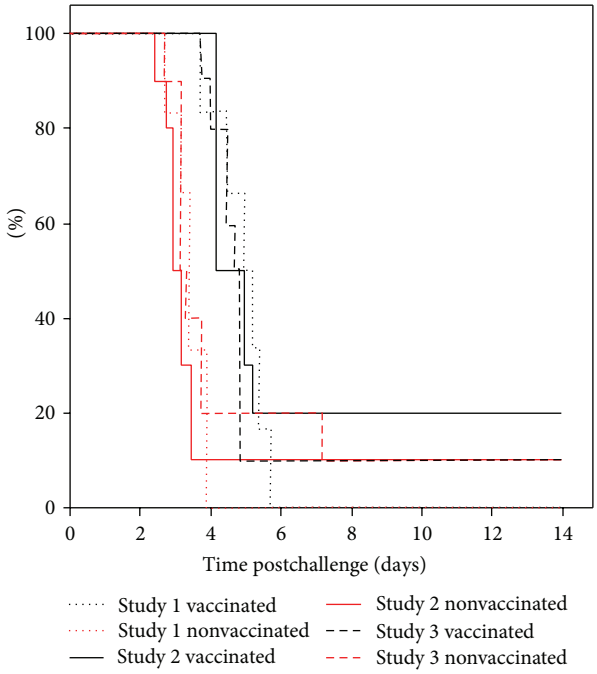

Figure 2: Combined survival plots of 3 studies following passive therapy of mice with either nonimmune or plague vaccinated volunteer serum. Study (1), $n = 6$ per group, study (2), $n = 10$ per group, and study (3), $n = 10$ per group. Mice were administered 250 μL human serum into the peritoneal cavity, 3 hours before being exposed to more than 10 LD_{50} aerosolised *Y. pestis* using a modified contained Henderson apparatus. The median time to death (MTD) was calculated using a Kaplan-Meier survival plot.

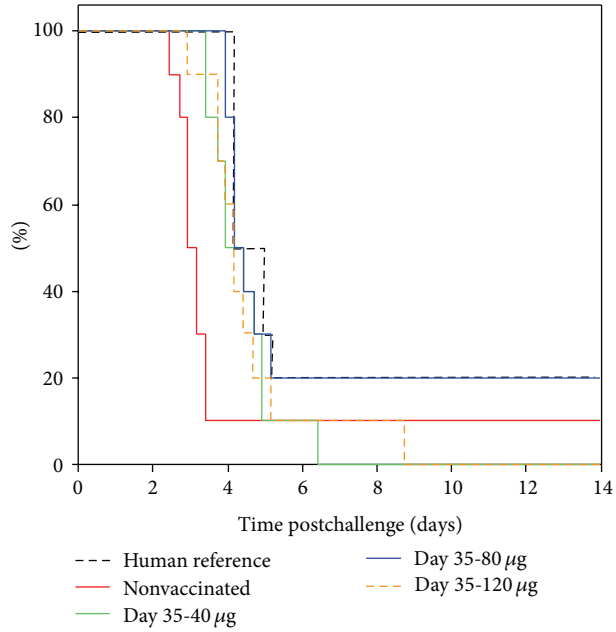

Figure 3: Combined survival plots of BALB/c mice following passive transfer of human serum from vaccines 35 days after receiving different doses of vaccine. Study (2), $n = 10$ per group. Mice were administered 250 μL human serum into the peritoneal cavity, 3 hours before being exposed to more than 10 LD_{50} aerosolised *Y. pestis* using a modified contained Henderson apparatus. The median time to death (MTD) was calculated using a Kaplan-Meier survival plot.

human antibodies. Results showed that there was no difference in the time to death of Hsd:NIHS mice ($P > 0.02$, Mann-Whitney) compared to BALB/c mice after aerosol challenge of *Y. pestis* (Figure 6), and Table 3 demonstrates that a presented dose of 2.4 LD_{50} or above results in an average MTD of 5.3 days (±0.8 SE).

3.5. Comparison of Passive Protection of Human Antibody within Hsd:NIHS and BALB/c Mice. The highest titre human serum available was used to compare the suitability of BALB/c and Hsd:NIHS mouse strains for the assessment of passive protection against pneumonic plague. After exposure to 10.6 LD_{50} of *Y. pestis*, the MTD of BALB/c and Hsd:NIHS with negative control sera was the same at 3.5 days (Figure 7). However, after intraperitoneal administration of high titre human vaccine serum, there were statistically significant ($P < 0.02$, Wilcoxon test) delays in the MTD in both BALB/c and Hsd:NIHS mice of 5.5 to 7.7 days, respectively (Table 3).

3.6. Use of Cynomolgus Macaque Serum to Provide Passive Protection

3.6.1. Cynomolgus Macaque Immunisation. To confirm that cynomolgus macaque serum can provide a significant level

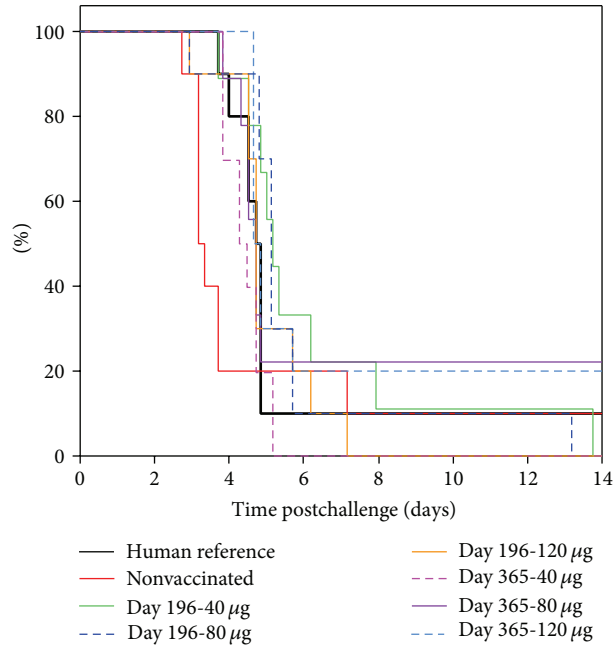

Figure 4: Combined survival plots of mice following passive therapy of either nonimmune or plague vaccinated volunteer serum from 196 to 365 days postinoculation. Study (3), $n = 10$ per group. BALB/c mice were administered 250 μL human serum into the peritoneal cavity, 3 hours before being exposed to *Y. pestis* using a modified contained Henderson apparatus. The median time to death (MTD) was calculated using a Kaplan-Meier survival plot.

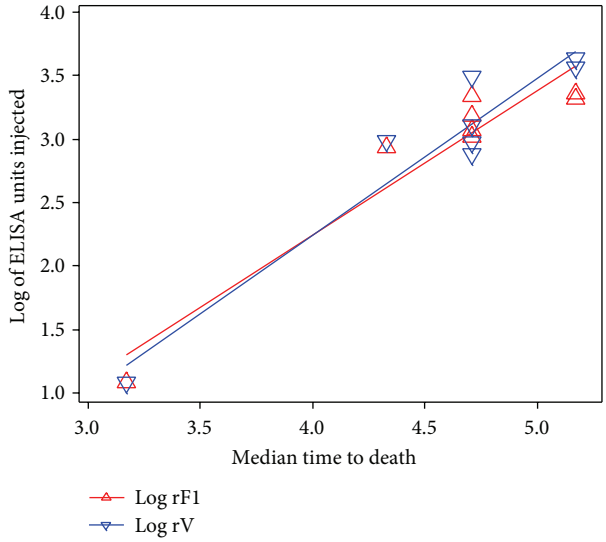

Figure 5: When all of the passive protection data from BALB/c mice were pooled, the log ELISA titre against both rF1 and rV correlated with survival time.

of protection against pneumonic plague, two cynomolgus macaques were immunised intramuscularly with three 10 μg doses of rF1 and rV vaccine 21 days apart. The antibody titres were monitored and the study terminated after the peak of the anti-rF1 and anti-rV antibody responses. The serum isolated at termination was pooled and the anti-rF1 and anti-rV antibody titres were assessed by ELISA (Figure 8).

3.6.2. Pharmacokinetics of Primate Antibody in Mice. To maximise the efficacy of passively transferred antibodies, we examined the pharmacokinetics of cynomolgus macaque serum in the circulating blood stream of Hsd:NIHS mice (Figure 1). The results showed that optimal primate antibody concentrations were reached between three and six hours after intraperitoneal administration of 250 μL. This had a similar profile to human antibodies in BALB/c mice.

3.6.3. Passive Protection with Primate Sera. The cynomolgus macaque serum was used in an assessment of passive protection in Hsd:NIHS mice against an aerosolised challenge of *Y. pestis*. The MTD of the untreated mice was observed to be 3.5 days, whereas the MTD of mice treated with the highest titre of human serum was 7.7 days (Figure 9). The MTD for the mice treated with the cynomolgus macaque serum could not be determined because 60% of the mice survived until day 14. However, there was no statistical difference ($P > 0.02$, Wilcoxon) between the passive protective effect of human and cynomolgus macaque vaccine sera in Hsd:NIHS mice.

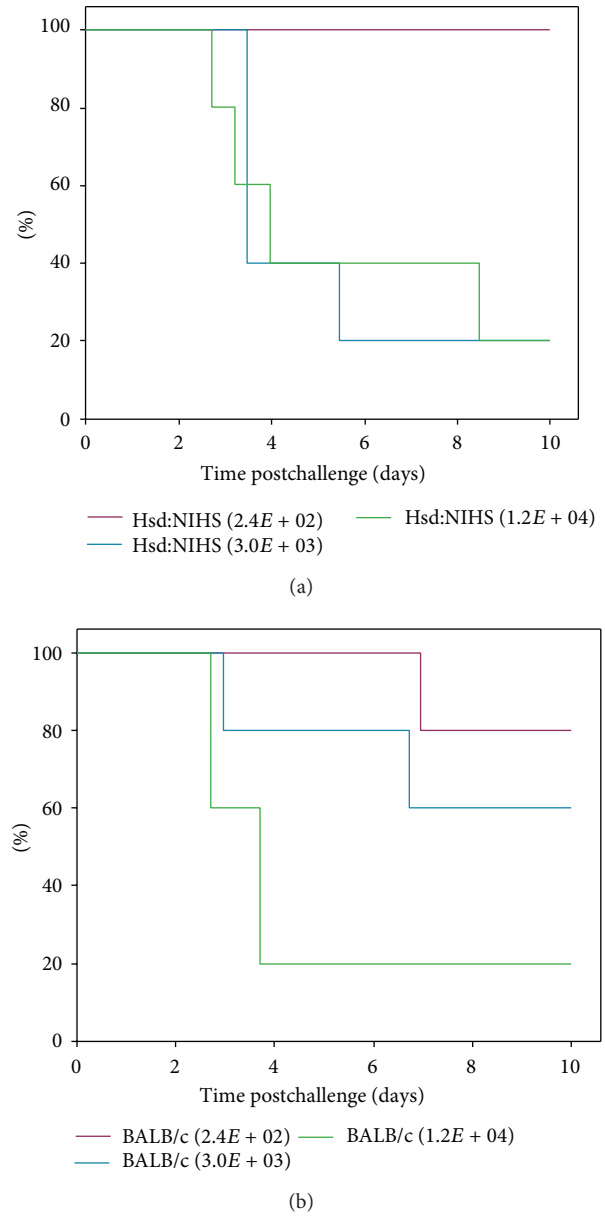

Figure 6: Mouse strain BALB/c and Hsd:NIHS had similar susceptibly to aerosolised *Y. pestis*. (a) shows the survival plots for Hsd:NIHS and (b) shows the survival plots for BALB/c mice. Study (4), $n = 5$ per group. The MTD was calculated using a Kaplan-Meier survival plot.

4. Discussion

The rF1 and rV vaccine was developed to protect against pneumonic plague in humans. In order to enable the licensure of the plague vaccine, information regarding efficacy will need to be provided using animals and the FDAs "animal rule" [32]. In addition, linkage between the human disease and animal studies is essential. An assessment of the protective effect following the passive transfer of antibodies from human vaccines to mice may provide this link.

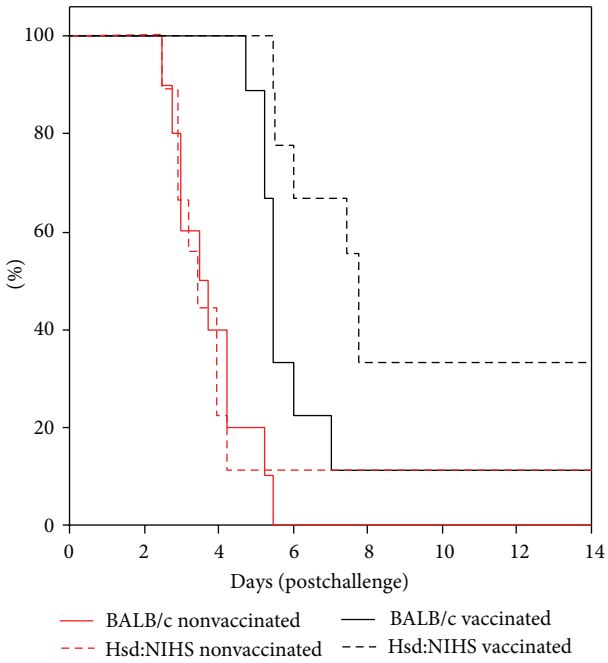

FIGURE 7: Hsd:NIHS mice had better survival outcomes than BALB/c mice after administration of human serum. Study (5), $n = 10$ mice per group. Mice were injected with 250 μL human serum into the peritoneal cavity, 3–6 hours before being exposed to aerosolised *Y. pestis* using a modified contained Henderson apparatus. The MTD was calculated using a Kaplan-Meier survival plot.

A model of pneumonic plague was successfully set up by challenging BALB/c mice with aerosolised *Y. pestis* (CO92). This system was both robust and reproducible. To determine whether the antibody response raised against the rF1 and rV plague vaccine was sufficient to protect against pneumonic plague, a passive transfer model in BALB/c mice using human serum was developed. Serum from rF1 and rV vaccines provided significant protection in the pneumonic plague mouse model, as defined by a delay in MTD of between 1 and 2 days. The protective effect of human vaccine sera in mice was found to extend up to 365 days postimmunisation. In addition, this protective effect was not found to be dose dependent as no difference was observed between sera from vaccines that received 40, 80, or 120 μg.

By examining the relationship between human IgG ELISA titre to either rF1 or rV and the MTD, we have demonstrated that the ELISA titres are proportional to the extent of the protective effect. This supports the findings by Fellows et al. [13, 32] which used the recombinant rF1V vaccine and Green et al. [33] who used the rF1 and rV vaccine used within this paper. However, in contrast with the findings of Fellows et al., [13] the passive transfer of human antibody was not providing complete protection as expected. Therefore, we used a mouse strain more closely related to that used by Fellows et al., the outbred Hsd:NIHS strain, and compared them to the inbred BALB/c mouse strain which was used in our earlier studies.

When we compared the susceptibility of Hsd:NIHS and BALB/c mice to aerosolised *Y. pestis* CO92, we found no statistical differences in the mean time to death. To determine whether the antibody response raised against the rF1 and rV plague vaccine was sufficient to protect against pneumonic plague, a passive transfer model in Hsd:NIHS mice using human serum was developed. This was compared to the BALB/c model. Serum from human rF1 and rV vaccines provided significant protection in both the BALB/c and Hsd:NIHS mice strains, as defined by a delay in MTD of between 2 and 4 days, respectively. Restrictions in the quantity of human vaccine trial serum available prevented a repeat pharmacokinetic study of human antibody in Hsd:NIHS mice. The outcome of the pharmacological analysis of cynomolgus macaque antibodies in Hsd:NIHS mice did, however, provide sufficient similarity in the clearance rate of primate antibody for us to be confident that the delay between passive antibody administration and infection was optimal in both murine species.

Cynomolgus macaque sera were also used to assess protection in Hsd:NIHS mice against an aerosolised challenge of *Y. pestis*. The MTD of untreated mice was 3.5 days, whereas those treated with the highest titre of human serum was 7.7. We were unable to provide a median time to death for the NHP serum, as 60% of the mice survived until the end of the experiment.

The passive transfer data presented in this paper supports the findings of previous passive transfer studies from plague vaccine studies [13, 25, 34]. However an interesting result from this study was the difference between the ability of the outbred Hsd:NIHS and the inbred BALB/c to utilise human serum to protect against pneumonic plague. The duration of protection with the human serum was significantly longer in Hsd:NIHS mice than in BALB/c mice. The reason for this difference in protection is unknown and could have important implications when evaluating the efficacy of human antibodies in other passive transfer experiments and should be investigated further. New murine IgG Fc receptors are continually being discovered [35] and are currently being evaluated for their specificity to human IgG. The possibility that Hsd:NIHS mice are able to bind human IgG more effectively than BALB/c mice should be further investigated.

In summary, the results presented in this study demonstrate that passive transfer of human and cynomolgus macaque antibodies raised in response to vaccination with rF1 and rV provides protection in the form of delay in the median time to death in murine pneumonic plague. The data indicate that increasing levels of antibodies result in an increase in the MTD. Our data also demonstrates a good correlation between IgG ELISA titres to rF1 and rV with biological protection. In addition, human serum was better utilized for protection in Hsd:NIHS mice than in BALB/c mice.

Conflict of Interests

The authors declare that there is no conflict of interests regarding the publication of this paper.

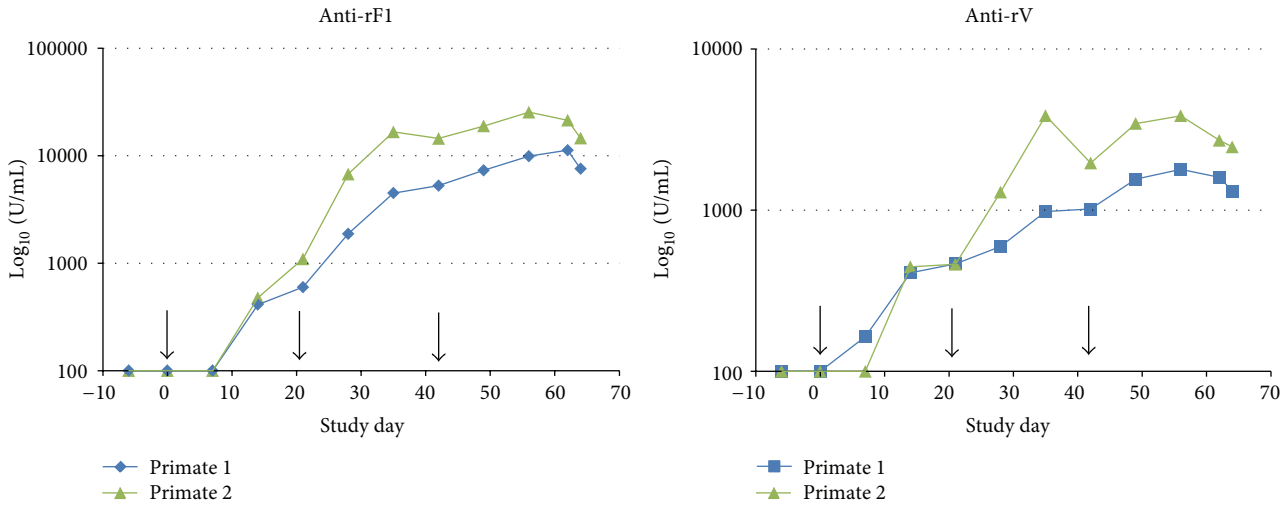

Figure 8: Assessment of anti-rF1 and anti-rV antibody titres in NHP serum after 3 intramuscular immunizations of 10 μg of rF1 and rV antigen. Detectable amounts of anti-rF1 and anti-rV antibodies were found in the serum 2 weeks after the primary immunization, with anti-rF1 consistently having a higher titre.

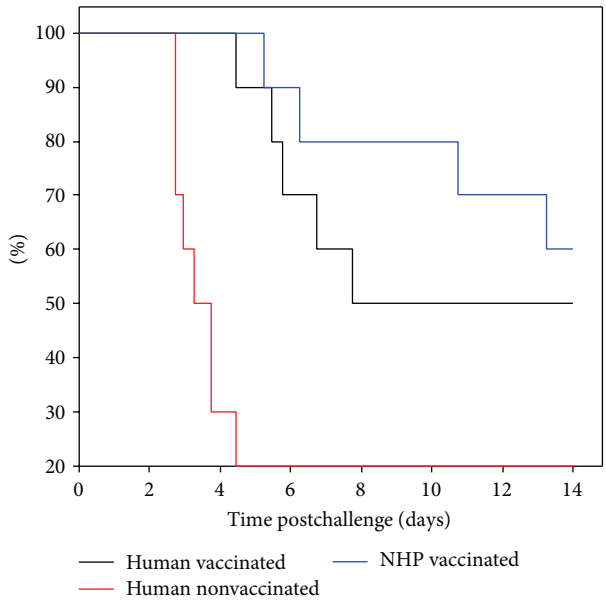

Figure 9: Passive immune therapy with NHP serum provided better protection in Hsd:NIHS mice than human serum after a lethal challenge of *Y. pestis*. Study (6), n = 10 mice per group. Mice were administered 250 μL serum into the peritoneal cavity, 3–6 hours before being exposed to aerosolised *Y. pestis* using a modified contained Henderson apparatus. The MTD was calculated using a Kaplan-Meier survival plot.

Acknowledgments

This study was funded by the National Institute for Allergy and Infectious Diseases, Contract no, N01-A1-30062. The authors would like to thank the Biological Investigation Group for their help and support with the animal work, all members of the bacteriology and immunology teams, past and present, who contributed to this work, HLS for performing and analysing the first pharmacokinetic study, NIAID for the provision of the vaccinated human serum, Allen Roberts for supervision and acquisition of funding, Julia Vipond, Julia Tree, and Stuart Dowall for their assistance and support with the preparation and reviewing of the paper. In addition, the authors thank Dstl for their permission to use the human ELISA assay conducted at HLS in the human PK study.

References

[1] M. B. Prentice and L. Rahalison, "Plague," *The Lancet*, vol. 369, no. 9568, pp. 1196–1207, 2007.

[2] E. D. Williamson, "Plague," *Vaccine*, vol. 27, supplement 4, pp. D56–D60, 2009.

[3] T. Butler, "Plague gives surprises in the first decade of the 21st century in the United States and worldwide," *The American Journal of Tropical Medicine and Hygiene*, vol. 89, no. 4, pp. 788–793, 2013.

[4] M. Galimand, A. Guiyoule, G. Gerbaud et al., "Multidrug resistance in Yersinia pestis mediated by a transferable plasmid," *The New England Journal of Medicine*, vol. 337, no. 10, pp. 677–680, 1997.

[5] A. Guiyoule, G. Gerbaud, C. Buchrieser et al., "Transferable plasmid-mediated resistance to streptomycin in a clinical isolate of Yersinia pestis," *Emerging Infectious Diseases*, vol. 7, no. 1, pp. 43–48, 2001.

[6] K. F. Meyer, "Effectiveness of live or killed plague vaccines in man," *Bulletin of the World Health Organization*, vol. 42, no. 5, pp. 653–666, 1970.

[7] J. D. Marshall Jr., P. J. Bartelloni, D. C. Cavanaugh, P. J. Kadull, and K. F. Meyer, "Plague immunization. II. Relation of adverse clinical reactions to multiple immunizations with killed vaccine," *Journal of Infectious Diseases*, vol. 129, pp. S19–S25, 1974.

[8] G. W. Anderson Jr., P. L. Worsham, C. R. Bolt et al., "Protection of mice from fatal bubonic and pneumonic plague by passive immunization with monoclonal antibodies against the F1 protein of Yersinia pestis," *The American Journal of Tropical Medicine and Hygiene*, vol. 56, no. 4, pp. 471–473, 1997.

[9] R. Kingston, F. Burke, J. H. Robinson et al., "The fraction 1 and V protein antigens of Yersinia pestis activate dendritic cells to induce primary T cell responses," *Clinical and Experimental Immunology*, vol. 149, no. 3, pp. 561–569, 2007.

[10] Y. Levy, Y. Flashner, A. Tidhar et al., "T cells play an essential role in anti-F1 mediated rapid protection against bubonic plague," *Vaccine*, vol. 29, no. 40, pp. 6866–6873, 2011.

[11] V. L. Motin, R. Nakajima, G. B. Smirnov, and R. R. Brubaker, "Passive immunity to yersiniae mediated by anti-recombinant V antigen and protein A-V antigen fusion peptide," *Infection and Immunity*, vol. 62, no. 10, pp. 4192–4201, 1994.

[12] E. D. Williamson, S. M. Eley, A. J. Stagg, M. Green, P. Russell, and R. W. Titball, "A sub-unit vaccine elicits IgG in serum, spleen cell cultures and bronchial washings and protects immunized animals against pneumonic plague," *Vaccine*, vol. 15, no. 10, pp. 1079–1084, 1997.

[13] P. Fellows, J. Adamovicz, J. Hartings et al., "Protection in mice passively immunized with serum from cynomolgus macaques and humans vaccinated with recombinant plague vaccine (rF1V)," *Vaccine*, vol. 28, no. 49, pp. 7748–7756, 2010.

[14] J. Hill, C. Copse, S. Leary, A. J. Stagg, E. D. Williamson, and R. W. Titball, "Synergistic protection of mice against plague with monoclonal antibodies specific for the F1 and V antigens of *Yersinia pestis*," *Infection and Immunity*, vol. 71, no. 4, pp. 2234–2238, 2003.

[15] J. Hill, J. E. Eyles, S. J. Elvin, G. D. Healey, R. A. Lukaszewski, and R. W. Titball, "Administration of antibody to the lung protects mice against pneumonic plague," *Infection and Immunity*, vol. 74, no. 5, pp. 3068–3070, 2006.

[16] S. M. Jones, F. Day, A. J. Stagg, and E. D. Williamson, "Protection conferred by a fully recombinant sub-unit vaccine against Yersinia pestis in male and female mice of four inbred strains," *Vaccine*, vol. 19, no. 2-3, pp. 358–366, 2000.

[17] D. G. Heath, G. W. Anderson Jr., J. M. Mauro et al., "Protection against experimental bubonic and pneumonic plague by a recombinant capsular F1-V antigen fusion protein vaccine," *Vaccine*, vol. 16, no. 11-12, pp. 1131–1137, 1998.

[18] S. M. Jones, K. F. Griffin, I. Hodgson, and E. D. Williamson, "Protective efficacy of a fully recombinant plague vaccine in the guinea pig," *Vaccine*, vol. 21, no. 25-26, pp. 3912–3918, 2003.

[19] L. E. Quenee, N. A. Ciletti, D. Elli, T. M. Hermanas, and O. Schneewind, "Prevention of pneumonic plague in mice, rats, guinea pigs and non-human primates with clinical grade rV10, rV10-2 or F1-V vaccines," *Vaccine*, vol. 29, no. 38, pp. 6572–6583, 2011.

[20] P. Russell, S. M. Eley, S. E. Hibbs, R. J. Manchee, A. J. Stagg, and R. W. Titball, "A comparison of Plague vaccine, USP and EV76 vaccine induced protection against Yersinia pestis in a murine model," *Vaccine*, vol. 13, no. 16, pp. 1551–1556, 1995.

[21] E. D. Williamson and P. C. F. Oyston, "Protecting against plague: towards a next-generation vaccine," *Clinical and Experimental Immunology*, vol. 172, no. 1, pp. 1–8, 2013.

[22] E. D. Williamson, S. M. Eley, K. F. Griffin et al., "A new improved sub-unit vaccine for plague: the basis of protection," *FEMS Immunology and Medical Microbiology*, vol. 12, no. 3-4, pp. 223–230, 1995.

[23] E. D. Williamson, S. M. Eley, A. J. Stagg, M. Green, P. Russell, and R. W. Titball, "A single dose sub-unit vaccine protects against pneumonic plague," *Vaccine*, vol. 19, no. 4-5, pp. 566–571, 2000.

[24] M. K. Hart, G. A. Saviolakis, S. L. Welkos, and R. V. House, "Advanced development of the rF1V and rBV A/B vaccines: progress and challenges," *Advances in Preventive Medicine*, vol. 2012, Article ID 731604, 14 pages, 2012.

[25] E. D. Williamson, H. C. Flick-Smith, E. Waters et al., "Immunogenicity of the rF1+rV vaccine for plague with identification of potential immune correlates," *Microbial Pathogenesis*, vol. 42, no. 1, pp. 11–21, 2007.

[26] E. D. Williamson, P. M. Vesey, K. J. Gillhespy, S. M. Eley, M. Green, and R. W. Titball, "An IgG1 titre to the F1 and V antigens correlates with protection against plague in the mouse model," *Clinical and Experimental Immunology*, vol. 116, no. 1, pp. 107–114, 1999.

[27] C. Buchrieser, M. Prentice, and E. Carniel, "The 102-kilobase unstable region of Yersinia pestis comprises a high—pathogenicity island linked to a pigmentation segment which undergoes internal rearrangement," *Journal of Bacteriology*, vol. 180, no. 9, pp. 2321–2329, 1998.

[28] H. A. Druett, "A mobile form of the Henderson apparatus," *Journal of Hygiene*, vol. 67, no. 3, pp. 437–448, 1969.

[29] K. R. MAY and G. J. HARPER, "The efficiency of various liquid impinger samplers in bacterial aerosols," *British Journal of Industrial Medicine*, vol. 14, no. 4, pp. 287–297, 1957.

[30] A. C. Guyton, "Measurement of the respiratory volumes of laboratory animals," *American Journal of Physiology*, vol. 150, no. 1, pp. 70–71, 1947.

[31] E. Pietersen, "Long-term outcomes of patients with extensively drug-resistant tuberculosis in South Africa: A Cohort Study," *The Lancet*, vol. 383, no. 9924, pp. 1230–1239, 2014.

[32] P. Fellows, W. Lin, C. Detrisac et al., "Establishment of a Swiss webster mouse model of pneumonic plague to meet essential data elements under the animal rule," *Clinical and Vaccine Immunology*, vol. 19, no. 4, pp. 468–476, 2012.

[33] M. Green, D. Rogers, P. Russell et al., "The SCID/Beige mouse as a model to investigate protection against Yersinia pestis," *FEMS Immunology and Medical Microbiology*, vol. 23, no. 2, pp. 107–113, 1999.

[34] E. D. Williamson, H. C. Flick-Smith, C. LeButt et al., "Human immune response to a plague vaccine comprising recombinant F1 and V antigens," *Infection and Immunity*, vol. 73, no. 6, pp. 3598–3608, 2005.

[35] P. Bruhns, "Properties of mouse and human IgG receptors and their contribution to disease models," *Blood*, vol. 119, no. 24, pp. 5640–5649, 2012.

Hindawi Publishing Corporation
Journal of Immunology Research
Volume 2014, Article ID 341820, 13 pages
http://dx.doi.org/10.1155/2014/341820

Research Article

Multiple Roles of Myd88 in the Immune Response to the Plague F1-V Vaccine and in Protection against an Aerosol Challenge of *Yersinia pestis* CO92 in Mice

Jennifer L. Dankmeyer,[1] Randy L. Fast,[1] Christopher K. Cote,[1] Patricia L. Worsham,[1] David Fritz,[1] Diana Fisher,[1] Steven J. Kern,[1] Tod Merkel,[2] Carsten J. Kirschning,[3] and Kei Amemiya[1]

[1] *US Army Medical Research Institute of Infectious Diseases, Fort Detrick, Frederick, MD 21703, USA*
[2] *Center of Biologics Evaluation and Research, US Food and Drug Administration, Bethesda, MD 20892, USA*
[3] *Institute of Medical Microbiology, University Duisburg-Essen, Essen, Germany*

Correspondence should be addressed to Kei Amemiya; kei.amemiya@us.army.mil

Received 15 February 2014; Revised 23 April 2014; Accepted 3 May 2014; Published 4 June 2014

Academic Editor: E. Diane Williamson

The current candidate vaccine against *Yersinia pestis* infection consists of two subunit proteins: the capsule protein or F1 protein and the low calcium response V protein or V-antigen. Little is known of the recognition of the vaccine by the host's innate immune system and how it affects the acquired immune response to the vaccine. Thus, we vaccinated Toll-like receptor (Tlr) *2*, *4*, and *2/4*-double deficient, as well as signal adaptor protein *Myd88*-deficient mice. We found that Tlr4 and Myd88 appeared to be required for an optimal immune response to the F1-V vaccine but not Tlr2 when compared to wild-type mice. However, there was a difference between the requirement for Tlr4 and MyD88 in vaccinated animals. When F1-V vaccinated *Tlr4* mutant (lipopolysaccharide tolerant) and *Myd88*-deficient mice were challenged by aerosol with *Y. pestis* CO92, all but one *Tlr4* mutant mice survived the challenge, but no vaccinated *Myd88*-deficient mice survived the challenge. Spleens from these latter nonsurviving mice showed that *Y. pestis* was not cleared from the infected mice. Our results suggest that MyD88 appears to be important for both an optimal immune response to F1-V and in protection against a lethal challenge of *Y. pestis* CO92 in F1-V vaccinated mice.

1. Introduction

The first vaccine developed against plague was a heat-inactivated, whole-cell vaccine used by Haffkine during the Third Pandemic of plague in India in 1897 [1]. For the next 100 years, heat-inactivated, formalin-inactivated, or live-attenuated whole-cell vaccines were used to vaccinate humans against plague infection. The current candidate plague vaccine consists of a F1 capsule protein and the low calcium response (Lcr) V protein or V-antigen either as a mixture of the two proteins or a recombinant fusion of the two proteins [2, 3].

A strong humoral immune response to the individual subunits F1 or V or combined subunits (F1-V or F1+V), or an altered V-antigen (V10) was initially believed to be sufficient to provide protection against a lethal *Y. pestis* challenge in both mouse and nonhuman primate models of plague [2–8]. Both murine and human monoclonal antibodies against the subunit components of the plague vaccine have been shown to mediate protection against a lethal plague challenge in mice [9–12].

There is evidence to suggest that cell mediated immune responses are also important for protection against *Y. pestis* infection [13–15]. Although there are still some questions as to the contribution of the humoral and cellular immune responses for protection mediated by the plague vaccine in animal models, the F1-V subunit vaccine is currently being evaluated in a human Phase 2b clinical trial [16]. Very little is known of the host's innate immune response to the F1-V vaccine, and its effect on the ability of the vaccinated host to

be protected from a lethal aerosol challenge by *Y. pestis* CO92. Thus we wanted to evaluate the involvement of Tlr2, Tlr4, and MyD88 in raising antibodies to the F1-V subunit vaccine, and then determine if vaccinated mice with specific deficiencies in these Tlrs or adaptor protein were protected in an aerosol challenge model with the virulent *Y. pestis* CO92 strain.

2. Materials and Methods

2.1. Reagents. The F1-V and V-antigen preparations were obtained from Dr. Brad Powell (USAMRIID, Ft. Detrick, MD). F1-V was prepared as previously described [17], and F1- and V-antigens were prepared as described by Heath et al. [18]. Endotoxin was removed from F1-V and V-antigens by Dr. Bill Gillette at the National Cancer Institute (NCI) (Frederick, Maryland). F1-V preparations contained endotoxin levels < 0.2 EU/μg as determined by Lonza (Walkersville, MD) using the kinetic chromogenic *Limulus* amebocyte lysate method. Anti-F1 monoclonal antibody (clone F1-04-A-G1) for immunohistochemical analysis was obtained from the USAMRIID cell culture division.

2.2. Animal Experiments

2.2.1. Mice. The original *Tlr2 deficiency* was in C57BL/6 mice which was a kind gift from Tularik (South San Francisco, CA), and backcrossed to C3H/HeJ. *Tlr2*, *Tlr4*, and *Tlr2*/*Tlr4* deficient C3H female mice were approximately 14 weeks old and backcrossed to C3H/HeN wild-type mice 9 times [19, 20]. In the first *Myd88* deficient vaccine study male C57BL/6 mice approximately 10 weeks old were used and were aged matched with control female C57BL/6 mice that were obtained from the NCI, Frederick, MD. The *Myd88* deficient mice were a kind gift from Dr. Shizuo Akira [21] and were backcrossed to a C57BL/6J background for over eight generations [22]. C57BL/6 *MyD88* deficient female mice used in the challenge study were approximately 6–10 weeks old. Sex and aged-matched C57BL/6 mice were obtained from NCI, Frederick, MD. C3H/HeJ [lipopolysaccharide (LPS) tolerant] 6–8 weeks old female mice (hereafter referred to as *Tlr4* mutant) were used for the *Tlr4* mutant challenge studies, and age and sex matched C3H/HeN control mice were obtained from NCI, Frederick, MD [23–25].

Research was conducted under an IACUC approved protocol in compliance with the Animal Welfare Act, PHS Policy, and other federal statutes and regulations relating to animals and experiments involving animals. The facility where this research was conducted is accredited by the Association for Assessment and Accreditation of Laboratory Animal Care, International and adheres to the principles stated in the 8th Edition of the Guide for the Care and Use of Laboratory Animals, National Research Council, 2011.

2.2.2. Vaccinations. Mice were vaccinated with F1-V twice subcutaneously as described previously [26] with Alhydrogel (500 ug) (Brenntag Biosector, Denmark). The amount of F1-V used is described in the tables or figure legends. Mice received either adjuvant or adjuvant with indicated amounts of F1-V. Serum was obtained from mice by intracardiac puncture or retroorbital bleeding approximately 4 weeks after the initial vaccination or 3-4 weeks after the boost vaccination. Mice were challenged by aerosol 22–30 days after the boost vaccination with *Y. pestis* CO92 where 1 LD_{50} is 6.8×10^4 colony forming units (cfus) for a whole body challenge with amounts specified in the figure legend [27]. Mice were observed for 21 days postchallenge.

2.3. Antibody, Cytokine, and Proliferation Assays

2.3.1. Antibody Titers. Antibody titers against the vaccine were determined by enzyme-linked immunosorbent assay (ELISA) as described previously [26] approximately 30 days after the initial vaccination and 22–30 days after the boost vaccination. All antibody titers were performed in triplicate for each mouse and reported as the geometric mean with standard error of the mean (SEM).

2.3.2. Cytokine Analysis. Cytokines expressed by stimulated splenocytes were determined as previously described [26]. Briefly, spleen cultures were prepared from mice approximately 30 days after the last vaccination. Spleens were combined in pairs within each group and duplicate cultures (5×10^6 cells/mL) were prepared and stimulated with F1-V (10 μg/mL) or V-antigen (10 μg/mL) for 40–45 h at 37 C with 5% CO_2. The culture supernatants were collected, and the amount of cytokine expression (in triplicate) was determined by BD FACSArray analysis (BD Pharmingen, San Diego, CA). The limits of detection were as follows: IFN-γ, 0.5 pg/mL; IL-12 (p70), 1.9 pg/mL; IL-4, 0.3 pg/mL; and IL-10, 9.6 pg/mL. The results were reported as the mean with the standard error of the mean.

2.3.3. Proliferation Analysis. Proliferation of splenocytes was determined as previously described [26]. Briefly, splenocyte cultures (0.2 mL) were prepared from spleens as previously described above except at 2×10^6 cells/mL and incubated with the antigen in triplicate for 40–45 h at 37 C with 5% CO2. Incubation was continued for 18–24 h with 1 μCi of [3H] thymidine at a specific activity of 5 Ci/mmol (Amersham Life Sciences, Arlington, IL) before collecting the cells and counting the amount of radioactivity incorporated. The results were reported as the mean with the standard error of the mean.

2.4. Histochemical/Immunohistochemical Analysis of Spleens. Spleens of mice in the *Myd88*-deficient vaccine study were removed as soon as we found the nonsurviving mouse early in the morning or through the work day up to 21 days after challenge. Mice that survived the challenge after 21 days or mice that were unchallenged control mice were deeply anesthetized and euthanized before removing their spleens. All spleens were placed into 4% buffered formalin for at least 21 days before histochemical or immunohistochemical analysis was performed by the Pathology Division at USAMRIID. Tissue sections were stained using an automated

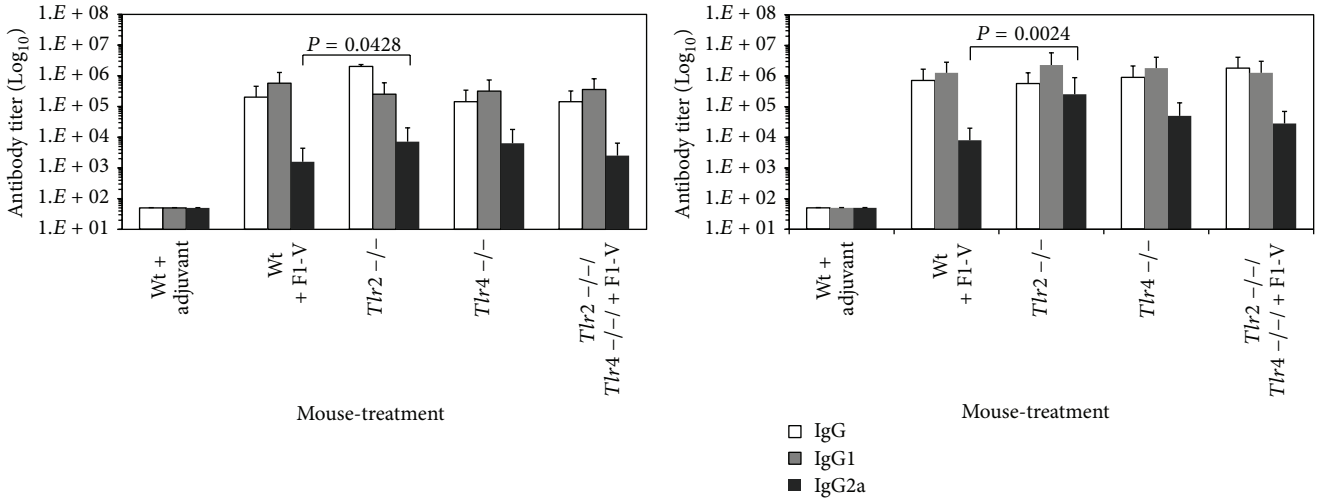

(a) After prime vaccination

(b) After boost vaccination

Figure 1: Comparison of the class and subclass antibody titers to the *Y. pestis* F1-V vaccine in wild-type C3H/NeN, *Tlr2*, *Tlr4*, and *Tlr2/4* deficient mice after the prime and boost vaccination. Blood was drawn 30 days after each vaccination for the antibody determination (IgG, IgG1, and IgG2a) that is reported as the geometric mean with geometric standard error of the mean. There were 6 mice in each group. There was a significant difference between the wild-type C3H/HeN mice and *Tlr2* deficient C3H/HeN mice in the levels of IgG2a after the prime vaccination ($P = 0.0428$) and boost vaccination ($P = 0.0024$).

hematoxylin and eosin Sakura Automated slide stainer. Immunohistochemical staining was performed using a Dako EnVision+ kit (Dako, Catalog no. K4007 or K4010) with the *Y. pestis* anticapsule F1 monoclonal antibody as the primary antibody. All photomicrographs were taken with a Nikon Eclipse 80i microscope using a 20X objective lens with the final magnification of 271X. The histological slides were read by the Veterinarian pathologist in the Bacteriology Division at USAMRIID.

2.5. Statistical Analysis. Log 10 transformations were applied to antibody titer values and cytokine responses before analysis to satisfy assumptions of normality and homoscedasticity. Antibody titers were compared between experimental groups using two-sample t-tests when comparing only two groups or Dunnett's tests when comparing multiple groups to a shared control. Mean times to death were compared with two-sample t-tests with stepdown Bonferroni corrections to account for multiple comparisons. Survival rates were compared with Fisher's exact tests with stepdown Bonferroni corrections to account for multiple comparisons. All statistical analyses were conducted using SAS Version 9 (SAS Institute Inc., Cary, NC, 2003). All hypothesis tests are two-sided and considered significant at the $\alpha = 0.05$ level.

3. Results

3.1. Antibody Response, Cytokine Expression, and Proliferative Response to the F1-V Vaccine. C3H/HeN mice with deficiencies in *Tlr2*, *Tlr4*, or both *Tlr2/4* were vaccinated twice with 1 μg of F1-V, and antibody titers determined 30 days after the prime and boost vaccinations. Figure 1 shows that 30 days after the first vaccination, there was not a significant difference in the levels of IgG between the wild-type and *Tlr2*, *Tlr4*, or *Tlr2/4* double deficient mice ($P = 1.000$). There was also little difference in the IgG1 and IgG2a subclass response to the vaccine in the same mice, except in one case there was a slight significant difference in the IgG1 response between the wild-type mice that received the vaccine and mice with the *Tlr2* deficiency ($P = 0.042$). The IgG or subclass response to the vaccine was also not in most cases significantly different 30 days after the boost vaccination ($P = 1.000$) between the wild-type C3H/HeN mice, *Tlr2*, *Tlr4*, and *Tlr2/4* double deficient mice (Figure 1). There was a significant difference between the IgG2a response between the wild-type mice and the *Tlr2* deficient mice ($P = 0.0024$). Nevertheless, our results suggest that overall, the antibody response to the plague F1-V vaccine did not depend on the presence of Tlr2 or Tlr4.

We then evaluated cytokine and proliferative responses to the vaccine by splenocytes from F1-V vaccinated wild-type, *Tlr2*, *Tlr4*, and *Tlr2/4* double deficient mice. Although we did not vaccinate these mice with only V-antigen, we wanted to compare its ability to stimulate splenocytes like the F1-V vaccine. We saw little IFN-γ, which is a T-cell helper type 1 (Th1-) like cytokine, produced by splenocytes from wild-type mice that received only adjuvant (Figure 2(a)). Splenocytes from wild-type C3H/HeN mice responded well to F1-V producing the most IFN-γ (1272 pg/mL), but splenocytes from *Tlr2* deficient mice produced a little more than half the amount of IFN-γ (710 pg/mL) as the splenocytes from wild-type C3H/HeN mice ($P = 0.2050$). Neither splenocyte preparations produced very much IFN-γ in response to the V-antigen. Splenocytes from F1-V vaccinated *Tlr4* deficient or *Tlr2/4* double deficient mice produced little IFN-γ (26.2 and 12.1 pg/mL, resp.) in response to F1-V ($P = 0.0042$ or $P = 0.0039$, resp.). We also examined the expression of IL-12 (p70)

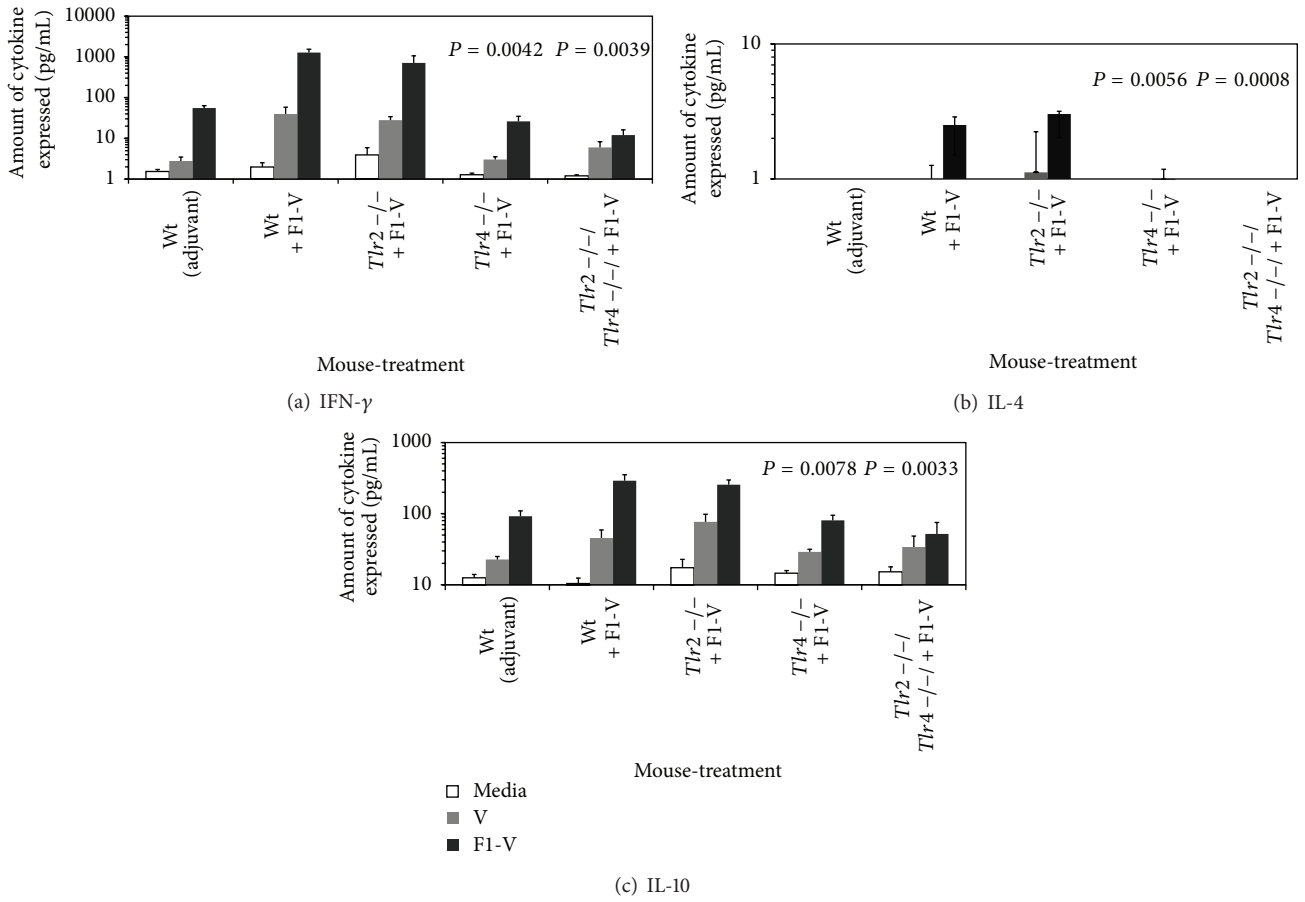

Figure 2: Cytokine expression by stimulated splenocytes from F1-V vaccinated wild-type C3H/HeN, *Tlr2*, *Tlr4*, and *Tlr2/4* deficient mice appears to be dependent on *Tlr4*. Mice were given a prime-boost vaccination of F1-V (1 μg) as shown in Figure 1, and splenocytes from these same mice were prepared and stimulated for 44 h in triplicate with medium only, 4 μg of F1-V or V antigen. Culture supernatants were collected and cytokine expression was determined: (a) IFN-γ; (b) IL-4; (c) IL-10. The results are reported as mean with standard error of the mean. Statistical significance shown above the respective bar was reported for differences in cytokine expression between splenocytes from wild-type C3H/HeN and *Tlr4* and *Tlr2/4*-deficient C3H/HeN mice stimulated with F1-V.

but very little was detected in all splenocyte preparations after stimulation with F1-V (data not shown).

We examined the expression of two Th2-type cytokines, IL-4 and IL-10. No IL-4 was detected in splenocyte cultures from mice that received only the adjuvant in response to V-antigen or F1-V (Figure 2(b)). Very low amounts of IL-4 were detected in splenocytes from wild-type C3H/HeN, *Tlr2* and *Tlr4* deficient mice (2.51, 3.03, and 0.59 pg/mL, resp.). No IL-4 was detected in splenocyte cultures from *Tlr2*/*Tlr4* double deficient mice after stimulation with the vaccine. There were significant differences in the amount of IL-4 produced by splenocytes from *Tlr4* and *Tlr2/4* deficient mice compared to splenocytes from the wild-type C3H/HeN mice ($P = 0.0056$ and $P = 0.0008$, resp.). Splenocytes from F1-V vaccinated wild-type C3H/HeN or *Tlr2* deficient mice produced comparable amounts of IL-10 (290 and 255 pg/mL, resp.) when stimulated with F1-V ($P = 0.9023$), but not with the V-antigen (Figure 2(c)). Significantly less IL-10 was expressed by splenocytes from F1-V vaccinated *Tlr4* and *Tlr2/4* deficient mice (80.5 and 51.9 pg/mL, resp.) when stimulated by the vaccine ($P = 0.0078$ and $P = 0.0033$, resp.). Little IL-10 was induced by V-antigen compared to that by F1-V at the same time.

The proliferative response to the F1-V vaccine and V-antigen was examined (Figure 3). When the amount of proliferation by splenocytes in response to the V-antigen alone between the wild-type C3H/HeN, *Tlr2*, *Tlr4*, and *Tlr2/4* deficient mice was compared, we saw a significant increase in proliferation by the splenocytes from the *Tlr2* deficient mice ($P = 0.0059$) but not by the other splenocytes. Splenocytes from wild-type C3H/HeN and *Tlr2* deficient mice that received the vaccine, proliferated well (12- to 10.5-fold, resp.) in response to the vaccine but with no significant difference between the two strains of mice ($P = 0.7013$). In contrast, there was a significant decrease in the proliferative response to the vaccine by splenocytes from *Tlr4* and *Tlr2/4* double deficient mice ($P = 0.0020$ and $P = 0.0001$, resp.). These results suggest that cellular immune responses to F1-V were more dependent on the presence of Tlr4 but not Tlr2 in mice vaccinated with F1-V.

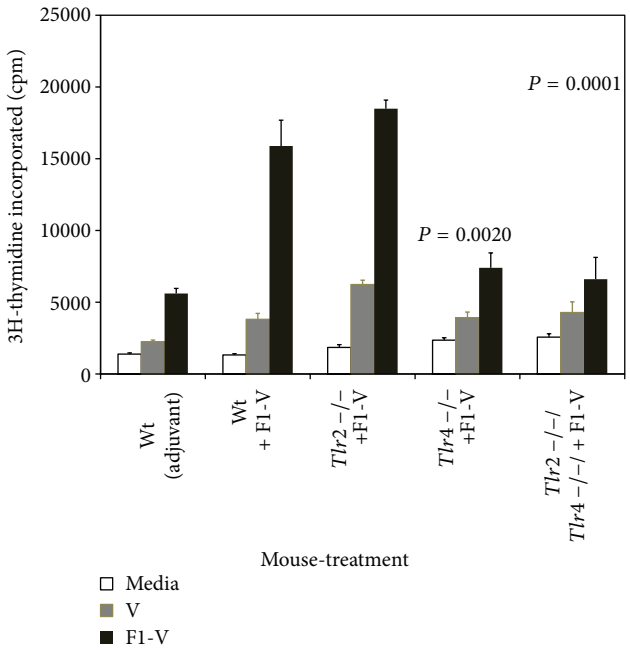

Figure 3: Proliferation by stimulated splenocytes from F1-V vaccinated wild-type C3H/HeN, *Tlr2*, *Tlr4*, and *Tlr2/4*-deficient mice appears to be dependent on Tlr4. Proliferation was determined after 44 h incubation in the presence of 4 μg of F1-V or V-antigen and a further 24 h incubation in the presence of 3[H]-Thymidine. Splenocytes used in the assay were prepared from the same groups of mice as shown in Figure 1. The results are reported as mean with standard error of the mean. The results on the y-axis are plotted in linear because of the overall low amount of stimulation. Statistical significance shown above the respective bar was reported for differences between the amount of proliferation between splenocytes from wild-type C3H/HeN and *Tlr2* and *Tlr2/4*-deficient C3H/HeN mice stimulated with F1-V.

3.2. Antibody Response, Cytokine Expression, and Proliferative Response by Myd88 Deficient Mice. Because the MyD88 adaptor protein is a pivotal molecule in the innate immune response, we wanted to examine the contribution of MyD88 to the antibody and cellular immune responses to the vaccine. We vaccinated 3 groups of mice with or without F1-V (Figure 4). After the initial vaccination, we saw significant differences in the IgG and IgG1 levels between the wild-type C57BL/6 mice and *Myd88* deficient mice ($P = 0.0153$ and $P = 0.0320$, resp.) 22 days later. However, after the boost vaccination, there was a difference but not significant ($P = 0.1161$) between the IgG levels of the wild-type C57BL/6 and *Myd88* deficient mice. There was no difference in the IgG1 response between the wild-type C57BL/6 and *Myd88* deficient mice. We saw little IgG2a produced in response to the vaccine (data not shown) because C57BL/6 mice do not have a functional IgG2a gene but produce a different isotype [IgG2c, 28-31].

We then examined the expression of IFN-γ, IL-4, and IL-10 by splenocytes cultures from F1-V vaccinated wild-type and *Myd88* deficient mice (Figure 5). IFN-γ (451 pg/mL) and IL-10 (106 pg/mL) were expressed in moderate amounts by splenocytes from F1-V vaccinated mice but not IL-4 (6.84 pg/mL). We saw significantly lower amounts of expression of IFN-γ (79.7 pg/mL, $P = 0.0176$) and IL-10 (42.04 pg/mL, $P = 0.0468$) but not IL-4 (3.92 pg/mL, $P = 0.0728$) by splenocytes from *Myd88* deficient mice. We also detected IL-12 (p70) produced in very low amounts (7.82 pg/mL) by vaccine stimulated splenocytes from wild-type C57Bl/6 mice but not from splenocytes from *Myd88* deficient mice (data not shown).

We compared the proliferative response of splenocytes from wild-type and *Myd88* deficient mice vaccinated with the plague vaccine (Figure 6) and saw close to a twofold decrease in proliferation between these two groups ($P = 0.0425$). Our results suggest that MyD88 protein appears to be intricately involved in the immune response to the F1-V vaccine.

3.3. MyD88 but Not Tlr4 Is Required for Survival against Y. pestis in F1-V Vaccinated Mice. It appeared that cell-mediated immune responses in F1-V vaccinated *Tlr4* and *Myd88* deficient mice were affected more than in *Tlr2* deficient mice. It had been previously suggested that weak or inefficient activation of Tlr2 by LcrV makes it unlikely that Tlr2 is involved in pathogenesis by plague [28, 29]. We, therefore, examined the contribution of Tlr4 and MyD88 in protection against an aerosol challenge by *Y. pestis* CO92 after F1-V vaccination. We used C3H/HeJ mice that have a missense mutation in the *Tlr4* coding region that makes it unresponsive to LPS [23–25] and C3H/HeN mice for the wild-type *Tlr4* (Figure 7(a)). One group of *Tlr4* mutant C3H/HeJ mice received adjuvant and another group received both adjuvant and F1-V (2.9 μg). Another group of wild-type C3H/HeN mice received only adjuvant and another group received adjuvant with F1-V. Before challenge there was a lower IgG response to the vaccine by the *Tlr4* mutant mice, but the difference in either IgG or IgG1 titers to the vaccine between the wild-type C3H/HeN and *Tlr4* mutant C3H/HeJ mice was not significant (1.87-fold and 1.07-fold, resp.). There was also no significant difference in the distribution of IgG levels against the F1- or V-antigens between the strains before challenge (data not shown). Twenty-two days after the boost vaccination all groups of mice were challenged with 21 LD_{50} of *Y. pestis* CO92 by aerosol. Figure 8 shows that only one F1-V vaccinated *Tlr4* mutant C3H/HeJ mouse died from the challenge, while no wild-type C3H/HeN vaccinated mice were lost. By comparison, C3H/HeN and C3H/HeJ mice that received only adjuvant all died by day 4-5 postchallenge. This study was repeated previously, with the same groups of vaccinated mice ($n = 10$ for all groups), except they were challenged with a lower dose (10 LD_{50}) of *Y. pestis* CO92. In this case there was complete protection of F1-V vaccinated *Tlr4* mutant mice (10/10) and no protection of the C3H/HeN and C3H/HeJ mice that received only adjuvant as in the study with the higher challenge dose (data not shown). Our results suggest that in F1-V vaccinated mice Tlr4 does not contribute significantly towards an antibody response to the vaccine or toward protection against a lethal aerosol challenge by *Y. pestis* CO92.

To examine the role of MyD88 in protection against a *Y. pestis* challenge in F1-V vaccinated mice, we vaccinated

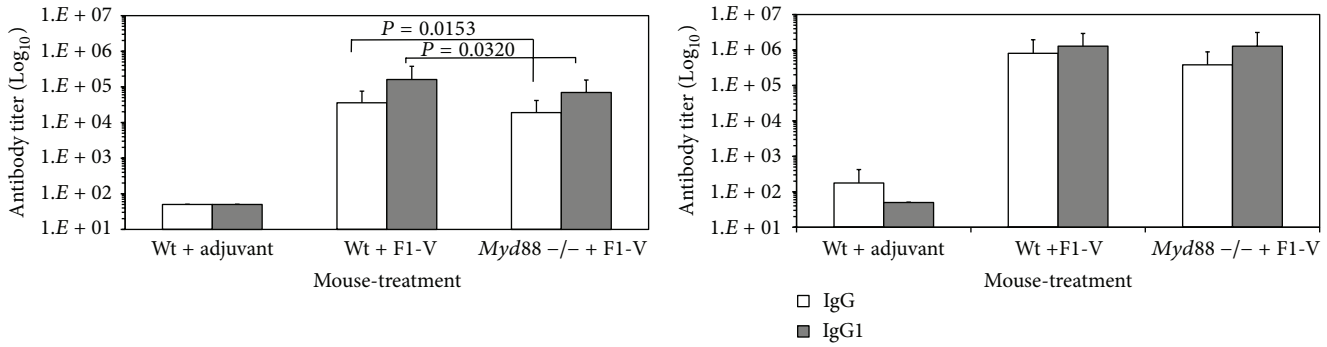

(a) After prime vaccination

(b) After boost vaccination

Figure 4: Antibody response to the plague F1-V vaccine in wild-type C57BL/6 and *Myd88* deficient mice after the prime and boost vaccination. Serum for the prime vaccination was drawn 22 days after vaccination and for the boost vaccination 29 days after vaccination. All mice received 2 μg of F1-V except mice in the adjuvant only group. N for wild-type C57BL/6 mice with adjuvant and wild-type C57BL/6 mice with F1-V was 6, while for the *Myd88* deficient C57BL/6 group with F1-V was 9. The titers are reported as geometric mean with geometric standard error of the mean. Significant differences in the antibody titer between the wild-type C57BL/6 mice that received F1-V and *Myd88*-deficient C57BL/6 mice that received F1-V which is shown above the respective bar after the prime vaccination (a).

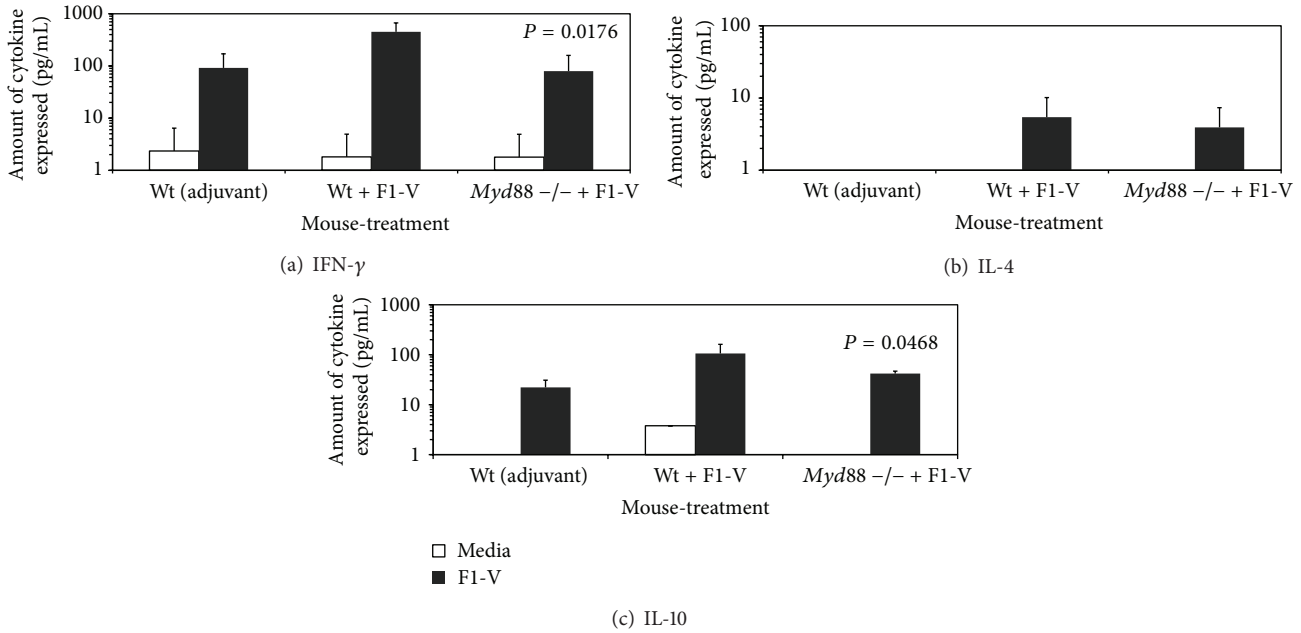

(a) IFN-γ

(b) IL-4

(c) IL-10

Figure 5: Cytokine expression by stimulated splenocytes from F1-V vaccinated wild-type C57BL/6 or *MyD88*-deficient mice appears to require MyD88. Splenocytes were stimulated with F1-V (5 μg) or medium alone for approximately 45 h before collecting the supernatant and determining the amount of cytokine present: (a), IFN-γ; (b), IL-4; (c), IL-10. Cells from three different groups of mice were used (see Figure 4): (1) wild-type (Wt) C57BL/6 mice that received only adjuvant, (2) Wt C57BL/6 mice that received F1-V (2 μg), and (3) *Myd88*-deficient C57BL/6 mice that received F1-V (2 μg). The results are reported as mean with standard error of the mean. Statistical significance shown above the respective bar was reported for differences between the amount of cytokine expressed between the wild-type C58BL/6 and *Myd88*-deficient splenocytes stimulated with F1-V ($P = 0.0176$ and $P = 0.0468$) in panels (a) and (c), respectively.

3 groups of mice (Figure 7(b)). The first group consisted of wild-type C57BL/6 mice that received only adjuvant, and the second group of wild-type C57BL/6 mice received adjuvant with F1-V (2.5 μg). The last group consisted of C57BL/6 *Myd88* deficient mice that received adjuvant with 2.5 μg of F1-V. Although the *Myd88* deficient F1-V vaccinated mice had a substantial IgG and IgG1 titer against the vaccine, there was a significantly lower antibody titer than in the wild-type mice ($P = 0.0020$ and $P = 0.0024$, resp.) against the vaccine and individual subunits ($P = 0.0053$ and $P = 0.0338$, resp., data not shown). When 10 mice from each group were challenged by aerosol with 10 LD_{50} of *Y. pestis* CO92, all mice that received only adjuvant died within 3–5 days after challenge, while F1-V vaccinated *Myd88* deficient mice all died within 5–7 days after challenge (Figure 9). There was no significant difference between the mean time to death (MTD)

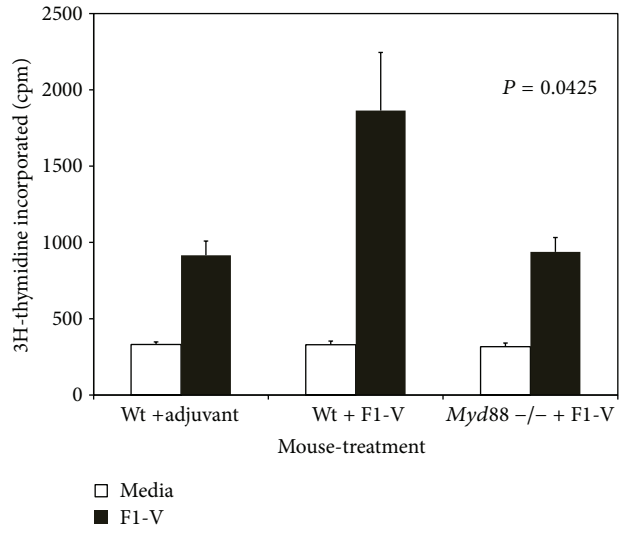

Figure 6: Proliferation by stimulated splenocytes from F1-V vaccinated wild-type C57BL/6 mice or *Myd88*-deficient C57BL/6 mice requires MyD88. Proliferation of stimulated splenocytes was determined as in Figure 3 except 2 μg of F1-V was used for stimulation in 0.25 mL. The same source of splenocytes stated in Figure 5 was used. The results are reported as mean with the standard error of the mean. Statistical significance shown above the respective bars was reported for differences between the amount of proliferation between splenocytes from wild-type C57BL/6 and *Myd88*-deficient C57BL/6 mice stimulated with F1-V.

of the adjuvant only wild-type group and the F1-V vaccinated *Myd88* deficient group ($P = 0.1151$). In contrast, 6 out of 10 mice survived the challenge in the wild-type F1-V vaccinated mice. The MTD for these three groups of mice were 4.5 days, 5.9 days, and 14.3 days, respectively. There was a significant difference between the MTD between the F1-V vaccinated wild-type mice and F1-V vaccinated *Myd88* deficient mice ($P < 0.0001$) and in the survival rate ($P = 0.0325$). Unlike Tlr4, the MyD88 adaptor protein appears to be required for an optimal antibody response to the vaccine and for protection against *Y. pestis* in F1-V vaccinated mice.

3.4. Spleens from Nonsurviving Challenged F1-V Vaccinated Myd88-Deficient Mice Showed That the Pathogen Was Not Cleared. Histochemical and immunohistochemical analyses were performed on spleens from mice from the *Myd88* deficient mice challenge study (Figure 10). There were no significant lesions noted in any of the spleens from the three groups of mice before challenge that includes the spleens from the *Myd88* deficient mice (Figures 10(a), 10(d), and 10(g)). In wild-type C57BL/6 mice that received only adjuvant and died after challenge (Figure 10, Gp1a-c), there was evidence of active infection (primarily of neutrophils and macrophages) and numerous bacilli in the marginal zone surrounding the white pulp. The presence of *Y. pestis* was confirmed with an anti-F1 monoclonal antibody (mAb) (Figure 10, Gp1c). There was a depletion of lymphocytes in this region compared to the wild-type mice that were not challenged (Figure 10, Gp1a).

In spleens of surviving wild-type C57BL/6 mice that were vaccinated with F1-V and challenged with *Y. pestis* CO92, there was an influx of lymphocytes in the white pulp and extramedullary hematopoiesis in the surrounding red pulp region. When the spleen sections were probed with the anti-F1 mAb, a few isolated anti-F1-positive spots were found in the marginal zone of the white pulp (Figure 10, Gp2f, arrows).

Spleens from *Myd88* deficient mice that were vaccinated with F1-V and challenged with *Y. pestis* CO92 appeared much like the wild-type mice that received only adjuvant. The presence of bacteria was seen in the marginal zone of the white pulp with mild to moderate lymphoid depletion observed in the white pulp, as well as mild extramedullary hematopoiesis in the red pulp (Figure 10, Gp3 h). A large amount of anti-F1 positive regions could be seen in the marginal zone of the white pulp and surrounding red pulp (Figure 10, Gp3i). Over all, the spleens from mice that did not survive the *Y. pestis* CO92 challenge from either wild-type mice that received only adjuvant or the *Myd88* deficient group that were vaccinated showed the presence of large amounts of the organism in the marginal zone of the white pulp as well as lymphoid depletion in the white pulp. The analysis of the spleens from F1-V vaccinated *Myd88* deficient mice suggested that MyD88 was required for clearance of the pathogen after a lethal challenge of *Y. pestis* CO92.

4. Discussion

The results of our studies with the *Tlr2*, *4*, and *2/4* double deficient or adaptor protein *Myd88* deficient mice suggest that Tlr4 and MyD88 appear to be important for an optimal antibody response to the subunit F1-V plague vaccine, but MyD88 also appears to be required for protection against a lethal *Y. pestis* CO92 challenge in F1-V vaccinated mice. Furthermore, cell-mediated immune responses to the vaccine appear to be more dependent on Tlr4 and MyD88 but not necessarily Tlr2. The expression of Th1- and Th2-like cytokines (IFN-γ, and IL-4, IL-10, resp.) and cell proliferation were moderately effected by the absence of Tlr2, but in the absence of Tlr4 or MyD88 the immune response to the vaccine was significantly affected. Still, there was distinction between the absence of Tlr4 or MyD88 in the immune response and protection against a *Y. pestis* CO92 challenge. We saw that in F1-V vaccinated mice, Tlr4 does not appear to be required for protection against a lethal challenge as long as antibodies to F1-V were present. In the absence of MyD88, however, the presence of a substantial level of antibody to the F1-V vaccine did not protect F1-V vaccinated mice from a lethal challenge of *Y. pestis*. Differences in the number of survivors between the wild-type C57BL/6 and *Myd88* deficient F1-V vaccinated mice might be attributed to both the difference in the antibody response to the vaccine (Figure 7(b), $P = 0.0020$) and differences in the cell-mediated response. Because of the critical role played by macrophages and neutrophils in the spread and control of *Y. pestis* in the infected host [30, 31], we cannot rule out if their involvement becomes limited in the clearance and survival of the host in the presence of a *Myd88*-deficiency at the same time

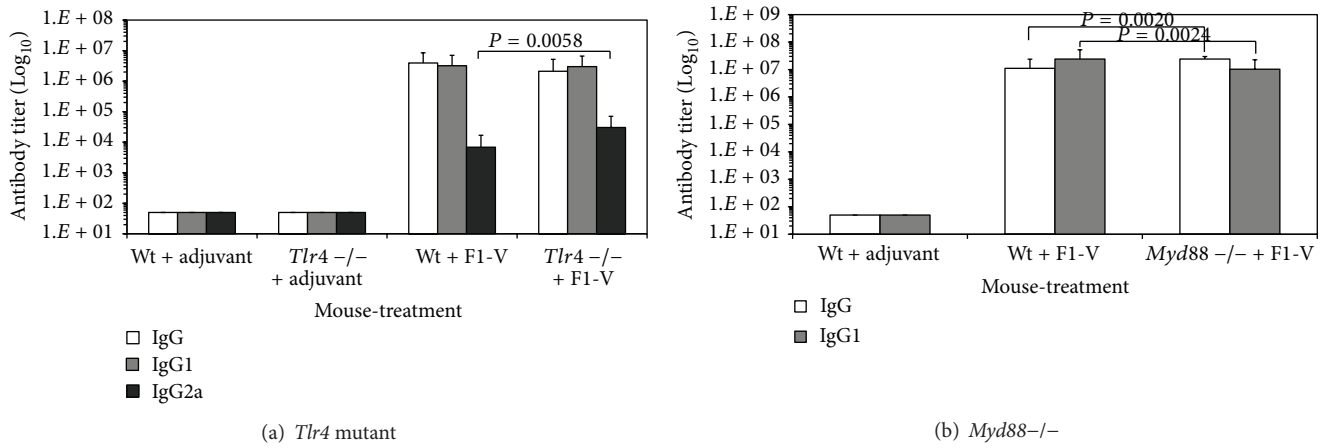

(a) *Tlr4* mutant (b) *Myd88*−/−

FIGURE 7: Antibody titers against the F1-V vaccine in (a) C3H/HeN wild-type and *Tlr4* mutant C3H/HeJ mice, and (b) C57BL/6 wild-type and *Myd88*-deficient C57BL/6 mice vaccinated with F1-V before *Y. pestis* CO92 aerosol challenge. (a) There were 4 groups of mice with 10 in each group: (1) Wt+adjuvant, (2) *Tlr4* mutant+adjuvant, (3) Wt+F1-V (2.9 μg), and (4) *Tlr4* mutant+F1-V (2.9 μg). Antibody titers are reported from serum collected 22 days after a boost vaccination. (b) There were 3 groups of mice with 15 in groups 1 and 2 and 14 in group 3: (1) Wt+adjuvant, (2) Wt+F1-V (2.5 μg), (3) *Myd88*-deficient mice+F1-V (2.5 μg). Antibody titers are reported as geometric mean with geometric standard error of the mean. Significant differences between the antibody class or subclass are reported above the respective bar between the (a) Wt+F1-V and *Tlr4* mutant+F1-V or (b) Wt+F1-V and *Myd88*-deficient+F1-V.

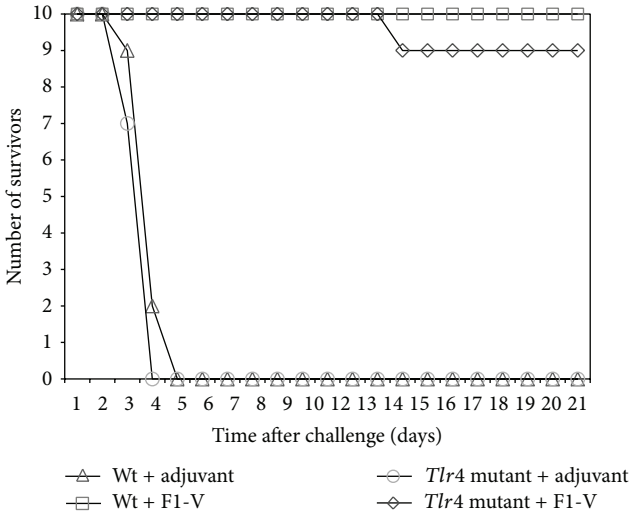

FIGURE 8: Survival of F1-V vaccinated C3H/HeN wild-type and C3H/HeJ *Tlr4* mutant mice after aerosol challenge with *Y. pestis* CO92. Mice were given two vaccinations of F1-V (2.9 μg), and 22 days after the boost vaccination, they were challenged by aerosol with 21 LD_{50} of *Y. pestis* CO92. There were four groups of mice (10 mice per group): wild-type C3H/HeN, with adjuvant only (△); *Tlr4* C3H/HeJ mutant, with adjuvant only (○); wild-type C3H/HeN, with F1-V (□); and *Tlr4* C3H/HeJ mutant, with F1-V (◊). After challenge, the mice were followed for 21 days. Previous results were essentially the same when the mice in the same vaccination groups were challenged with half the dose (10 LD_{50}) of *Y. pestis* CO92 except all (10/10) the F1-V vaccinated C3H/HeJ *Tlr4* mutant mice survived.

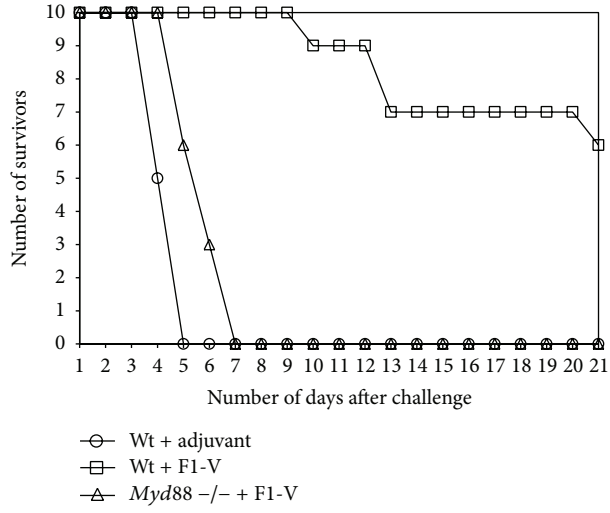

FIGURE 9: Survival of F1-V vaccinated C57BL/6 wild-type and C57BL/6 *Myd88*-deficient mice after aerosol challenge with *Y. pestis* CO92. Mice were given two vaccinations of F1-V (2.5 μg) (see Figure 7(b)), and 33 days after the boost vaccination they were challenged by aerosol with 19 LD_{50} of *Y. pestis* CO92. There were three groups of mice that were challenged (10 mice per group): wild-type C57BL/6+adjuvant only (○); wild-type C57BL/6+F1-V (□); and C57BL/6 *Myd88*-deficient mice+ F1-V (△). After challenge, the mice were followed for 21 days. The mean time to death (MTD) was the following: wild-type with adjuvant only: 4.50 days; wild-type with F1-V: 14.25 days; *Myd88*-deficient mice with F1-V: 5.90 days.

that the host's immune system is being compromised [28]. Although we did not include a *Myd88* deficient group that received only adjuvant, we believe that like the wild-type C57BL/6 mice that received only adjuvant, this group would not survive the lethal challenge by *Y. pestis* CO92. Without any protective anti-F1-V antibody, we would anticipate that the number and rate of survival would be similar to the wild-type C57BL/6 mice that did not receive the vaccine. As a comparison, although Tlr4 is upstream from MyD88 but the

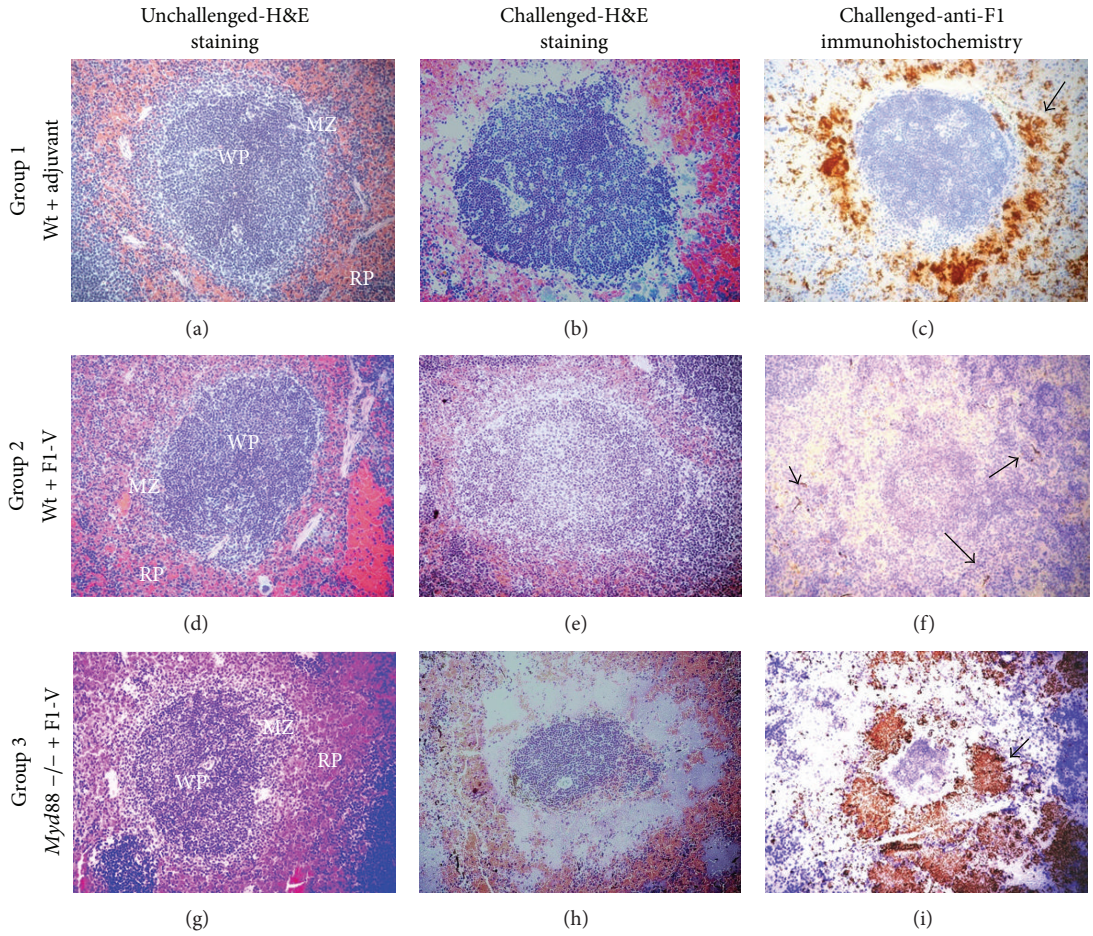

Figure 10: Histochemical and immunohistochemical analysis of spleens from unchallenged and challenged mice from adjuvant only C57BL/6 wild-type, F1-V vaccinated C57BL/6 wild-type, and F1-V vaccinated C57BL/6 *Myd88*-deficient mice. Mice were obtained from the corresponding group of mice as described in Figures 7(b) and 9. Spleens from additional mice from each group were used as controls (Unchallenged-H&E, panels (a), (d), and (g)). Regions in the spleen were labeled: white pulp, WP; red pulp, RP; and marginal zone, MZ. Spleen sections from challenged mice are shown stained (Challenged-H&E, panels (b), (e), and (h)) or probed with an anti-F1 monoclonal antibody (Challenged-Anti-F1, panels (c), (f), and (i)). The spleen section shown from Group 2, wild-type+F1-V was from a mouse that survived challenge (panels (e) and (f)). Arrows in panel (c) and (i) point to F1 positive regions in the marginal zone. Arrows in panel (f) point to isolated F1 positive spots.

signal transduction pathway would still not be activated, in the previous challenge study with *Tlr4* mutants, the number of survivors and MTD of *Tlr4* mutant mice that did not receive F1-V was similar to the wild-type mice that did not receive the vaccine (between 4-5 days). Furthermore, there was no significant difference in the number of survivors and the survival rate of the *Myd88* deficient mice that did receive F1-V and the wild-type C57BL/6 group. We saw that in the absence of MyD88, *Y. pestis* accumulates in the marginal zone of the spleen in mice that succumb to the lethal challenge, but they did not accumulate in spleens of F1-V vaccinated wild-type C57BL/6 mice, although we could see a few isolated organisms in the latter case. It is not clear at this time how much of the accumulation of *Y. pestis* in the spleen could be attributed to the possible attenuation of neutrophils in the absence of MyD88 [32, 33] or other biological events in the infected host (see discussion further below).

Although it could be said that part of our observation on the requirement of Tlr4 or MyD88 on the immune response to the F1-V vaccine could be attributed to the presence of endotoxin in our vaccine preparations, there were very minor amounts in our vaccine preparations. In the initial *Tlr2* and *4* deficient mouse immune studies, each mouse received 1 μg of F1-V (Figure 1), which contained approximately 0.18 EU per vaccination (see Section 2). This amount of endotoxin is approximately equivalent to 0.018 ng according to a reported estimated value of 1 EU/mL which is approximately 0.1 ng/mL of endotoxin (Pierce LAL chromogenic endotoxin quantitation kit, Thermo Scientific, Rockford, IL). This amount of estimated endotoxin did not have a significant effect on the antibody response between the wild-type C3H/HeN and *Tlr2* or *Tlr4* deficient mice to the vaccine (Figure 1). At the same time, in the initial *Myd88* deficient study, each mouse received 2 μg of F1-V (Figure 4) or 0.36 EU per vaccination,

which was estimated to be 0.036 ng per mouse. We saw a lower but not significant difference in the IgG response to the vaccine in the *Myd88* deficient mice when compared to the wild-type C57BL/6 mice ($P = 0.1161$). For the *Tlr4* mutant and *Myd88*-deficient challenge studies, we used a different F1-V preparation (Figures 7(a) and 7(b), resp.). Excluding the adjuvant control mice, each mouse in the *Tlr4* mutant challenge study received 2.9 μg of F1-V or an estimated amount of 0.0087 EU, and in the *Myd88* deficient challenge study, each test mouse received 2.5 μg of F1-V or 0.0075 EU, which corresponds to approximately 0.00087 ng and 0.00075 ng of endotoxin for the *Tlr4* mutant mice and *Myd88* deficient mice, respectively. For the antibody response to the vaccine in the *Tlr4* mutant C3H/HeJ mice, it was lower than the wild-type C3H/HeN mice but not significantly ($P = 0.1486$). In the case of the *Myd88* deficient mice that were challenged, the *Myd88* deficient mice did have a significantly lower but still a substantial antibody response to the vaccine when compared to the wild-type C57BL/6 mice ($P = 0.0020$). The differences in the antibody response and cell-mediated immune response to the vaccine between the wild-type mice and corresponding *Tlr4* mutant or *Myd88* deficient mice suggest that MyD88 may be more important for an optimal immune response to the F1-V vaccine than Tlr4.

Numerous reports suggest that MyD88, Tlr2, or Tlr4, is required for clearance or protection against a bacterial pathogen [34–46]. Our report is the first to describe that MyD88 is required even in the presence of a substantial level of F1-V specific antibody for protection against *Y. pestis* infection. That MyD88 may be involved in activities other than as a signal adaptor protein cannot be completely excluded. Blander and Medzhitov [47] reported that uptake of *Escherichia coli* through phagosome/lysosome fusion was slower in bone marrow derived macrophages (BMDM) from *Tlr2/4* double deficient and *Myd88* deficient mice compared to BMDM from wild-type mice. Yates and Russell [48] reported a significant decrease in phagosome/lysosome fusion in BMDM from *Myd88* deficient mice after particle internalization was independent of Tlr2 or Tlr4. Sun and Ding [49] demonstrated that MyD88 adaptor protein increased the half-life of IFN-γ-induced mRNA for both TNF-α and IP-10. Stabilization of the mRNA was dependent on the activation of p38 and the presence of adenine-uridine-rich elements in the 3′-untranslated region of the mRNA. A physical association between IFN-γ R1 and MyD88 was noted. These reports suggest that MyD88 plays a pivotal role in the innate immune process as an adaptor protein, in phagosome/lysosome fusion after pathogen internalization, and cell-mediated immune events that affect the response to the pathogen.

The F1-V subunit vaccine has been formulated with aluminum hydroxide in animal and human studies [2, 8, 16, 18, 26, 50, 51]. It has been proposed that activation of the immune response by aluminum hydroxide adjuvants occurs through a protein complex called the inflammasome [52]. Activation of the inflammasome leads to activation of caspase-1 resulting in cleavage of pro-IL-1B and pro-IL-18 to mature molecules that are excreted [53–56]. However, there are conflicting reports on the dependency of the inflammasome on specific antibody responses [54–59]. Furthermore, there are conflicting reports on the requirement for Tlr activation in general for antigen specific antibody responses [60, 61]. It is not clear if inflammasome activation can possibly replace Tlr activation for antigen recognition for specific antibody responses, but equally important is the potential roles of MyD88 in the immune response for protection and clearance of the pathogen from the infected host as we have shown in the present study.

5. Conclusion

We have shown by using mice with deficiencies in specific components of the innate immune system that the antibody response to the plague F1-V vaccine could be affected, but we still observed a substantial antibody response in most cases in the absence of these components. An optimal immune response to F1-V appears to require the presence of Tlr4 or MyD88 but not Tlr2. In addition, the antibody response to the vaccine in the absence of Tlr4 still protected the mouse from a lethal challenge by *Y. pestis* CO92, but it did not in the absence of MyD88. Further, it may be that part of the reason for the lack of protection against plague in *Myd88* deficient mice was possibly a combination of a suboptimal antibody response to the vaccine and attenuated cell-mediated immune responses that led to the inability to clear the pathogen from the mouse. The latter possibility may also include attenuation of macrophage or neutrophil recruitment or phagocytosis of the pathogen. MyD88 appears to be involved in multiple aspects of the immune response to the plague vaccine and protection against plague infection.

Conflict of Interests

The authors listed in this paper certify that they have no affiliations with or involvement in any organization or entity with any financial interest (such as honoraria, education grants, participation in speakers' bureaus, membership, employment, consultancies, stock ownership or other equity interest, and expert testimony or patent-licensing arrangements) or nonfinancial interest (such as personal or professional relationships, affiliations, knowledge, or beliefs) in the subject matter or materials discussed in this paper.

Acknowledgments

The authors thank Steven Tobery and Anthony Bassett for their excellent technical assistance throughout this study. The authors thank Sarah Cohen for technical assistance in photomicroscopy. We also thank Stephen Little for critical reading of this paper. The authors thank the Joint Science and Technology Office/Defense Threat Reduction Agency for support for this research (Project no. 1.1A0018_07_RD_B). Opinions, interpretations, conclusions, and recommendations are those of the authors and are not necessarily endorsed by the U.S. Army.

References

[1] W. M. Haffkine, "Remarks on the plague prophylactic fluid," *British Medical Journal*, vol. 1, pp. 1461–1462, 1897.

[2] E. D. Williamson, S. M. Eley, K. F. Griffin et al., "A new improved sub-unit vaccine for plague: the basis of protection," *FEMS Immunology and Medical Microbiology*, vol. 12, no. 3-4, pp. 223–230, 1995.

[3] D. G. Heath, G. W. Anderson, S. L. Welkos, G. P. Andrews, A. M. Friedlander, and J. M. Mauro, "A recombinant capsular F1-V antigen fusion protein vaccine protects against experimental bubonic and pneumonic plague," in *Vaccine 97*, F. Brown, D. Burton, P. Doherty, J. Mekalanos, and E. Norrby, Eds., pp. 197–200, Cold Spring Harbor Laboratory Press, New York, NY, USA, 1997.

[4] S. E. C. Leary, E. D. Williamson, K. F. Griffin, P. Russell, S. M. Eley, and R. W. Titball, "Active immunization with recombinant V antigen from *Yersinia pestis* protects mice against plague," *Infection and Immunity*, vol. 63, no. 8, pp. 2854–2858, 1995.

[5] G. W. Anderson, S. E. C. Leary, E. D. Williamson et al., "Recombinant V antigen protects mice against pneumonic and bubonic plague caused by F1-capsule positive and -negative strains of *Yersinia pestis*," *Infection and Immunity*, vol. 64, no. 11, pp. 4580–4585, 1996.

[6] K. L. DeBord, D. M. Anderson, M. M. Marketon et al., "Immunogenicity and protective immunity against bubonic plague and pneumonic plague by immunization of mice with the recombinant V10 antigen, a variant of LcrV," *Infection and Immunity*, vol. 74, no. 8, pp. 4910–4914, 2006.

[7] C. A. Cornelius, L. E. Quenee, K. A. Overheim et al., "Immunization with recombinant V10 protects cynomolgus macaques from lethal pneumonic plague," *Infection and Immunity*, vol. 76, no. 12, pp. 5588–5597, 2008.

[8] E. D. Williamson, P. J. Packer, E. L. Waters et al., "Recombinant (F1 + V) vaccine protects cynomolgus macaques against pneumonic plague," *Vaccine*, vol. 29, no. 29-30, pp. 4771–4777, 2011.

[9] G. W. Anderson, P. L. Worsham, C. R. Bolt et al., "Protection of mice from fatal bubonic and pneumonic plague by passive immunization with monoclonal antibodies against the F1 protein of *Yersinia pestis*," *American Journal of Tropical Medicine and Hygene*, vol. 56, no. 4, pp. 471–473, 1997.

[10] J. Hill, S. E. C. Leary, K. F. Griffin, E. D. Willliamson, and R. W. Titball, "Regions of *Yersinia pestis* V antigen that contribute to protection against plague identified by passive and active immunization," *Infection and Immunity*, vol. 65, no. 11, pp. 4476–4482, 1997.

[11] J. Hill, C. Copse, S. Leary, A. J. Stagg, E. D. Williamson, and R. W. Titball, "Synergistic protection of mice against plague with monoclonal antibodies specific for the F1 and V antigens of *Yersinia pestis*," *Infection and Immunity*, vol. 71, no. 4, pp. 2234–2238, 2003.

[12] X. Xiao, Z. Zhu, J. L. Dankmeyer et al., "Human anti-plague monoclonal antibodies protect mice from *Yersinia pestis* in a bubonic plague model," *PLoS ONE*, vol. 5, no. 10, Article ID e13047, 2010.

[13] M. A. Parent, L. B. Wilhelm, L. W. Kummer, F. M. Szaba, I. K. Mullarky, and S. T. Smiley, "Gamma interferon, tumor necrosis factor alpha, and nitric oxide synthase 2, key elements of cellular immunity, perform critical protective functions during humoral defense against lethal pulmonary *Yersinia pestis* infection," *Infection and Immunity*, vol. 74, no. 6, pp. 3381–3386, 2006.

[14] S. T. Smiley, "Immune defense against pneumonic plague," *Immunological Reviews*, vol. 225, no. 1, pp. 256–271, 2008.

[15] J.-S. Lin, S. Park, J. J. Adamovicz et al., "TNFα and IFNγ contribute to F1/LcrV-targeted immune defense in mouse models of fully virulent pneumonic plague," *Vaccine*, vol. 29, no. 2, pp. 357–362, 2010.

[16] M. K. Hart, G. A. Saviolakis, S. L. Welkos, and R. V. House, "Advanced development of the rF1V and rBV vaccines: progress and challenges," *Advances in Preventive Medicine*, vol. 2012, Article ID 731604, 14 pages, 2012.

[17] B. S. Powell, G. P. Andrews, J. T. Enama et al., "Design and testing for a nontagged F1-V fusion protein as vaccine antigen against bubonic and pneumonic plague," *Biotechnology Progress*, vol. 21, no. 5, pp. 1490–1510, 2005.

[18] D. G. Heath, G. W. Anderson Jr., J. M. Mauro et al., "Protection against experimental bubonic and pneumonic plague by a recombinant capsular F1-V antigen fusion protein vaccine," *Vaccine*, vol. 16, no. 11-12, pp. 1131–1137, 1998.

[19] H. Weighardt, S. Kaiser-Moore, R. M. Vabulas, C. J. Kirschning, H. Wagner, and B. Holzmann, "Myeloid differentiation factor 88 deficiency improves resistance against sepsis caused by polymicrobial infection," *Journal of Immunology*, vol. 169, no. 6, pp. 2823–2827, 2002.

[20] S. Spiller, S. Dreher, G. Meng et al., "Cellular recognition of trimyristoylated peptide or enterobacterial lipopolysaccharide via both TLR2 and TLR4," *The Journal of Biological Chemistry*, vol. 282, no. 18, pp. 13190–13198, 2007.

[21] O. Adachi, T. Kawai, K. Takeda et al., "Targeted disruption of the MyD88 gene results in loss of IL-1- and IL- 18-mediated function," *Immunity*, vol. 9, no. 1, pp. 143–150, 1998.

[22] M. A. Hughes, C. S. Green, L. Lowchyj et al., "MyD88-dependent signaling contributes to protection following Bacillus anthracis spore challenge of mice: implications for toll-like receptor signaling," *Infection and Immunity*, vol. 73, no. 11, pp. 7535–7540, 2005.

[23] A. Poltorak, X. He, I. Smirnova et al., "Defective LPS signaling in C3H/HeJ and C57BL/10ScCr mice: mutations in Tlr4 gene," *Science*, vol. 282, no. 5396, pp. 2085–2088, 1998.

[24] K. Hoshino, O. Takeuchi, T. Kawai et al., "Toll-like receptor 4 (TLR4)-deficient mice are hyporesponsive to lipopolysaccharide evidence for TLR4 as the Lps gene product," *Journal of Immunology*, vol. 162, no. 7, pp. 3749–3752, 1999.

[25] S. T. Qureshi, L. Larivière, G. Leveque et al., "Endotoxin-tolerant mice have mutations in toll-like receptor 4 (Tlr4)," *The Journal of Experimental Medicine*, vol. 189, no. 4, pp. 615–625, 1999.

[26] K. Amemiya, J. L. Meyers, T. E. Rogers et al., "CpG oligodeoxynucleotides augment the murine immune response to the *Yersinia pestis* F1-V vaccine in bubonic and pneumonic models of plague," *Vaccine*, vol. 27, no. 16, pp. 2220–2229, 2009.

[27] H. S. Heine, A. Louie, F. Sorgel et al., "Comparison of 2 antibiotics that inhibit protein synthesis for the treatment of infection with *Yersinia pestis* delivered by aerosol in a mouse model of pneumonic plague," *Journal of Infectious Diseases*, vol. 196, no. 5, pp. 782–787, 2007.

[28] K. Pouliot, N. Pan, S. Wang, S. Lu, E. Lien, and J. D. Goguen, "Evaluation of the role of LcrV-toll-like receptor 2-mediated immunomodulation in the virulence of *Yersinia pestis*," *Infection and Immunity*, vol. 75, no. 7, pp. 3571–3580, 2007.

[29] D. Reithmeier-Rost, J. Hill, S. J. Elvin et al., "The weak interaction of LcrV and TLR2 does not contribute to the virulence

of *Yersinia pestis*," *Microbes and Infection*, vol. 9, no. 8, pp. 997–1002, 2007.

[30] R. M. Martin, A. Silva, and A. M. Lew, "The Igh-1 sequence of the non-obese diabetic (NOD) mouse assigns it to the IgG2c isotype," *Immunogenetics*, vol. 46, no. 2, pp. 167–168, 1997.

[31] R. M. Martin, J. L. Brady, and A. M. Lew, "The need for IgG2c specific antiserum when isotyping antibodies from C57BL/6 and NOD mice," *Journal of Immunological Methods*, vol. 212, no. 2, pp. 187–192, 1998.

[32] R. A. Lukaszewski, D. J. Kenny, R. Taylor, D. G. C. Rees, M. G. Hartley, and P. C. F. Oyston, "Pathogenesis of *Yersinia pestis* infection in BALB/c mice: effects on host macrophages and neutrophils," *Infection and Immunity*, vol. 73, no. 11, pp. 7142–7150, 2005.

[33] M. M. Marketon, R. W. DePaolo, K. L. DeBord, B. Jabri, and O. Schneewind, "Microbiology: plague bacteria target immune cells during infection," *Science*, vol. 309, no. 5741, pp. 1739–1741, 2005.

[34] O. Takeuchi, K. Hoshino, and S. Akira, "TLR2-deficient and MyD88-deficient mice are highly susceptible to *Staphylococcus aureus* infection," *Journal of Immunology*, vol. 165, no. 10, pp. 5392–5396, 2000.

[35] B. T. Edelson and E. R. Unanue, "MyD88-dependent but toll-like receptor 2-independent innate immunity to Listeria: no role for either in macrophage listericidal activity," *Journal of Immunology*, vol. 169, no. 7, pp. 3869–3875, 2002.

[36] E. Seki, H. Tsutsui, N. M. Tsuji et al., "Critical roles of myeloid differentiation factor 88-dependent proinflammatory cytokine release in early phase clearance of *Listeria monocytogenes* in mice," *Journal of Immunology*, vol. 169, no. 7, pp. 3863–3868, 2002.

[37] C. G. Feng, C. A. Scanga, C. M. Collazo-Custodio et al., "Mice lacking myeloid differentiation factor 88 display profound defects in host resistance and immune response to *Mycobacterium avium* infection not exhibited by Toll-like receptor 2 (TLR2)- and TLR4-deficient animals," *Journal of Immunology*, vol. 171, no. 9, pp. 4758–4764, 2003.

[38] U. M. Nagarajan, D. M. Ojcius, L. Stahl, R. G. Rank, and T. Darville, "*Chlamydia trachomatis* induces expression of IFN-γ-inducible protein 10 and IFN-β independent of TLR2 and TLR4, but largely dependent on MyD88," *Journal of Immunology*, vol. 175, no. 1, pp. 450–460, 2005.

[39] D. S. Weiss, K. Takeda, S. Akira, A. Zychlinsky, and E. Moreno, "MyD88, but not toll-like receptors 4 and 2, is required for efficient clearance of *Brucella abortus*," *Infection and Immunity*, vol. 73, no. 8, pp. 5137–5143, 2005.

[40] K. A. Archer and C. R. Roy, "MyD88-dependent responses involving Toll-like receptor 2 are important for protection and clearance of *Legionella pneumophila* in a mouse model of Legionnaires' disease," *Infection and Immunity*, vol. 74, no. 6, pp. 3325–3333, 2006.

[41] C. M. Collazo, A. Sher, A. I. Meierovics, and K. L. Elkins, "Myeloid differentiation factor-88 (MyD88) is essential for control of primary in vivo *Francisella tularensis* LVS infection, but not for control of intramacrophage bacterial replication," *Microbes and Infection*, vol. 8, no. 3, pp. 779–790, 2006.

[42] T. R. Hawn, K. D. Smith, A. Aderem, and S. J. Skerrett, "Myeloid differentiation primary response gene (88)- and toll-like receptor 2-deficient mice are susceptible to infection with aerosolized *Legionella pneumophila*," *Journal of Infectious Diseases*, vol. 193, no. 12, pp. 1693–1702, 2006.

[43] R. Spörri, N. Joller, U. Albers, H. Hilbi, and A. Oxenius, "MyD88-dependent IFN-γ production by NK cells is key for control of *Legionella pneumophila* infection," *Journal of Immunology*, vol. 176, no. 10, pp. 6162–6171, 2006.

[44] S. L. Lebeis, B. Bommarius, C. A. Parkos, M. A. Sherman, and D. Kalman, "TLR signaling mediated by MyD88 is required for a protective innate immune response by neutrophils to *Citrobacter rodentium*," *Journal of Immunology*, vol. 179, no. 1, pp. 566–577, 2007.

[45] E. Burns, T. Eliyahu, S. Uematsu, S. Akira, and G. Nussbaum, "TLR2-dependent inflammatory response to *Porphyromonas gingivalis* is MyD88 independent, whereas MyD88 is required to clear infection," *Journal of Immunology*, vol. 184, no. 3, pp. 1455–1462, 2010.

[46] Y. Shen, I. Kawamura, T. Nomura et al., "Toll-like receptor 2- and MyD88-dependent phosphatidylinositol 3-kinase and Rac1 activation facilitates the phagocytosis of *Listeria monocytogenes* by murine macrophages," *Infection and Immunity*, vol. 78, no. 6, pp. 2857–2867, 2010.

[47] J. M. Blander and R. Medzhitov, "Regulation of phagosome maturation by signals from Toll-like receptors," *Science*, vol. 304, no. 5673, pp. 1014–1018, 2004.

[48] R. M. Yates and D. G. Russell, "Phagosome maturation proceeds independently of stimulation of toll-like receptors 2 and 4," *Immunity*, vol. 23, no. 4, pp. 409–417, 2005.

[49] D. Sun and A. Ding, "MyD88-mediated stabilization of interferon-γ-induced cytokine and chemokine mRNA," *Nature Immunology*, vol. 7, no. 4, pp. 375–381, 2006.

[50] A. Glynn, C. J. Roy, B. S. Powell, J. J. Adamovicz, L. C. Freytag, and J. D. Clements, "Protection against aerosolized *Yersinia pestis* challenge following homologous and heterologous prime-boost with recombinant plague antigens," *Infection and Immunity*, vol. 73, no. 8, pp. 5256–5261, 2005.

[51] L. E. Quenee and O. Schneewind, "Plague vaccines and the molecular basis of immunity against *Yersinia pestis*," *Human Vaccines*, vol. 5, no. 12, pp. 817–823, 2009.

[52] F. Martinon, A. Mayor, and J. Tschopp, "The inflammasomes: guardians of the body," *Annual Review of Immunology*, vol. 27, pp. 229–265, 2009.

[53] S. C. Eisenbarth, O. R. Colegio, W. O'Connor Jr., F. S. Sutterwala, and R. A. Flavell, "Crucial role for the Nalp3 inflammasome in the immunostimulatory properties of aluminium adjuvants," *Nature*, vol. 453, no. 7198, pp. 1122–1126, 2008.

[54] L. Franchi and G. Núñez, "The Nlrp3 inflammasome is critical for aluminum hydroxide-mediated IL-1β secretion but dispensable for adjuvant activity," *European Journal of Immunology*, vol. 38, no. 8, pp. 2085–2089, 2008.

[55] M. Kool, V. Pétrilli, T. De Smedt et al., "Alum adjuvant stimulates inflammatory dendritic cells through activation of the NALP3 inflammasome," *Journal of Immunology*, vol. 181, no. 6, pp. 3755–3759, 2008.

[56] H. Li, S. B. Willingham, J. P.-Y. Ting, and F. Re, "Inflammasome activation by alum and alum's adjuvant effect are mediated by NLRP3," *Journal of Immunology*, vol. 181, no. 1, pp. 17–21, 2008.

[57] A. S. McKee, M. W. Munks, M. K. L. MacLeod et al., "Alum induces innate immune responses through macrophage and mast cell sensors, but these sensors are not required for alum to act as an adjuvant for specific immunity," *Journal of Immunology*, vol. 183, no. 7, pp. 4403–4414, 2009.

[58] F. A. Sharp, D. Ruane, B. Claass et al., "Uptake of particulate vaccine adjuvants by dendritic cells activates the NALP3 inflammasome," *Proceedings of the National Academy of Sciences of the United States of America*, vol. 106, no. 3, pp. 870–875, 2009.

[59] J. Harris, F. A. Sharp, and E. C. Lavelle, "The role of inflammasomes in the immunostimulatory effects of particulate vaccine adjuvants," *European Journal of Immunology*, vol. 40, no. 3, pp. 634–638, 2010.

[60] A. L. Gavin, K. Hoebe, B. Duong et al., "Adjutant-enhanced antibody responses in the absence of toll-like receptor signaling," *Science*, vol. 314, no. 5807, pp. 1936–1938, 2006.

[61] C. Pasare and R. Medzhitov, "Control of B-cell responses by Toll-like receptors," *Nature*, vol. 438, no. 7066, pp. 364–368, 2005.

Hindawi Publishing Corporation
Journal of Immunology Research
Volume 2014, Article ID 395302, 6 pages
http://dx.doi.org/10.1155/2014/395302

Review Article

Approaches to Modelling the Human Immune Response in Transition of Candidates from Research to Development

Diane Williamson

Defence Science and Technology Laboratory (DSTL), Porton Down, Salisbury, Wilts SP4 0JQ, UK

Correspondence should be addressed to Diane Williamson; dewilliamson@dstl.gov.uk

Received 14 December 2013; Accepted 11 March 2014; Published 7 May 2014

Academic Editor: Julia Tree

This review considers the steps required to evaluate a candidate biodefense vaccine or therapy as it emerges from the research phase, in order to transition it to development. The options for preclinical modelling of efficacy are considered in the context of the FDA's Animal Rule.

1. Introduction

The development of any product for ultimate clinical use is a lengthy process, requiring the progression from proof-of-principle research into nonclinical models and safety testing and progressive phases of testing in humans, through clinical trials. The different phases of clinical trial are generally designed to progressively test the safety and immunogenicity of the candidate vaccine or therapy, usually starting with a dose-escalating design followed by dose and schedule optimisation, before pivotal trials at the selected dose and schedule.

Ordinarily, where a vaccine or therapy is directed against a disease of public health relevance which occurs predictably and regularly in a percentage of the healthy adult or pediatric population, efficacy trials of the candidate can progress in this population under authorized protocols, as long as there is sufficient nonclinical evidence that it is likely to confer benefit to this susceptible population. The endpoint of such trials is a quantifiable impact on the occurrence of, or recovery from, the disease.

However, where the vaccine or therapy is directed against a disease which is not normally prevalent, but which erupts from time-to-time in regions of the world where the disease is endemic, clinical trialling of efficacy is much more difficult. This is due not only to the unpredictability of the eruption but also the unknown size of the affected population. Furthermore, it is not ethical to deliberately expose a healthy population in a nonendemic area to potentially life-threatening disease, in order to test the efficacy of a candidate vaccine or therapy.

This situation is true for the clinical testing of vaccines or therapies directed against potential bioterrorist agents, or against pathogens that lack adequate diagnostics, or new products where a vaccine is already available but the use of a placebo arm would be unethical. All of these situations present circumstances which are both ethically challenging and which make carrying out a clinical trial of efficacy with sufficient statistical power very difficult to achieve.

In such circumstances, where clinical efficacy trials are not feasible for reasons of either logistics and/or ethics, the approval of novel vaccines for clinical use will rely on the demonstration of immune correlates of protection and the approval of novel therapies on predetermined immune readout or other endpoints [1]. This entails a clinical trial design where the endpoints are the measurement of surrogate markers of efficacy, based on immunological readouts which have been found to correlate statistically with protective efficacy in appropriate animal models. Depending on how closely the animal model mimics the human infection, more

than one animal model of the infection may be required to provide immune correlates, with the following assumptions:

(1) there is a well-understood pathophysiological mechanism of the toxicity of the pathogen and its prevention or substantial reduction by the vaccine or inhibition by the therapy;

(2) the effect is demonstrated in one or more animal species expected to react with a response predictive for humans, unless the effect is demonstrated in a single animal species that represents a sufficiently well-characterized animal model for predicting the response in humans;

(3) the animal study endpoint is clearly related to the desired benefit in humans, generally the enhancement of survival or prevention of major morbidity;

(4) The data or information on the kinetics and pharmacodynamics of the vaccine or therapy or other relevant data or information, in animals and humans, allows selection of an effective dose in humans.

These concepts are embodied in the Animal Rule by the Food and Drug Agency in the USA and are discussed in detail elsewhere [1]. In a subsequent section, we will focus on how immune correlates of protection can be derived in nonclinical models and how they can be applied to predict the protection likely to be achieved in human subjects during clinical trials.

This is not to say that there are not circumstances under which non-life-threatening infections can be deliberately caused in human volunteers with their fully informed consent, in order to test a new vaccine or therapy. Indeed many such studies are authorized by ethical review bodies every year in the UK and elsewhere to test prophylaxes or therapies for influenza [2, 3]. Additionally human volunteers have given informed consent to test prophylaxes and therapies for malaria and other non-life-threatening conditions [4].

2. Approaches to Modelling the Human Immune Response to Candidate Vaccines or Therapies

In transitioning vaccines and therapies to the clinic, it is essential to model the human immune response as closely as possible. This is particularly important in the case of vaccines and therapies intended for use to protect against biodefense agents, since for these, it will be neither ethical nor feasible to conduct conventional phase III efficacy trials in human volunteers. Thus, for these biodefense agents it will be important to establish safety and efficacy in appropriate animal models prior to transition to Phase I safety studies [5].

In the R&D of vaccines and therapies for biodefense, the traditional approach has involved a progression from early evaluation in tissue and organ culture through an appropriate small animal model(s) to higher animal models, with the latter being engaged in the early to advanced development phases. This approach also supports a 3R's philosophy, that is, the reduction, refinement, and replacement of the use of whole animals in research, with appropriate alternatives, a policy promoted in the UK by the Home Office [6] and in the USA by the Animal Welfare Act [7] and by the Association for assessment and accreditation of laboratory animal care international (AAALAC) [8]. Tissue culture systems provide an early evaluation of candidate vaccines and therapies for their potential cytotoxic effects *in vitro* or *ex vivo* and may be of greatest value if both animal and human cell lines are available for comparison. Additionally, the ability to grow cells in a three-dimensional structure, for example, in a rotating vessel, may provide a more authentic model of the tissue or organ being simulated [9]. As a step beyond tissue culture, it is possible to maintain individual organs in a physiological medium in order to interrogate their responses to a therapeutic candidate and this has been successful, for example, with isolated, perfused lungs [10]. Furthermore, *in silico* modelling to predict what might be antigenic in microorganisms may help to make large microbial genomes more tractable and focus efforts prior to embarking on animal models [11]. There are an increasing number of algorithms available to analyse structure-function relationships, to determine surface-exposed, hydrophilic chemical groups in order to predict surface-exposed conformational or buried linear epitopes [12]. Beyond organogenic tissue culture, simple *in vivo* models such as the waxmoth larva (*Galleria mellonella*) or the nematode worm *Caenorhabditis elegans* may be used for an initial evaluation of potential toxicity and an early indication of efficacy against an administered challenge [13]. For example, the Galleria model has been demonstrated to be susceptible to challenge with bacteria of the *Burkholderia* species and can be used to evaluate approaches to therapy of these infections. Although a simple structure, Galleria provides an attractive holistic *in vivo* model in which to screen for efficacy and which does not require any of the supporting infrastructure needed to house laboratory rodents, for example [14]. Similarly, *C. elegans* has a primitive physiology and immune system and has been used to study mechanisms of infectivity and virulence used, for example, by *Pseudomonas aeruginosa* and *Staphylococcal aureus* [15]. In recent years, the zebrafish (*Dario rerio*) has gained ground as an alternative to mammalian models of infectious disease and since the sequencing of its genome, several laboratories have developed bacterial and viral disease models using the zebrafish [16]. Zebrafish have been reported to be a useful model for streptococcal infection being susceptible to the human pathogen *Streptococcus pyogenes* [17], whilst the pathology and immune response of zebrafish to *Franciscella tularensis* are similar in many aspects to that in mammals [18]. Zebrafish have also been mooted as a useful model of toll-like receptor (TLR) signalling in immunity and disease [19] and as a model for inflammatory disorders [20].

At the next level, laboratory rodents may be used to evaluate the safety, immunogenicity, and efficacy of candidate vaccines and therapies. Traditionally, the mouse has been the species of choice and over many years, a comprehensive repertoire of reagents has become available to assess the physiological and particularly the immune responses of mice. Inbred strains of mice have the advantage that their genotypes are defined and so relative differences in observed response may be related to genotype, if all other influences are

standardised [21]. Non-laboratory strain, outbred mice on the other hand, may respond differently to some infections and thus may be a more authentic model for certain infections such as a Gammaherpesvirus, for which the wood mouse is a natural host [22]. Another outbred rodent model, the prairie dog, which is a zoonotic vector for *Yersinia pestis*, has recently been used to evaluate the efficacy of a candidate subunit vaccine for plague using vaccination in the wild by spiked bait [23], allowing confirmation that the vaccine is effective in both natural and laboratory models of infection [24]. Starting with a defined genotype such as that of the C57Bl6 mouse with H-2b haplotype, specific single gene deletions can be made to knock out specific cytokines or cytokine receptors or to confer sensitivity to a toxin such as diphtheria toxin [25]. The effect of these deletions may be to alter the polarity of the immune response; for example, IL10 or IL10 receptor knockouts may have a Th1-polarised response [26]; or to delete a subset of cells, for example, regulatory T-cells (Treg) in mice transgenic for diphtheria toxin (DT) receptor under the control of the *foxp3* gene locus, allowing the selective and efficient depletion of $Foxp3^+$ T reg cells by the injection of diphtheria toxin [27].

Such transgenic mice still express murine major histocompatibility locus (MHC) proteins, so that their immune responses are authentically murine, hence their antigen-presenting cells (APC) will process foreign material and antigens and present peptides processed from them in the cleft of the MHCII complex on the surface of APC to murine CD4+ T-cell receptors; a T-cell response will be initiated if the T-cell receives a second signal transmitted between a B7 molecule on the APC surface and the CD28 receptor on the T-cell surface. Alternatively, processing and presentation of foreign proteins as peptides in the cleft of MHC1 molecules results in presentation to CD8+ T-cells and if a second signal is also received the CD8+ T-cell is induced to become cytotoxic. In man, the analogous system to the murine MHC system is the human leucocyte antigen (HLA) complex. HLA molecules A, B, and C correspond to MHC class 1 molecules, whereas HLA molecules DR, DQ, and DP are analogous to MHCII molecules. To exploit murine models fully to predict human immune responses, HLA transgenic mice have been developed which carry full-length genomic constructs for HLA-DR or DQ molecules and which have been crossed for many generations with C57BL/6 Ab-null mice, so that they lack expression of endogenous mouse MHC class II molecules [28]. These HLA transgenic mice thus allow an evaluation of human immune responses in a murine framework. This approach to immunoanalysis is of particular value, for example, in T-cell epitope-mapping studies where the objective is to determine the immunodominant regions of an immunogen and to assign function to structure.

Other rodent species used in the laboratory include rats, guinea pigs, and hamsters. These generally are used less frequently than mice but may be selected based on a greater resistance to microbial challenge, as with the Fischer rat [29] or on susceptibility to aerosol challenge (as with the guinea pig) [30] or as a second model of, for example, *Burkholderia* infection (hamster) [31]. Rabbits, which are classed as lagomorphs, may provide an intermediate model between rodents and non-human primates. In some cases, rabbits are a superior model to the non-human primate. For instance, in the case of modelling infection with *Bacillus anthracis* (causative of anthrax), the rabbit may be the model of choice [32] since mice are supersensitive to the capsule [33] surrounding the bacterium and the routine use of non-human primates, such as macaques, is expensive and raises ethical issues [34]. Rabbits, on the other hand, respond in a dose-related manner to spore challenge and can be protected by vaccines or therapies designed to prevent the effects of anthrax toxins [35]. In this context, the utility of HLA transgenic mice to predict human sensitivity to anthrax has been demonstrated. Using an unencapsulated strain of *B. anthracis* to avoid the supersensitivity of mice, HLA transgenic mice have been shown to be differentially susceptible, so that compared with inbred strains such as the A/J [33] and C57Bl6, HLA-transgenic mice were less susceptible [36]. Awareness of such differential resistances may help to extrapolate murine data to man or aid the selection of the most appropriate animal models with which to predict the human immune response.

Non-human primates are at the maximum level of sentience for laboratory species and should be used only with the highest level of justification and where there is no alternative [6]. Amongst NHPs, however, Rhesus and cynomolgus macaques are the most frequently used members of this Old World monkey species. Although evolutionarily most akin to humans, it cannot be assumed that NHPs will always exactly represent the human response to the testing of candidate vaccines or therapies. This was illustrated recently in the lessons learned from the testing of the superagonistic monoclonal antibody (Mab) TGN1412 for CD28. Designed as an immune downregulator to treat inflammatory conditions such as rheumatoid arthritis, leukaemia, and multiple sclerosis, this Mab was found to be safe on extensive toxicity testing in macaques, but on testing in a Phase 1 trial in healthy human volunteers it induced pronounced inflammation with a cytokine storm, requiring intensive care of the volunteers involved [37]. This was an unexpected result since the CD28 receptor is homologous between macaques and humans and the unexpected toxicity in clinical trial volunteers prompted extensive subsequent investigation [38]. After extensive analysis of cell subtypes and their activation status it was found that, unlike in man, the CD28 receptor is not expressed on central memory effector T-cells in macaques, so that the macaques were unable to respond through this cell subset with the cytokine storm that occurred in the volunteers [39]. This investigation and analysis of the cause of the cytokine storm have led to a better understanding of some potential limitations in preclinical testing and highlighted the benefit of applying such molecular immunological approaches to preclinical testing, particularly perhaps of immunotherapeutics [39].

New World monkeys are more evolutionarily distant from man than are the Old World monkeys and comprise a group including the marmoset which may be ethically and practically (because of their small size) more acceptable as a laboratory model [40]. Recently, there has been renewed

interest in the common marmoset (*Callithrix jacchus*) as a model for vaccination and therapy of microbial disease [41]. This in turn has led to the identification of a range of immunoreagents suitable for the assessment of marmoset responses [42].

For some microbial diseases, the animal model may need to be selected based on a display of similar symptomatology to that seen in man. Thus, where emesis is a common symptom, the ferret may be selected for use, as the most suitable model [43]. In the same vein, rodents are not ideal models for human inhalational exposure since they are nasal obligate breathers unlike non-human primates who can breathe through the mouth as well as the nose [44].

Infrequently, species which in the wild may transmit zoonoses may be used in captivity to test candidate vaccines or therapies. For example, the black-footed ferret, as well as the prairie dog mentioned above, has been used successfully to evaluate a recombinant subunit vaccine for *Yersinia pestis*, since both these species are able to transmit plague to man [24].

3. Surrogate Markers of Efficacy and Correlates of Protection

Surrogate markers of efficacy for an antimicrobial vaccine or therapy encompass immunological or microbiological readouts which explain, and are causally related to, protective efficacy and which provide endpoints which are surrogates for survival [45]. Usually, it would be expected that a number of surrogate markers would be required to predict that the candidate had induced an appropriate antimicrobial or protective immune response in man to a pathogen. The observation of statistically significant immune correlates of protection in an animal model can lead to the identification of the same immunological readouts in man, which will then serve as surrogate marker(s) of efficacy [46].

Thus, in clinical trials where the protective efficacy of the vaccine or therapy cannot be tested directly, surrogate markers of efficacy can be measured instead. For a candidate vaccine, these measurements may encompass some of the following: vaccine-specific antibody titre and functionality (e.g., toxin-neutralisation, viral plaque reduction, or bactericidal/bacteriostatic activity), cytokine secretion patterns, the induction of cell-mediated immunity with display of activation markers on immune effector cells, and an *ex vivo* proliferative or cytotoxic T cell response towards the vaccine antigen(s) or infected eukaryotic cells [47]. For a candidate therapy, these measurements may encompass the induction of appropriate responses to inhibit the binding of viruses or bacteria to host cells to prevent entry or invasion, leading to bacterial or viral clearance, or inhibition of an essential factor (e.g., bacterial cell wall assembly) for the survival and replication of bacteria or viruses in the human host [48]. Clearly, the deliberate exposure of the host to life-threatening infection to test the therapy is not ethical, so these parameters could be tested in human cells *ex vivo*. Some of these measurements may be defined as surrogate markers to substitute for survival as an endpoint in efficacy testing in man, as long as (1) the animal model in which they were derived authentically represents the human infection and (2) a statistically valid association with protection has been demonstrated in the animal model [1]. Under these conditions, the observed induction of such surrogate markers of efficacy in a clinical trial volunteer is predictive that the candidate vaccine has induced protective immunity.

Of course, it may not always be possible to identify true surrogate markers of efficacy, for example, where the entirety of the mechanism of protection is unknown. This could happen where only a single parameter in an animal model has been observed to correlate with protection but does not explain the entirety of the protective effect observed. Several scenarios have been suggested where putative surrogate markers of efficacy would not serve that function, for example, where a disease process has multiple causes and the intervention does not impact these directly, so that caution needs to be exercised to ensure that the risk : benefit ratio remains acceptable and the product being considered for licensure has tangible clinical benefit [49]. Having identified immune correlates of protection, there are various mathematical approaches which can be applied to extrapolate these nonclinical data to man in order to predict degrees of protection or therapeutic effect, which may be related to the scale of the immunological responses observed in the clinic [50].

4. Progress and Prospects for Licensure

Successful licensure of next generation biodefense vaccines and therapies will depend on the successful use of the FDA's Animal Rule [1], the satisfactory demonstration of immune correlates of protection across the animal species used as efficacy models and the subsequent identification of suitable surrogate markers of efficacy with which to monitor the responses of clinical trial volunteers. Recently, on the basis of the Animal Rule, several medical countermeasures have been licensed: levofloxacin (US FDA, April 2012) for inhalational anthrax, ciprofloxacin (US FDA, April 2013) for inhalational plague, and raxibacumab (US FDA, December 2012) for anthrax intoxication.

Other products which contribute to biodefense have also been licensed by the FDA, amongst which are a heptavalent botulinum antitoxin, licensed for the treatment of symptomatic botulism (2013); a reduced primary schedule with booster doses at 12 and 18 months has been approved for the FDA-licensed anthrax vaccine, AVA (Biothrax) (2012); an updated vaccinia vaccine (ACAM2000) for smallpox was approved in 2007; vaccinia immune globulin has been approved for the treatment of complications of vaccinia vaccine (2005); and an immunoglobulin for infant botulism (BabyBIG) was approved in 2003 [51].

Steady progress is being made in developing a stockpile of biodefense-related projects and subsequent papers in this issue deal with the impact of non-human primate models on understanding pathogenesis and the use of emerging technologies to understand the molecular basis of infection,

prophylaxis and therapy and specific infectious disease syndromes. These advances together with guidance from the Animal Rule will have impact on the development to licensure in the long term. However, the pathway to the licensure of new biodefense vaccines is still long and challenging and current regulatory guidance is based on uncharted territory so far.

Conflict of Interests

The author declares that there is no conflict of interests regarding the publication of this paper.

References

[1] US FDA HHS, "New drug and biological drug products; evidence needed to demonstrate effectiveness of new drugs when human efficacy studies are not ethical or feasible," *Federal Register*, vol. 67, pp. 37988–37998, 2002.

[2] http://www.niaid.nih.gov/news/newsreleases/2013/Pages/flu-Pathogenesis.aspx.

[3] http://www.retroscreen.com/news-publications/story/first-swine-flu-vaccine-cleared-for-uk-use/.

[4] http://www.malariavaccine.org/rd-clinical-trials.php.

[5] D. N. Wolfe, W. Florence, and P. Bryant, "Current biodefense vaccine programs and challenges," *Human Vaccines and Immunotherapeutics*, vol. 9, pp. 1591–1597, 2013.

[6] National Centre for the Replacement, Refinement and Reduction of animals in research, http://www.nc3rs.org.uk/.

[7] Animal Welfare Act , USA, 1966, https://awic.nal.usda.gov/public-law-89-544-act-august-24-1966.

[8] Association for the Assessment And Accreditation of Laboratory Animal Care international (AAALAC), http://www.aaalac.org/.

[9] J. Barrila, A. L. Radtke, A. Crabbé et al., "Organotypic 3D cell culture models: using the rotating wall vessel to study host-pathogen interactions," *Nature Reviews Microbiology*, vol. 8, no. 11, pp. 791–801, 2010.

[10] P. G. Sanchez, G. J. Bittle, L. Burdorf, R. N. Pierson III, and B. P. Griffith, "State of Art: clinical ex vivo lung perfusion: rationale, current status, and future directions," *Journal of Heart and Lung Transplantation*, vol. 31, no. 4, pp. 339–348, 2012.

[11] B. de la Caridad Addine Ramírez, R. Marrón, R. Calero et al., "In silico identification of common epitopes from pathogenic mycobacteria," *BMC Immunology*, vol. 14, supplement, article S6, 2013.

[12] J. V. Kringelum, C. Lundegaard, O. Lund, and M. Nielsen, "Reliable B cell epitope predictions: impacts of method development and improved benchmarking," *PLOS Computational Biology*, vol. 8, no. 12, Article ID e1002829, 2012.

[13] K. D. Seed and J. J. Dennis, "Development of *Galleria mellonella* as an alternative infection model for the Burkholderia cepacia complex," *Infection and Immunity*, vol. 76, no. 3, pp. 1267–1275, 2008.

[14] S. Uehlinger, S. Schwager, S. P. Bernier et al., "Identification of specific and universal virulence factors in Burkholderia cenocepacia strains by using multiple infection hosts," *Infection and Immunity*, vol. 77, no. 9, pp. 4102–4110, 2009.

[15] J. E. Irazoqui, E. R. Troemel, R. L. Feinbaum, L. G. Luhachack, B. O. Cezairliyan, and F. M. Ausubel, "Distinct pathogenesis and host responses during infection of *C. elegans* by *P. aeruginosa* and *S. aureus*," *PLoS Pathogens*, vol. 6, Article ID e1000982, 2010.

[16] C. Sullivan and C. H. Kim, "Zebrafish as a model for infectious disease and immune function," *Fish and Shellfish Immunology*, vol. 25, no. 4, pp. 341–350, 2008.

[17] M. N. Neely, J. D. Pfeifer, and M. Caparon, "Streptococcus-zebrafish model of bacterial pathogenesis," *Infection and Immunity*, vol. 70, no. 7, pp. 3904–3914, 2002.

[18] L. N. Vojtech, G. E. Sanders, C. Conway, V. Ostland, and J. D. Hansen, "Host immune response and acute disease in a zebrafish model of francisella pathogenesis," *Infection and Immunity*, vol. 77, no. 2, pp. 914–925, 2009.

[19] M. van der Vaart, J. J. van Soest, H. P. Spaink, and A. H. Meijer, "Functional analysis of a zebrafish *myd88* mutant identifies key transcriptional components of the innate immune system," *Disease Models and Mechanisms*, 2013.

[20] Z. Kanwal, A. Zakrzewska, and J. denHertog, "Deficiency in hematopoietic phosphatase ptpn6/shp1 hyperactivates the innate immune system and impairs control of bacterial infections in zebrafish embryos," *Journal of Immunology*, 2013.

[21] M. F. W. Festing, "Invited review: inbred strains should replace outbred stocks in toxicology, safety testing, and drug development," *Toxicologic Pathology*, vol. 38, no. 5, pp. 681–690, 2010.

[22] D. J. Hughes, A. Kipar, J. T. Sample, and J. P. Stewart, "Pathogenesis of a model gammaherpesvirus in a natural host," *Journal of Virology*, vol. 84, no. 8, pp. 3949–3961, 2010.

[23] T. E. Rocke, S. R. Smith, D. T. Stinchcomb, and J. E. Osorio, "Immunization of black-tailed prairie dog against plague through consumption of vaccine-laden baits," *Journal of Wildlife Diseases*, vol. 44, no. 4, pp. 930–937, 2008.

[24] E. D. Williamson and P. C. F. Oyston, "Protecting against plague: towards a next generation vaccine," *Clinical & Experimental Immunology*, vol. 172, no. 1, pp. 1–8, 2013.

[25] M. Saito, T. Iwawaki, C. Taya et al., "Diphtheria toxin receptor-mediated conditional and targeted cell ablation in transgenic mice," *Nature Biotechnology*, vol. 19, no. 8, pp. 746–750, 2001.

[26] X. Yang, J. Gartner, L. Zhu, S. Wang, and R. C. Brunham, "IL-10 gene knockout mice show enhanced Th1-like protective immunity and absent granuloma formation following *Chlamydia trachomatis* lung infection," *Journal of Immunology*, vol. 162, no. 2, pp. 1010–1017, 1999.

[27] K. Lahl and T. Sparwasser, "In vivo depletion of FoxP3+ Tregs using the DEREG mouse model," *Methods in Molecular Biology*, vol. 707, pp. 157–172, 2011.

[28] D. M. Altmann, D. C. Douek, A. J. Frater, C. M. Hetherington, H. Inoko, and J. I. Elliott, "The T cell response of HLA-DR transgenic mice to human myelin basic protein and other antigens in the presence and absence of human CD4," *Journal of Experimental Medicine*, vol. 181, no. 3, pp. 867–875, 1995.

[29] C. R. Raymond and J. W. Conlan, "Differential susceptibility of Sprague-Dawley and Fischer 344 rats to infection by *Francisella tularensis*," *Microbial Pathogenesis*, vol. 46, no. 4, pp. 231–234, 2009.

[30] V. Savransky, D. C. Sanford, E. Syar et al., "Pathology and pathophysiology of inhalational anthrax in a guinea pig model," *Infection and Immunity*, vol. 81, pp. 1152–1163, 2013.

[31] D. L. Fritz, P. Vogel, D. R. Brown, and D. M. Waag, "The hamster model of intraperitoneal burkholderia mallei (Glanders)," *Veterinary Pathology*, vol. 36, no. 4, pp. 276–291, 1999.

[32] G. M. Zaucha, M. L. M. Pitt, J. Estep, B. E. Ivins, and A. M. Friedlander, "The pathology of experimental anthrax in rabbits

exposed by inhalation and subcutaneous inoculation," *Archives of Pathology and Laboratory Medicine*, vol. 122, no. 11, pp. 982–992, 1998.

[33] H. C. Flick-Smith, E. L. Waters, N. J. Walker et al., "Mouse model characterisation for anthrax vaccine development: comparison of one inbred and one outbred mouse strain," *Microbial Pathogenesis*, vol. 38, no. 1, pp. 33–40, 2005.

[34] N. A. Twenhafel, "Pathology of inhalational anthrax animal models," *Veterinary Pathology*, vol. 47, no. 5, pp. 819–830, 2010.

[35] S. F. Little, B. E. Ivins, P. F. Fellows, M. L. M. Pitt, S. L. W. Norris, and G. P. Andrews, "Defining a serological correlate of protection in rabbits for a recombinant anthrax vaccine," *Vaccine*, vol. 22, no. 3-4, pp. 422–430, 2004.

[36] S. Ascough, R. J. Ingram, K. K. Chu et al., "Anthrax lethal factor as an immune target in humans and transgenic mice and the impact of HLA polymorphism on $CD4^+$ T cell immunity," *PLOS Pathogens*. In press.

[37] E. W. St. Clair, "The calm after the cytokine storm: lessons from the TGN1412 trial," *Journal of Clinical Investigation*, vol. 118, no. 4, pp. 1344–1347, 2008.

[38] R. Stebbings, L. Findlay, C. Edwards et al., ""Cytokine storm" in the Phase I trial of monoclonal antibody TGN1412: better understanding the causes to improve preclinical testing of immunotherapeutics," *Journal of Immunology*, vol. 179, no. 5, pp. 3325–3331, 2007.

[39] R. Stebbings, D. Eastwood, S. Poole, and R. Thorpe, "After TGN1412: recent developments in cytokine release assays," *Journal of Immunotoxicology*, vol. 10, no. 1, pp. 75–82, 2013.

[40] J. McKinley, H. M. Buchanan-Smith, L. Bassett, and K. Morris, "Training common marmosets (*Callithrix jacchus*) to cooperate during routine laboratory procedures: ease of training and time investment," *Journal of Applied Animal Welfare Science*, vol. 6, no. 3, pp. 209–220, 2003.

[41] M. S. Lever, A. J. Stagg, M. Nelson et al., "Experimental respiratory anthrax infection in the common marmoset (*Callithrix jacchus*)," *International Journal of Experimental Pathology*, vol. 89, no. 3, pp. 171–179, 2008.

[42] R. J. Hornby, P. C. Pearce, A. P. Bowditch, L. Scott, and G. D. Griffiths, "Multiple vaccine and pyridostigmine bromide interactions in the common marmoset *Callithrix jacchus*: immunological and endocrinological effects," *International Immunopharmacology*, vol. 6, no. 12, pp. 1765–1779, 2006.

[43] N. Percie du Sert, J. A. Rudd, C. C. Apfel, and P. L. R. Andrews, "Cisplatin-induced emesis: systematic review and meta-analysis of the ferret model and the effects of 5-HT_3 receptor antagonists," *Cancer Chemotherapy and Pharmacology*, vol. 67, no. 3, pp. 667–686, 2011.

[44] J. R. Harkema, S. A. Carey, and J. G. Wagner, "The nose revisited: a brief review of the comparative structure, function, and toxicologic pathology of the nasal epithelium," *Toxicologic Pathology*, vol. 34, no. 3, pp. 252–259, 2006.

[45] M. Mueller, A. de la Peña, and H. Derendorf, "Issues in pharmacokinetics and pharmacodynamics of anti-infective agents: kill curves versus MIC," *Antimicrobial Agents and Chemotherapy*, vol. 48, no. 2, pp. 369–377, 2004.

[46] S. A. Plotkin and P. B. Gilbert, "Nomenclature for immune correlates of protection after vaccination," *Clinical Infectious Diseases*, vol. 54, no. 11, pp. 1615–1617, 2012.

[47] J. Hombach, T. Solomon, I. Kurane, J. Jacobson, and D. Wood, "Report on a WHO consultation on immunological endpoints for evaluation of new Japanese encephalitis vaccines, WHO, Geneva, 2-3 September, 2004," *Vaccine*, vol. 25, pp. 4130–4139, 2004.

[48] R. Wise, "Maximizing efficacy and reducing the emergence of resistance," *Journal of Antimicrobial Chemotherapy*, vol. 51, no. 1, supplement S1, pp. 37–42, 2003.

[49] T. R. Fleming, "Surrogate endpoints and FDA's accelerated approval process," *Health Affairs*, vol. 24, no. 1, pp. 67–78, 2005.

[50] E. D. Williamson, M. G. Duchars, and R. Kohberger, "Recent advances in predictive models and correlates of protection in testing biodefence vaccines," *Expert Review of Vaccines*, vol. 9, no. 5, pp. 527–537, 2010.

[51] FDA, Vaccines, blood and biologics development and approval process (Biologics). Biological approvals by year, http://www.fda.gov/.

Hindawi Publishing Corporation
Journal of Immunology Research
Volume 2014, Article ID 308732, 6 pages
http://dx.doi.org/10.1155/2014/308732

Research Article

Fusion-Expressed CTB Improves Both Systemic and Mucosal T-Cell Responses Elicited by an Intranasal DNA Priming/Intramuscular Recombinant Vaccinia Boosting Regimen

Sugan Qiu,[1] Xiaonan Ren,[1] Yinyin Ben,[1] Yanqin Ren,[1] Jing Wang,[1,2] Xiaoyan Zhang,[1,2] Yanmin Wan,[1] and Jianqing Xu[1,2]

[1] *Shanghai Public Health Clinical Center, Fudan University, Shanghai 201508, China*
[2] *Institute of Biomedical Science, Fudan University, Shanghai 200032, China*

Correspondence should be addressed to Yanmin Wan; wanyanmin_2004@163.com and Jianqing Xu; jianqingxu2008@gmail.com

Received 13 November 2013; Accepted 7 March 2014; Published 1 April 2014

Academic Editor: Diane Williamson

Previous study showed that CTB (Cholera toxin subunit B) can be used as a genetic adjuvant to enhance the systemic immune responses. To further investigate whether it can also be used as a genetic adjuvant to improve mucosal immune responses, we constructed DNA and recombinant Tiantan vaccinia (rTTV) vaccines expressing OVA-CTB fusion antigen. Female C57BL/6 mice were immunized with an intranasal DNA priming/intramuscular rTTV boosting regimen. OVA specific T-cell responses were measured by IFN-γ ELISPOT and specific antibody responses were determined by ELISA. Compared to the nonadjuvant group (pSV-OVA intranasal priming/rTTV-OVA intramuscular boosting), pSV-OVA-CTB intranasal priming/rTTV-OVA-CTB intramuscular boosting group significantly improved the magnitudes of T-cell responses at spleen (1562 ± 567 SFCs/10^6 splenocytes versus 330 ± 182 SFCs/10^6 splenocytes, $P < 0.01$), mesenteric LN (96 ± 83 SFCs/10^6 lymphocytes versus 1 ± 2 SFCs/10^6 lymphocytes, $P < 0.05$), draining LNs of respiratory tract (109 ± 60 SFCs/10^6 lymphocytes versus 2 ± 2 SFCs/10^6 lymphocytes, $P < 0.01$) and female genital tract (89 ± 48 SFCs/10^6 lymphocytes versus 23 ± 21 SFCs/10^6 lymphocytes, $P < 0.01$). These results collectively demonstrated that fusion-expressed CTB could act as a potent adjuvant to improve both systemic and mucosal T-cell responses.

1. Introduction

DNA vaccines are insufficient to stimulate strong mucosal and systemic immunity when inoculated alone [1]. Various approaches have been taken to improve the immunogenicity of DNA vaccine, such as delivering DNA by using electroporation or enhancing host response by coadminstration of genetic adjuvants [1].

Cholera toxin (CT) is a strong mucosal immunogen as well as an effective adjuvant [2]; both the holotoxin and its subunits can be used as adjuvants for protein based vaccines [3, 4]. Recent studies suggested that both CTA (Cholera toxin subunit A) and CTB (Cholera toxin subunit B) can also be used as genetic adjuvants to boost the systemic immune responses elicited by DNA vaccines [5, 6]. To investigate whether CTB can also be used as a genetic adjuvant to improve antigen specific mucosal immune responses, in this study, we constructed DNA and recombinant Tiantan vaccinia (rTTV) vaccines encoding OVA-CTB fusion antigen and tested their immunogenicity in an intranasal DNA priming/intramuscular rTTV boosting regimen, which has been proved to be able to raise vigorous mucosal and systemic immune response [7].

2. Materials and Methods

2.1. Vaccines and Mice. All DNA and recombinant vaccinia virus vaccines were constructed in our previous work. The 6–8-week-old female C57BL/6 mice were bred and maintained

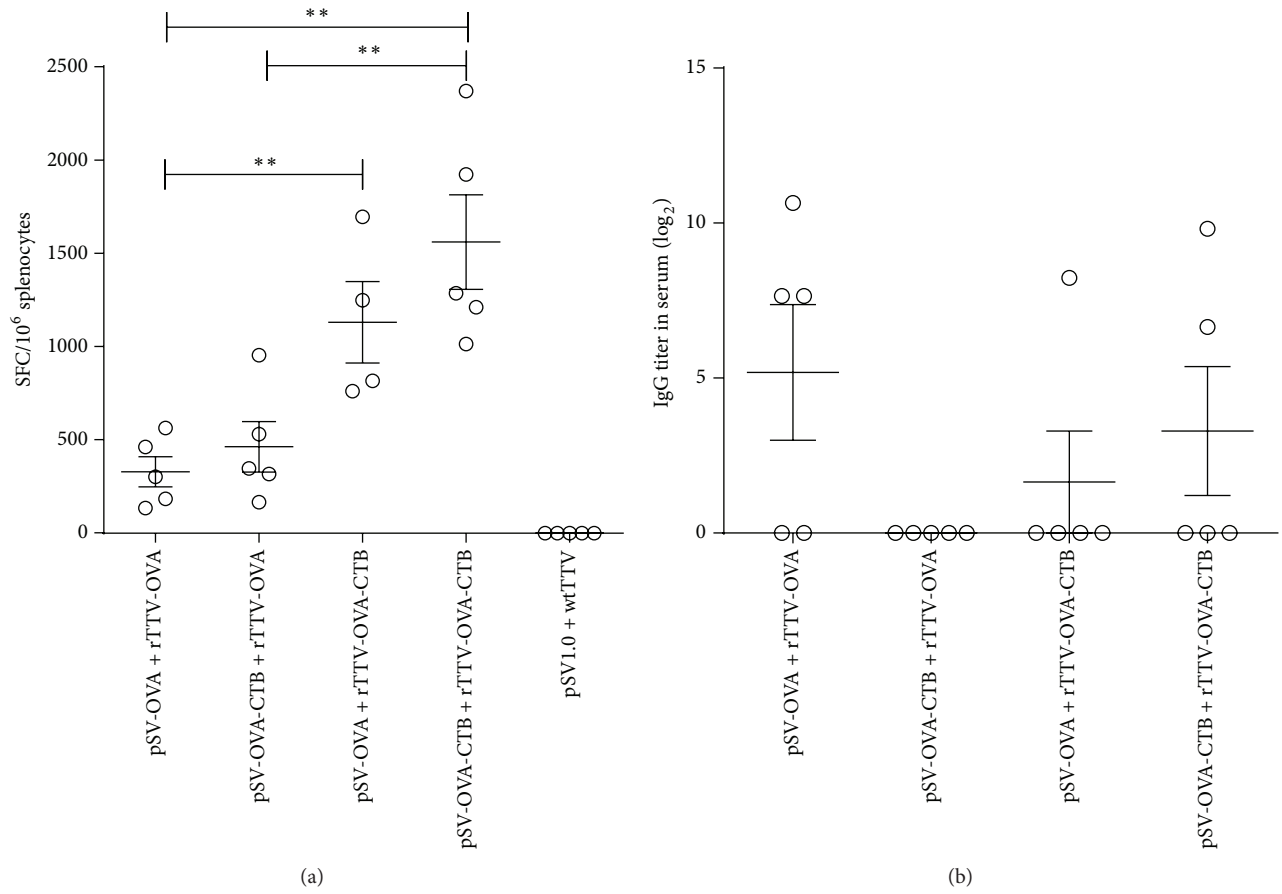

Figure 1: Humoral and cellular immune responses at systemic level. (a) Ovalbumin specific T-cell responses in spleen. The cellular responses elicited in rTTV-OVA-CTB boosting groups were significantly stronger than those elicited in rTTV-OVA boosting groups. (b) Ovalbumin specific antibody responses in serum. OVA specific IgG titers elicited by adjuvant groups tended to be lower than the nonadjuvant group, but no statistical significance was reached. $^{**}P < 0.01$.

under specific pathogen-free condition. All animal experiments were reviewed by the Institutional Animal Care and Use Committee (IACUC) of Shanghai Public Health Clinical Center.

2.2. Mice Immunization and Sampling. DNA vaccine (5 μg/mouse) mixed with Turbofect (Fermentas, Cat. number R0541) was given intranasally on weeks 0, 2, and 4. And on week 7, mice were boosted intramuscularly with recombinant Tiantan vaccinia vaccine (1×10^6 pfu/mouse). Two weeks after the final vaccination, mice were euthanized. Vaginal lavage, bronchial alveolar lavage, and serum were collected for the detection of specific antibody response. Spleen, cervical, axillary, iliac, inguinal, and mesenteric lymph nodes were isolated for T-cell response assay.

2.3. IFN-γ ELISPOT Assay. Freshly isolated mouse splenocytes were adjusted to the concentration of 4×10^6 cells/mL and plated into 96-well ELISPOT plate (BD Bioscience, Cat. number 551083) coated with anti-mouse IFN-γ antibody at 50 μL/well (2×10^5 cells/well). The splenocytes were stimulated with OVA peptide (amino acids 257–264) at the final concentration of 5 μg/mL. After incubation at 37°C with 5% CO_2 for 20 hours, the ELISPOT plates were developed according to the manufacturer's manual and read with Immunospot Reader (ChampspotIII, Beijing Sage Creation Science, China).

2.4. ELISA Assay. ELISA plates coated with 2 μg/mL OVA were used for the detection of anti-OVA antibodies (Abs). Serum, bronchial lavage, or vaginal lavage samples were 2-fold serially diluted in PBS containing 5% skimmed milk and 0.5% TWEEN-20. OVA specific IgG and IgA were detected by peroxidase conjugated anti-mouse IgG and anti-mouse IgA, respectively. End point titers were determined by the last dilution, whose OD was beyond or equal to 2-fold that of the corresponding dilution of mice sera immunized with mock control.

2.5. Statistical Analysis. Comparisons between two groups were done by the method of unpaired t-test and comparisons among three or more groups were done by using the method

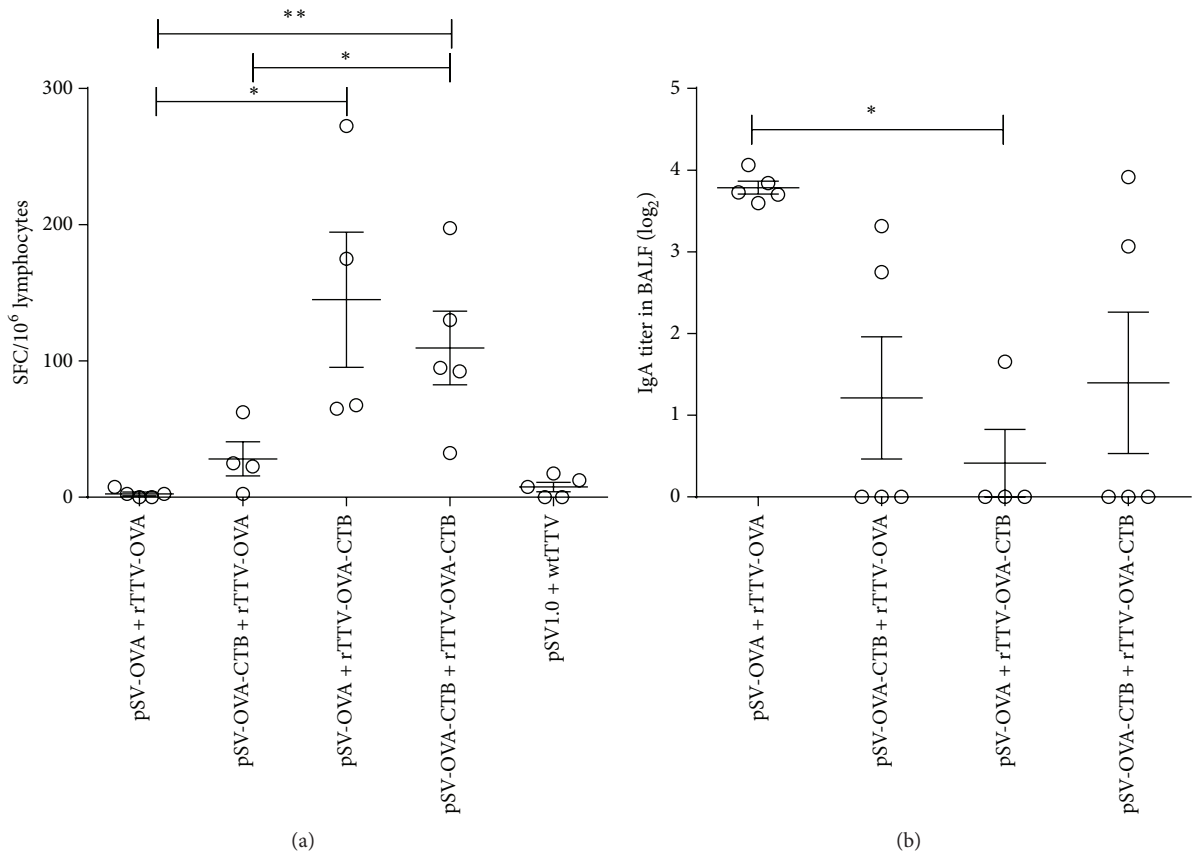

Figure 2: Specific antibody and T-cell immune responses elicited in respiratory tract. (a) Ovalbumin specific T-cell response in cervical and axillary lymph nodes. Significant differences were observed between rTTV-OVA-CTB boosting groups and rTTV-OVA boosting groups. (b) Specific IgA titer in bronchial alveolar lavage. The average OVA specific IgA titer induced by pSV-OVA priming/rTTV-OVA boosting was significantly higher than pSV-OVA priming/rTTV-OVA-CTB boosting group. $^{*}P < 0.05$, $^{**}P < 0.01$.

of one-way ANOVA (Prism6, GraphPad Software, Inc.). Significant difference was defined as $P \leq 0.05$.

3. Results

3.1. Systemic Immune Responses. Mice were immunized according to the schedule shown in Table 1. Two weeks after the final immunization, splenocytes were isolated and OVA-specific T-cell responses were quantified by IFN-γ ELISPOT assay. Specific binding antibody in serum was detected by ELISA.

ELISPOT results showed that all the rTTV-OVA-CTB boosting groups mounted significantly stronger T-cell immune responses (1132 ± 436 SFCs/10^6 splenocytes for pSV-OVA intranasal priming/rTTV-OVA-CTB intramuscular boosting group and 1562 ± 567 SFCs/10^6 splenocytes for pSV-OVA-CTB intranasal priming/rTTV-OVA-CTB intramuscular boosting group) than rTTV-OVA boosting groups (330 ± 182 SFCs/10^6 splenocytes for pSV-OVA intranasal priming/rTTV-OVA intramuscular boosting group and 464 ± 303 SFCs/10^6 splenocytes for pSV-OVA-CTB intranasal priming/rTTV-OVA intramuscular boosting group) (Figure 1(a)). OVA specific IgG titers elicited by adjuvant groups tended to be lower than the nonadjuvant group, but no statistical significance was observed (Figure 1(b)).

3.2. Humoral and Cellular Immune Responses Elicited in Respiratory Tract. We collected the bronchi alveolar lavage for specific IgA titration, cervical, and axillary lymph nodes for analysis of mucosal T-cell responses. The ELISPOT data showed that pSV-OVA intranasal priming/rTTV-OVA-CTB intramuscular boosting induced the highest T-cell responses (145 ± 99 SFCs/10^6 lymphocytes) and pSV-OVA-CTB intranasal priming/rTTV-OVA-CTB intramuscular boosting group was the second (109 ± 60 SFCs/10^6 lymphocytes). Both were significantly higher than the nonadjuvant group (pSV-OVA intranasal priming/rTTV-OVA intramuscular boosting, 2 ± 2 SFCs/10^6 lymphocytes) (Figure 2(a)).

The mean titer of OVA specific IgA in bronchi alveolar lavage induced by adjuvant groups was lower than the non-adjuvant group. Significant difference was observed between pSV-OVA intranasal priming/rTTV-OVA intramuscular boosting group and pSV-OVA intranasal priming/rTTV-OVA-CTB intramuscular boosting group (Figure 2(b)).

Table 1: Mice immunization schedule.

Group	No. of mice	Week 0 (50 μg/mouse)	Week 2 (50 μg/mouse)	Week 4 (50 μg/mouse)	Week 7 (1E6pfu/mouse)	Week 9
A	5	pSV1.0	pSV1.0	pSV1.0	WT TTV	Euthanized
B	5	pSV-OVA	pSV-OVA	pSV-OVA	rTTV-OVA	Euthanized
C	5	pSV-OVA	pSV-OVA	pSV-OVA	rTTV-OVA-CTB	Euthanized
D	4	pSV-OVA-CTB	pSV-OVA-CTB	pSV-OVA-CTB	rTTV-OVA	Euthanized
E	5	pSV-OVA-CTB	pSV-OVA-CTB	pSV-OVA-CTB	rTTV-OVA-CTB	Euthanized

3.3. Humoral and Cellular Immune Responses Elicited in Female Genital Tract. Inguinal and iliac LNs were collected for ELISPOT assay and vaginal lavage was collected for specific IgA and IgG titration. T-cell responses of pSV-OVA-CTB intranasal priming/rTTV-OVA-CTB intramuscular boosting group (89 ± 48 SFCs/10^6 lymphocytes) were significantly higher than rTTV-OVA boosting groups (23 ± 21 SFCs/10^6 lymphocytes for pSV-OVA intranasal priming/rTTV-OVA intramuscular boosting group; 63 ± 26 SFCs/10^6 lymphocytes for pSV-OVA-CTB intranasal priming/rTTV-OVA intramuscular boosting group) (Figure 3(a)).

No significant difference was observed among the OVA specific IgG titers in vaginal lavage of all groups (Figure 3(b)). OVA specific IgA titers of pSV-OVA-CTB intranasal priming/rTTV-OVA-CTB intramuscular boosting group were significantly higher than pSV-OVA intranasal priming/rTTV-OVA-CTB intramuscular boosting group (Figure 3(c)).

3.4. Ovalbumin Specific T-Cell Responses in Mesenteric Lymph Nodes. To investigate specific T-cell responses in intestinal mucosa, we isolated mesenteric LN and measured OVA specific T-cell responses by ELISPOT assay. The results suggested that both rTTV-OVA-CTB boosting groups (138 ± 102 SFCs/10^6 lymphocytes for pSV-OVA intranasal priming/rTTV-OVA-CTB intramuscular boosting group and 96 ± 84 SFCs/10^6 lymphocytes for pSV-OVA-CTB intranasal priming/rTTV-OVA-CTB intramuscular boosting group) elicited significantly higher T-cell responses than rTTV-OVA boosting groups (1 ± 2 SFCs/10^6 lymphocytes for pSV-OVA intranasal priming/rTTV-OVA intramuscular boosting group and 1 ± 2 SFCs/10^6 lymphocytes for pSV-OVA-CTB intranasal priming/rTTV-OVA intramuscular boosting group) (Figure 4).

4. Discussion

The mucosae constitute the major portal of entry of infectious agents. An ideal vaccine should induce both systemic and mucosal immune responses in order to block the entry of pathogens and contain infections *in vivo*. Majority of previous studies seek to induce mucosal immune responses by mucosal immunization [8–11]; however, this may not be applicable for naked DNA vaccines due to the relative weak immunogenicity [7].

In this study, we constructed DNA and recombinant Tiantan vaccinia (rTTV) vaccines encoding OVA-CTB fusion antigen and immunized C57/BL mice in an intranasal DNA priming/intramuscular rTTV boosting regimen. Our data showed that pSV-OVA-CTB priming (i.n.)/rTTV-OVA-CTB boosting (i.m.) elicited the highest magnitude of T-cell responses in spleen (system level). And the genetic adjuvant effect of CTB was more significant for recombinant vaccinia vaccine than for DNA vaccine, since the T-cell responses induced by pSV-OVA priming (i.n.)/rTTV-OVA-CTB boosting (i.m.) were significantly higher than pSV-OVA priming (i.n.)/rTTV-OVA boosting (i.m.) and the T-cell responses elicited by pSV-OVA-CTB priming (i.n.)/rTTV-OVA boosting (i.m.) were only slightly higher than the nonadjuvant group. In contrast, OVA specific IgG responses elicited by adjuvant groups tended to be lower than the nonadjuvant group although no statistical significance was reached.

We further tested specific immune responses at different mucosal sites and found that pSV-OVA-CTB priming (i.n.)/rTTV-OVA-CTB boosting (i.m.) consistently raised significant higher cellular immune response than the nonadjuvant group at respiratory, intestinal, and female genital tract, which indicated that the fused-expression of CTB in both DNA and rTTV vaccines is essential for eliciting robust T-cell responses at mucosal sites. Very interestingly, we found that rTTV-OVA-CTB boosting was especially efficient at improving specific T-cell responses in mesenteric lymph node. Besides, similar to the observations of antibody responses in serum, we found that the adjuvant groups tended to induce lower specific IgA titer in both bronchi alveolar lavage and vaginal lavage.

When being used as an adjuvant of protein vaccine, CTB can enhance specific immune response through either GM1 receptor-mediated antigen uptake [12] or stimulating expression of B7.2 on APCs [13]. As OVA is a secretory protein, we thus postulate that the secreted OVA-CTB fusion expressed by the DNA or recombinant vaccinia vaccines can also bind with GM1 receptor or interact with APCs *in vivo*, which may facilitate the uptake and presentation of OVA. This hypothesis was supported by our previous work, in which we found that the adjuvant effect decreased when separating CTB and the antigen into two plasmids (see Supplementary Figure 1 available online at http://dx.doi.org/10.1155/2014/308732). Further experiments will be conducted to confirm the proposed mechanisms and clarify the missing details.

5. Conclusions

Taken together, in spite of being short of mechanistic explanation, our data clearly showed that fusion-expressed CTB could serve as a potent adjuvant to enhance both systemic

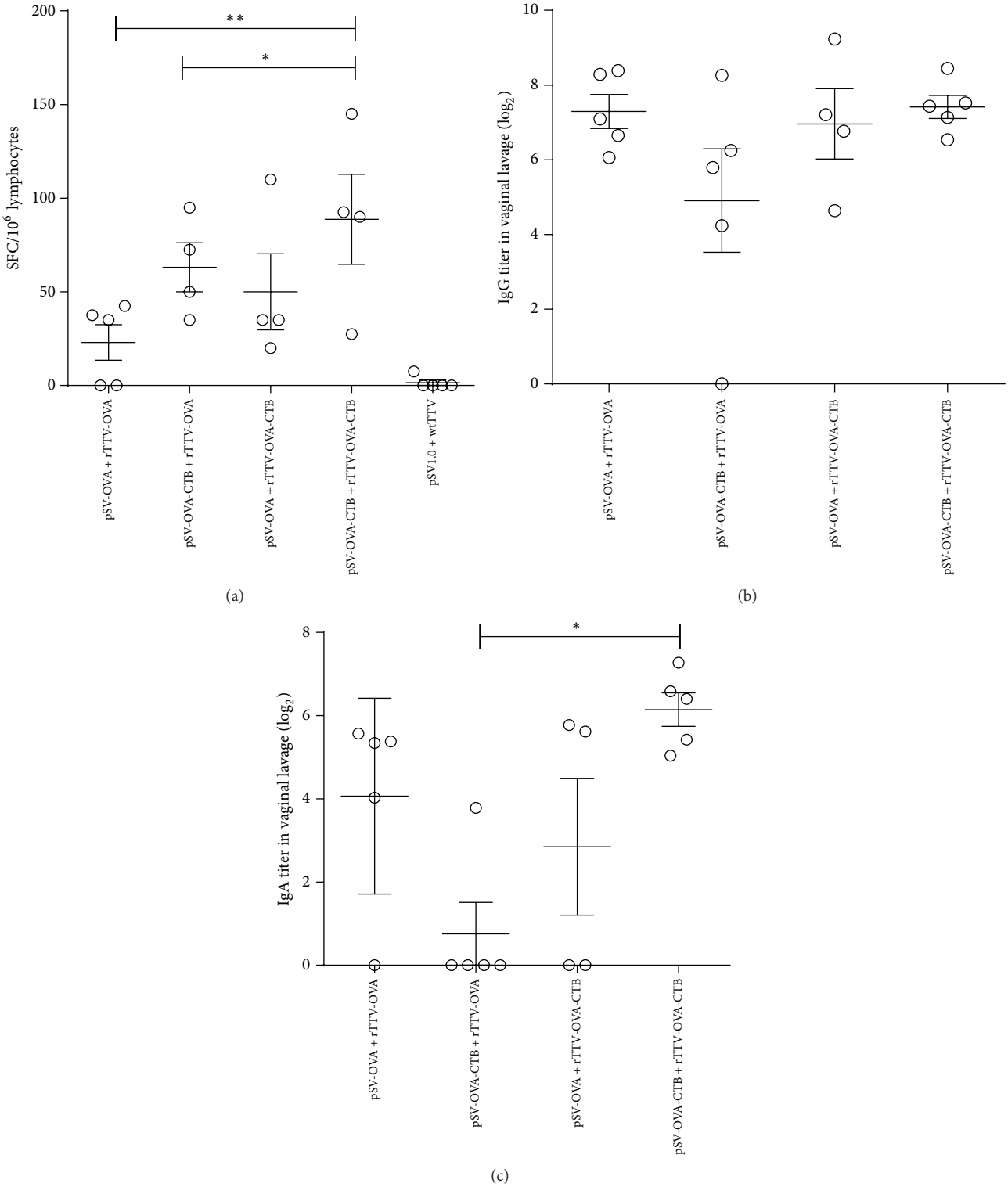

Figure 3: Specific antibody and T-cell immune responses elicited in female genital tract. (a) T lymphocytes responses in inguinal and iliac lymph nodes. The T-cell responses of rTTV-OVA-CTB boosting groups were significantly higher than those of rTTV-OVA boosting groups. (b) Specific IgG responses in vaginal lavage. No significant difference was found among different groups. (c) Specific IgA responses in vaginal lavage. IgA titer elicited by pSV-OVA-CTB priming/rTTV-OVA-CTB boosting group was significantly higher than pSV-OVA priming/rTTV-OVA-CTB boosting group. $^{*}P < 0.05$, $^{**}P < 0.01$.

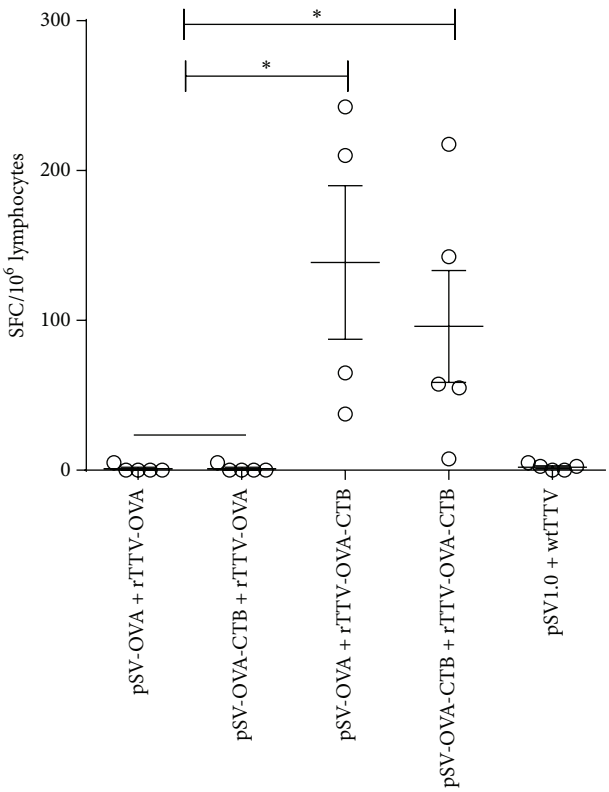

Figure 4: T-cell responses elicited in mesenteric lymph node. rTTV-OVA-CTB boosting raised significantly more rigorous T-cell responses than rTTV-OVA boosting groups. $^{*}P < 0.05$.

and mucosal T-cell response, not only for DNA vaccine but also for viral vectored vaccine.

Conflict of Interests

The authors declare that there is no conflict of interests regarding the publication of this paper.

Acknowledgments

The authors thank Dr. Zhaoqin Zhu for her kind help during the paper preparation. This research was supported by National Natural Science Foundation of China (81302605 and 31200108), Shanghai Science and Technology Committee Grants (11XD1404200 and 11ZR1430600), and Shanghai Municipal Health and Family Planning Commission Grant (XBR2011042).

References

[1] C. Coban, K. Kobiyama, T. Aoshi et al., "Novel strategies to improve DNA vaccine immunogenicity," *Current Gene Therapy*, vol. 11, no. 6, pp. 479–484, 2011.

[2] C. O. Elson and W. Ealding, "Cholera toxin feeding did not induce oral tolerance in mice and abrogated oral tolerance to an unrelated protein antigen," *The Journal of Immunology*, vol. 133, no. 6, pp. 2892–2897, 1984.

[3] A. D. Wilson, C. J. Clarke, and C. R. Stokes, "Whole cholera toxin and B subunit act synergistically as an adjuvant for the mucosal immune response of mice to keyhole limpet haemocyanin," *The Journal of Immunology*, vol. 31, no. 4, pp. 443–451, 1990.

[4] S. J. McKenzie and J. F. Halsey, "Cholera toxin B subunit as a carrier protein to stimulate a mucosal immune response," *The Journal of Immunology*, vol. 133, no. 4, pp. 1818–1824, 1984.

[5] H. Cong, M. Zhang, Q. Xin et al., "Compound DNA vaccine encoding SAG1/ SAG3 with A_2/B subunit of cholera toxin as a genetic adjuvant protects BALB/c mice against *Toxoplasma gondii*," *Parasites & Vectors*, no. 6, article 63, 2013.

[6] K. C. Bagley, G. K. Lewis, and T. R. Fouts, "Adjuvant activity of the catalytic A1 domain of cholera toxin for retroviral antigens delivered by GeneGun," *Clinical and Vaccine Immunology*, vol. 18, no. 6, pp. 922–930, 2011.

[7] X. Huang, J. Xu, C. Qiu et al., "Mucosal priming with PEI/DNA complex and systemic boosting with recombinant TianTan vaccinia stimulate vigorous mucosal and systemic immune responses," *Vaccine*, vol. 25, no. 14, pp. 2620–2629, 2007.

[8] M. R. Neutra and P. A. Kozlowski, "Mucosal vaccines: the promise and the challenge," *Nature Reviews Immunology*, vol. 6, no. 2, pp. 148–158, 2006.

[9] J. Holmgren and C. Czerkinsky, "Mucosal immunity and vaccines," *Nature Medicine*, vol. 11, pp. S45–S53, 2005.

[10] M. B. Parr and E. L. Parr, "Vaginal immunity in the HSV-2 mouse model," *International Reviews of Immunology*, vol. 22, no. 1, pp. 43–63, 2003.

[11] R. P. Morrison and H. D. Caldwell, "Immunity to murine chlamydial genital infection," *Infection and Immunity*, vol. 70, no. 6, pp. 2741–2751, 2002.

[12] J. Sánchez and J. Holmgren, "Cholera toxin: a foe & a friend," *Indian Journal of Medical Research*, vol. 133, no. 2, pp. 153–163, 2011.

[13] S. Park, S. Chun, and P. Kim, "Intraperitoneal delivery of cholera toxin B subunit enhances systemic and mucosal antibody responses," *Molecules and Cells*, vol. 16, no. 1, pp. 106–112, 2003.